University of Alberta

CHARACTERIZATION OF PEROXISOME BIOGENESIS AND FUNCTION IN *CAENORHABDITIS ELEGANS*

by

Oleh Ihorovych Petriv ©

A thesis submitted to the Faculty of Graduate Studies and Research in partial fulfillment of the requirements for the degree of Doctor of Philosophy

Department of Cell Biology

Edmonton, Alberta

Spring 2005

Library and
Archives Canada

Published Heritage
Branch

395 Wellington Street
Ottawa ON K1A 0N4
Canada

Bibliothèque et
Archives Canada

Direction du
Patrimoine de l'édition

395, rue Wellington
Ottawa ON K1A 0N4
Canada

0-494-08289-5

Your file Votre référence
ISBN
Our file Notre reference
ISBN

NOTICE:
The author has granted a non-exclusive license allowing Library and Archives Canada to reproduce, publish, archive, preserve, conserve, communicate to the public by telecommunication or on the Internet, loan, distribute and sell theses worldwide, for commercial or non-commercial purposes, in microform, paper, electronic and/or any other formats.

The author retains copyright ownership and moral rights in this thesis. Neither the thesis nor substantial extracts from it may be printed or otherwise reproduced without the author's permission.

AVIS:
L'auteur a accordé une licence non exclusive permettant à la Bibliothèque et Archives Canada de reproduire, publier, archiver, sauvegarder, conserver, transmettre au public par télécommunication ou par l'Internet, prêter, distribuer et vendre des thèses partout dans le monde, à des fins commerciales ou autres, sur support microforme, papier, électronique et/ou autres formats.

L'auteur conserve la propriété du droit d'auteur et des droits moraux qui protège cette thèse. Ni la thèse ni des extraits substantiels de celle-ci ne doivent être imprimés ou autrement reproduits sans son autorisation.

In compliance with the Canadian Privacy Act some supporting forms may have been removed from this thesis.

While these forms may be included in the document page count, their removal does not represent any loss of content from the thesis.

Conformément à la loi canadienne sur la protection de la vie privée, quelques formulaires secondaires ont été enlevés de cette thèse.

Bien que ces formulaires aient inclus dans la pagination, il n'y aura aucun contenu manquant.

Canada

For
my Ukraine
and
the Orange revolution

ABSTRACT

Peroxisomes are organelles that perform multiple roles in the cell, most notably in lipid metabolism. Loss of peroxisomal function in humans results in lethal neurodegenerative disorders. This thesis investigates the use and advantages of the nematode *Caenorhabditis elegans* as a model organism for the human peroxisomal disorders.

Eleven sequence homologs of fourteen known human PEX genes (genes encoding proteins necessary for peroxisome biogenesis) were identified in the nematode genome: Pex1p, -2p, -3p, -5p, -6p, -10p, -11p, -12p, -13p, -14p and -19p. Pex3p, -5p, -12p, -13p, -14p and -19p were found to be required for peroxisome biogenesis and to be involved in the regulation of developmental decisions in the nematode. Our analysis by RNA interference did not demonstrate any apparent function in peroxisome biogenesis for the remaining *C. elegans* homologs of the human PEX genes and for the homologs of human Pex2p and Pex11p in nematode development.

The developmental role of fifteen nematode genes that are homologs of human peroxisomal enzymes has also been assessed. Genes coding for alkyldihydroxyacetonephosphate synthase and $\Delta^{3,5}$-$\Delta^{2,4}$-dienoyl-CoA isomerase were found to be indispensable for normal nematode development. A *C. elegans* mutant lacking peroxisomal catalase was found to exhibit a progeric phenotype. The mammalian peroxisomal protein SCPx (Sterol Carrier Protein x) has thiolase and sterol carrier protein domains that are encoded by two separate genes in *C. elegans*, which permits the ready dissection of the functions of these domains. Using strains deleted individually for these genes, it was demonstrated that, like SCPx, the *C. elegans* P-44 type II thiolase and the Fat-2 protein are involved in the metabolism of branched chain fatty acids.

Most soluble proteins are targeted to the peroxisomal matrix by one of two peroxisomal targeting signals (PTS), PTS1 or PTS2. The PTS2 pathway has been suggested to be absent in *C. elegans*. This thesis presents conclusive evidence that PTS2 pathway is indeed absent in *C. elegans*. Computational analysis of both functional and nonfunctional PTS2s has led to two re-evaluated PTS2 consensus sequences that describe more accurately all variants of the PTS2 motif.

The work reported in this thesis supports the utility of *C. elegans* as a model system with which to study peroxisome biogenesis and function in a multicellular organismal setting under both normal developmental and disease conditions.

ACKNOWLEDGEMENTS

I am sincerely grateful to my supervisor Dr. Richard Rachubinski who has allowed me to work independently and to develop my own ideas. He has assembled a lab with the research environment that greatly contributed to my confidence and growth as a researcher. I was happy to work in this team. I am sorry for Rick as he constantly had to fight with my English, but that was the best course of English I could dream of.

My sincere appreciation to the members of my Supervisory Committee and Candidacy Examining Committee who provided the invaluable guidance and excellent ideas that helped in my research: professors Rick Rachubinski, David Pilgrim, Paul Melançon, Bernard Lemire and Andrew Simmonds. I also want to thank to my external supervisor, Dr. Paul Watkins for his invaluable expertise of my work. Thank you all for numerous advises, consultations and help.

I would also like to recognize past and present colleagues in the Rachubinski's lab who have taught me and shared ideas with me: Vladimir Titorenko, Roger Bascom, Juan Carlos Torres, Andrei and Monica Fagarasanu, Chris Tam, Franco Joseph, Cleofe Hurtado, Jenny Chang, Melissa Dobson, Martine Ooms.

My deep appreciation also to Hanna Kroliczak, Elena Savidov, Rick Poirier, Dwayne Weber, Cecilia Acat and Preterita Zegarra for their friendship and excellent technical assistance and to the office staff of the Department of Cell Biology (Robert Venketrman, Melanie Grams, Claire Lavergne, Veronica Clough, Coleen Langard and James Kendall) for guidenace through the study process.

I also thank Barbara Knoblach for a critical reading of this manuscript and to Drs. David Pilgrim, Bernard Lemire and Zhixiang Wang for allowing me to use their equipment.

I am very thankful to Honey Chan for help with confocal and electron microscopy, and to Dr Randy Whittal for help with gas chromatography, to Ling Tang for computer programming and to Steven Pennock and Yi Wang for help with mammalian cell culture and transfection.

TABLE OF CONTENTS

CHAPTER 1 **INTRODUCTION** 1

1.1 What are peroxisomes? 2

1.2 Biochemical roles of peroxisomes 2

1.3 PEX genes and biogenesis of peroxisomes 4

1.4 Peroxisome targeting signals 9

1.5 Peroxisomal diseases 10

1.6 A new model for the peroxisomal disorders? 12

1.7 What is *Caenorhabditis elegans*? 13

1.8 Why *C. elegans*? 16

1.9 What do we know about peroxisomes in *C. elegans*? 17

1.10 Thesis rationale 20

CHAPTER 2 **MATERIALS AND METHODS** 21

2.1 Materials 22

2.2 Methods 30

2.2.1 Purification of genomic DNA from nematodes 30

2.2.2 Purification of mRNA from nematodes 30

2.2.3 *In vitro* dsRNA synthesis 31

2.2.4 dsRNA interference 31

2.2.5 Genomic integration of the CFP-SKL expression construct 31

2.2.6 DNA sequencing 32

2.2.7 Polymerase Chain Reactions (PCR) 32

2.2.8 Digestion of DNA by restriction endonucleases 33

2.2.9 Dephosphorylation of 5' DNA ends 33

2.2.10 Gel electrophoresis of DNA fragments 33

2.2.11 Purification of DNA fragments from agarose 34

2.2.12 Ligation of DNA fragments 34

2.2.13 Preparation of anti-thiolase antibodies 34

2.2.14 Determination of protein concentration 34

2.2.15 Electrophoresis of proteins 35
2.2.16 Detection of proteins by immunoblotting 35
2.2.17 Immunofluorescence microscopy 36
2.2.18 Determination of catalase activity 36
2.2.19 Determination of lifespan 37
2.2.20 Measurement of protein carbonylation 37
2.2.21 Confocal microscopy 37
2.2.22 Computational analysis of PTS2 motifs 38
2.2.23 Isolation and sequencing of mevalonate kinase cDNA from *C. elegans* 38
2.2.24 Morphometric analysis of peroxisomes and lipid droplets 39
2.2.25 Growth synchronization 39
2.2.26 Electron microscopy 39
2.2.27 Single worm PCR 40
2.2.28 Selection of the *ctl-2* mutant 40
2.2.29 Cloning of pRS315/pgk::PTS2-GFP plasmids 41
2.2.30 *In silico* search for *C. elegans* orthologs of human peroxins and peroxisomal enzymes 41
2.2.31 Gas chromatography 42
2.2.32 Supplementation of the nematode diet with pristanic acid 43

CHAPTER 3 **THE ROLE OF *CAENORHABDITIS ELEGANS* PEROXINS AND PEROXISOMAL ENZYMES IN NEMATODE ONTOGENESIS** 44
3.1 Overview 45
3.2 *In silico* search for the *C. elegans* orthologs of human peroxins and peroxisomal enzymes 45
3.2.1 Orthologs of human peroxins 49
3.2.2 Orthologs of human peroxisomal enzymes 50
3.3 RNAi silencing of putative nematode peroxins and peroxisomal enzymes 54

3.3.1 Deficiency in most of the *C. elegans* homologs of peroxins causes a developmental delay in the worm 54
3.4 Effects of deficiency in some nematode putative peroxisomal enzymes on nematode development 57
3.5 Functional and morphological changes in nematode peroxisomes lacking subsets of peroxins and peroxisomal enzymes 59
3.5.1 Impairment of PTS1-import in functional knockouts of peroxins 61
3.5.2 Morphological abnormalities of peroxisomes in thiolase-deficient worms 61
3.6 DISCUSSION 64
3.6.1 Functions of *C. elegans* peroxins 65
3.6.2 Deficiency in *C. elegans* peroxisomal enzymes 75

CHAPTER 4 **ASPECTS OF PEROXISOMAL PROTEIN IMPORT PATHWAYS IN *CAENORHABDITIS ELEGANS*** 79
4.1 Overview 80
4.2 Search for components of the PTS2-dependent peroxisomal import pathway and PTS2-containing proteins in *C. elegans* 81
4.3 Subcellular localization of *C. elegans* mevalonate kinase and two other putative PTS2-containing proteins 83
4.4 Computational analysis of PTS2 motifs from eukaryotic genomes 88
4.5 DISCUSSION 93
4.5.1 No evidence for the PTS2-dependent import pathway in *C. elegans* 93
4.5.2 A new definition for the consensus sequence of the peroxisome targeting signal type 2 96

CHAPTER 5 **ROLE OF PEROXISOMAL CATALASE IN *CAENORHABDITIS ELEGANS* LONGEVITY** 102
5.1 Overview 103
5.2 Characterization of the catalase genes of *C. elegans* and analysis of catalase enzymatic activity in the nematode 103

5.3 Lack of peroxisomal, but not cytosolic, catalase causes a progeric phenotype in *C. elegans* 110
5.4 Cells of the *Δctl-2* mutant exhibit abnormal peroxisome morphology 112
5.5 DISCUSSION 115

CHAPTER 6 **FUNCTIONAL DISSECTION OF THE THIOLASE AND STEROL-CARRIER DOMAINS OF SCPx OF *CAENORHABDITIS ELEGANS*** 123
6.1 Overview 124
6.2 Genetic and phenotypic characterization of *C. elegans* P-44 deficiency 124
6.3 Fatty acids composition of P-44 mutant and wild-type *C. elegans* 127
6.4 DISCUSSION 140

CHAPTER 7 **PERSPECTIVES** 146
7.1 Peroxisome biogenesis and peroxisome biogenesis diseases in the nematode *C. elegans* and in humans 147
7.2 Peroxisomal import pathways in *C. elegans* 149
7.3 Nematode catalases and longevity 149
7.4 Nematode metabolism of specific classes of fatty acids 152
7.5 Is *C. elegans* a good system to model human peroxisome function? 153

CHAPTER 8 **REFERENCES** 156

APPENDIX 180

LIST OF TABLES

Table 1.3.1. Peroxins and their functions in humans and other organisms 5

Table 1.5.1. Human peroxisomal diseases 11

Table 2.1.1. List of chemicals and reagents 22

Table 2.1.2. List of enzymes 23

Table 2.1.3. Plasmids 24

Table 2.1.4. Strains 24

Table 2.1.5. Antibodies 27

Table 2.1.6. Oligonucleotides 27

Table 2.1.7. Standard media, buffers and solutions 29

Table 3.2.1. Human peroxins and their homologs in *C. elegans* 46

Table 3.2.2. Human peroxisomal enzymes and their homologs in *C. elegans* 47

Table 3.2.3. Peroxins from other organisms and their homologs in *C. elegans* 48

Table 3.3.1. ORFs targeted in RNAi experiments 55

Table 3.7.1. BLAST alignments for *H. sapiens* PEX1 vs *C. elegans* proteins 70

Table 3.7.2. BLAST alignments for *H. sapiens* PEX6 vs *C. elegans* proteins 72

Table 4.2.1. Occurrence of the PTS2 consensus sequence in peroxisomal proteins across different eukaryotes 82

Table 4.4.1. Sequences of functional PTS2 motifs 92

Table 4.5.1. Comparison of PTS2 sequences of MeKs from different eukaryotes 94

Table 4.5.2. List of PTS2 sequences and their variants tested for their functionality in importing proteins into peroxisomes 98

Table 5.2.1. Three genes encode catalases in *C. elegans* 108

Table 5.2.2. Lifespan, catalase activity and egg laying in *C. elegans* mutants 108

Table 6.3.1. Structure of some fatty acids and their derivatives 134

LIST OF FIGURES

Figure 1.3.1. Role of peroxins in peroxisome biogenesis and maintenance 7
Figure 1.7.1. Life cycle of the nematode *C. elegans* at 25°C 15
Figure 2.1.1. Maps of plasmid vectors used for expression in mammalian cells, *C. elegans*, *S. cerevisiae* and *E. coli* 25
Figure 3.3.1. Percentages of adults in the offspring, and phenotypes of F1 progeny, of worms injected with dsRNAs to target genes encoding various peroxisomal enzymes of lipid metabolism and peroxins 56
Figure 3.3.2. RNAi reduction of the levels of the type 2 thiolase P44 58
Figure 3.5.1. Localization of CFP-SKL in various nematode cells using direct fluorescence and immunofluorescence microscopy 60
Figure 3.5.2. Effect of RNAi on the subcellular localization of the peroxisomal marker CFP-SKL 62
Figure 3.5.3. The size and morphology of peroxisomes in worms injected with dsRNA to Pex12p or to P-44 (type 2 peroxisomal thiolase). 63
Figure 3.7.1. Peroxisomal metabolic pathways and peroxins involved in the development of *C. elegans* 66
Figure 3.7.2. Characteristic phenotypes of dsRNA$_{Pex1p}$- and dsRNA$_{Pex6p}$-injected worms 69
Figure 3.7.3. Alignment of *pmp* cDNAs 76
Figure 4.3.1. Gene structure and cDNA sequence for *C. elegans* mevalonate kinase 84
Figure 4.3.2. Subcellular localization of chimeras of *Ce*MeK and GFP 85
Figure 4.3.3. Subcellular localization of two putative PTS2-containing proteins of *C. elegans* 85
Figure 4.3.4. The putative PTS2s of the proteins encoded by the ORFs W10G11.11 and D1053.2 do not function in targeting to peroxisomes in cells from other organisms with functional PTS2 targeting systems 87

Figure 4.4.1. Distribution and composition of PTS2 motifs 89

Figure 4.4.2. Distribution and amino acid composition of PTS2 motifs with consensus –(R/K)(L/V/I)X_5(H/Q)(L/A)– in peroxisomal proteins 90

Figure 5.2.1. Structure of the *ctl* locus in the *C. elegans* genome 104

Figure 5.2.2. Detection of the deletions of catalase genes 105

Figure 5.2.3. Multiple alignment of *C. elegans* catalase genes 106

Figure 5.2.4. Activity of catalases in *C. elegans* 109

Figure 5.3.1. Effects of mutation of the *ctl-1* and *ctl-2* genes on lifespan and egg laying capacity of wild-type and *Δclk-1* mutant worms 111

Figure 5.3.2. Carbonylation levels of the major proteins of wild-type and catalase mutant worms 111

Figure 5.4.1. Cells of *Δctl-2* mutant worms contain enlarged peroxisomes but lipid droplets of normal size 113

Figure 5.4.2. Peroxisomes exhibit altered morphology in *Δctl-2* mutant worms 114

Figure 5.4.3. Gas Chromatography spectra of methyl esters of fatty acids derived from the *C.elegans* wild-type (N2) and catalase mutant (Δ*ctl-1*, Δ*ctl-2*) worms 116

Figure 5.5.1. Reporter GFP expression from the *ctl-3* gene promoter 119

Figure 5.5.2. Survival of *S. cerevisiae* wild-type (WT) and mutant strains lacking cytosolic (Δ*ctt1*) or peroxisomal (Δ*cta1*) catalase 119

Figure 6.2.1. Alignment of human SCPx and *C. elegans* homologs 125

Figure 6.2.2. Molecular and phenotypic features of thiolase type I deficiency in the *Δp-44* mutant strain RB859 126

Figure 6.2.3. Egg laying in wild-type and P-44 mutant worms 128

Figure 6.2.4. Electron microscopy of peroxisomes in P-44 mutant worms 129

Figure 6.3.1. Gas chromatogram of total lipids derived from *C. elegans* wild-type (N2) and P-44 mutant worms fed *E. coli* OP50 131

Figure 6.3.2. Gas chromatogram of methyl esters of fatty acids extracted from *E. coli* OP50 132

Figure 6.3.3. Gas chromatogram of lipids extracted from wild-type worms fed *E. coli* OP50 133

Figure 6.3.4. Gas chromatogram of methyl esters of fatty acids derived from *C. elegans* wild-type (N2) and P-44 mutant worms fed pristanic acid 136
Figure 6.3.5. Ion impact mass spectra of phytanic, pristanic, and TMTD acids 137
Figure 6.3.6. Comparison of ion impact mass spectra obtained from an unknown C15 fatty acid and the cycplopropane-containing fatty acids C17Δ and C19Δ 138
Figure 6.3.7. Gas chromatogram of methyl esters of fatty acids extracted from wild-type worms fed *E. coli* strains OP50 and FT17 139
Figure 6.3.8. Gas chromatogram of methyl esters of fatty acids derived from *C. elegans* wild-type (N2) and fat-2 mutant worms fed with pristanic acid 141
Figure 6.4.1. Catabolism of phytanic acid in humans 142
Figure A1. Gas chromatogram spectra of the standard lipid mixture ST1 and of lipids extracted from wild-type worms fed *E. coli* OP50
Figure A2. Gas chromatogram spectra of the standard lipid mixture ST2 and of lipids extracted from wild-type worms fed *E. coli* OP50
Figure A3. Gas chromatogram spectra of the standard lipid mixture ST3 and of lipids extracted from wild-type worms fed *E. coli* OP50
Figure A4. Gas chromatogram spectra of the standard lipid mixture ST4 and of lipids extracted from wild-type worms fed *E. coli* OP50
Figure A5. Gas chromatogram spectra of the standard lipid mixture ST5 and of lipids extracted from wild-type worms fed *E. coli* OP50

LIST OF SYMBOLS AND ABBREVIATIONS

°C	degrees Celsius
ADHAPS	alkyldihydroxyacetonephosphate synthase
ALDP	adrenoleukodystrophy related protein
APS	ammonium persulfate
ATPase	adenosine triphosphatase
bp	base pair
BSA	bovine serum albumin
*Ce*MeK	*C. elegans* mevalonate kinase
CFP	cyan fluorescent protein
CIAP	calf intestinal alkaline phosphatase
CSM	complete supplement mixture
D	dalton
DHAP	dihydroxyacetonephosphate
dNTP	deoxyribonucleoside triphosphate
dsRNA	double-stranded RNA
DTT	dithiothreitol
ECL	enhanced chemiluminescence
EDTA	ethylenediaminetetraacetic acid
EMS	ethyl methane sulfonate
ER	endoplasmic reticulum
FATP2	fatty acid transporter protein 2
GC	gas chromatography
GFP	green fluorescent protein
*Hs*MeK	*Homo sapiens* mevalonate kinase
IPTG	isopropyl β-D-thiogalactopyranoside
IRD	infantile Refsum disease
J	Joule
LCFAs	long-chain fatty acids
LDL	low density lipoprotein
MBP	maltose-binding protein
MS	mass spectrometry
NALD	neonatal adrenoleukodystrophy
NCBI	National Center for Biotechnology Information
OMIM	Online Mendelian Inheritance in Man[1]
ORF	open reading frame
PAHX	phytanoyl-CoA 2-hydroxylase
PCR	polymerase chain reaction
PEX#	gene required for peroxisome biogenesis and maintenance
Pex#p	protein required for peroxisome biogenesis and maintenance
PGK1	phosphoglycerate kinase 1
PhyH	phytanoyl-CoA 2-hydroxylase
PMP	peroxisomal membrane protein
PMSF	phenylmethylsulfonylfluoride

---

[1] http://www.ncbi.nlm.nih.gov/entrez/query.fcgi?db=OMIM

pTH1	peroxisomal thiolase 1
pTH2	peroxisomal thiolase 2
PTS	peroxisomal targeting signal
RCDP	rhizomelic chondrodysplasia punctata
RNAi	RNA interference
ROS	reactive oxygen species
SCPx	sterol carrier protein x
SDS	sodium dodecyl sulfate
SDS-PAGE	sodium dodecyl sulfate-polyacrylamide gel electrophoresis
SOD	superoxide dismutase
ssRNA	single-stranded RNA
TEMED	*N,N,N',N'*-tetramethylethylenediamine
TPR	tetratricopeptide repeat
UV	ultraviolet
v	volume
VLCFA	very-long chain fatty acid
VLCFAS	very-long chain fatty acids synthetase
w	weight
X-ALD	X-linked adrenoleukodystrophy
X-gal	5-bromo-4-chloro-3-indolyl-β-D-galactoside
YNB	yeast nitrogen base
ZS	Zellweger cerebro-hepato-renal syndrome

CHAPTER 1

INTRODUCTION

1.1 What are peroxisomes?

Contemporary textbooks give us the following classical definitions of peroxisomes: "small vesicular compartments that contain enzymes utilized in a variety of oxidative reactions" (Alberts *et al.*, 2002); "containers for enzymes involved in oxidative reactions" (Pollard and Earnshaw, 2002); "Peroxisomes contain at least 50 different enzymes, which are involved in a variety of biochemical pathways in different types of cells" (Cooper, 2000). Since the time when peroxisomes were first found and described in mouse kidney (Rhodin, 1954), and later also discovered in plants (Porter and Kaulfield, 1958), thousands of scientific papers have been published on the topic, and our understanding of peroxisomal functions and biogenesis has progressed significantly (Titorenko and Rachubinski, 2001b). Interest in understanding peroxisomes is explained by findings showing peroxisomes are involved in a great variety of important cellular functions and are associated with a number of severe human diseases (Wanders *et al.*, 2001).

1.2 Biochemical roles of peroxisomes

Microbodies, the class of subcellular compartments that includes the peroxisomes, the glyoxysomes of plants, the glycosomes of Trypanosomes and Woronin bodies in some fungi, are found in virtually all eukaryotic cells (Purdue and Lazarow, 2001). Microbodies have similar enzymatic properties, with some variations in their metabolic pathways depending on the type of tissue or cell (Tolbert and Essner, 1981). This work is focused on peroxisomes - microbodies of eukaryotes from yeasts to metazoans, including mammals.

Peroxisomes are known to carry out α- and β-oxidation of fatty acids and the decomposition of hydrogen peroxide. Depending on the cell type, peroxisomes also take part in the biosynthesis of plasmalogens, cholesterol and bile acids, polyunsaturated fatty acids (in metazoans), penicillin (in fungi), and lysine (in yeasts). Peroxisomes also compartmentalize the catabolism of amino acids, purines, polyamines and prostaglandins (in metazoans); the glyoxylate cycle (in fungi and yeasts); and methanol, ethanol and amine oxidation (in yeasts) (Lazarow and Moser, 1989; Purdue and Lazarow, 2001; Titorenko and Rachubinski, 2001a). In addition, peroxisomes take part in respiration. They consume oxygen while catabolizing different classes of fatty acids (Tolbert and Essner, 1981).

The majority of all biochemical reactions happening in peroxisomes are catalyzed by enzymes located in the peroxisomal matrix. Due to their high concentration, some enzymes (*e.g.*, urate oxidase) can form a crystal core within the organelle (Tolbert and Essner, 1981). All peroxisomal proteins are encoded by nuclear genes and synthesized in the cytosol (Titorenko and Rachubinski, 2001b). The peroxisomal matrix is surrounded by a single, semi-permeable membrane.

Morphologically, peroxisomes are very diverse. In rat liver, their shapes range from multiple isolated round vesicles to a single convoluted compartment consisting of a cup-shaped structure and torturously branched tubules (Purdue and Lazarow, 2001) or tubulo-reticular clusters (Schrader, 2001). Peroxisomes range in size from 0.1 to 1.5 μm (Tolbert and Essner, 1981). The number, size, protein composition and even the shapes of peroxisomes vary not only depending on the organism and cell type but also on environmental conditions (Titorenko and Rachubinski, 2001a).

1.3 PEX genes and biogenesis of peroxisomes

In all organisms studied, as many as 32 different proteins that control peroxisome biogenesis and maintenance, called PEXes, are found (Table 1.3.1). In humans, there are 14 such proteins identified and designated as Pex1p, Pex2p, Pex3p, Pex5p, Pex6p, Pex7p, Pex10p, Pex11p, Pex12p, Pex13p, Pex14p, Pex16p, Pex19p and Pex26p (shaded in gray in Table 1.3.1). At least 13 of these genes, when mutated, cause lethal peroxisome biogenesis disorders in humans (Shimozawa *et al.*, 2004; Section 1.4).

PEX genes encode proteins belonging to various functional classes, including shuttling receptors, integral membrane proteins and ATPases (Fig. 1.3.1). The best studied PEX proteins are the receptors for peroxisomal protein import, Pex5p (Terlecky *et al.*, 1995) and Pex7p (Marzioch *et al.*, 1994). Both receptors are located in the cytosol when unbound by their cargo. They specifically recognize and bind proteins carrying peroxisome targeting signals (PTS). To date, PTS1 (recognized by Pex5p) and PTS2 (recognized by Pex7p) are the best defined (Rachubinski and Subramani, 1995). Another putative cytosolic receptor for peroxisomal proteins is Pex19p. Pex19p is able to recognize and bind the membrane PTS1 (mPTS1) motif found in peroxisomal membrane proteins such as Pex11p, Pex14p and PMP70 (Titorenko and Rachubinski, 2001b). The initial docking site for both the Pex5p-PTS1 and Pex7p-PTS2 complexes at the cytosolic surface of the peroxisomal membrane consists of two membrane-associated peroxins, Pex13p and Pex14p (Sacksteder and Gould, 2000; Titorenko and Rachubinski, 2001b; Fig. 1.3.1). After docking, the PTS1 and PTS2 receptors, together with their cargoes, are transferred to other membrane-associated components of the import machinery consisting of the peroxins Pex2p, Pex10p and Pex12p (Hettema *et al.*, 1999; Terlecky and Fransen, 2000). These

Table 1.3.1. Peroxins and their functions in humans and other organisms

Peroxin[1]	Function in humans or other organism	*Sp*[2]
Pex1p	Putative AAA-ATPase. Interacts with Pex6p and is required for peroxisomal protein import. Mutations are detected in patients with Zellweger syndrome, neonatal adrenoleukodystrophy, and infantile Refsum disease	***Hs*** ***Mm*** ***Sc*** ***Ca***
Pex2p	Peroxisomal membrane protein 3. Involved in protein-peroxisome targeting and peroxisome biogenesis. Increased expression may be therapeutic for Zellweger syndrome	***Hs*** ***Mm*** ***Sc***
Pex3p	A peroxisomal protein required for the early stages of peroxisomal biogenesis. Mutations in the corresponding gene cause Zellweger syndrome. Docking factor for Pex19p	***Hs*** ***Mm*** ***Rn*** ***Sc*** ***Ca***
Pex4p	Ubiquitin-conjugating enzyme required for peroxisomal biogenesis	***Sc*** ***Pa*** ***Ca***
Pex5p	Peroxisome receptor 1. Targets proteins to the peroxisome via PTS1 signal recognition. Mutations cause neonatal adrenoleukodystrophy, Zellweger syndrome, and infantile Refsum disease	***Hs*** ***Mm*** ***Sc*** ***Sp*** ***Ca***
Pex6p	Peroxisome assembly factor 2. AAA-ATPase family member that interacts with Pex1p and is involved in peroxisomal protein import and peroxisome assembly. Mutations correlate with peroxisome biogenesis disorders and complementation group C Zellweger syndrome	***Hs*** ***Mm*** ***Rn*** ***Sc***
Pex7p	Peroxisome receptor 2. A peroxisomal import receptor for proteins containing peroxisomal targeting signal 2 (PTS2). Mutations in the *PEX7* gene cause rhizomelic chondrodysplasia puncta	***Hs*** ***Mm*** ***Sc*** ***Sp*** ***Ca***
Pex8p	Peroxin involved in protein import into peroxisomes	***Sc***
Pex9p	Peroxin involved in protein import and peroxisome enlargement	***Yl***
Pex10p	Peroxin has a C3HC4 zinc finger RING motif. Interacts with Pex12p. Required for the import of peroxisomal matrix proteins. Mutation is detected in patients with Zellweger syndrome and neonatal adrenoleukodystrophy. Involved in the import of tryptophanyl (W) tRNA synthetase predicted to be mitochondrial	***Hs*** ***Sc***
Pex11p	Peroxisomal biogenesis factor 11α. May regulate peroxisome abundance in response to external stimuli. May recruit ADP-ribosylation factor (ARF) and coatomer. May mediate peroxisome biogenesis from existing peroxisomes	***Hs*** ***Mm*** ***Rn*** ***Sp*** ***Sc***
	Peroxisomal biogenesis factor 11β. A peroxisomal integral membrane protein that is involved in regulating peroxisome proliferation and abundance through a multistep process	***Hs*** ***Mm*** ***Rn*** ***Ca***
	Peroxisomal biogenesis factor 11γ. A putative integral peroxisomal membrane protein that may function in peroxisome division or homeostasis	***Hs*** ***Mm*** ***Rn***
Pex12p	An integral peroxisomal membrane protein that interacts with Pex5p and Pex10p and acts in peroxisomal matrix protein import downstream of receptor docking. Mutations in the zinc ring domain result in Zellweger syndrome	***Hs*** ***Mm*** ***Rn*** ***Sc***
Pex13p	A peroxisomal membrane protein. Acts in peroxisomal matrix protein import, receptor docking, and biogenesis. Deficiency is associated with peroxisome biogenesis disorder complementation group H	***Hs*** ***Mm*** ***Sc*** ***Ca***

---

[1] Human peroxins are shaded in gray.

[2] ***Sp****, species;* ***Hs****, Homo sapiens;* ***Mm****, Mus musculus;* ***Rn****, Rattus norvegicus;* ***Ca****, Candida albicans;* ***Sc****, Saccharomyces cerevisiae;* ***Sp****, Schizosaccharomyces pombe;* ***Yl****, Yarrowia lipolytica;* ***Pp****, Pichia pastoris;* ***Nc****, Neurospora crassa.*

Pex14p	A peroxisomal membrane protein that provides a docking target for Pex5p and is required for peroxisomal import of PTS1- and PTS2-containing proteins, altered expression is associated with neuroblastoma	*Hs* *Mm* *Rn* *Ca*
Pex15p	Peroxisomal integral membrane protein required for peroxisome assembly. Promotes peroxisomal membrane association of Pex6p	*Sc*
Pex16p	Peroxisomal integral membrane protein involved in the initial stages of peroxisomal membrane formation during peroxisomal biogenesis. Mutations cause Zellweger syndrome of the complementation group IX	*Hs* *Mm*
Pex17p	Peroxisomal peripheral membrane protein required for peroxisome biogenesis	*Sc* *Pp* *Ca*
Pex18p	Peroxin involved with Pex21p in Pex7p-mediated peroxisomal protein targeting	*Sc*
Pex19p	Peroxisomal farnesylated protein. Binds several peroxisomal membrane proteins (PMP). Involved in early stages of PMP import and peroxisomal biogenesis. Deficiency is associated with Zellweger syndrome complementation group J	*Hs* *Mm* *Sc* *Ca*
Pex20p	Peroxin that functions together with Pex7p in PTS2-dependent protein import	*Nc*
Pex21p	Peroxin involved with Pex18p in Pex7p-mediated peroxisomal protein targeting. Enhances the seryl-tRNA aminoacylation activity of seryl-tRNA synthetase (Ses1p) *in vitro*	*Sc*
Pex22p	Peroxisomal matrix protein import	*Sc* *Pp*
Pex23p	Peroxin required for the import of matrix proteins	*Yl*
Pex24p	Peroxin. Integral peroxisomal membrane protein	*Yl*
Pex25p	Peroxisomal membrane-associated protein involved in peroxisome biogenesis and peroxisomal protein import. Required for regulation of peroxisome size and maintenance	*Sc*
Pex26p	Peroxisomal membrane protein. Recruits the Pex1p-Pex6p AAA-ATPase complexes to peroxisomes. Binds Pex6p. Loss of function mutation correlates with peroxisome biogenesis disorder CG8 (CG-A)	*Hs*
Pex27p	Protein involved in regulating peroxisome size and number	*Sc*
Pex28p	Integral peroxisomal membrane protein required for normal peroxisome morphology and distribution	*Sc*
Pex29p	Integral peroxisomal membrane protein required for normal peroxisome morphology and distribution	*Sc*
Pex30p	Integral peroxisomal membrane protein. Functions as a negative regulator of peroxisome size	*Sc*
Pex31p	Integral peroxisomal membrane protein. Functions as a negative regulator of peroxisome size	*Sc*
Pex32p	Integral peroxisomal membrane protein. Functions as a negative regulator of peroxisome size	*Sc*

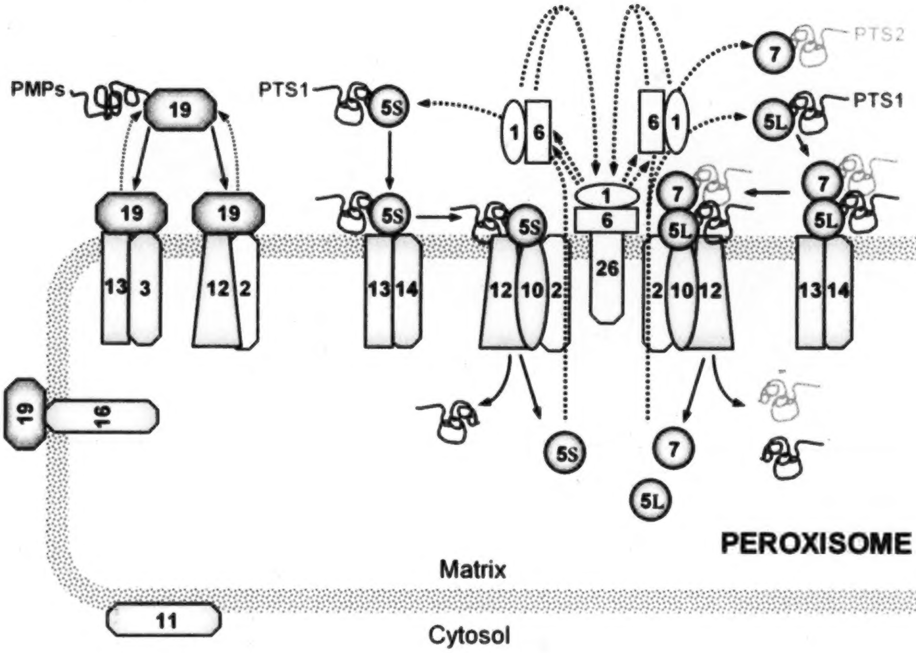
PMPs
19
PTS1
5S
1
6
PTS2
7
5L
13
3
12
2
14
10
26
16
11
PEROXISOME
Matrix
Cytosol

Figure 1.3.1. Role of peroxins in peroxisome biogenesis and maintenance. The designated peroxins Pex1p (**1**), Pex2p (**2**), Pex3p (**3**), Pex5p (**5**) (L, long form, S, short), Pex6p (**6**), Pex7p (**7**), Pex10p (**10**), Pex11p (**11**), Pex12p (**12**), Pex13p (**13**), Pex14p (**14**), Pex19p (**19**) and Pex26p (**26**) act in the following processes: membrane protein targeting, insertion and assembly (green); matrix protein docking and translocation (pink); matrix protein import by PTS1 and PTS2 receptors (blue and orange, respectively); recycling of the PTS1 receptor (yellow).

components function in the translocation of cargo proteins, either alone or together with their receptors, across the peroxisomal membrane into the peroxisomal matrix (Fujiki, 2000; Subramani *et al.*, 2000). In human cells, Pex2p, together with two cytosolic peroxins, Pex1p and Pex6p, may act to recycle the PTS1 receptor to the cytosol (Fujiki, 2000; Gould and Valle, 2000; Sacksteder and Gould, 2000). In humans, alternative splicing of the *pex5* gene results in the generation of the short (Pex5pS), and long (Pex5pL) forms of the PTS1 receptor. Whereas Pex5pS is implicated in PTS1 import only, Pex5pL is also involved in PTS2 import, acting in a complex with Pex7p (Braverman *et al.*, 1998; Titorenko and Rachubinski, 2001b). The peroxin Pex16p, together with Pex3p, is an integral peroxisomal membrane protein that is inserted into the lipid bilayer upon binding to Pex19p (Sacksteder *et al.*, 2000). This step seems to be required for the subsequent targeting of other peroxisomal membrane proteins in a Pex19p-dependent manner (Gould and Valle, 2000; Titorenko and Rachubinski, 2001b). The recently discovered peroxin Pex26p recruits the Pex1p-Pex6p AAA-ATPase complexes to peroxisomes via its binding to Pex6p (Matsumoto, *et al.*, 2003). Finally, to maintain a stable population of peroxisomes in the dividing cell or proliferating tissue, effective control of peroxisome number is necessary. Pex11p, and its functional homologs Pex25p and Pex27p, are thought to be positive regulators of peroxisome division in the yeast *Saccharomyces cerevisiae* (Erdmann and Blobel, 1995; Smith *et al.*, 2002; Tam *et al.*, 2003; Rottensteiner *et al.*, 2003). In humans three isoforms of Pex11p, α, β, and γ are known to exist (Schrader *et al.*, 1998; Tanaka *et al.*, 2003), but their individual roles remain unknown.

1.4 Peroxisome targeting signals

Chapter 4 of this work describes an analysis of specific protein motifs that constitute signals recognized by peroxisomal receptors. Therefore, it is necessary to give some introduction to this issue. PTSs are distinct and conserved among eukaryotes (de Hoop and AB, 1992; Blattner *et al.*, 1995). Interestingly, even viral proteins have been found to be imported into peroxisomes and to use targeting signals identical to eukaryotic PTSs (Mohan and Atreya, 2003). The majority of peroxisomal matrix proteins are targeted by PTS1. PTS1 is a carboxyl-terminal tripeptide with the consensus sequence –(S/C/A)(K/R/H)(L/M) (Subramani, 1993). The efficiency of various tripeptides to function as PTS1s can be enhanced by adjacent "accessory" sequences (Purdue *et al.*, 1996; Mullen *et al.*, 1997; Mizuno *et al.*, 2002; Klein *et al.*, 2002). SKL has been found to be the most effective PTS1, and it functions in most organisms (Swinkels *et al.*, 1992). A recent re-evaluation of the PTS1 motif (Neuberger *et al.*, 2003a) found that the PTS1 signal is comprised of the 12 carboxyl-terminal residues of the targeted protein. The peroxin Pex5p that mediates PTS1-dependent transport is a shuttling receptor. After recognition and delivery of the cargo across the peroxisomal membrane, Pex5p is recycled to the cytosol. Dysfunctional Pex5p has been shown to cause the human peroxisome biogenesis disorder, Zellweger syndrome (Wanders, 1999; Gould and Valle, 2000). A small subset of peroxisomal matrix proteins is targeted by PTS2. The PTS2 is located at the amino terminus of proteins at variable distances from the initiating methionine. The amino terminus of a PTS2-containing protein is sometimes cleaved from the protein molecule inside the peroxisome by a specific protease (de Hoop and AB, 1992). The consensus PTS2 was first defined as a nonapeptide with the sequence –RLX$_5$(H/Q)L– (de

Hoop and AB, 1992), which was later modified to –(R/K)(L/V/I)X_5(H/Q)(L/A)– (Rachubinski and Subramani, 1995). Defective PTS2-dependent import results in the peroxisome biogenesis disorder, rhizomelic chondrodysplasia punctata (Wanders, 1999; Gould and Valle, 2000).

Some peroxisomal matrix proteins contain neither an apparent PTS1 nor a PTS2 but instead have internal targeting signals, sometimes called PTS3, which remain poorly defined (Kragler *et al.*, 1993; Elgersma *et al.*, 1995). Often these proteins use the PTS1-dependent targeting machinery for their import into peroxisomes (Elgersma *et al.*, 1995). Similarly, a peroxisomal membrane targeting signal, mPTS1 is not well defined, but two of the reported consensus sequences for the mPTS1 are (K/R)(K/R)X_{3-7}(T/S)X_2(D/E) and (Y)X_3(L)X_3(K/Q/N) (Titorenko and Rachubinski, 2001b).

1.5 Peroxisomal diseases

Every biological system or process that plays an important or indispensable role in the functioning of the organism is prone to malfunctions. This is also true for peroxisomes. Loss of some metabolic function or complete absence of these organelles in humans gives rise to severe polysymptomatic syndromes. Two classes of peroxisomal disorders are defined. Mutations that affect PEX genes are the recognized causes of the peroxisome biogenesis disorders (Lazarow and Moser, 1989; Gould and Valle, 2000). This class encompasses such syndromes as Zellweger cerebro-hepato-renal syndrome (ZS), neonatal adrenoleukodystrophy (NALD), infantile Refsum disease (IRD), and rhizomelic chondrodysplasia punctata (RCDP) (Table 1.5.1). The common symptoms for these diseases are the neurodegeneration and improper axon migration, cognitive and

Table 1.5.1. Human peroxisomal diseases

Peroxisome biogenesis disorders (PBDs)		
Syndrome	**OMIM #**	**Abbreviation**
Zellweger syndrome	214100	ZS
Neonatal adrenoleykodystrophy	202370	NALD
Infantile Refsum disease	266510	IRD
Rhizomelic chondrodysplasia punctata Type 1	215100	RCDP1

Peroxisome single enzyme diseases		
Enzyme	**Phenotype**	**Reference**
acyl-CoA oxidase	ZS, NALD, IRD	Poll-Thé *et al.*, 1988
L-bifunctional enzyme	ZS, NALD, IRD	
D-bifunctional enzyme		van Grunsven *et al.*, 1999
alkyl-DHAP synthase	ZS	Datta *et al.*, 1984
DHAP acyl trasferase	ZS	
catalase	acatalasemia	Ogata, 1991
phytanoyl-CoA hydroxylase	Refsum disease	Jansen *et al.*, 1997; Mihalick *et al.*, 1997
α-methylacyl-CoA racemase	NALD, Refsum disease	Ferdinandusse *et al.*, 2000
ALDP	X-linked ALD	Mosser *et al.*, 1993

Complementation groups of the PBDs			
PBD group		**Affected gene**	**Phenotypes**
1	E*	PEX1	ZS, NALD, IRD
2		PEX5	ZS, NALD, IRD
3		PEX12	ZS, NALD, IRD
4	C	PEX6	ZS, NALD
7	B	PEX10	ZS, NALD
8	A	PEX26	ZS, NALD, IRD
9	D	PEX16	ZS
10	F	PEX2	ZS, IRD
11	R	PEX7	RCDP
12	G	PEX3	ZS
13	H	PEX13	ZS, NALD
14	J	PEX19	ZS
	K	PEX14	ZS

*complementation grouping of Gifu University School of Medicine (Shimozawa *et al.*, 2004) motor dysfunction, retinopathy, sensorineural hearing impairment and hepatic involvement.

The second class of peroxisomal disorders encompasses single enzyme disorders that result from a deficiency of an enzyme in the peroxisome (Table 1.5.1) (Powers and Moser, 1998; Fijiki, 2000; Gould and Valle, 2000). This class includes deficiencies of peroxisomal acyl-CoA oxidase, D-bifunctional enzyme and L-bifunctional enzyme, alkyl-dihydroxyacetonephosphate (ADHAP) synthase and DHAP acyl transferase, catalase, phytanoyl-CoA hydroxylase, α-methylacyl-CoA racemase, and adrenoleukodystrophy protein (ALDP) (a peroxisomal transporter of the ATP-binding cassette (ABC) transporter superfamily).

The pattern of inheritance of peroxisomal diseases is compatible with an autosomal recessive mode of inheritance (for ZS and NALD) or an X-linked mode of inheritance (ALDP deficiency). The frequency of disorders is estimated at 1:25 000 to 1:50 000 (Lazarow and Moser, 1989). The treatment of peroxisomal diseases is limited by the multiple malformations and defects that arise during human embryogenesis. Some dietary approaches are used for patients with milder forms of the disorders to compensate for a loss of metabolic functions (McGuinness *et al.*, 2000).

1.6 A new model for the peroxisomal disorders?

To date, the machinery for peroxisome biogenesis and maintenance has been studied most extensively in yeasts and cultured human cells (Lazarow and Fujiki, 1985; Titorenko and Rachubinski, 2001). However, clinical data show that peroxisomal deficiencies manifest themselves at the level of the organism rather than of the single cell.

Degeneration of neuronal connectivity observed in the brains of patients with peroxisomal disorders may well be caused by the absence of peroxisomes in glial cells, as well as in the neurons themselves (Lazarow and Moser, 1989). A model multicellular organism rather than a model unicellular system is therefore preferable for studying the physiological effects of the peroxisomal disorders. A model multicellular organism also provides the possibility of differentiating the physiological roles of peroxisomes in different organs and of studying the tissue specificities of peroxisome-related processes. A requirement for a model multicellular organism for the peroxisome disorders is the possession of a nervous system, as this is the system primarily affected in patients with peroxisome disorders. Accessibility to genetic manipulation and the extent of knowledge available for the organism are also important factors for selecting a model organism for research. This thesis attempts to analyze systematically the benefits and drawbacks of the nematode *Caenorhabditis elegans* as a model organism for peroxisome-related research and, in partiuclar, for the peroxisome disorders.

1.7 What is *Caenorhabditis elegans*?

C. elegans is a rhabditid nematode (Blaxter, 1998). Nematodes are a group of metazoan organisms that encompasses at least 20,000 described species including numerous parasites of plants and animals. Among the human parasites are the large gut roundworm *Ascaris lumbricoides*, the blood-sucking human hookworms, and the pork trichina worm. *C. elegans* is a small (approximately 1 mm in length), non-parasitic, free-living nematode found in soil across most of the temperature regions of the world (Hope, 1999). For development, *C. elegans* requires only a humid environment, ambient temperature, atmospheric oxygen, and bacteria as food. Under laboratory conditions, *C. elegans* is maintained on agar plates seeded with the slowly growing *Escherichia coli* strain, OP50 (Stiernagle, 1999). Media must be supplemented with cholesterol, which *C. elegans* cannot synthesize (Kurzchalia and Ward, 2003). The optimal temperature for the maintenance of *C. elegans* is between 16°C and 25°C. *C. elegans* ontogenesis starts in the egg. The development of the nematode to the adult stage requires 3 days at 25°C (Lewis and Fleming, 1995). During this time, worms undergo several postembryonic molts (without metamorphosis) called larval stages L1, L2, L3 and L4 (Fig. 1.7.1). After reaching adult stage, *C. elegans* lays eggs for the first 3 to 4 days. The mean lifespan of *C. elegans* is approximately two weeks. In the absence of food or during overcrowding, L2 nematodes can transform into special dauer larvae (Riddle, 1988). During this developmental stage, the nematode does not feed and can survive for several months. Three to four hours after dauers are presented with food, they resume feeding and reach the L4 stage after 8 hours (Lewis and Fleming, 1995).

C. elegans has two sexes: self-fertilized XX hermaphrodites and XO males that differ in the arrangement of the gonad and in tail shape. The ratio between XX hermaphrodites and XO males in a wild-type population is 500:1 or greater. The shape of animals does not change markedly in stages L1 through L3, and therefore they are monitored mainly by characteristic cell divisions. The entire cell lineage of *C. elegans* is known (Sulston *et al.*, 1983). During postembryonic development, the number of somatic cells increases from 558 (hermaphrodite) or 560 (male) cells in the L1 stage to 959 (hermaphrodite) or 1031 (male) cells in adult worms (Lewis and Fleming, 1995). Almost one-third (302) of the hermaphrodite's cells are nerve cells (White *et al.*, 1986). The male

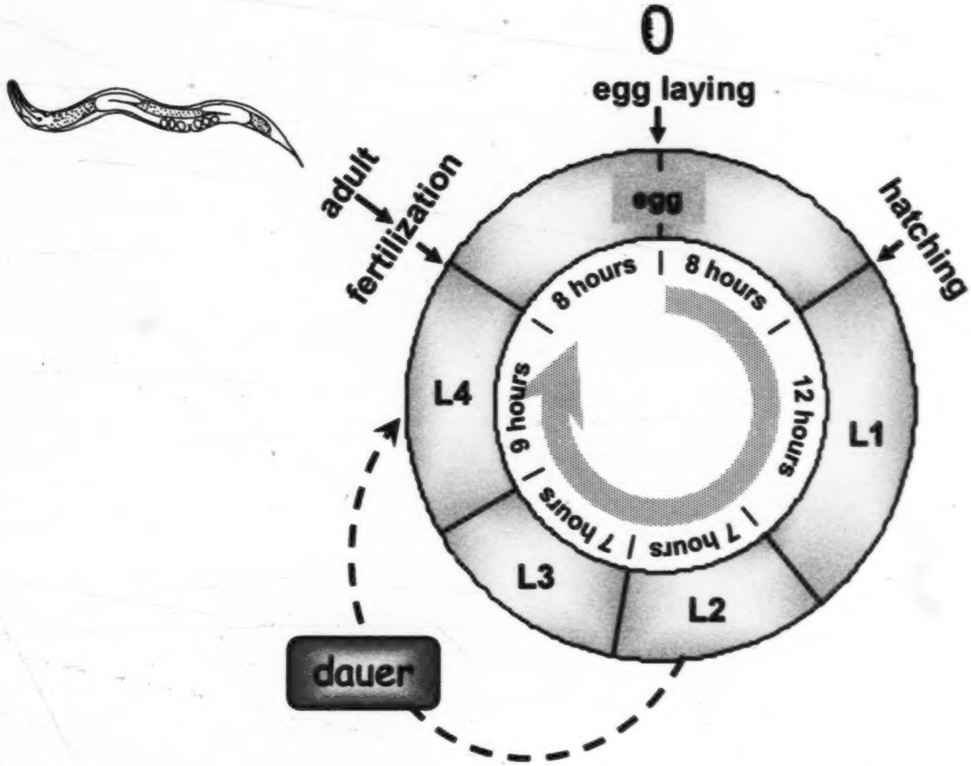
egg laying
adult
fertilization
hatching
egg
8 hours
8 hours
12 hours
7 hours
7 hours
9 hours
L1
L2
L3
L4
dauer

Figure 1.7.1. Life cycle of the nematode *C. elegans* at 25°C. Duration of larval stages (L1-L4) is presented. After fertilization, the egg remains in the nematode body for 8 hours before being laid. It takes a further 8 hours for the laid eggs to hatch. In starved populations, nematodes can enter the alternative dauer stage.

has an additional 79 neurons. *C. elegans* can sense temperature, mechanical stimuli and a wide range of chemical stimuli (Hope, 1999).

The genome of *C. elegans* is completely sequenced (The *C. elegans* Sequencing Consortium, 1998), and some 20,000 genes have been identified (Kim *et al.*, 2001). About 40% of these genes have apparent homologs in humans (Sternberg, 2001). Almost all functional domains of human proteins are present in the worm.

These features make *C. elegans* an attractive model organism with which to study aspects of peroxisome function in metazoans.

1.8 Why *C. elegans*?

Why not continue studying peroxisomes using yeast, cultured fibroblasts or the plant *Arabidopsis* as model organisms? Although the clinical phenotypes of the various peroxisomal disorders (Moser, 1999) and some aspects of peroxisome biogenesis in cultured fibroblasts of PBD patients (Gould and Valle, 2000) and yeasts (Purdue and Lazarow, 2001) are well studied, the importance of peroxisomes in the normal development of a multicellular organism remains largely unknown. *Arabidopsis* simply stands too far from humans on the evolutionary tree, and it does not have neuronal tissue. From this perspective, the metazoan *C. elegans* provides several important advantages as a model system. First, *C. elegans* is a genetically tractable multicellular organism with a sequenced genome and a well studied lifecycle (Blaxter, 1998; Hope, 2001; Sternberg, 2001). Second, *C. elegans* has a relatively simple multicellular organization (Lewis and Fleming 1995; Hope 1999). The pedigrees of cells have been established from the egg to the adult stage of the organism (Huang and Sternberg 1995; Hope 1999), and individual cells can be followed as they divide, migrate, differentiate, and die in the embryo. Moreover, the transparent cuticle of the worm permits the visualization of all cells, fluorescently tagged proteins and vital dyes within the living organism (Koushika and Nonet, 2000). Third, since the cell lineage, location, and synaptic connectivity of neurons during development of the *C. elegans* nervous system have been completely described (Blaxter 1998; Thomas and Lockery 1999), the nematode should prove extremely useful in the analysis of the molecular basis underlying the impaired neuronal development and neurodegeneration observed in patients with peroxisomal disorders (Wanders and Tager, 1998; Wanders, 1999; Sacksteder and Gould, 2000; Wanders *et al.*, 2001). Lastly, although studies with cultured human fibroblasts have opened up the option for pre- or postnatal diagnosis of peroxisomal disorders (Wanders *et al.*, 1996), they have not yet provided any prospect for therapeutic treatment of these disorders. In contrast, *C. elegans* has been used extensively for testing various pharmaceutical agents and for new drug discovery (Rand and Johnson, 1995; Thomas and Lockery 1999). Therefore, the *C. elegans* mutants carrying various, well defined peroxisomal defects that are reported in this thesis could prove useful in the future for the high-throughput screening of pharmaceuticals to treat the different peroxisomal disorders.

1.9 What do we know about peroxisomes in *C. elegans*?

At the time when work on this project started, there were few publications reporting specifically on the peroxisomes of *C. elegans*. A series of papers described the cloning of the gene encoding thiolase type II (Bun-ya *et al.*, 1997), the catalytic functions of thiolase type II (Bun-ya *et al.*, 1998), its peroxisomal localization (Maebuchi *et al.*, 1999), and its expression pattern throughout nematode ontogenesis (Bun-ya *et al.*, 2000). The pH optimum of nematode peroxisomal catalase was also reported, and the enzyme was localized to peroxisomes (Togo *et al.*, 2000). Togo and coworkers also presented the first electron microscopy analysis of *C. elegans* peroxisomes (Togo *et al.*, 2000). The gene encoding a potential peroxisomal enzyme, alkyl-dihydroxyacetonephosphate synthase (ADHAPS), was cloned, and ADHAPS in the nematode was found to carry a PTS1 rather than a PTS2 (de Vet *et al.*, 1998). This observation prompted a deeper analysis of the peroxisomal targeting pathways in *C. elegans* and the suggestion that the PTS2-mediated pathway is absent in the nematode (Motley *et al.*, 2000). However, there was no experimental evidence for a peroxisomal localization of ADHAPS in *C. elegans*. *C. elegans* was shown to have a functional PTS1-dependent pathway by its import of a protein chimera consisting of green fluorescent protein tagged at its carboxyl terminus with PTS1 (GFP-PTS1) into peroxisomes (Motley *et al.*, 1998).

Special attention must be given to a manuscript reporting on the role of cytosolic catalase in nematode aging (Taub *et al.*, 1999). Although the results reported in this manuscript were later retracted (Taub *et al.*, 2003), it prompted our laboratory to start to investigate the role of peroxisomal catalase in nematode aging. The results of this study are presented in Chapter 5 of this thesis.

During the course of the work presented in this thesis, the tetratricopeptide repeat (TPR) domain from the predicted *C. elegans* Pex5p protein (PTS1 receptor) was found to be able to functionally substitute for the TPR domain of *Saccharomyces cerevisiae* Pex5p (Gurvitz *et al.*, 2001). This work was a practical continuation of previous experiments done by the same group in which potential nematode open reading frames (ORF) encoding the

PTS1 receptor and a number of putative PTS1-containing peroxisomal proteins were predicted (Gurvitz *et al.*, 2000). Interestingly, this publication was the first to suggest *C. elegans* as "an attractive model system for studying the importance of peroxisomes and affiliated processes in neurodegeneration, and also for studying a β-oxidation process that is potentially compartmentalized in both mitochondria and peroxisomes". The genes encoding three additional nematode homologs of known peroxisomal proteins - Pex1p and Pex6p (Ghenea *et al.*, 2001) and a Nudix hydrolase (AbdelRaheim and McLennan, 2002) - were cloned, but no experimental evidence for a peroxisomal location for these proteins in the nematode was presented, except that the Nudix hydrolase was shown to be imported into peroxisomes via the PTS1 pathway when heterologously expressed in *S. cerevisiae* (AbdelRaheim and McLennan, 2002). *C. elegans* Pex1p did not complement a *pex1* mutant of *S. cerevisiae* when expressed heterologously (Ghenea *et al.*, 2001). A comprehensive morphological study of *C. elegans* peroxisomes using electron microscopy was published by Yokota and coworkers (Yokota *et al.*, 2002). Finally, following the publication of our manuscript on the role of peroxins in the ontogenesis of *C. elegans* (Petriv *et al.*, 2002), Thieringer and coworkers (Thieringer *et al.*, 2003) published a similar analysis. They concluded that "*C. elegans* peroxisomes seem to be more similar to the human than to yeast peroxisomes". This publication also analyzed the nature of observed developmental arrest and indicated that a deficiency in the peroxin Pex5p arrests postembryonic development of the nematode at the L1 larval stage and impairs axonal migration during development of the nematode nervous system.

1.10 Thesis rationale

The objective of the work reported in this thesis was to reinforce the utility of the nematode *C. elegans* in peroxisome research. The thesis reports the advantages of using *C. elegans* as a valuable model system with which to study the molecular defects underlying the human peroxisomal disorders. It addresses specific features that make the nematode preferable to other popular model systems and examines the similarities and differences between human and nematode peroxisomes. This thesis also addresses a variety of other peroxisome-related topics, including the role of peroxisomes in aging, the import of peroxisomal proteins via specific targeting signals, and some aspects of peroxisomal metabolism of branched fatty acids. The studies reported in this thesis also demonstrate the potential of *C. elegans* as a model to investigate the lethal neurological peroxisomal disorders known to disrupt peroxisome biogenesis and affect human development.

CHAPTER 2

MATERIALS AND METHODS

2.1 Materials

2.1.1 List of chemicals and reagents

Reagent	Source
2-mercaptoethanol	Bioshop
3-methyl-1-butanol (isoamyl alcohol)	Caledon
5-bromo-4-chloro-3-indolyl-β-D-galactoside (X-gal)	Vector Biosystems
812 Resin	Marivac
acrylamide	Invitrogen
agarose, electrophoresis grade	Invitrogen
albumin, bovine serum (BSA)	Roche
ammonium persulfate [$(NH_4)_2S_2O_8$]	BDH
ammonium sulfate [$(NH_4)_2SO_4$]	BDH
ampicillin	Sigma
antipain	Roche
aprotinin	Roche
Bacto agar	BD
Bacto tryptone	BD
benzamidine hydrochloride	Sigma
protein assay dye reagent	Bio-Rad
bromophenol blue	BDH
chloroform ($CHCl_3$)	Fisher
cholesterol	Sigma
complete supplement mixture (CSM)	BIO 101
complete supplement mixture minus leucine (CSM-leu)	BIO 101
Coomassie Brilliant Blue R-250	ICN
D-(+)-glucose	Sigma
diethylpyrocarbonate (DEPC)	Sigma
dimethylsulfoxide (DMSO)	Caledon
dithiothreitol (DTT)	ICN
DNA molecular size standards	NEB
dodecenyl succinic anhydride	Marivac
Dulbecco's modified Eagle's medium (DMEM)	Gibco
ethanol	Commercial Alcohols
ethylenediaminetetraacetic acid (EDTA)	Sigma
Ficoll PM400	Pharmacia
formaldehyde, 37% (v/v)	BDH
FuGENE 6 Transfection Reagent	Roche
glycerol	BDH
hexane (*n*-hexanes, GC grade)	EMD
hydrochloric acid	Fisher
hydrogen peroxide solution, 30% (w/v)	Sigma
isopropanol	Fisher
isopropyl β-D-thiogalactopyranoside (IPTG)	Vector Biosystems

leucine	Sigma
leupeptin	Roche
lithium acetate	Sigma
methyl nadic anhydride	Marivac
methanol	Commercial Alcohols
N,N,N',N'-tetramethylethylenediamine (TEMED)	Invitrogen
N,N'-methylene bisacrylamide	Invitrogen
N-propyl gallate	Calbiochem
pepstatin A	Sigma
peptone	Difco
phenol, buffer-saturated	Invitrogen
phenylmethylsulfonylfluoride (PMSF)	Roche
phytanic acid	Sigma, Larodan
Ponceau S	Sigma
potassium chloride	BDH
potassium ferricyanide	Sigma
potassium phosphate, dibasic (K_2HPO_4)	Merck
potassium phosphate, monobasic (KH_2PO_4)	Merck
pristanic acid	Larodan, Malmö, Sweden
protein molecular size standards	NEB
RNA molecular size standards	NEB
sodium acetate	BDH
sodium chloride	Merck
sodium citrate	BDH
sodium dodecyl sulfate (SDS)	Sigma
sodium hydroxide	BDH
sodium hypochlorite, 5.25% (w/w)	Commercial Cleaners
sodium phosphate, dibasic (Na_2HPO_4)	BDH
sodium thiosulfate	Sigma
standard mixtures for gas chromatography	Larodan, Malmö, Sweden
sulfuric acid (H_2SO_4)	Merck
Tris-base, (tris[hydroxymethyl]aminomethane)	Roche
Triton X-100	Sigma
TRIZMA hydrochloride (tris[hydroxymethyl]aminomethane hydrochloride)	Sigma
tryptone	Difco
Tween 20 (polyoxyethylenesorbitan monolaurate)	Sigma
xylene cyanol FF	Sigma
yeast extract	Difco
yeast nitrogen base without amino acids (YNB)	Difco

2.1.2 List of enzymes

Enzyme	**Source**
calf intestinal alkaline phosphatase (CIAP)	NEB

proteinase, type K	Sigma
restriction endonucleases	NEB
ribonuclease A, DNase-free	Sigma
T4 DNA ligase	NEB
Taq polymerase	NEB

2.1.3 Plasmids

Plasmid (see also plasmid maps, Fig. 2.1.1)	**Source**
pPD118.25	Dr. A. Fire
pGEM-T	Promega
pDSRed2-Peroxi	Clontech
pECFP-N1	Clontech
pMAL-c2X	NEB
pRS315	NEB
pDP#MM016	Dr. D. Pilgrim
pRF4	Dr. A. Fire

2.1.4 Strains

Strain	**Source**
NIH 3T3 murine fibroblasts	Dr. Z. Wang
COS-7 monkey kidney epithelial cells	Dr. Z. Wang
Caenorhabditis elegans variety Bristol, strain N2	CGC
Caenorhabditis elegans, strain CB4845, *unc-119(e2498)III*	Dr. D. Pilgrim
Caenorhabditis elegans, strain CB1489, *him-8(e1489)IV*	CGC
Caenorhabditis elegans, strain LB90 *ctl-2* (*ua90*)*II*	This study
Caenorhabditis elegans, strain TU2463 *ctl-1(u800) II*	CGC
Caenorhabditis elegans, strain MQ130 *clk-1(qm30)III*	CGC
Caenorhabditis elegans, strain RB859 *Y57A10C.6(ok693) II*	CGC
Caenorhabditis elegans, strain VC262 *dhs-28&gei-15(ok450) X*	CGC
Caenorhabditis elegans, strain RB675 *pmp-4*(*ok396*) IV	CGC
Saccharomyces cerevisiae, strain *BY4741*, (*MATa, his3Δ1, leu2Δ0, met15Δ0, ura3Δ0*)	Giaever *et al.*, 2002
Saccharomyces cerevisiae, strain *WT-POT1-mRFP*, (*MATa, his3Δ1, leu2Δ0, met15Δ0, ura3Δ0, pot1::POT1-mRFP(HIS5)*)	Ms. Y.Y.C. Tam
Escherichia coli OP50	Dr. D. Pilgrim
Escherichia coli DH5α, F$^-$ φ80d*lac*ZΔM15 Δ(*lac*ZYA-*arg*F) U169 *rec*A1 *end*A1 *hsd*R17(r$_k^-$, m$_k^+$) *pho*A *sup*E44 λ$^-$ *thi*-1 *gyr*A96 *rel*A1	Invitrogen
Escherichia coli FT17, F$^-$ *araC14?, Sec 206(aziR)?, lacZ36, proC32, purE42, glnV44*(AS), λ$^-$, *trpE38, rfbD1, rpsL109*(strR), *xylA5, mtl-1, metE70, metB1, thi-1, cfa-1*	Yale University collection

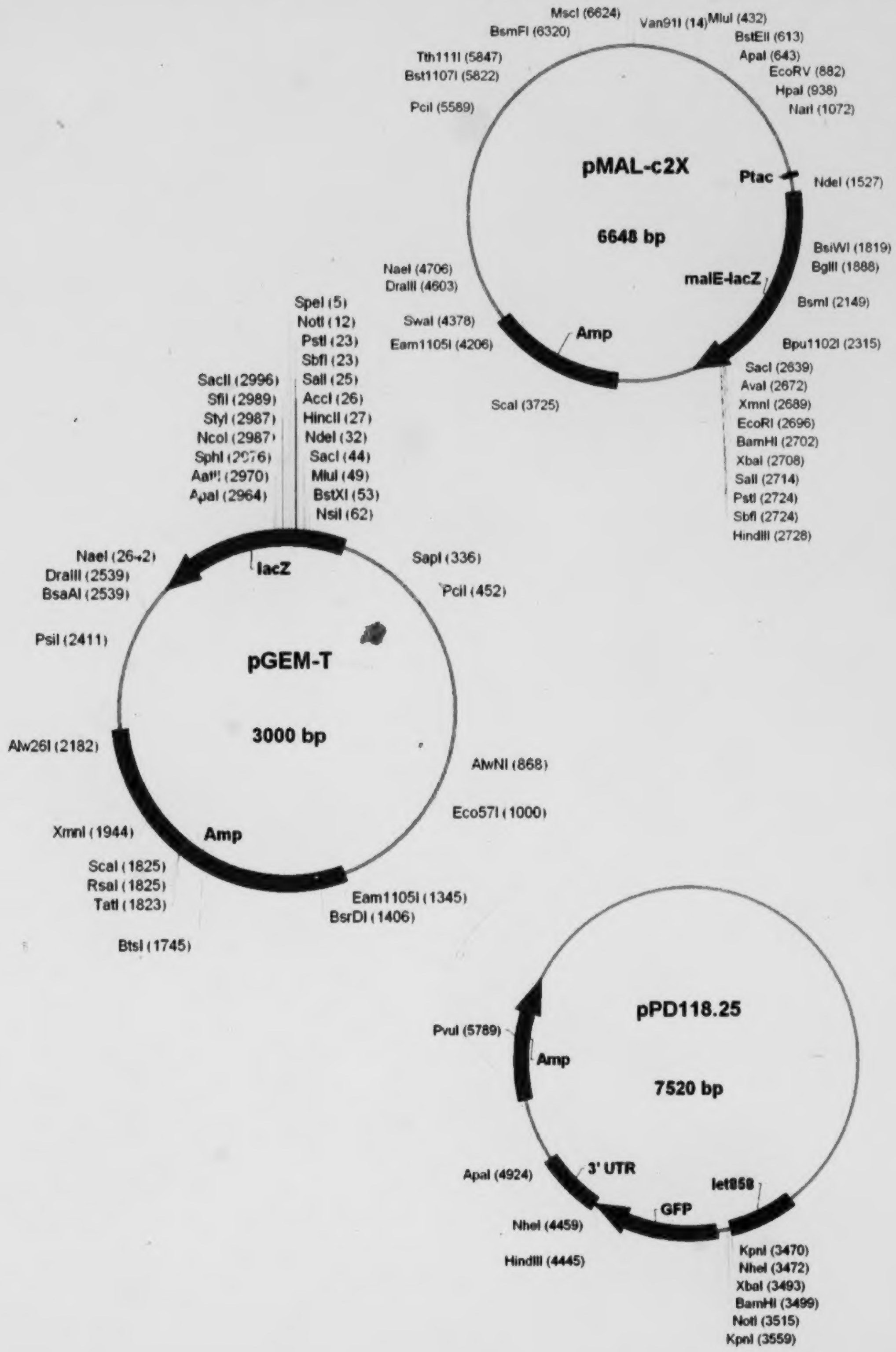
pMAL-c2X
6648 bp
MscI (6624)
BsmFI (6320)
Van91I (14)
MluI (432)
BstEII (613)
ApaI (643)
EcoRV (882)
HpaI (938)
NarI (1072)
Tth111I (5847)
Bst1107I (5822)
PciI (5589)
Ptac
NdeI (1527)
BsiWI (1819)
BglII (1888)
malE-lacZ
BsmI (2149)
NaeI (4706)
DraIII (4603)
SwaI (4378)
Eam1105I (4206)
Amp
Bpu1102I (2315)
SacI (2639)
AvaI (2672)
XmnI (2689)
EcoRI (2696)
BamHI (2702)
XbaI (2708)
SalI (2714)
PstI (2724)
SbfI (2724)
HindIII (2728)
ScaI (3725)
pGEM-T
3000 bp
SpeI (5)
NotI (12)
PstI (23)
SbfI (23)
SalI (25)
AccI (26)
HincII (27)
NdeI (32)
SacI (44)
MluI (49)
BstXI (53)
NsiI (62)
SacII (2996)
SfiI (2989)
StyI (2987)
NcoI (2987)
SphI (2976)
AatII (2970)
ApaI (2964)
NaeI (2642)
DraIII (2539)
BsaAI (2539)
lacZ
SapI (336)
PciI (452)
PsiI (2411)
AlwNI (868)
Eco57I (1000)
Alw26I (2182)
XmnI (1944)
Amp
ScaI (1825)
RsaI (1825)
TatI (1823)
Eam1105I (1345)
BsrDI (1406)
BtsI (1745)
pPD118.25
7520 bp
PvuI (5789)
Amp
ApaI (4924)
3' UTR
let858
GFP
NheI (4459)
HindIII (4445)
KpnI (3470)
NheI (3472)
XbaI (3493)
BamHI (3499)
NotI (3515)
KpnI (3559)

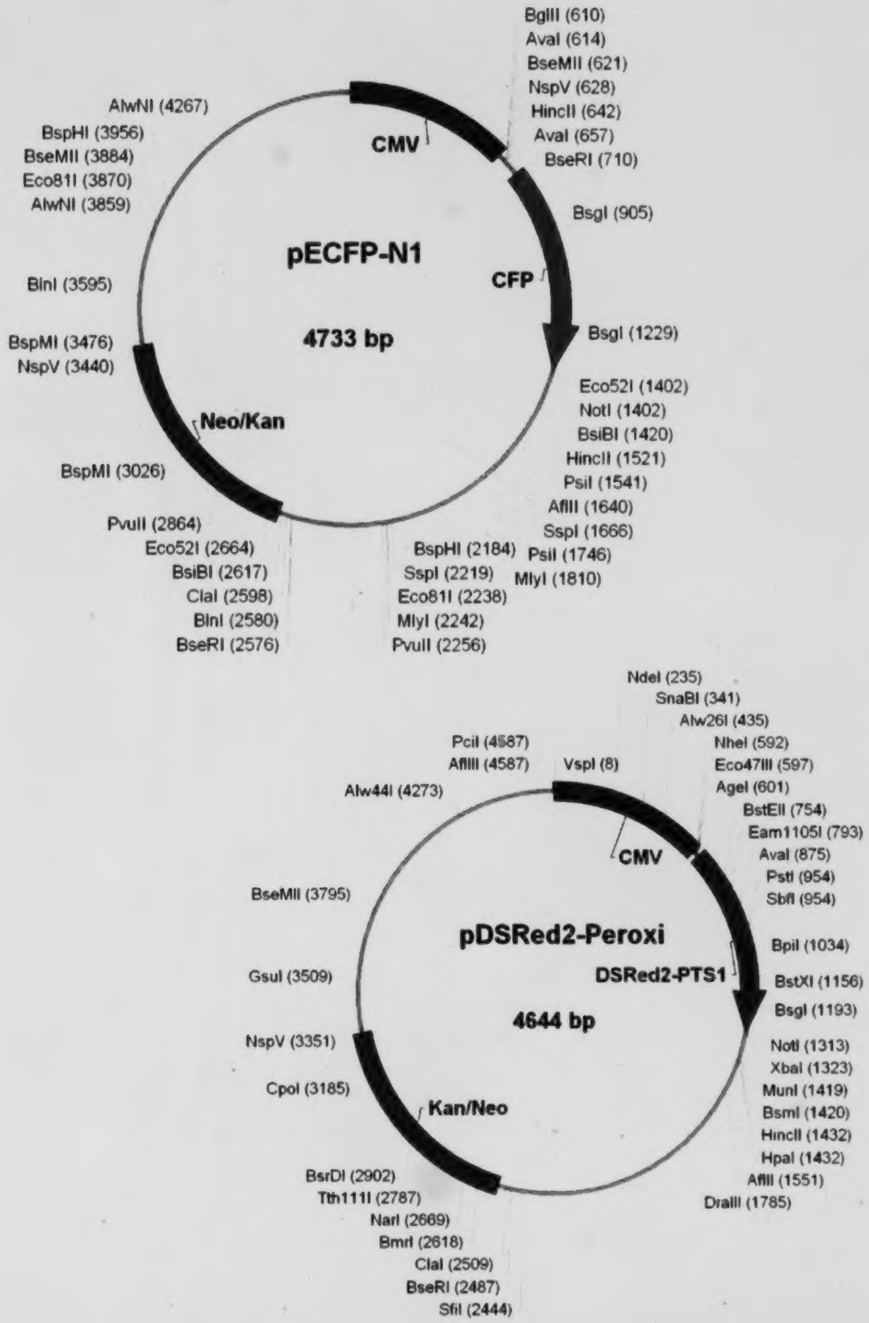
BglII (610)
AvaI (614)
BseMII (621)
NspV (628)
HincII (642)
AvaI (657)
BseRI (710)
BsgI (905)
BsgI (1229)
Eco52I (1402)
NotI (1402)
BsiBI (1420)
HincII (1521)
PsiI (1541)
AflII (1640)
SspI (1666)
PsiI (1746)
MlyI (1810)
BspHI (2184)
SspI (2219)
Eco81I (2238)
MlyI (2242)
PvuII (2256)
PvuII (2864)
Eco52I (2664)
BsiBI (2617)
ClaI (2598)
BlnI (2580)
BseRI (2576)
BspMI (3026)
BspMI (3476)
NspV (3440)
BlnI (3595)
AlwNI (4267)
BspHI (3956)
BseMII (3884)
Eco81I (3870)
AlwNI (3859)
CMV
CFP
Neo/Kan
pECFP-N1
4733 bp
NdeI (235)
SnaBI (341)
Alw26I (435)
NheI (592)
Eco47III (597)
AgeI (601)
BstEII (754)
Eam1105I (793)
AvaI (875)
PstI (954)
SbfI (954)
BpiI (1034)
BstXI (1156)
BsgI (1193)
NotI (1313)
XbaI (1323)
MunI (1419)
BsmI (1420)
HincII (1432)
HpaI (1432)
AflII (1551)
DraIII (1785)
Sfil (2444)
BseRI (2487)
ClaI (2509)
BmrI (2618)
NarI (2669)
Tth111I (2787)
BsrDI (2902)
CpoI (3185)
NspV (3351)
GsuI (3509)
BseMII (3795)
Alw44I (4273)
PciI (4587)
AflIII (4587)
VspI (8)
CMV
DSRed2-PTS1
Kan/Neo
pDSRed2-Peroxi
4644 bp

Figure 2.1.1. Maps of plasmid vectors used for expression in mammalian cells, *C. elegans*, *S. cerevisiae* and *E. coli*. Black regions, promoters; purple regions, genes encoding selection markers. Genes of interest are designated by other colours.

2.1.5 Antibodies

Antibodies	Source
FITC-conjugated donkey anti-guinea pig IgG	Jackson
Guinea pig anti-thiolase polyclonal	This study
rabbit anti-GFP, affinity purified	Dr. L. Berthiaume

2.1.6 Oligonucleotides[1]

Application	Sequence	Name
PEX1 RNAi	TATTTAATACGACTCACTATAGGGAGAAATGAATCAAAGCTATCCGGCTTTC	SG0759
	GCGCTAATASGACTCACTATAGGGAGAACTCTTTCTCCATCATAATTTCACAATATCTC	SG0760
PEX2 RNAi	TATTTAATACGACTCACTATAGGGAGAATGATTCACCACTTTAGGTACCACCA	AA1303
	CGCCTAATACGACTCACTATAGGGAGATTGAGCAGACTCTTCTAGAAAATAGAAAGATAC	AA1304
PEX3 RNAi	TATTTAATACGACTCACTATAGGGAGAAATGTTGGCATCTGCATGGGA	SG0757
	CGCCTAATACGACTCACTATAGGGAGAATCAAAAATGTTTCAGGAATTGTGC	SG0758
PEX5 RNAi	CCGGGTACCAAGCAAACCCTTTCACAACCATG	AA1262
	CTAGACTAGAGAGGCTTTTACAGCTGCCGAATTCCCG	AA1263
PEX6 RNAi	TATTTAATACGACTCACTATAGGGAGAACCGCCGTATCTTACAGTACATG	SG 0086
	CGCGTAATACGACTCACTATAGGGAGAGATGTCTCTGAGCAACCCGTATT	SG 0087
PEX10 RNAi	TATTTAATACGACTCACTATAGGGAGAAGTCAGCAAAGAGCTTCTGGGC	SG0741
	CGCCTAATACGACTCACTATAGGGAGAAAGGAATATCCGAATGAGCACTGG	SG0742
PEX11 RNAi	TATTTAATACGACTCACTATAGGGAGAAATGGTAAACTCAACAACACTTGCCC	SG0743
	CGCCTAATACGACTCACTATAGGGAGAACCAATAATCGAAGCCAACAATG	SG0744
PEX12 RNAi	TATTTAATACGACTCACTATAGGGAGAGAGCGTCGTTCACGGAAAACT	AA1307
	CGCCTAATACGACTCACTATAGGGAGATTGTTATAAGTGTTTACGTATTGGTTGATACA	AA1308
PEX13 RNAi	TATTTAATACGACTCACTATAGGGAGAGTATATTGTTTAGGTATGGTGGTGGGG	AA1301
	CGCCTAATACGACTCACTATAGGGAGATGAATTCAAATCTCTTGGTGGAAAAG	AA1302
PEX14 RNAi	TATTTAATACGACTCACTATAGGGAGAAATGACTGACCCATCTAGTTCCCC	SG0745
	CGCCTAATACGACTCACTATAGGGAGAAATCTGCCAACTCGTCAGCTAATGA	SG0746
PEX19 RNAi	TATTTAATACGACTCACTATAGGGAGAATGACTGACGAAACAACCCAAAATAT	AA1305

---

[1] Restriction sites are underlined

	CGCCTAATACGACTCACTATAGGGAGACTCGAATTGTTTCTCATATCGTTCCT	AA1306
Thiolase RNAi	TATTTAATACGACTCACTATAGGGAGAAACCTGCTGTGGTCAACGTGC	AA1289
	CGCCTAATASGACTCACTATAGGGAGATCAAATCTTGGACTGTGCAGCTC	AA1290
CTL-2 RNAi	TATTTAATACGACTCACTATAGGGAGAATGCCAAACGATCCATCGG	AA1287
	CGCCTAATASGACTCACTATAGGGAGAACCTCAGCGAAGTAGTTCCTTGC	AA1288
ADHAPS RNAi	TATTTAATACGACTCACTATAGGGAGAATGTCGGCGTCCTATCAAACAA	AA1291
	CGCCTAATACGACTCACTATAGGGAGATCTACAACTTGCAATGCGGTGA	AA1292
Enoyl-CoA RNAi	TATTTAATACGACTCACTATAGGGAGAATGCTCGCCTCTCGCCGT	AA1309
	CGCCTAATACGACTCACTATAGGGAGATCTAATCGAGAAAATCGCATCCTGT	AA1310
Synth RNAi	TATTTAATACGACTCACTATAGGGAGAGATGGTTCCCGCATCAGC	AA1311
	CGCCTAATACGACTCACTATAGGGAGACTCAGCATCAGGTACAACAATAGCA	AA1312
ABC RNAi	TATTTAATACGACTCACTATAGGGAGA(G/C)(A/T)GAAGAAAT(T/C)GCATT(T/C)TA(C/T)(G/C)(G/A)AGG	AA1313
	CGCCTAATACGACTCACTATAGGGAGACCTTCAACATC(T/A)A(T/C)(T/A)(G/C)(T/A)(T/A)ACTGCAGA(G/A)GT	AA1314
Thiolases RNAi	TATTTAATACGACTCACTATAGGGAGATTG(T/G)(T/C)G(G/T)(A/T)GGAA(T/C)(G/T)GA(G/A)A(G/A)(T/C)ATG(T/A)(G/C)(A/T)CAAGT(A/T)CCATTTT	AA1377
	CGCCTAATACGACTCACTATAGGGAGATCC(G/A)T(C/T)(G/A)CAAA(G/T)(G/T)GCAGC(T/A)AC(T/A)CCGA	AA1378
VLCFAS RNAi	TATTTAATACGACTCACTATAGGGAGACAGGGTCTTGGCTATCGATCC	AA1389
	CGCCTAATACGACTCACTATAGGGAGATCAACATCCTGACAAATTGGCA	AA1390
pPD118.25/CFP-SKL	ACGGGGTACCATGAGTAAAGGAGAAGAACTTTTCACTGG	AA1153
	ACTAGCTAGCTTAAAGTTTGCTTTTGTATAGTTCATCCATGCCATGTGT	AA1154
Mevalonate kinase cDNA cloning	GATGGTCGTCATAGGAGGTGATCAA	AA1536
	ATTAAGCTTGCTGAATGTATCCACAT	0029SG
	GAGGAGTTGCCAGCTTCAAGC	0017SG
	TCATTTATGTTTTGAAGCCGGC	0018SG
pPD118.25/D1053.2-GFP	CAAGGTACCATGAGGCTGCTCCCAACTCTTC	AA1124
	ACCGGTACCCCCATTGACGCACTGAGAAGAGACTGAGG	AA1125
pPD118.25/W10G11.11-GFP	CAAGGTACCATGAGGATCTTCCTGAATACTGTTCATTTA	AA1126
	ACCGGTACCCCTTGGGCAAAATGACAAATGTAGCC	AA1145
pRS315/*pgk*::PTS2$_{W10G11.11}$-GFP, pRS315/*pgk*::PTS2$_{D1053.2}$-GFP	GAAGATCTTTACTTGTACAGCTCGTCCATGCCCGA	AA1434
pECFP-N1/PTS2$_{D1053.2}$-CFP, pRS315/*pgk*::PTS2$_{D1053.2}$-GFP	GAAGATCTATGAGGCTGCTCCCAACTCTTGCCCAAGCTGTGAGCAAGGGCGAGGAGCTGTTCA	AA1435
pECFP-N1/PTS2$_{W10G11.11}$-CFP, pRS315/*pgk*::PTS2$_{W10G11.11}$-GFP	GAAGATCTATGAGGATCTTCCTGAATACTGTTCATTTAGTGAGCAAGGGCGAGGAGCTGTTCA	AA1436

pRS315/*pgk*::PTS2-GFP	GAAGATCTTTACTTGTATGGCCGGCTAGCGAATTCCAAAGCTTGTGGGCTTTTGTATAGTTCGTCCATGCCATGTGTAA	AA1419
pECFP-N1/PTS2$_{W10G11.11}$-CFP pECFP-N1/PTS2$_{D1053.2}$-CFP	GAGCGGCCGCTTACTTGTACAGCTCGTCCATGC	AA1486
pPD118.25/Mev-GFP pPD118.25/GFP-Mev	GGGGTACCGCGGCCGCTAGCAGATCCCCGCGGATGGTCGTCATAGGAGGTGATCAA	AA1531
	CTAGCTAGCTCGAATCATTAGCCTCAGGATCCTTTATGTTTTGAAGCCGGC	AA1532
	ATTAAGCTTGCTGAATGTATCCACAT	SG0029
	GATCTATGTCGGATAAACAATCAATTG	SG0030
	GAGGAGTTGCCAGCTTCAAGC	SG0017
	TCATTTATGTTTTGAAGCCGGC	SG0018
pPD118.25 3'-5' sequencing	AATAATCAGGGTTAGTTAGTATATA	AA1140
pPD118.25 5'-3' sequencing	GATTTATCGTTCGTTTGTGAGAAATTTAATT	AA1144
pRS315 sequencing 5'-3'	ACGGCCAGTGAATTGTAATACG	AA1360
pRS315 sequencing 3'-5'	CATGATTACGCCAAGCTCGGA	SG0722
pECFP-N1 5'-3' sequencing	GCAGAGCTGGTTTAGTGAACCGTC	AA1489
pMA91 sequencing	TAGTAGAACCTCGTGAAACTTACA	AA1462
Confirmation of PTS2$_{D1053.2}$	CTGCTCCCAACTCTTGCCCAAGCT	AA1487
Confirmation of PTS2 $_{W10G11.11}$	ATCTTCCTGAATACTGTTCATTTA	AA1488
Cloning of PGK promoter	CGCGGATCCAAGCTTTCTAACTGATCTATCCAAAACTG	AA1482
	CCGGAATTCTAACGAACGCAGAATTTTCGAGT	AA1483
Ctl-2 knockout selection	TTAGATATGAGAGCGAGCCTGTTTC	AA1494
	TGCACATATGCACCATACAGCA	AA1495
	CTAGTGGTACATCCATGCAAATGC	AA1497
	CTGAAGCATGACTCGCTGTTG	AA1513
pMAL-p2X/ MBP-Thio	CGAGGATCCTCAAAACGCGAGCATTACGC	AA1137
	TTGCTGCAGTCAAATCTTGGACTGTGCAGCTC	AA1117
pPD118.25/*ctl-1,2*::GFP	GGCTGCAGATTGTTTGATATTCAAACTTTTGTATATAGAATC	QC0499
	CAGCGGCCGCTTTGGTTCTGAAATTTTAGTTAGGA	QC0500
pPD118.25/*ctl-3*::GFP	CGGAATTCCTCGTAGCGAAAGCTACAGTAATTCT	SG0071
	GAGAATGCTTTGAAGATTTACTGTTGAATTTCCG	SG0072

2.1.7 Standard media, buffers and solutions

Medium, solution or buffer	Composition[a]	Reference
LB	1% tryptone, 0.5% yeast extract, 1% NaCl	Maniatis *et al.*, 1982
CSM	0.67% YNB without amino acids, 0.08% CSM, 2% glucose	Maniatis *et al.*, 1982
YEPD	1% yeast extract, 2% peptone, 2% glucose	Maniatis *et al.*, 1982
MYOB	0.55 g TRIZMA-hydrochloride, 0.24 g Tris, 4.6 g tryptone, 8 mg cholesterol, 2 g NaCl/L	Church *et al.*, 1995
YNO	0.67% YNB without amino acids, 0.05% yeast extract, 0.5% (w/v) Tween 40, 0.1% (w/v) oleic acid	Maniatis *et al.*, 1982
DMEM	10% calf serum, penicillin and streptomycin, each at 100	Maniatis *et al.*, 1982

	units/ml	
Worm Lysis Solution	0.1 M NaCl, 10 mM Tris-HCl, pH 8.0, 10 mM EDTA, 1% SDS, 1% 2-mercaptoethanol, 100 µg Proteinase K/ml	Hope, 1999
TE	1 mM Tris-HCl, pH 8.0, 1 mM EDTA	Hope, 1999
Worm Injection Buffer	2% PEG-6000, 20 mM potassium phosphate, 2 mM potassium citrate, pH 7.5	Mello and Fire, 1995
TBST	20 mM Tris-HCl, pH 7.5, 100 mM EDTA, 0.05% (w/v) Tween 20	Maniatis *et al.*, 1982

[a] For solid media, agar was added to 2%.

2.2 Methods

2.2.1 Purification of genomic DNA from nematodes

Mixed stage animals were harvested from MYOB agar plates and washed thoroughly in M9 buffer to clean the sample of bacteria. A 10× volume of Worm Lysis Solution was added. The sample was frozen for at least 10 min at -80°C and afterwards incubated at 65°C with occasional shaking until animals were completely digested. Nucleic acids were extracted from the lysate with phenol-chloroform (25:24:1, phenol:chloroform:isoamyl alcohol followed by 24:1, chloroform:isoamyl alcohol) extraction and precipitated by the addition of 2.5 volumes of ethanol to the final aqueous phase. RNA was digested 37°C for 1 hour by DNase-free RNase A at a final concentration of 10 µg/ml. DNA was pelleted by centrifugation for 10 min at 16,000 × *g*, washed twice with 70% ethanol and dissolved in water or TE buffer.

2.2.2 Purification of mRNA from nematodes

Total RNA was isolated from the nematode using the RNAqueous Small Scale Phenol-Free Total RNA Isolation Kit (Ambion, Austin, TX) following the recommendations of the manufacturer.

2.2.3 *In vitro* dsRNA synthesis

The T7-MEGAscript High Yield Transcription Kit (Ambion) was used to produce ssRNA *in vitro*. Template for the transcription reaction was produced by PCR using oligonucleotides incorporating the T7 phage RNA polymerase promoter. Both RNA strands were generated in a single reaction and annealed after completion of their synthesis by incubation for 10 min at 65°C followed by slow cooling.

2.2.4 dsRNA interference

dsRNA was dissolved in Worm Injection Buffer at a concentration of 0.5-1.0 mg/ml and injected into one or both gonad arms of young adult hermaphrodites as described (Mello and Fire, 1995). Injected animals were transferred to MYOB agar plates seeded with the OP50 strain of *Escherichia coli*. After 12 hours, the surviving animals were transferred to fresh culture plates, on which they were allowed to lay eggs. The percentage of adult F1 progeny was evaluated 3 days after injection. The percentage of adults in the offspring of worms injected with control dsRNA was set at 100% in each independent experiment. 300-700 animals were examined in each experiment. Experiments were repeated a minimum of 3 times.

2.2.5 Genomic integration of the CFP-SKL expression construct

The nematode strain CB4845 was injected with the plasmid pPD118.25/CFP-SKL containing the chimeric gene encoding CFP tagged with the PTS1-tripeptide SKL at its carboxyl terminus downstream of the *let-858* promoter. pPD118.25/CFP-SKL was made using oligonucleotides AA1153 and AA1154. Plasmid pDP#MM016 containing the entire *unc-119* gene, including promoter and 3' untranslated regions, was coinjected with pPD118.25/CFP-SKL to allow for selection of transgenic animals. Worms that reverted from the Unc$^-$ phenotype to the wild-type phenotype were selected as those containing extrachromosomal arrays. These worms were exposed to an ultraviolet radiation dose of 350 µJ from a UV Stratalinker 1800 (Stratagene, La Jolla, CA). Homozygotes stably (100% of population) expressing the CFP-SKL construct were selected.

2.2.6 DNA sequencing

Automated dideoxynucleotide termination DNA sequencing (Sanger *et al.*, 1977) was performed using the BigDye Terminator Cyrcle Sequencing Ready Reaction Kit (Applied Biosystems, Foster City, CA). This PCR-based methodology randomly incorporates fluorescently labeled dideoxynucleotides into DNA using a modified version of *Taq* polymerase. 3-5 µg of supercoiled plasmid DNA as template and 3.2 pmol of oligonucleotide primer were used in each reaction. PCR was performed in a RoboCycler 40 equipped with a Hot Top (Stratagene). PCR parameters were: 2 min initial denaturation at 96°C, followed by 25 cycles of 96°C, 50°C and 60°C for 46 sec, 51 sec, and 4 min 10 sec, respectively. Reaction products were precipitated by addition of alcohol and separated by capillary electrophoresis in an ABI 310 Genetic Analyzer (Applied Biosystems).

2.2.7 Polymerase chain reactions (PCR)

PCR reactions were performed in a Robocycler 40 or a Robocycler 96, each equipped with a Hot Top attachment. To screen mutant libraries, Ready-To-Go PCR beads were used according to the specifications of the manufacturer (Amersham, Piscataway, NJ). Reactions were performed in a volume of 10 µl. For mutation-sensitive applications, reactions typically contained 100-300 pmol of oligonucleotide primers, 0.5 mM of each dNTP, and 5 U of Taq polymerase in a 25 µl buffered reaction. The Expand Long Template PCR System (Roche) was used according to the manufacturer's recommendations to make PCR products longer than 5 kilobase pairs.

2.2.8 Digestion of DNA by restriction endonucleases

DNA was digested under conditions optimal for the specific restriction enzyme according to the manufacturer's instructions. For diagnostic and preparative purposes, 1 to 5 µg of DNA was digested. Double enzyme digests were done in buffers recommended by New England Biolabs.

2.2.9 Dephosphorylation of 5' DNA ends

5' DNA ends were dephosphorylated in a buffered reaction containing 5 U of calf intestinal alkaline phosphatase for 20 min at 37°C.

2.2.10 Gel electrophoresis of DNA fragments

Samples of DNA containing an appropriate volume of 6× sample dye (0.25% bromophenol blue, 0.25% xylene cyanol FF, 15% Ficol PM 400) (Sambrook and Russell, 2001) were subjected to electrophoresis on 1% agarose gels containing 1× TBE buffer and 0.5 µg ethidium bromide/ml. DNA fragments were visualized by ultraviolet illumination.

2.2.11 Purification of DNA fragments from agarose

DNA fragments were excised from gel, and DNA was purified using the QIAquick Gel Extraction Kit (Qiagen, Valencia, CA) according to the manufacturer's recommendations.

2.2.12 Ligation of DNA fragments

DNA fragments were ligated at a 1:3 to 1:5 molar ratio of plasmid:insert in a 10 µl buffered reaction containing T_4 DNA ligase at 4°C overnight. DNA fragments obtained by PCR were ligated into the pGEM-T shuttle vector (Promega, Madison, WI) following the manufacturer's instructions.

2.2.13 Preparation of anti-thiolase antibodies

The last exon of the gene Y57A10C.6 encoding the 242 carboxyl-terminal amino acids of the *C. elegans* type II peroxisomal thiolase P-44 was fused in-frame and downstream of the open reading frame (ORF) encoding *E. coli* maltose binding protein (MBP) to make the vector pMAL-p2X/Thio. The chimeric protein product was synthesized in *E. coli* DH5α, purified by affinity chromatography on amylose resin and cleaved with Factor Xa. The thiolase polypeptide fragment was separated from MBP by SDS-PAGE, excised from the gel and isolated by electroelution. Antibodies to the polypeptide were raised in rabbit and Guinea pig.

2.2.14 Determination of protein concentration

The concentration of proteins in lysates was determined by the Bradford method using a commercial protein assay dye reagent (Bio-Rad, Hercules, CA). 1 ml of reagent was added to 100 µl of diluted sample, vortexed briefly and incubated at room temperature for 10 min. The absorbances of samples was measured at 595 nm. A standard curve was used to determine the protein content of a sample from its absorbance value. The standard curve was made by measuring the absorbances of known amounts of bovine serum albumin.

2.2.15 Electrophoresis of proteins

Proteins were separated by sodium dodecylsulfate-polyacrylamide gel electrophoresis (SDS-PAGE) by the method of Laemmli (Laemmli, 1970). Proteins were dissolved in a sample buffer to yield a final buffer concentration of 62.5 mM Tris-HCl, pH 6.8, 2% SDS, 10 mM DTT, 10% sucrose and 0.001% bromphenol blue. Samples were denaturated by boiling for 5 min. Discontinuous slab gels for protein separation consisted of a stacking gel (3% acrylamide/*N,N'*-methylene bisacrylamide (30:0.8), 60 mM Tris-HCl, pH 6.8, 0.1% SDS, 0.1% (v/v) TEMED, 0.1% ammonium persulfate) and a resolving gel (7% to 18% acrylamide/*N,N'*-methylene bisacrylamide (30:0.8), 375 mM Tris-HCl, pH 8.3, 0.1% SDS, 0.1% (v/v) TEMED, 0.042% ammonium persulfate). Electrophoresis running buffer consisted of 50 mM Tris-HCl, pH 8.8, 0.4 M glycine, 0.1% SDS.

2.2.16 Detection of proteins by immunoblotting

Immunoblotting analysis and detection of antigen-antibody complexes by enhanced chemiluminescence were performed as follows. Proteins separated by SDS-PAGE were transferred to nitrocellulose membrane for 40 min at 60 mA/cm^2 using a semi-dry transfer system (Tyler Research Instruments). Transfer buffer consisted of 20 mM Tris, 150 mM glycine, 20% (v/v) methanol. After transfer, the nitrocellulose membrane was blocked by incubation in a 5% solution of dry fat-free milk in TBST (20 mM Tris-HCl, pH 7.5, 150 mM NaCl, 0.05% (w/v) Tween 20) for 40 min at room temperature. Antibodies bound to specific proteins were detected by enhanced chemiluminescence using a commercially available kit (Amersham-Pharmacia) according to the manufacturer's instructions.

2.2.17 Immunofluorescence microscopy

Double-labeling, immunofluorescence microscopy was performed as described (Miller and Shakes, 1995). Rabbit and guinea pig anti-thiolase antibodies were used at a dilution of 1:100. Affinity-purified rabbit antibodies to green fluorescent protein (GFP) were used at a dilution of 1:500. Primary antibodies were detected with rhodamine- or FITC-conjugated donkey anti-rabbit IgG antibodies or with rhodamine- or FITC-conjugated donkey anti-guinea pig IgG antibodies. Samples were viewed with an Olympus BX50 microscope.

2.2.18 Determination of catalase activity

The catalase activity of lysates of mixed stage animals prepared by sonication in 20 mM Tris-HCl, pH 7.5, 50 mM potassium acetate, 2 mM EDTA, 100 mM sorbitol was measured either colorimetrically (Leighton *et al.*, 1968) or by staining *in situ* with ferricyanide following native gel electrophoresis (Woodbury *et al.*, 1971).

2.2.19 Determination of lifespan

To measure nematode lifespan, plates containing 10 to 14 worms were incubated at 20°C and scored daily for surviving animals. Worms were transferred to fresh plates every 2 to 3 days. The starting point for lifespan determination was at hatching. Lost, bagged and exploded animals were excluded from analysis.

To measure chronological lifespan in wild-type and mutant strains of the yeast *Saccharomyces cerevisiae*, cells were grown to stationary phase in YEPD medium, pelleted and washed three times in distilled, deionized water, and transferred to distilled, deionized water at a density of 2-3 cells/µl. Cells were incubated at 30°C with rotational shaking (220 rpm) in Erlenmeyer flasks at a flask volume/medium volume ratio of 5:1. To score for surviving cells, cell suspensions were seeded onto YEPD agar plates, and the number of individual yeast colonies was counted.

2.2.20 Measurement of protein carbonylation

Protein carbonylation was determined using the OxyBlot Protein Oxidation Detection Kit (Intergen, Burlington, MA) according to the manufacturer's protocol and quantitated by analysis of autoradiograms with a GS-800 Calibrated Densitometer using Quantity One 4.3.1 software (Bio-Rad).

2.2.21 Confocal microscopy

Confocal microscopy was performed with a LSM510 META laser scanning microscope (Carl Zeiss). Peroxisomes were visualized with a fluorescent protein chimera of CFP tagged at its carboxyl terminus with the peroxisome targeting signal 1 (PTS1) tripeptide Ser-Lys-Leu (Petriv *et al.*, 2002).

2.2.22 Computational analysis of PTS2 motifs

The learning database for computational analysis contained peroxisomal proteins extracted from the Swiss-Prot protein database (Release 42.0) (Boeckmann *et al.*, 2003) according to the annotation: proteins from eukaryotic organisms localized to peroxisomes OR glyoxysomes OR microbodies OR glycosomes but NOT to nucleus or cytoplasm or endoplasmic reticulum or associated with the cytoskeleton. All putative PTS1-containing proteins were removed using the on-line application at http://mendel.imp.univie.ac.at/PTS1/ (Neuberger *et al.*, 2003b). Proteins derived from ORFs less than 30 amino acids in length were not included in the computational analysis. The resulting database consisted of 845 protein sequences. The length of each protein was set at 100% to calculate the position of putative PTS2 signals along the protein molecule. All codes for database analysis were written using JAVA language.

2.2.23 Isolation and sequencing of mevalonate kinase cDNA from *C. elegans*

The full-length cDNA of *C. elegans* mevalonate kinase (*Ce*MeK) (corresponding to ORF Y42G9A.4) was cloned as two fragments and inserted into expression vector pPD118.25. Using the RNA-queous-4PCR Kit (Ambion), RT-PCR with the pairs of primers SG0029/SG0030 and SG0017/SG0018 was performed to generate overlapping cDNA fragments of 1216 bp and 787 bp, respectively. The fragments were joined following cleavage at a unique *Eco*RI restriction site in the overlapping regions of the two fragments. The full-length cDNA was sequenced using oligonucleotides AA1531 and AA1532 and inserted into nematode expression vector pPD118.25 in-frame with the ORF for GFP. Two vectors were generated, the first encoding *Ce*MeK tagged at its amino terminus with GFP and the second with *Ce*MeK tagged at its carboxyl terminus with GFP.

2.2.24 Morphometric analysis of peroxisomes and lipid droplets

The area of cross section of peroxisomes and lipid droplets was determined using UTHSCSA Image Tool 2.00 software from electron microscopic images and confocal microscopic images captured with CCD cameras.

2.2.25 Growth synchronization

Gravid adult worms were washed from plates with M9 buffer and treated with basic hypochlorite (0.25 M KOH, 1-1.5% hypochlorite) to harvest eggs. Eggs were washed with M9 buffer and distributed across fresh plates seeded with *E. coli* OP50.

2.2.26 Electron microscopy

Electron microscopy of worms was performed as previously described (Hall, 1995). Essentially, worms were washed from plates with M9 buffer, fixed in 1% paraformaldehyde, 2.5% glutaraldehyde, 50 mM sodium cacodylate, pH 7.2, at 4°C overnight with rotation. After fixation, worms were washed 5 times for 10 min in 50 mM sodium cacodylate, pH 7.2, and placed in a buffered solution of 1% osmium tetroxide, 0.05 M $K_3Fe(CN)_6$ for 40 min. Worms were washed 3 times for 5 min each with water and then dehydrated in increasing concentrations of ethanol from 60% to 100%. Dehydrated worms were embedded in epon resin. Sectioned samples were examined with a Philips 410 electron microscope. Electron microscopic images were captured with a MegaView III CCD camera (Soft Imaging System, Lakewood, CO).

2.2.27 Single worm PCR

A nested PCR method (Plasterk, 1995) was used for single worm PCR. Individual worms were put in a 96-well format plate in 2.5 µl of worm lysis solution (Table 2.1.7), lysed by incubation for 90 min at 65°C, and then maintained for 30 min at 90°C to inactivate proteinase K. The PCR master mix containing an external pair of primers for nested PCR was dispersed into wells (10 µl each). The PCR reaction was performed on a Robocycler 96 machine equipped with a Hot Top. After the first round of PCR (35 cycles), the reaction mixture was removed from the wells, and PCR master mix containing an internal pair of primers was dispersed, and the cycling was again performed. The resulting PCR products were analyzed by electrophoresis on an agarose gel.

2.2.28 Selection of the *ctl-2* mutant

The *ctl-2* deletion was found by screening a mutant genome library kindly provided by Dr. Bernard Lemire, Department of Biochemistry, University of Alberta. A PCR reaction with nested primers (AA1494 as outer left, AA1513 as inner left, AA1497 as outer right, AA1495 as inner right) was performed using the following conditions in both rounds of PCR: 35 cycles of denaturation for 45 sec at 95°C; annealing for 45 sec at 45°C; elongation for 90 sec at 72°C. The reaction volume was 10 µl in a 96-well format. The reaction mixture was removed after the first round of PCR using the outer primers, and a fresh mixture with the inner primers was dispensed into the wells for the next round of PCR. After the homozygous *ctl-2* mutant (*ua90*) was selected, it was outcrossed with the wild-type N2 strain six times.

2.2.29 Cloning of pRS315/pgk::PTS2-GFP plasmids

GFP was tagged with PTS2 by amplification of the gene encoding GFP from vector pEGFP-N1 using as forward primers oligonucleotide AA1435 for $\mathrm{PTS2}_{\mathrm{D1053.2}}$-GFP and oligonucleotide AA1436 for $\mathrm{PTS2}_{\mathrm{W10G11.11}}$-GFP and oligonucleotide AA1434 as the reverse primer. This amplification product was inserted into *Bgl*II site of vector pMA91 (Mellor *et al.*, 1983) (Fig. 2.1.1) between the PGK promoter and terminator sequences. *pgk*::PTS2-GFP was then excised with *Hin*dIII and cloned into the corresponding site of the plasmid pRS315 (Fig. 2.1.1).

2.2.30 *In silico* search for *C. elegans* orthologs of human peroxins and peroxisomal enzymes

The gene and protein sequences of human peroxins and peroxisomal enzymes were retrieved from National Center for Biotechnology Information (NCBI) data bank[2]. To identify potential orthologs of human peroxins and peroxisomal enzymes involved in lipid metabolism in the nematode, we performed a computer search of the *C. elegans* genome WormPD[3] and The Sanger Centre[4] databases against protein sequences of known human peroxins and peroxisomal enzymes using the Gapped BLAST (v2.0.10)[5] algorithm with

---

[2] http://www.ncbi.nlm.nih.gov/

[3] http://www.proteome.com

[4] http://www.sanger.ac.uk

[5] http://www.ncbi.nlm.nih.gov/blast/

SEG and COIL filters. Alignments were refined by the Smith-Waterman alignment algorithms from the UCS Sequence alignment package (v2.0). Sequences yielding the highest score were aligned pairwise with the human counterpart proteins using the BLASTP (v2.2.6) algorithm with the following settings: BLOSUM62 matrix; expectation value 10.0; gap x_dropoff 50; open gap 9; extension gap of 1 penalties; word size 3; low complexity filter off. The cut-off based on E-value was equal 0.00001. The alignment results are presented in Tables 3.2.1, 3.2.2 and 3.2.3.

The Proteome BioKnowledge Library[6] and WormBase[7] databases were used to retrieve information related to RNAi and mutant phenotypes, if available, for chosen nematode counterparts of human peroxins and peroxisomal proteins.

2.2.31 Gas chromatography

To analyze the fatty acids composition in the nematode, a mixed-age population of worms was washed from agar plates, rinsed several times with water, submerged in 1 ml of 2.5% H_2SO_4 in methanol and incubated at 80°C for 1 hour. 200 µl of hexane and 1.5 ml of water was then added to extract methyl esters. The solution was concentrated under vacuum. Samples were analyzed by GC-MS according to the method of Watts and Browse (Watts and Browse, 2002) using a Hewlett-Packard (HP) Gas Chromatograph 5890 Series II equipped with a DB-225 column. The initial temperature was 50°C, and the gas chromatograph was programmed to increase temperature at 10°C/min to 180°C, to hold for 5 min, and then increase temperature to 220°C at 5°C/min, and then to hold for 5 min.

---

[6] https://proteome.incyte.com/

[7] http://www.wormbase.org

2.2.32 Supplementation of the nematode diet with pristanic acid

Pristanic acid was found to be catabolized by *E. coli.* Therefore, bacteria had to be removed from all experiments involving the analysis of pristanic acid. Worms grown on agar plates and fed OP50 *E. coli* were washed with M9 buffer and cleaned of remaining bacteria by several consecutive washes with M9 buffer. Cleaned worms were resuspended in 250 µl of M9 buffer in a capped glass vial 1.5-cm in diameter and with a flat bottom. 2 µl of pristanic acid was added to the vial, and worms were left at room temperature for 16 hours. Worms were washed thoroughly with M9 buffer and then water and subjected to GC-MS analysis.

CHAPTER 3

THE ROLE OF *CAENORHABDITIS ELEGANS* PEROXINS AND PEROXISOMAL ENZYMES IN NEMATODE ONTOGENESIS

A version of this chapter has previously been published as "RNA interference of peroxisome-related genes in *C. elegans*: a new model for human peroxisomal disorders" (Petriv, O.I., D.B. Pilgrim, R.A. Rachubinski, and V.I. Titorenko. 2002. *Physiol. Genomics*. 10:79-91).

3.1 Overview

Extensive database searches yielded a number of nematode genes encoding putative homologs of human peroxins and peroxisomal enzymes. RNAi screening suggested that most of the peroxins and some of the peroxisomal enzymes are indispensable for normal development of *C. elegans*. A peroxisomal fluorescent reporter allowed monitoring of both PTS1-dependent protein import into peroxisomes and the morphology of organelles. It revealed that abnormal functioning of peroxisomes correlates with developmental defects in the nematode. These experimental data suggest that the biogenesis of nematode and human peroxisomes is closely related.

3.2 *In silico* search for the *C. elegans* orthologs of human peroxins and peroxisomal enzymes

Extensive searches of *C. elegans* genomic databases (see Materials and Methods) resulted in the identification of 11 genes encoding putative nematode peroxins, homologs[8] of the 14 known human peroxins (Table 3.2.1). Similarly, based on their high level of sequence identity with human genes, 14 genes encoding putative nematode peroxisomal enzymes were selected. Interestingly, computer analysis also revealed that 18 other peroxins known to function in yeasts, but not in humans, have only six putative nematode counterparts (one with high, and five with moderate to low, levels of sequence identity). The homologous pairs were aligned using BLAST pairwise alignment. The alignment results are presented in Tables 3.2.1, 3.2.2 and 3.2.3.

---

[8] Homologs of human genes in the nematode were identified using sequence identity/similarity as main selection criteria.

Table 3.2.1. Human peroxins and their homologs in *C. elegans*

Human	Gene Bank #	Alignment[1]	Nematode	Worm Base #
Pex1p	NP_000457.1	Score = 225 bits (736), Expect = 6e-57 Identities = 269/992 (27%), Positives = 448/992 (45%), Gaps = 135/992 (13%) 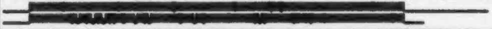	**prx-1**	C11H1.4
Pex2p	NP_000309.1	Score = 58.7 bits (175), Expect = 1e-07 Identities = 70/299 (23%), Positives = 118/299 (39%), Gaps = 77/299 (25%) 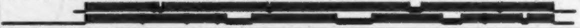	**prx-2**	ZK809.7
Pex3p	NP_003621.1	Score = 55.1 bits (163), Expect = 2e-06 Identities = 35/115 (30%), Positives = 62/115 (53%), Gaps = 8/115 (6%) 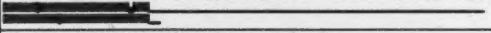	**prx-3**	C15H9.8
Pex5p	NP_000310.2	Score = 201 bits (655), Expect = 3e-50 Identities = 187/629 (29%), Positives = 288/629 (45%), Gaps = 140/629 (22%) 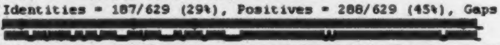	**prx-5**	C34C6.6
Pex6p	NP_000278.2	Score = 234 bits (767), Expect = 6e-60 Identities = 183/494 (37%), Positives = 280/494 (56%), Gaps = 42/494 (8%) 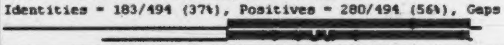	**prx-6**	F39G3.7
Pex7p	NP_000279.1		**51 ORFs**	
Pex10p	NP_722540.1	Score = 114 bits (364), Expect = 2e-24 Identities = 105/346 (30%), Positives = 163/346 (46%), Gaps = 67/346 (19%) 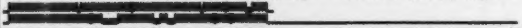	**wrs-2**	C34E10.4
Pex11p	NP_542393.1-γ	Score = 52.7 bits (155), Expect = 9e-06 Identities = 55/231 (23%), Positives = 99/231 (42%), Gaps = 36/231 (15%) 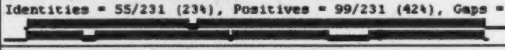	**prx-11**	C47B2.8
Pex12p	NP_000277.1	Score = 170 bits (553), Expect = 2e-41 Identities = 130/352 (36%), Positives = 198/352 (55%), Gaps = 24/352 (6%) 	**prx-12**	F08B12.2
Pex13p	NP_002609.1	Score = 160 bits (517), Expect = 4e-38 Identities = 123/302 (40%), Positives = 172/302 (56%), Gaps = 19/302 (6%) 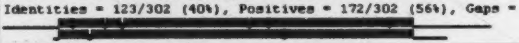	**prx-13**	F32A5.6
Pex14p	NP_004556.1	Score = 59.8 bits (179), Expect = 6e-08 Identities = 67/282 (23%), Positives = 131/282 (45%), Gaps = 55/282 (19%) 	**prx-14**	R07H5.1
Pex16p	NP_476515.1		**No homology**	
Pex19p	AAH00496.1	Score = 94.0 bits (294), Expect = 3e-18 Identities = 92/302 (30%), Positives = 136/302 (44%), Gaps = 46/302 (15%) 	**prx-19**	F54F2.8
Pex26p	NP_060399.1		**No homology**	

---

[1] Upper protein - human peroxin, lower protein - nematode homolog. Blue colour, regions of homology, red colour, gaps.

Table 3.2.2. Human peroxisomal enzymes and their homologs in *C. elegans*

Human	Gene Bank #	Alignment[1]	Nematode	Worm Base #
CAT	NP_001743.1	Score = 522 bits (1736), Expect = e-147 Identities = 311/478 (65%), Positives = 382/478 (79%), Gaps = 1/478 (0%) 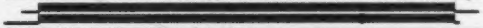	**ctl-2**	Y54G11A.5a
ACAA1	NP_001598.1	Score = 146 bits (470), Expect = 6e-34 Identities = 129/399 (32%), Positives = 205/399 (51%), Gaps = 32/399 (8%) 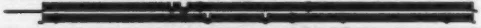		T02G5.7
		Score = 149 bits (480), Expect = 7e-35 Identities = 122/390 (31%), Positives = 198/390 (50%), Gaps = 19/390 (4%) 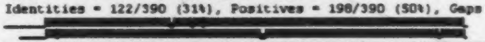	**kat-1**	T02G5.8
		Score = 101 bits (319), Expect = 2e-20 Identities = 105/393 (26%), Positives = 173/393 (43%), Gaps = 38/393 (9%) 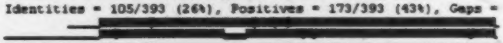		T02G5.4
SCPx	NP_002970.2	Score = 382 bits (1266), Expect = e-105 Identities = 238/408 (58%), Positives = 311/408 (75%), Gaps = 5/408 (1%) 	**P-44**	Y57A10C.6
ADHAPS	NP_003650.1	Score = 505 bits (1679), Expect = e-141 Identities = 310/578 (53%), Positives = 411/578 (70%), Gaps = 4/578 (0%) 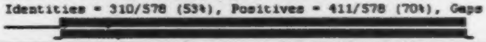	**ads-1**	Y50D7A.7
ABCD1	NP_000024.2	Score = 587 bits (1955), Expect = e-166 Identities = 376/664 (56%), Positives = 499/664 (74%), Gaps = 17/664 (2%) 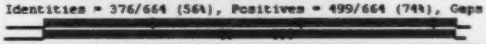 ABCD1/pmp-4	**pmp-4**	T02D1.5
ABCD2	NP_005155.1	Score = 355 bits (1174), Expect = 2e-96 Identities = 244/615 (39%), Positives = 367/615 (59%), Gaps = 19/615 (3%) 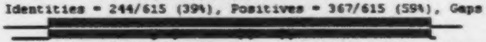 ABCD2/pmp-1	**pmp-1**	C44B7.6
ABCD3	NP_002849.1	Score = 602 bits (2004), Expect = e-170 Identities = 377/612 (61%), Positives = 480/612 (77%), Gaps = 2/612 (0%) ABCD3/pmp-2	**pmp-2**	C44B7.9
ABCD4	NP_005041.1	Score = 261 bits (856), Expect = 5e-68 Identities = 202/577 (35%), Positives = 324/577 (56%), Gaps = 33/577 (5%) 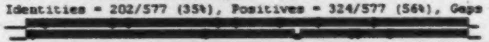 ABCD4/pmp-5	**pmp-5**	T10H9.5a
		Score = 337 bits (1112), Expect = 6e-91 Identities = 251/639 (39%), Positives = 377/639 (58%), Gaps = 54/639 (8%) 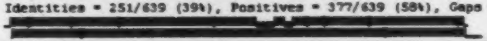 ABCD4/pmp-3	**pmp-3**	C54G10.3
FATP2	NP_003636.1	Score = 291 bits (957), Expect = 5e-77 Identities = 220/574 (38%), Positives = 317/574 (54%), Gaps = 28/574 (4%) 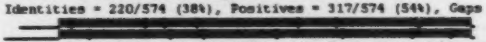		F28D1.9
LACS	NP_001986.2	Score = 510 bits (1697), Expect = e-143 Identities = 340/685 (49%), Positives = 461/685 (66%), Gaps = 23/685 (3%) 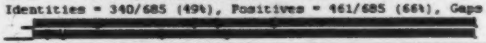		Y65B4BL.5
ECH1	NP_001389.1	Score = 193 bits (629), Expect = 3e-48 Identities = 121/282 (42%), Positives = 177/282 (61%), Gaps = 3/282 (1%) 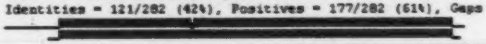		Y25C1A.13

---

[1] Upper protein - human enzyme, lower protein - nematode homolog. Blue colour, regions of homology, red colour, gaps.

Table 3.2.3. Peroxins from other organisms and their homologs in *C. elegans*[1]

Peroxin	Gene Bank #	Alignment[2]	Nematode ORF
Pex4p *Sc*[3]	NP_011649	Score = 63.4 bits (191), Expect = 5e-09 Identities = 50/153 (32%), Positives = 76/153 (48%), Gaps = 16/153 (10%) 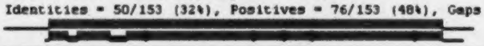	M7.1
Pex4p *Pa*	AAC16238	Score = 78.9 bits (243), Expect = 1e-13 Identities = 52/146 (35%), Positives = 74/146 (50%), Gaps = 24/146 (16%) 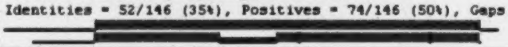	M7.1
Pex8p *Sc*	NP_011591		N/A
Pex9p *Yl*	P45817		N/A
Pex15p *Sc*	NP_014598		N/A
Pex17p *Sc*	NP_014185		N/A
Pex17p *Yl*	P87200		N/A
Pex17p *Pp*	AAF19606		N/A
Pex18p *Sc*	NP_012030		N/A
Pex20p *Yl*	AAC23564	Score = 42.6 bits (121), Expect = 0.009 Identities = 82/419 (19%), Positives = 152/419 (35%), Gaps = 60/419 (14%) 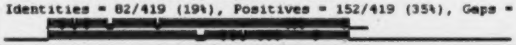	F16D3.2
		Score = 44.7 bits (128), Expect = 0.002 Identities = 59/217 (27%), Positives = 86/217 (39%), Gaps = 31/217 (14%) 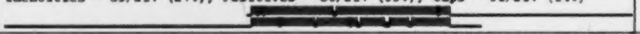	C34E7.1
Pex20p *Nc*	AAN39561	Score = 39.0 bits (109), Expect = 0.11 Identities = 67/317 (21%), Positives = 126/317 (39%), Gaps = 46/317 (14%) 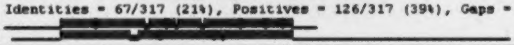	Y59A8A.3
Pex21p *Sc*	AAS56603		N/A
Pex22p *Pp*	AAD45664		N/A
Pex22p *Sc*	NP_009346		N/A
Pex23p *Yl*	AAF22254		N/A
Pex24p *Yl*	AAM68970		N/A
Pex25p *Sc*	NP_015213		N/A
Pex27p *Sc*	NP_014836		N/A
Pex28p *Sc*	NP_012020		N/A
Pex29p *Sc*	NP_010767		N/A
Pex30p *Sc*	NP_013428	Score = 34.6 bits (94), Expect = 5.1 Identities = 36/142 (25%), Positives = 65/142 (45%), Gaps = 10/142 (7%) 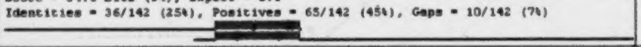	T04A8.13
Pex31p *Sc*	NP_011518		N/A
Pex32p *Sc*	NP_009727		N/A

---

[1] The Expectation values here are much higher than the cut-off 0.00001.

[2] Upper protein - peroxin, lower protein - nematode homolog. This illustrates how little identity there is between nematode and yeast peroxins. Blue colour, regions of homology, red colour, gaps.

[3] *Nc, Neurospora crassa; Pa, Pichia angusta; Pp, Pichia pastoris; Sc, Saccharomyces cerevisiae; Yl, Yarrowia lipolytica; Hp, Hansenula polymorpha; Ct, Candida tropicalis*

3.2.1 Orthologs of human peroxins

All known human peroxins have been analyzed for their potential *C. elegans* counterparts using sequence alignment followed by a homology search.

The search revealed candidate orthologs of two of three known human peroxisomal receptors, the PTS1-receptor (Pex5p) and the mPTS receptor (Pex19p) encoded by the ORFs C34C6.6 and F54F2.8, respectively (Table 3.2.1). No distinct homolog of the human PTS2-receptor, Pex7p, was found in the nematode. In fact, an analysis of the interactions between the *C. elegans* ortholog of human Pex5p and PTS1-containing peroxisomal matrix proteins revealed that the Pex5p-dependent route for the peroxisomal targeting of PTS1 proteins is conserved between humans and nematodes (Gurvitz *et al.*, 2000). In contrast, no evidence of a PTS2-dependent import pathway in the nematode was found (Motley *et al.*, 2000; Petriv *et al.*, 2004).

Candidate orthologs of components of the docking complex for the PTS receptors found in the peroxisomal membrane, the peroxins Pex2p, Pex3p, Pex10p, Pex12p, Pex13p and Pex14p, were found to be encoded by ORFs ZK809.7, C15H9.8, C34E10.4, F08B12.2, F32A5.6 and R07H5.1, respectively. Pex11p (γ isoform), involved in the control of division and inheritance of peroxisomes in humans is represented in *C. elegans* by a protein encoded by the ORF C47B2.8. Two AAA-ATPases that are implicated in peroxisomal protein import and PTS1 receptor recycling, the peroxins Pex1p and Pex6p, have their *C. elegans* homologs encoded by the ORFs C11H1.6 and F39G3.7, respectively (Ghenea *et al.*, 2001).

In addition to a lack of Pex7p, no nematode orthologs were found for the human peroxins Pex16p or Pex26p.

3.2.2 Orthologs of human peroxisomal enzymes

The following candidate *C. elegans* orthologs of human peroxisomal enzymes implicated in lipid metabolism were identified:

Orthologs of human catalase. Catalase converts hydrogen peroxide to water and molecular oxygen. *In silico* searching revealed three candidate *C. elegans* orthologs, Y54G11A.6, Y54G11A.5(A), and Y54G11A.13 of the only known human catalase. Two of these *C. elegans* ORFs have been shown to encode two distinct forms of catalase, a cytosolic catalase, CTL-1, encoded by the ORF Y54G11A.6 (Taub *et al.*, 1999), and a peroxisomal catalase, CTL-2, encoded by the ORF Y54G11A.5(A) (Togo *et al.*, 2000). The third form of catalase encoded by the ORF Y54G11A.13 has not been characterized to date (Petriv and Rachubinski, 2004). Of the three nematode catalases, only peroxisomal catalase CTL-2 contains a PTS1 tripeptide at its carboxyl terminus.

Orthologs of human thiolases. Two human peroxisomal thiolases have been identified. Peroxisomal thiolase 1 (pTH1) acts only on straight-chain substrates and is not reactive with 3-ketoacyl-CoA esters carrying a methyl group at the α carbon (Hashimoto, 1999; Wanders *et al.*, 2001). pTH1 is therefore not involved in the α-oxidation of branched fatty acids (Wanders and Tager, 1998; Hashimoto, 1999). *In silico* searching revealed three candidate *C. elegans* orthologs of human pTH1 (encoded by the gene ACAA1): T02G5.8, T02G5.7 and T02G5.4. The carboxyl termini of all three potential *C. elegans* orthologs of human pTH1 carry tripeptides that closely resemble the PTS1 signal for matrix proteins, namely QKL for T02G5.8, KKL for T02G5.7 and QKL for T02G5.4, all of which have been shown to function in targeting proteins to peroxisomes in other organisms (Motley *et al.*, 2000). Previous studies have also predicted that the *C. elegans* ORFs T02G5.8, T02G5.7 and T02G5.4 represent orthologs of human pTH1 (Gurvitz *et al.*, 2000; Motley *et al.*, 2000).

Peroxisomal thiolase type II (pTH2) is the second human peroxisomal thiolase. pTH2 (which is alternatively termed SCP2/3-ketothiolase or SCPx, for Sterol Carrier Protein x) is required for the metabolism of 3-oxoacyl-CoA esters with an α-methyl branched chain and a very-long straight chain (Hashimoto, 1999; Wanders *et al.*, 2001; Ferdinandusse, 2001, 2004). These CoA esters include intermediates of peroxisomal α-oxidation of tetramethyl-branched phytanic acid (C20), 2-hydroxytetracosanoic (cerebronic, C:24) acid, as well as very-long chain fatty acids (VLCFAs) such as C24:0, C26:0 and C24:6n-3. Oxidation of branched fatty acids and VLCFAs has been shown to be impaired in ZS patients (Sandhir *et al.*, 2000; Jansen *et al.*, 2001). During α-oxidation, phytanic acid is shortened to pristanic acid, which then enters peroxisomal β-oxidation, with the last step catalyzed by pTH2 (Fig. 5.8.1) (Hashimoto, 1999; Wanders *et al.*, 2001). *In silico* searching revealed the ORF Y57A10C.6 of *C. elegans* as a potential ortholog of human pTH2. This ORF encodes the *C. elegans* peroxisomal thiolase, P-44 (Maebuchi *et al.*, 1999), which is required for the metabolism of 3-oxoacyl-CoA esters with a methyl branched chain at the α carbon (Togo *et al.*, 2000). P-44 is homologous to the amino-terminal part, but not to the SCP2 (sterol carrier protein 2) domain, of SCPx (Table 3.2.2), and therefore does not possess lipid transfer activity (Seedorf *et al.*, 1998).

Ortholog of human alkyldihydroxyacetonephosphate synthase. ADHAPS catalyzes the second step in the biosynthesis of plasmalogen in peroxisomes (Hajra and Das, 1996). In humans, defects in ADHAPS result in a peroxisomal single enzyme disorder, RCDP type 3 (de Vet *et al.*, 1999). ADHAPS, which is targeted to peroxisomes by a PTS2 in mammals (de Vet *et al.*, 1997b), contains a PTS1 in *C. elegans* (de Vet *et al.*, 1998). The *C. elegans* counterpart of human ADHAPS is encoded by ORF Y50D7A.7 (Motley *et al.*, 2000).

Orthologs of human ATP-binding cassette (ABC) half-transporters. Four human peroxisomal membrane ABC half-transporters have been identified, namely ALDP (ABCD1), ALDRP (ABCD2), PMP70 (ABCD3) and PMP69 (ABCD4) (Wanders and Tager, 1998; Wanders *et al.*, 2001). They are all members of the so-called ABCD subfamily of the ABC transporters, a family of various membrane transporters (Dean *et al.*, 2001). Different combinations of ABC half-transporters in dimers (peroxisomal half-transporter heterodimers) have been proposed to mediate the transport of distinct subsets of their substrates across the peroxisomal membrane (Dean *et al.*, 2001). ALDP is implicated in the uptake of VLCFA-CoAs, as a deficiency in this ABC half-transporter leads to the accumulation of $C_{26:0}$ VLCFA in the plasma of patients and causes X-ALD (Holzinger *et al.*, 1999). The functions of the other three transporters remain to be established, although, considering their high similarity to each other and to ALDP, they may be involved in fatty acid transport across the peroxisomal membrane (Dean *et al.*, 2001). Indeed, PMP70 has recently been implicated in the peroxisomal transport of 2-methylacyl-CoA esters (Wanders *et al.*, 2001). *In silico* searching revealed five candidate *C. elegans* orthologs of human ABC half-transporters, *i.e.* proteins pmp-1 through 5. Pmp-1 and Pmp-2 show high similarity to two human ALDP-like transporters, ABCD2 and ABCD3. Pmp-4 is also a putative ortholog of human ABCD2.

Orthologs of human acyl-CoA synthetases. An initial step of fatty acid metabolism in humans is catalyzed by one of several acyl-CoA synthetases (Watkins, 1997), all of which ligate CoA to free fatty acid but have different substrate specificities. Their substrates range from LCFAs to VLCFAs (Stanczak *et al.*, 1992; Oikawa *et al.*, 1998; Fujino *et al.*, 2000). Acyl-CoAs formed in the acyl-CoA synthetase-catalyzed reaction are key intermediates in the biosynthesis of various lipids, including triacylglycerols, phospholipids, cholesterol esters and sphingomyelin, and in the β-oxidation of fatty acids (Wanders and Tager, 1998; Wanders *et al.*, 2001). CoA activation was also found to be necessary for activation of phytanic acid prior its α-oxidation in peroxisomes (Watkins *et al.*, 1994), but the enzyme responsible for this action has not yet been identified (Verhoeven and Jacobs, 2001).

Activation of VLCFAs in humans is found both in the ER (Steinberg *et al.*, 2000) and in peroxisomes (Steinberg *et al.*, 1999), but not in mitochondria (Singh and Poulos, 1988). It is performed by a fatty acid transporter family member, FATP2 (Steinberg *et al.*, 1999). A number of *C. elegans* ORFs encode proteins homologous to human FATP2, with the highest similarity scored by a fatty acid transport protein, *Ce*FATPa, encoded by ORF F28D1.9.

The protein encoded by *C. elegans* ORF Y65B4BL.5 has the highest similarity to human acyl-CoA synthetase, FACL1, which has been found to be implicated in LCFA activation at the peroxisomal membrane (Singh *et al.*, 1992). Y65B4BL.5 is also an ortholog of two *S. cerevisiae* peroxisomal acyl-CoA synthetases, Faa1p and Faa2p.

Ortholog of human $\Delta^{3,5}$*-*$\Delta^{2,4}$*-dienoyl-CoA isomerase.* This enzyme catalyzes the first step of auxiliary reactions that allow polyunsaturated fatty acids to enter the normal pathway for the β-oxidation of fatty acids (Filppula *et al.*, 1998). The *C. elegans* genome contains a number of genes encoding likely orthologs of the human peroxisomal $\Delta^{3,5}$-$\Delta^{2,4}$-

dienoyl-CoA isomerase-like protein, ECH1. The candidate nematode ortholog protein with the highest score is encoded by ORF Y25C1A.13.

3.3 RNAi silencing of putative nematode peroxins and peroxisomal enzymes

A comprehensive list of the orthologs chosen for post-transcriptional silencing of their encoding genes by RNAi, along with a graphical representation of the genes themselves, is presented in Table 3.3.1. The high level of sequence identity between ORFs encoding thiolases type 1 (T02G5.4, T02G5.7 and T02G5.8), as well as between ORFs encoding ABC half-transporters selected for silencing (T02D1.5, C44B7.8 and C44B7.9), permitted the use of redundant oligonucleotides (see Materials and Methods and Table 3.3.1). Of note, the ORFs C44B7.8 and C44B7.9, as well as the ORFs T02G5.7 and T02G5.8, are closely positioned in the nematode genome, being separated by approximately 380 bp and 220 bp, respectively. Therefore, discrete silencing of these genes is not possible if they are transcribed as a polycistronic pre-mRNA (Blumenthal and Gleason, 2003). These genes were targeted by triplicate dsRNA.

3.3.1 Deficiency in most of the *C. elegans* homologs of peroxins causes a developmental delay in the worm

The effect of RNAi on *C. elegans* genes encoding various peroxins was evaluated. The offspring of worms 3 days following injection with dsRNAs specific to Pex1p, Pex5p, Pex6p, Pex10p, Pex12p, Pex13p, Pex14p or Pex19p (Fig. 3.3.1) did not produce eggs, an indicative of retarded development and larval stage. On the other hand, at the same time, large number of adults and eggs were found in the offspring of worms that had been injected with control dsRNA or dsRNAs specific to the genes encoding Pex11p or Pex2p (Fig. 3.3.1).

Table 3.3.1. ORFs targeted in RNAi experiments

ORF name	ORF similarity to *H. sapiens* proteins	Gene and dsRNA structure[1]
C11H1.4	Pex1p	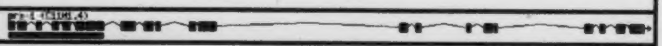 prx-1 (C11H1.4)
ZK809.7	Pex2p	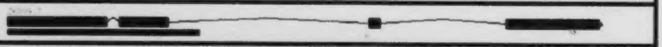
C15H9.8	Pex3p	prx-3 (C15H9.8)
C34C6.6	Pex5p	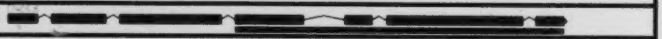
F39G3.7	Pex6p	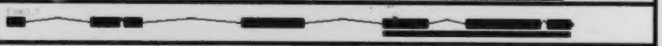
C34E10.4	Pex10p	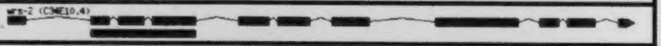
C47B2.8	Pex11p	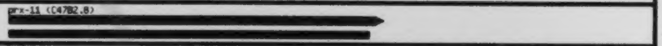 prx-11 (C47B2.8)
F08B12.2	Pex12p	
F32A5.6	Pex13p	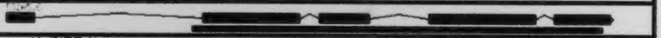
R07H5.1	Pex14p	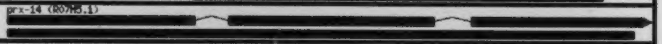 prx-14 (R07H5.1)
F54F2.8	Pex19p	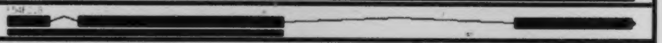
Y54G11A.5A	CAT	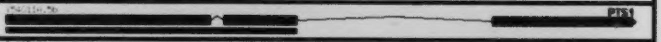
T02G5.4 T02G5.7 T02G5.8	ACAA1	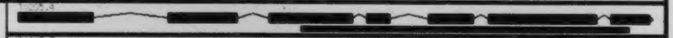 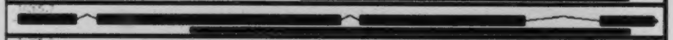 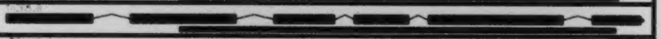
Y57A10C.6	SCP2	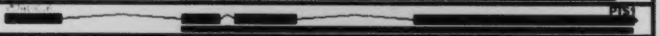
Y50D7A.7	AGPS	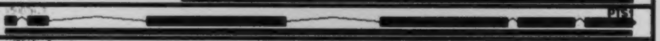
Y65B4BL.5	ACSL1	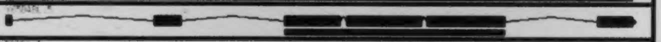
F28D1.9	SLC27A2	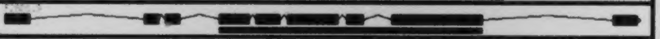
T02D1.5 C44B7.9 C44B7.8	ABCD1,2,3,4	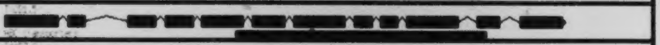 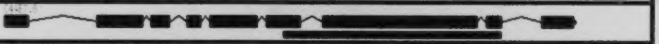
Y25C1A.13	ECH1	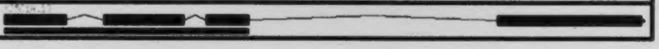

---

[1] dsRNA - pink; exons - blue; introns - line; PTS1 signal - red. Different genes are drawn to different scales.

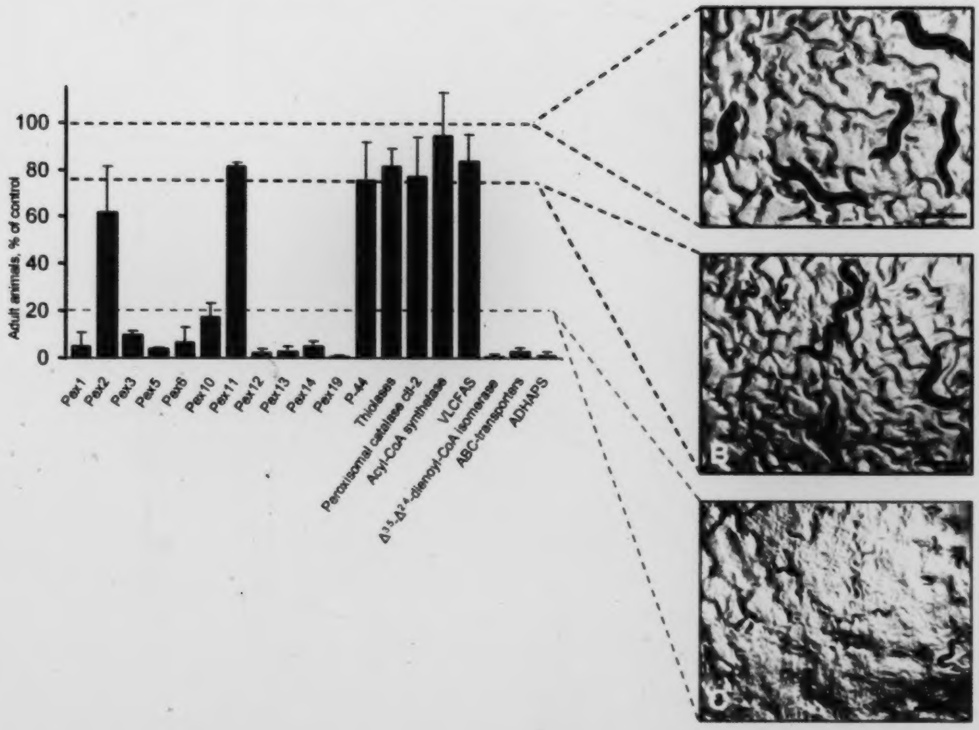

Figure 3.3.1. Percentages of adults in the offspring, and phenotypes of F1 progeny, of worms injected with dsRNAs to target genes encoding various peroxisomal enzymes of lipid metabolism and peroxins. The percentages of adults were evaluated 3 days after injection. The percentage of adults in the offspring of control worms injected with control dsRNA was set at 100% in each independent experiment. Data from 3 to 7 independent experiments are presented (300-700 worms counted). Bright-field photomicrographs represent typical phenotypes and were taken 3 days postinjection. Panel **B** shows worms with slightly delayed development. Panel **C** shows worms that remain at the L1-L2 developmental stage, while panel **A** shows a control experiment in which worms reach the adult stage. Bars, 0.5 mm.

3.4 Effects of deficiency in some nematode putative peroxisomal enzymes on nematode development

The offspring of worms injected with dsRNAs specific to ORFs for various peroxisomal enzymes of lipid metabolism can be divided into two distinct phenotypes (Fig. 3.3.1). The first phenotype showed significant developmental delay in the worms, with almost no adult worms being found 3 days postinjection. The second phenotype was almost indistinguishable from that of control worms, and, compared to control values, 60% to 100% of the F1 progeny of worms injected with dsRNA reached adult stage.

No adults were found in the offspring of worms 3 days after injection with dsRNAs specific to the genes for homologs of ADHAPS, $\Delta^{3,5}$-$\Delta^{2,4}$-dienoyl-CoA isomerase, or the three ABC half-transporters (Fig. 3.3.1). Most of these worms were the size of larvae at the L1, L2 or L3 stage. In contrast, at the same time, large numbers of adults and eggs were observed in the offspring of worms injected with either control dsRNA or dsRNAs specific to genes encoding the type 2 thiolase P-44, the three type 1 thiolases, the three type 1 thiolases and thiolase P-44, catalase ctl-2, the ortholog of yeast acyl-CoA synthetases Faa1p and Faa2p encoded by the ORF Y65B4BL.5, or the ortholog of human VLCFA-CoA synthetase encoded by the ORF F28D1.9 (Fig. 3.3.1). Nevertheless, injection of dsRNA to the gene encoding type 2 thiolase P-44 was effective in reducing the amount of this protein to approximately 10% of its normal levels (Fig. 3.3.2), demonstrating the effectiveness of RNAi in the post-transcriptional silencing of specific genes.

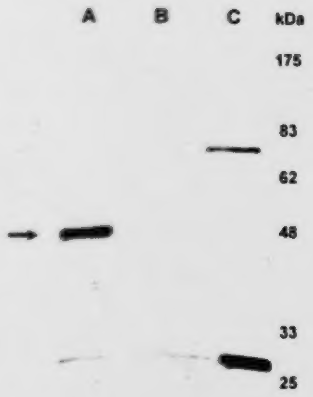

Figure 3.3.2. RNAi reduction of the levels of the type 2 thiolase P44. Lysates of (**A**) worms injected with control dsRNA, (**B**) worms injected with dsRNA specific to the ORF Y57A10C.6 for thiolase P-44 and (**C**) *E. coli* OP50 (a food source for *C. elegans*) were separated by SDS-PAGE, transferred to nitrocellulose, and subjected to immunoblotting with anti-thiolase P-44 antibodies. Equal amounts of protein were loaded in lanes A and B. The position of migration of P-44 is designated by the arrow. The numbers at right indicate the migrations of molecular mass standards (in kDa).

3.5 Functional and morphological changes in nematode peroxisomes lacking subsets of peroxins and peroxisomal enzymes

Motley and coworkers constructed fusions of GFP to a PTS1 to morphologically define peroxisomes within the cells of *C. elegans* (Motley *et al.*, 2000). We have used a similar approach and have integrated an extrachromosomal array encoding a CFP-SKL fusion protein into the genome of *C. elegans* in order to monitor the peroxisomal import of PTS1-targeted matrix proteins and to evaluate the size, number and morphology of peroxisomes in various dsRNA-injected worms. The integrated construct was expressed under the *let858* promoter, which is active in all tissues and at all stages of *C. elegans* development[9]. Expression of this fusion protein in worms produced a punctate pattern of fluorescence characteristic of peroxisomes and which can be visualized in the living organism by fluorescence microscopy (Fig. 3.5.1). The peroxisomal targeting of CFP-SKL was confirmed by double-labeling, immunofluorescence microscopy with antibodies to the well established marker of peroxisomes, P-44 thiolase type 2, and to CFP (Fig. 3.5.1). The punctate fluorescence patterns generated by antibodies to thiolase and to CFP were superimposable and characteristic of peroxisomes.

Visualization of peroxisomes *in vivo* using CFP-SKL unexpectedly revealed considerable differences in peroxisome size and number between various cells. Whereas the hypodermal cells contained high numbers of peroxisomes of uniform size, the gonads, pharyngeal muscle, body wall muscle, and sperm contained almost no detectable peroxisomes. The gut cells displayed significantly smaller, but more abundant peroxisomes than the hypodermal cells. Peroxisomes in the adult worm were smaller and more numerous than peroxisomes in worms at various larval stages. Remarkably, only a diffuse

---

[9] http://ftp.ciwemb.edu/PNF:byName:/FireLabWeb/FireLabInfo/FireLabVectors

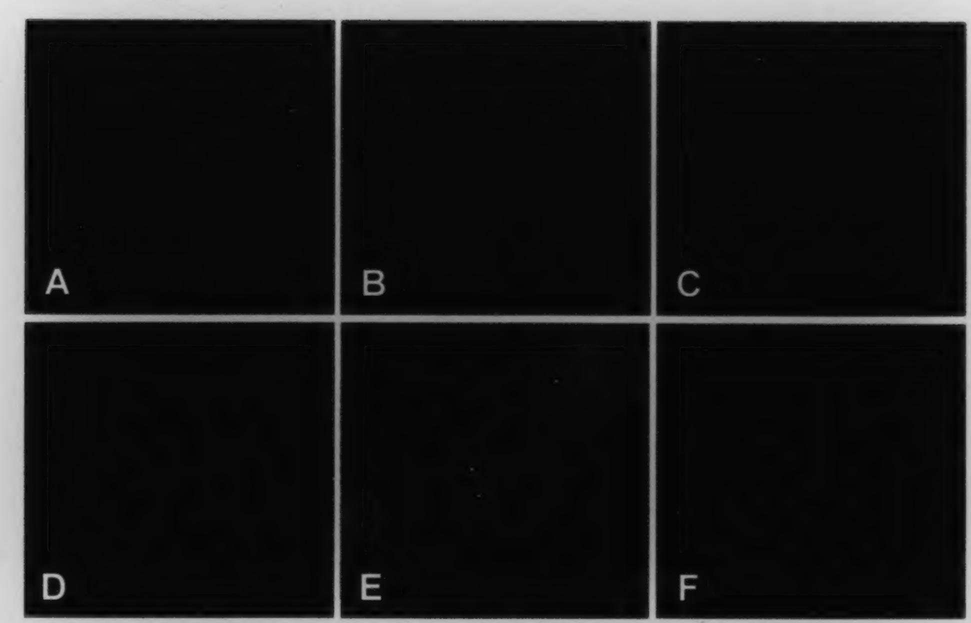

Figure 3.5.1. Localization of CFP-SKL in various nematode cells using direct fluorescence and immunofluorescence microscopy. CFP-SKL shows a diffuse pattern of fluorescence in seam cells, suggesting a lack of peroxisomes in these cells (**A**). In hypodermal cells, anti-thiolase (**D**) and anti-GFP (**F**) antibodies show a punctate pattern characteristic of peroxisomes. The merged image of panels **D** and **F** is shown in panel **E**. Panels **B** and **C**, the fluorescence patterns generated by preimmune sera.

pattern of fluorescence was seen in seam cells, one of the groups of cells from which the hypodermis forms, suggesting a lack of peroxisomes or PTS1-dependant peroxisomal import pathway in these cells (Fig. 3.5.1).

3.5.1 Impairment of PTS1-import in functional knockouts of peroxins

In worms injected with dsRNAs specific to the ORFs encoding Pex3p, Pex5p, Pex12p, Pex13p, Pex14p or Pex19p (Fig. 3.5.2, panels D, E, I, J, K and L, respectively), a diffuse pattern of fluorescence of CFP-SKL, which is characteristic of a cytosolic localization, was observed. Therefore, these worms are deficient in the peroxisomal import of PTS1-targeted matrix proteins. In contrast, injection of dsRNAs specific to ORFs encoding the other peroxins or the other peroxisomal enzymes did not compromise the punctate fluorescence pattern of CFP-SKL characteristic of peroxisomes. It should be noted that a low number of peroxisomes was observed in worms injected with dsRNA to the Pex12p homolog (Fig. 3.5.3 B). The peroxisomes were significantly larger and found in large groups. A similar effect was observed in experiments with Pex3p and Pex14p in those animals that did not display a complete suppression of the targeted genes.

No defect in peroxisome size and/or morphology was found in worms injected with dsRNA specific to the ORFs encoding homologs of Pex1p, Pex2p, Pex6p, Pex10p and Pex11p.

3.5.2 Morphological abnormalities of peroxisomes in thiolase-deficient worms

A difference from the wild-type phenotype of peroxisomes was also observed in experiments with RNAi to P-44 (type 2 peroxisomal thiolase) or the three homologs of

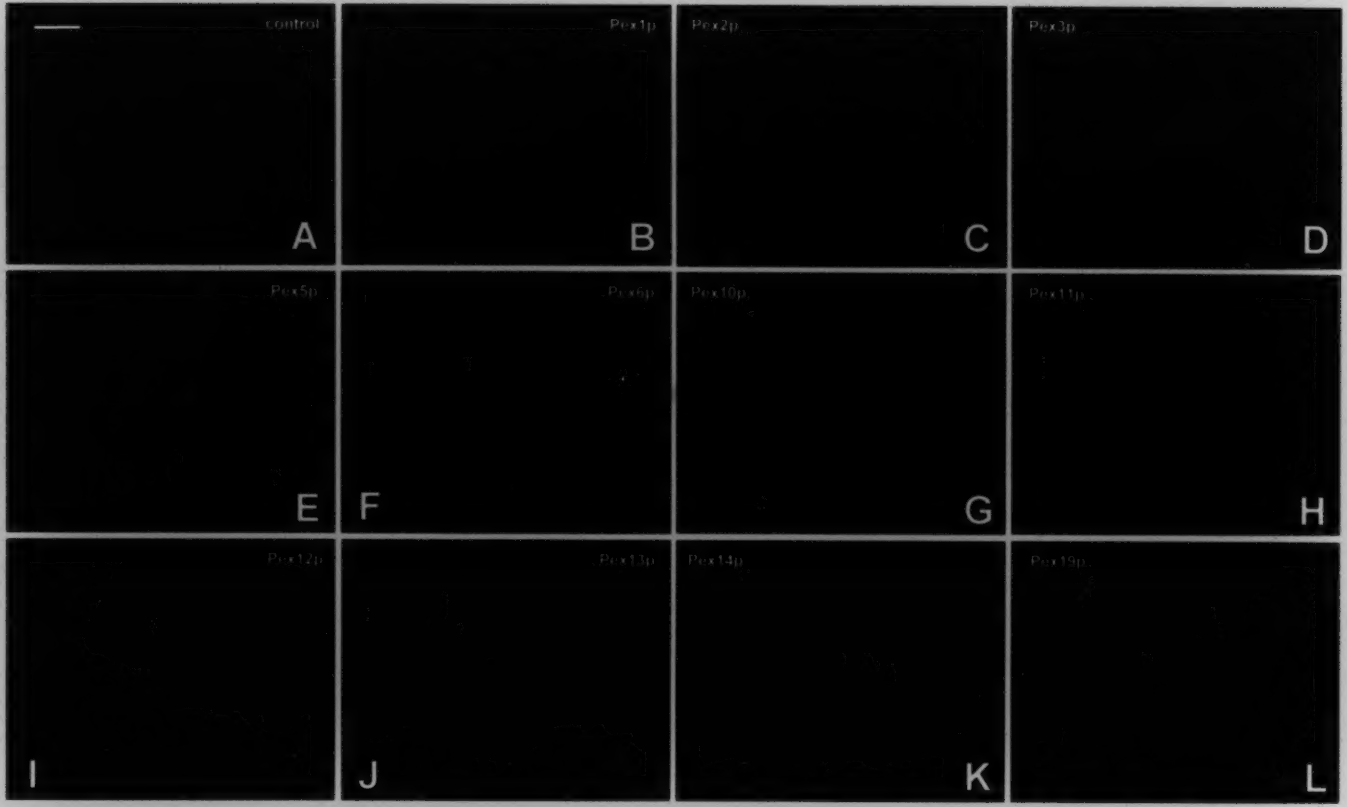
control
A
Pex1p
B
Pex2p
C
Pex3p
D
Pex5p
E
Pex6p
F
Pex10p
G
Pex11p
H
Pex12p
I
Pex13p
J
Pex14p
K
Pex19p
L

Figure 3.5.2. Effect of RNAi on the subcellular localization of the peroxisomal marker CFP-SKL. Worms were injected with control (**A**), Pex1p (**B**), Pex2p (**C**), Pex1p and Pex3p (**D**), Pex5p (**E**), Pex6p (**F**), Pex10p (**G**), Pex11p (**H**), Pex12p (**I**), Pex13p (**J**), Pex14p (**K**), and Pex19p (**L**)-dsRNAs. The punctate pattern of fluorescence is characteristic of peroxisomes, while the diffuse pattern of fluorescence is characteristic of cytosol. Bar, 20 μm.

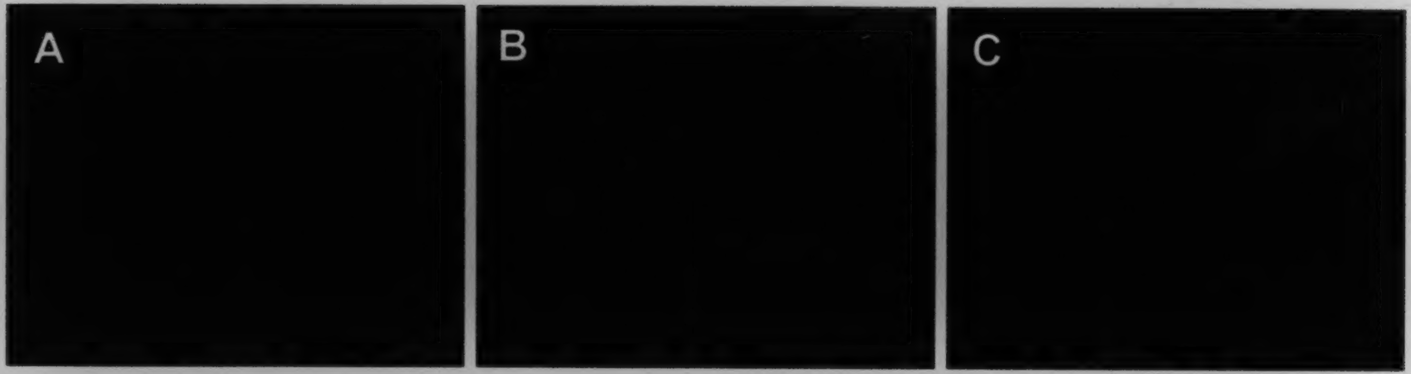

Figure 3.5.3. The size and morphology of peroxisomes in the hypodermis of worms injected with dsRNA to Pex12p or to P-44 (type 2 peroxisomal thiolase). Worms injected with Pex12p-dsRNA (**B**) accumulate peroxisomes that are fewer in number and of much larger size than those found in worms injected with control dsRNA (**A**). The injection of P-44-dsRNA (**C**) causes the accumulation of clusters of fewer irregularly shaped peroxisomes of variable size, most of which are larger than the round, uniformly sized and randomly distributed peroxisomes found in worms injected with control dsRNA (**A**).

type 1 thiolases plus P-44. Whereas peroxisomes in worms injected with control dsRNA were round in shape, of uniform size and randomly distributed in the organism, the injection of dsRNA to P-44 caused the accumulation of clusters of peroxisomes that were fewer in number, irregular in shape and of variable size (Fig. 3.5.3 C), with most peroxisomes being larger than those found in worms injected with control dsRNA (Fig. 3.5.3 A). A similar phenomenon has been observed in human, mammalian and yeast mutant cells deficient in other enzymes of β-oxidation. In these mutant cells, loss of the enzymatic activity of acyl-CoA oxidase (Fan *et al.*, 1998; Chang *et al.*, 1999; van Roermund *et al.*, 2000), fatty acyl-CoA synthetase (van Roermund *et al.*, 2000), and/or another peroxisomal β-oxidation enzyme, 2-enoyl-CoA hydratase/*D*-3-hydroxyacyl-CoA dehydrogenase (Chang *et al.*, 1999; Smith *et al.*, 2000), resulted in significant changes in peroxisome size and/or number. The primary targets for this so called metabolic control of peroxisome abundance (Chang *et al.*, 1999) are likely the levels of other peroxisomal β-oxidation enzymes that are dramatically increased by the loss of acyl-CoA oxidase (Fan *et al.*, 1998) or 2-enoyl-CoA hydratase/*D*-3-hydroxyacyl-CoA dehydrogenase (Smith *et al.*, 2000) enzymatic activity. The resultant overproduction of abundant matrix proteins leads to a significant change in peroxisome size (Chang *et al.*, 1999; Smith *et al.*, 2000; van Roermund *et al.*, 2000) and/or number (Fan *et al.*, 1998; Smith *et al.*, 2000).

3.6 DISCUSSION

RNAi, using dsRNA specific to a particular target locus, is now routinely employed to determine the likely loss-of-function phenotype of a gene (Bosher and Labouesse, 2000). The specificity and potency of RNAi make it ideal for investigating gene function starting only with genomic sequence (Gonczy *et al.*, 2000). However, as with all RNAi experiments, there is a strong possibility that post-transcriptional silencing may not have reduced the expression of some genes below a threshold necessary to display a phenotype. We should note also that nearly all mRNAs from *C. elegans* neurons are refractory to RNA interference (Kennedy *et al.*, 2004), but peroxisomes are known to be of major importance for normal development of the nervous system (Powers and Moser, 1998). Thus, results obtained using RNAi must be interpreted with caution until confirmed by gene knockouts.

Despite some caveats, this study evaluates the roles for various peroxisomal enzymes and peroxins in peroxisome function and biogenesis in the nematode *C. elegans* and compares these roles to those established for the homologous proteins in classical systems such as yeast and human. It also defines the peroxisomal metabolic functions and peroxins essential for normal development of *C. elegans* (Fig. 3.7.1). Our data suggest that the nematode model has unique features in peroxisome function and, within certain parameters, can be employed as a powerful tool with which to study the molecular defects underlying the human peroxisomal disorders.

3.6.1 Functions of *C. elegans* peroxins.

RNAi phenotypes of *C. elegans* peroxisomes labeled with a fluorescent marker confirm that most ORFs selected as candidate genes encoding orthologs of human peroxins are indeed involved in peroxisome biogenesis/peroxisomal import processes. According to *in silico* analysis, the peroxin Pex3p is encoded by ORF C15H9.8, Pex5p by ORF C34.C6.6, Pex12p by ORF F08B12.2, Pex13p by ORF F32A5.6, Pex14p by ORF

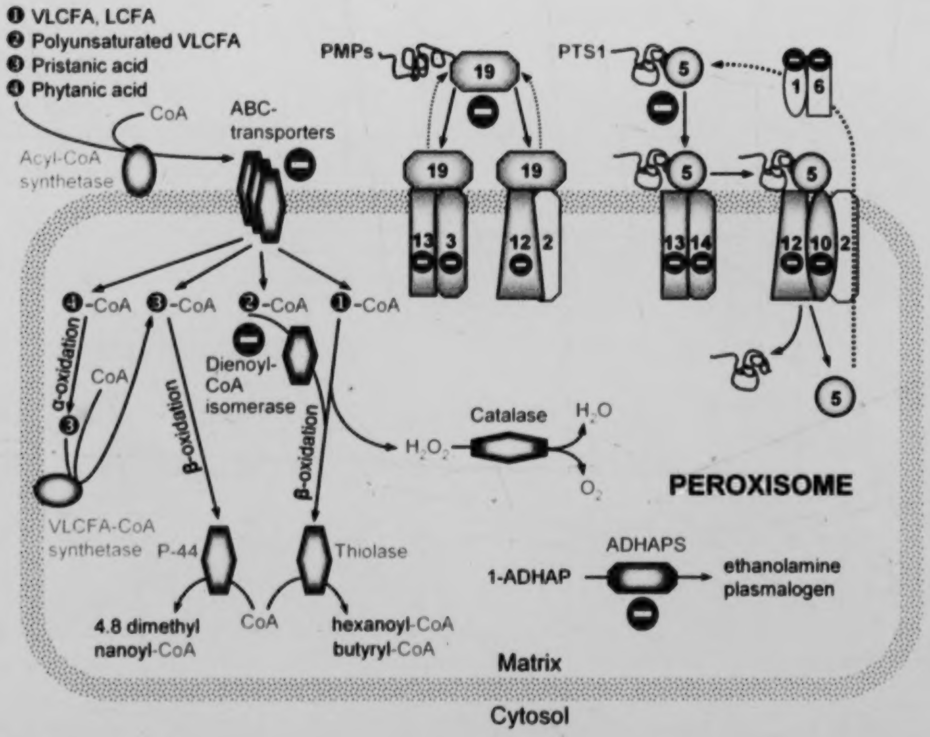
❶ VLCFA, LCFA
❷ Polyunsaturated VLCFA
❸ Pristanic acid
❹ Phytanic acid
CoA
Acyl-CoA synthetase
ABC-transporters
PMPs
19
PTS1
5
1
6
13
3
12
2
14
10
❹-CoA
❸-CoA
❷-CoA
❶-CoA
α-oxidation
CoA
❸
Dienoyl-CoA isomerase
β-oxidation
β-oxidation
Catalase
H₂O
H₂O₂
O₂
PEROXISOME
VLCFA-CoA synthetase
P-44
Thiolase
ADHAPS
1-ADHAP
ethanolamine plasmalogen
4.8 dimethyl nanoyl-CoA
CoA
hexanoyl-CoA butyryl-CoA
Matrix
Cytosol

Figure 3.7.1. Peroxisomal metabolic pathways and peroxins involved in the development of *C. elegans*. Pex1p (**1**), Pex2p (**2**), Pex3p (**3**), Pex5p (**5**), Pex6p (**6**), Pex10p (**10**), Pex12p (**12**), Pex13p (**13**), Pex14p (**14**), Pex19p (**19**) and peroxisomal enzymes were targeted by RNAi, and the next progeny of worms was analyzed for developmental delay. Interference causing developmental delay is indicated in red. Developmental delays that did not correlate with peroxisomal defects are shown in black.

R07H5.1, and Pex19p by ORF F54F2.8 (Table 3.2.1). RNAi to these genes not only led to defects in peroxisomal function but also drastically inhibited nematode ontogenesis, suggesting a link between the two processes. Notably, a similar link for the above named peroxins was found in humans (Moser, 1998; Wanders, 1999).

Human peroxisomal ABC half-transporters, including ALDP and ALDRP, and their *C. elegans* counterparts are PMPs (Dean *et al.*, 2001). In *C. elegans*, ADHAPS is targeted to peroxisomes by a PTS1 (de Vet *et al.*, 1998; Motley *et al.*, 2000). This study shows that these proteins are required for the normal development of *C. elegans* (Section 3.7.2). In light of this finding, it is not surprising that deficiencies in the cytosolic shuttling receptors for the peroxisomal sorting of PMPs and PTS1-targeted proteins (Pex19p and Pex5p, respectively) as well as deficiencies in the membrane "anchor" for Pex19p (Pex3p), as well as components of the docking (Pex13p and Pex14p) and translocation (Pex12p) machineries for PTS1-containing matrix proteins are essential for the development of *C. elegans*.

As for candidate genes for the peroxins Pex1p, Pex2p, Pex6p, Pex10p and Pex11p (encoded by ORFs C11H1.4, ZK809.7, F39G3.7, C34E10.4 and C47B2.8, respectively), no defect in peroxisomal import was detected in RNAi experiments (Fig. 3.5.2). This finding is rather surprising, since in all other organisms studied so far, Pex1p, Pex2p, Pex6p and Pex10p are essential for the peroxisomal import of matrix proteins (Subramani *et al.*, 2000; Titorenko and Rachubinski, 2001b; Hazra *et al.*, 2002;) and, in human cells, Pex1, Pex2p, Pex6p and Pex10p are required for recycling of the PTS1 receptor to the cytosol (Titorenko and Rachubinski, 2001b). In addition, we observed significant developmental delay in Pex1p and Pex6p RNAi experiments (Fig. 3.3.1). dsRNA$_{Pex1p}$- and dsRNA$_{\mathrm{Pex\ 6p}}$-treated worms displayed a similar phenotype of a short, undeveloped body (Fig. 3.7.2), yet imported a CFP-SKL peroxisomal reporter. This fact indicates that the ORFs C11H1.4 and F39G3.7 do not encode peroxins but rather proteins with high similarity to Pex1p and Pex6p and having other cellular functions. In fact, due to the highly conserved AAA-ATPase domain that is found in Pex1p and Pex6p and is shared among many families of proteins (Lupas and Martin, 2002), a BLAST comparison of human Pex1p and Pex6p and proteins encoded by the *C. elegans* genome results in a large number of hits (Tables 3.7.1. and 3.7.2). This demonstrates a high probability that the nematode counterparts of these human peroxins are encoded by ORFs other than those predicted earlier (Ghenea *et al.*, 2001). This is supported by the observation that heterologous expression of *C. elegans* Pex1p in the *S. cerevisiae pex1* mutant did not complement the mutation (Ghenea *et al.*, 2001). On the other hand, one should consider the fact that the PTS2 pathway for the peroxisomal import of matrix proteins, which had previously been found in all organisms studied, has been shown to be absent in *C. elegans* (Motley *et al.*, 2000; Petriv *et al.*, 2004). Moreover, proteins that in all other studied organisms are targeted to the peroxisome by a PTS2 have acquired a PTS1 in *C. elegans* (Gurvitz *et al.*, 2000; Motley et al, 2000). It is possible that, due to the lack of a PTS2 import machinery and the great abundance of PTS1-targeted proteins, the levels of the cytosolic shuttling receptor Pex5p and/or other components of the PTS1-dependent import machinery may be significantly higher in *C. elegans* than in other organisms. Furthermore, a homolog of mammalian Pex26p, which recruits Pex1p/Pex6p complex to the membrane (Matsumoto *et al.*, 2003), is not found in *C. elegans* (Table 3.2.1). Therefore, Pex1p-, Pex6p-, Pex2p- and Pex10p-dependent recycling of the PTS1 receptor in the nematode may not be essential for

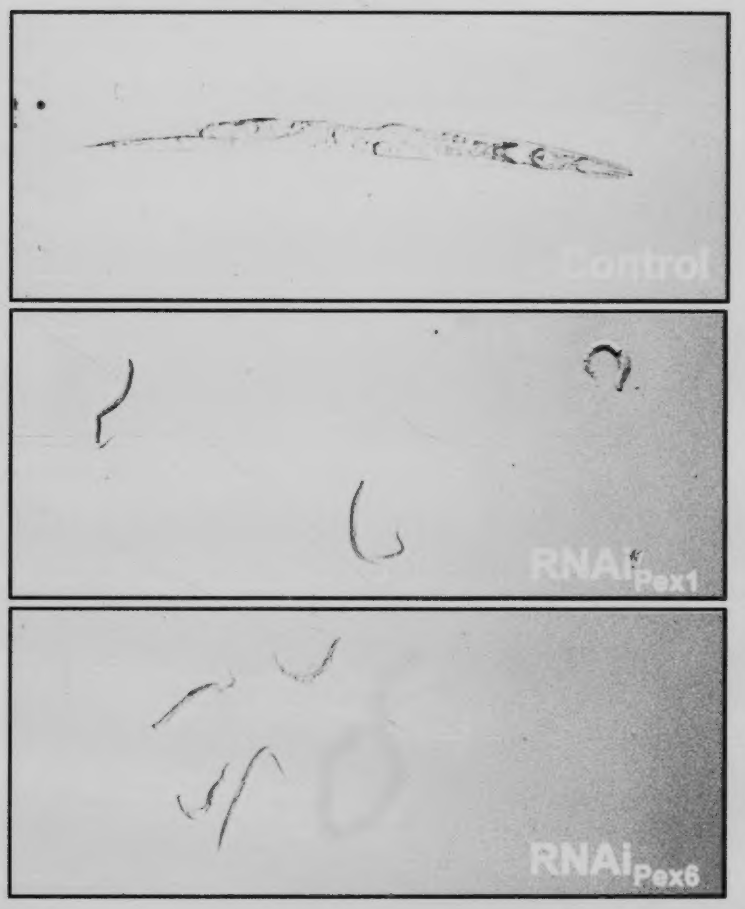
Control
RNAi$_{Pex1}$
RNAi$_{Pex6}$

Figure 3.7.2. Characteristic phenotypes of dsRNA$_{Pex1}$- and dsRNA$_{Pex6}$-injected worms. Morphology of 3-day old worms treated with dsRNA$_{Pex1}$, dsRNA$_{Pex6}$, or RNAi$_{control}$. Bar, 0.1 mm.

Table 3.7.1. BLAST alignments for *H. sapiens* Pex1p vs *C. elegans* proteins[1]	HITS
prx-1 phi-31 C41C4.8 Y48C3A.7 mac-1 prx-6 K04G2.3 rpt-4 rpt-6 F56F11.4 rpt-3 rpt-2 rpt-5 rpt-1 F11A10.1 C10G11.8 M03C11.5 nsf-1 C24B5.2 phi-23 F32D1.1 K04D7.2 mei-1 phi-25 Y38F2AR.7 Y47C4A.1 Y108F1.1 F10B5.5 F54B3.3	29

Gene	GenBank	Synonyms/Description	Match Length	% Iden	% Sim	High Score	E Val
prx-1	CAA94120.2	prx-1, pex1, C11H1.6, C11H1.4 Peroxisome assembly factor 1, putative ATPase involved in growth rate regulation	991	27%	45%	703	5e-70
phi-31	CAA90050.1	phi-31, C06A1.1 Putative ATPase that is involved in suppression of polyglutamylation	553	34%	51%	693	2e-68
C41C4.8	CAA88105.1	C41C4.8 Putative ATPase that is involved in suppression of polyglutamylation, positive regulation of growth rate, and locomotory behavior	543	33%	51%	696	1e-67
Y48C3A.7	CAB55106.2	Y48C3A.7, Y48C3A.1 Protein with very strong similarity to C. elegans MAC-1, which is an AAA-ATPase that blocks cell death caused by *C. elegans* CED-4, member of the ATPase family associated with various cellular activities	538	33%	51%	617	8e-60
mac-1	AAL05624.1	mac-1, Y48C3A.6 AAA-ATPase that blocks cell death caused by CED-4, required for fat accumulation	538	33%	50%	606	4e-58
prx-6	BAA76440.1	prx-6, pex6, pex-6, F39G3.7 Peroxin 6, unessential putative peroxisomal target signal type I (PTS1) receptor, required for normal development at the first larval stage	313	38%	60%	520	7e-50
K04G2.3	CAB00040.1	K04G2.3 Member of the ATPase family associated with various cellular activities that is involved in embryogenesis and positive growth regulation	331	39%	57%	526	3e-49
rpt-4	AAB70326.2	rpt-4, F23F1.8 Proteasome regulatory particle ATPase-like 4, putative 26S proteasome 19S regulatory complex ATPase subunit that is required for embryogenesis, morphogenesis, positive growth regulation, locomotory behavior, and reproduction	291	36%	57%	457	8e-46
rpt-6	CAB11558.1	rpt-6, Y49E10.B, Y49E10.1 Putative ATPase subunit of the 19S regulatory complex of the 26S proteasome that functions in embryonic and larval development	279	35%	57%	443	3e-44
F56F11.4	AAM48537.1	F56F11.4 Protein with strong similarity to *C. elegans* RPT-6, which is involved in embryonic and larval development and is a putative ATPase and part of the 26S proteasome, member of the ATPase family associated with various cellular activities	280	36%	55%	438	8e-44
rpt-3	AAA20608.1	rpt-3, F23F12.6 Proteasome regulatory particle ATPase-like 3, putative 26S proteasome 19S regulatory complex ATPase subunit that is required for embryonic development and reproduction	253	36%	58%	426	3e-42
rpt-2	AAB65906.1	rpt-2, F29G9.5 Proteasome regulatory particle ATPase-like 2, putative 26S proteaseome 19S regulatory complex ATPase subunit required for embryonic development	254	34%	57%	414	6e-41
rpt-5	AAC19196.1	rpt-5, F56H1.4 Proteasome regulatory particle, ATPase-like 5, putative ATPase subunit of the 19S regulatory complex of the 26S proteasome that is required for embryonic, post-embryonic development, and reproduction	225	38%	60%	407	5e-40
rpt-1	CAB01414.1	rpt-1, C52E4.4 Proteasome regulatory particle ATPase-like 1, subunit of the 19S regulatory complex of the 26S proteasome that is required for embryonic, post-embryonic development, and reproduction	245	35%	57%	402	2e-39
F11A10.1	CAA92684.1	F11A10.1 Putative ATPase of the AAA-family of ATPases, functions in germ line meiosis	232	38%	58%	391	1e-37
C10G11.8	AAB42248.2	C10G11.8 Protein with high similarity to proteasome 26S subunit ATPase 1 (human PSMC1), which is an ATPase subunit of the 26S proteasome complex that interacts with viral proteins, member of the ATPase family associated with various cellular activities	235	34%	54%	373	3e-36
M03C11.5	CAA88955.1	M03C11.5 Member of the ATPase family associated with various	213	39%	60%	374	7e-36

---

[1] www.incyte.com on-line service was used for BLAST comparison

		cellular activities and the M41 peptidase family of zinc metalloproteases, has a region of high similarity to a region of *S. cerevisiae* Yme1p, which acts in the degradation of improperly folded proteins					
nsf-1	CAB09531.1	nsf-1, H15N14.2 **NSF (*N*-ethylmaleimide sensitive secretion factor) homolog 1, protein involved in embryonic development**	269	36%	55%	373	5e-35
C24B5.2	AAM29664.1	C24B5.2 **Member of the ATPase family associated with various cellular activities, has moderate similarity to *C. elegans* MEI-1, which is a putative ATPase involved in microtubule disassembly during meiotic spindle formation and is required for embryonic development**	258	34%	53%	337	3e-31
phi-23	AAL60660.2	phi-23, Y47G6A.10 **Protein involved in embryogenesis, larval growth, and reproduction**	249	36%	53%	344	3e-30
F32D1.1	AAB65351.1	F32D1.1 **Member of the ATPase family associated with various cellular activities, has a region of high similarity to a region of spastic paraplegia 4 (spastin, human SPG4), which is an ATPase that is associated with hereditary spastic paraplegia upon gene mutation**	250	30%	53%	330	3e-28
K04D7.2	CAA93516.2	K04D7.2 **Member of the ATPase family associated with various cellular activities, has low similarity to *C. elegans* RPT-1, which is a putative ATPase subunit of the 19S regulatory complex of the 26S proteasome that is required for development and reproduction**	236	34%	53%	308	3e-28
mei-1	CAD56596.1	mei-1, T01G9.5B, T01G9.5 **Meiosis 1, putative ATPase that is involved in microtubule disassembly during meiotic spindle formation and is required for early embryonic development**	226	37%	59%	339	4e-27
phi-25	AAK29883.3	phi-25, Y34D9A.10, Y34D9A.A **Protein involved in larval development, regulation of movement, locomotory behavior, embryogenesis, and positive growth regulation**	286	25%	44%	222	1e-16
Y38F2AR.7	AAK68448.2	Y38F2AR.7, Y38F2A_5743.B, Y38F2AR.H **Member of the ATPase family associated with various cellular activities and the M41 peptidase family of zinc metalloproteases, has high similarity to a region of spastic paraplegia 7 (paraplegin, human SPG7), which is a putative metalloprotease**	165	30%	52%	215	5e-16
Y47C4A.1	AAK85500.1	Y47C4A.1, Y47C4A_211.A, Y47C4A.A **Member of the ATPase family associated with various cellular activities and of the M41 peptidase family of Zn metalloproteases, has high similarity to a region of *S. cerevisiae* Afg3p, which is involved in proteolysis and chaperon activity in mitochondria**	108	34%	56%	146	5e-09
Y108F1.1	AAN01432.2	Y108F1.1 **Member of the ATPase family associated with various cellular activities and the M41 peptidase family of zinc metalloproteases, has very strong similarity to uncharacterized *C. elegans* Y47C4A.1**	108	34%	56%	146	5e-09
F10B5.5	CAA88312.1	F10B5.5 **Member of the ATPase family associated with various cellular activities, has moderate similarity to thyroid hormone receptor-interacting protein 13 (human TRIP13), which is a transcription cofactor that binds the thyroid hormone receptor**	198	27%	41%	126	8e-06
F54B3.3	CAA88471.2	F54B3.3 **Protein involved in reproduction, larval growth, and embryogenesis**	254	25%	43%	116	3e-04

Table 3.7.2. BLAST alignments for *H. sapiens* Pex6p vs *C. elegans* proteins[1]	HITS
C41C4.8 prx-6 phi-31 Y48C3A.7 mac-1 K04G2.3 prx-1 rpt-6 F56F11.4 rpt-5 rpt-2 rpt-1 rpt-3 rpt-4 C10G11.8 F11A10.1 phi-23 F32D1.1 C24B5.2 M03C11.5 nsf-1 mei-1 K04D7.2 Y38F2AR.7 phi-25 Y47C4A.1 Y108F1.1 F10B5.5 F54C9.6 F54B3.3 rfc-1 C34B2.6	32

Gene	GenBank	Synonyms/Description	Match Length	% Iden	% Sim	High Score	E Val
C41C4.8	[illegible]	C41C4.8 Putative ATPase that is involved in suppression of polyglutamylation, positive regulation of growth rate, and locomotory behavior	473	39%	60%	809	2e-77
prx-6	[illegible]	prx-6, pex6, pex-6, F39G3.7 Peroxin 6, unessential putative peroxisomal target signal type I (PTS1) receptor, required for normal development at the first larval stage	494	36%	56%	758	9e-77
phi-31	[illegible]	phi-31, C06A1.1 Putative ATPase that is involved in suppression of polyglutamylation	473	38%	58%	785	1e-76
Y48C3A.7	[illegible]	Y48C3A.7, Y48C3A.1 Protein with very strong similarity to C. elegans MAC-1, which is an AAA-ATPase that blocks cell death caused by *C. elegans* CED-4, member of the ATPase family associated with various cellular activities	663	32%	49%	753	7e-76
mac-1	[illegible]	mac-1, Y48C3A.6 AAA-ATPase that blocks cell death caused by CED-4, required for fat accumulation	663	32%	48%	737	5e-74
K04G2.3	[illegible]	K04G2.3 Member of the ATPase family associated with various cellular activities that is involved in embryogenesis and positive growth regulation	365	36%	56%	539	4e-50
prx-1	[illegible]	prx-1, pex1, C11H1.6, C11H1.4 Peroxisome assembly factor 1, putative ATPase involved in growth rate regulation	493	34%	50%	508	1e-49
rpt-6	[illegible]	rpt-6, Y49E10.B, Y49E10.1 Putative ATPase subunit of the 19S regulatory complex of the 26S proteasome that functions in embryonic and larval development	253	43%	64%	477	1e-47
F56F11.4	[illegible]	F56F11.4 Protein with strong similarity to *C. elegans* RPT-6, which is involved in embryonic and larval development and is a putative ATPase and part of the 26S proteasome, member of the ATPase family associated with various cellular activities	254	43%	63%	468	1e-46
rpt-5	[illegible]	rpt-5, F56H1.4 Proteasome regulatory particle, ATPase-like 5, putative ATPase subunit of the 19S regulatory complex of the 26S proteasome that is required for embryonic, post-embryonic development, and reproduction	338	34%	54%	425	4e-41
rpt-2	[illegible]	rpt-2, F29G9.5 Proteasome regulatory particle ATPase-like 2, putative 26S protcaseome 19S regulatory complex ATPase subunit required for embryonic development	236	42%	61%	420	4e-41
rpt-1	[illegible]	rpt-1, C52E4.4 Proteasome regulatory particle ATPase-like 1, subunit of the 19S regulatory complex of the 26S proteasome that is required for embryonic, post-embryonic development, and reproduction	233	39%	60%	415	1e-40
rpt-3	[illegible]	rpt-3, F23F12.6 Proteasome regulatory particle ATPase-like 3, putative 26S proteasome 19S regulatory complex ATPase subunit that is required for embryonic development and reproduction	245	40%	60%	410	8e-40
rpt-4	[illegible]	rpt-4, F23F1.8 Proteasome regulatory particle ATPase-like 4, putative 26S proteasome 19S regulatory complex ATPase subunit that is required for embryogenesis, morphogenesis, positive growth regulation, locomotory behavior, and reproduction	230	40%	60%	406	1e-39
C10G11.8	[illegible]	C10G11.8 Protein with high similarity to proteasome 26S subunit ATPase 1 (human PSMC1), which is an ATPase subunit of the 26S proteasome complex that interacts with viral proteins, member of the ATPase family associated with various cellular activities	242	37%	60%	389	2e-37
F11A10.1	[illegible]	F11A10.1 Putative ATPase of the AAA-family of ATPases, functions in germ line meiosis	275	37%	55%	382	5e-36
phi-23	[illegible]	phi-23, Y47G6A.10 Protein involved in embryogenesis, larval growth, and reproduction	311	36%	53%	413	2e-35

---

[1] www.incyte.com on-line service was used for BLAST comparison

F32D1.1	AAB65351.1	F32D1.1 Member of the ATPase family associated with various cellular activities, has a region of high similarity to a region of spastic paraplegia 4 (spastin, human SPG4), which is an ATPase that is associated with hereditary spastic paraplegia upon gene mutation	282	33%	54%	371	2e-31
C24B5.2	AAM29664.1	C24B5.2 Member of the ATPase family associated with various cellular activities, has moderate similarity to *C. elegans* MEI-1, which is a putative ATPase involved in microtubule disassembly during meiotic spindle formation and is required for embryonic development	281	32%	50%	336	4e-31
M03C11.5	CAA88955.1	M03C11.5 Member of the ATPase family associated with various cellular activities and the M41 peptidase family of zinc metalloproteases, has a region of high similarity to a region of *S. cerevisiae* Yme1p, which acts in the degradation of improperly folded proteins	266	38%	53%	336	1e-30
nsf-1	CAB09531.1	nsf-1, H15N14.2 NSF (*N*-ethylmaleimide sensitive secretion factor) homolog 1, protein involved in embryonic development	221	38%	59%	327	1e-29
mei-1	CAD56596.1	mei-1, T01G9.5B, T01G9.5 Meiosis 1, putative ATPase that is involved in microtubule disassembly during meiotic spindle formation and is required for early embryonic development	295	35%	51%	336	6e-26
K04D7.2	CAA93516.2	K04D7.2 Member of the ATPase family associated with various cellular activities, has low similarity to *C. elegans* RPT-1, which is a putative ATPase subunit of the 19S regulatory complex of the 26S proteasome that is required for development and reproduction	245	34%	51%	282	8e-25
Y38F2AR.7	AAK68448.2	Y38F2AR.7, Y38F2A_5743.B, Y38F2AR.H Member of the ATPase family associated with various cellular activities and the M41 peptidase family of zinc metalloproteases, has high similarity to a region of spastic paraplegia 7 (paraplegin, human SPG7), which is a putative metalloprotease	188	32%	52%	245	3e-18
phi-25	AAK29883.3	phi-25, Y34D9A.10, Y34D9A.A Protein involved in larval development, regulation of movement, locomotory behavior, embryogenesis, and positive growth regulation	291	30%	49%	247	2e-14
Y47C4A.1	AAK85500.1	Y47C4A.1, Y47C4A_211.A, Y47C4A.A Member of the ATPase family associated with various cellular activities and of the M41 peptidase family of Zn metalloproteases, has high similarity to a region of S. cerevisiae Afg3p, which is involved in proteolysis and chaperon activity in mitochondria	130	32%	53%	146	6e-09
Y108F1.1	AAN91432.2	Y108F1.1 Member of the ATPase family associated with various cellular activities and the M41 peptidase family of zinc metalloproteases, has very strong similarity to uncharacterized *C. elegans* Y47C4A.1	130	32%	53%	146	6e-09
F10B5.5	CAA88312.1	F10B5.5 Member of the ATPase family associated with various cellular activities, has moderate similarity to thyroid hormone receptor-interacting protein 13 (human TRIP13), which is a transcription cofactor that binds the thyroid hormone receptor	191	28%	45%	143	1e-07
F54C9.6	CAA90252.1	F54C9.6 Protein involved in embryogenesis, osmoregulation, and positive growth regulation	170	28%	46%	134	1e-07
F54B3.3	CAA88471.1	F54B3.3 Protein involved in reproduction, larval growth, and embryogenesis	137	31%	53%	123	5e-06
rfc-1	CAA99812.1	rfc-1, C54G10.2 Replication factor C1, the large subunit of clamp-loading protein replication factor C complex, functions in embryonic development, germ line mitosis, gonad development, fertility, and genome stability of somatic cells	121	31%	46%	108	3e-04
C34B2.6	AAB97538.1	C34B2.6 Protein with high similarity to protease serine 15 (rat Prss15), which may be a mitochondrial matrix peptidase, member of the ATPase and ATP-dependent protease La (LON) domain containing families, has a Lon protease (S16) C-terminal proteolytic domain	125	26%	44%	105	7e-04

the process of matrix protein import. Possibly, these proteins took over different, or lost their original cellular functions during the evolutionary process. Experimental confirmation of this hypothesis awaits evaluation of the efficiency of peroxisomal protein import in Pex1p-, Pex2p-, Pex6p- and Pex10p-deficient worms in which the expression levels of Pex5p and/or other components of the peroxisomal targeting/docking/translocation machinery could be precisely manipulated and varied over a wide range.

The nematode ORF C47B2.8 encodes a putative homologue of one of the three isoforms of the human peroxin Pex11p, Pex11p-γ (Tanaka *et al.*, 2003). Pex11p-γ, similarly to the other two isoforms of Pex11p, Pex11p-α and Pex11p-β, is proposed to be involved in control of peroxisome division in mammals (Titorenko and Rachubinski, 2001b). No particular difference in peroxisome size, number or morphology was observed in worms injected with dsRNA specific to ORF C47B2.8. Neither affected the ontogenesis of these worms. Similarly, knock-out mice devoid of both Pex11p-α and Pex11p-β contain numerous peroxisomes, exhibit no obvious peroxisomal protein import defect and are only mildly affected in several key biochemical activities (Li *et al.*, 2002). Yet, these mice die early after birth because of severe neurological defects. As nearly all mRNAs from *C. elegans* neurons are refractory to RNA interference (Kennedy *et al.*, 2004), we cannot rule out a possible important role for the nematode Pex11p-γ homolog in the nervous system.

In conclusion, it must be emphasized that it would be premature at this time to dismiss a requirement for Pex2p and Pex11p and in the development of *C. elegans*.

3.6.2 Deficiency in *C. elegans* peroxisomal enzymes

Injection of dsRNAs specific to the ORFs encoding the three *C. elegans* orthologs of the membrane-embedded ABC half-transporters caused a substantial delay in the development of the nematode. In humans, ALDP has been implicated in the transport of VLCFA-CoAs across the peroxisomal membrane (Wanders *et al.*, 2001), and a similar role has been suggested for other ABC half-transporters (Dean *et al.*, 2001). A defect in ALDP in humans causes developmental delay and severe neurological deficits and leads to the most common peroxisomal disease, X-ALD (Wanders and Tager, 1998; Sasckteder and Gould, 2000).

In silico searching shows *C. elegans* possesses five *pmp* genes, homologs of human ABC half-transporters. In worms displaying defective development, the *pmp-1*, *pmp-2*, and *pmp-4* genes were silenced simultaneously. Mutants of two of the targeted ABC half-transporters (strains RB675 and VC189 mutant for pmp-4 and strain RB908 mutant for pmp-1) do not display any obvious developmental delay[10]. Similarly, there is no obvious phenotype for the *pmp-3* mutant (strain RB1108). mRNAs of *pmp-2* and *pmp-5* cannot be targeted individually by RNAi due to the high level of sequence identity with other *pmp* RNAs (Fig. 3.7.3). Moreover, dsRNA used in targeting the *pmp-1*, *pmp-2* and *pmp-4* genes can possibly silence the *pmp-3* and *pmp-5* genes as well.

ABC half transporters assemble as either homodimers or heterodimers to create a functional transporter (Dean *et al.*, 2001). RNAi experiments suggest that the *pmp* genes of *C. elegans* are involved in important physiological processes that, when affected, are able to interfere with normal development of the nematode. Most likely the nematode ABC transporters function in heterogenic complexes consisting of specific pmp proteins.

---

[10] http://biosci.umn.edu/CGC/CGChomepage.htm

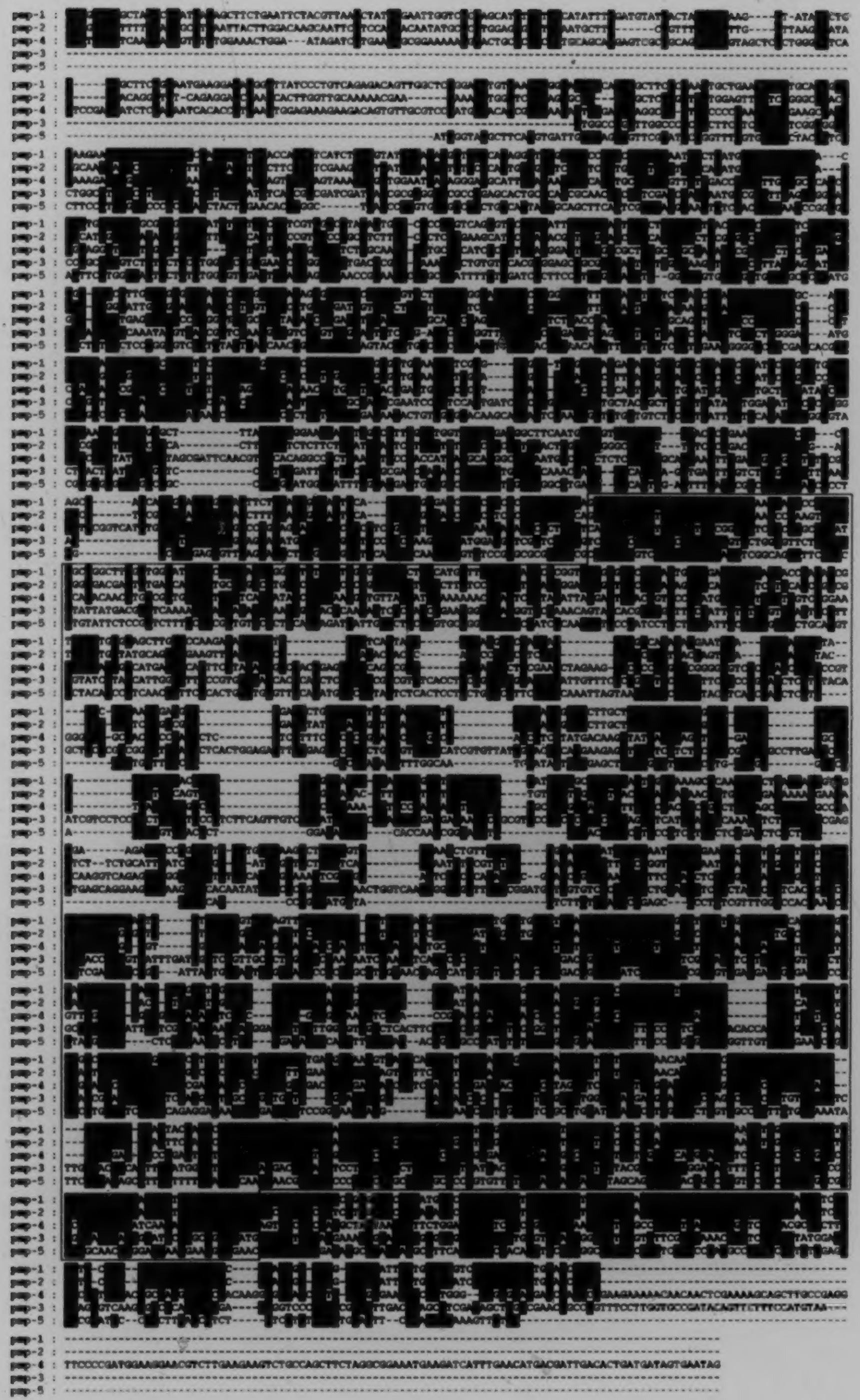

Figure 3.7.3. Alignment of *pmp* cDNAs. Area targeted by dsRNA is boxed in red. Identical bases, black.

Differentiation of the roles of individual pmp proteins in these complexes will be possible only after the construction and analysis of mutants carrying different combinations of pmp deficiencies, including deficiencies of pmp-2 and pmp-5.

Another peroxisome-associated metabolic process that is essential for the development of *C. elegans* involves an auxiliary metabolic pathway that allows polyunsaturated fatty acids to enter the normal peroxisomal β-oxidation spiral. In fact, injection of dsRNA specific to the ORF encoding the first enzyme in this auxiliary pathway, $\Delta^{3,5}$-$\Delta^{2,4}$-dienoyl-CoA isomerase, caused a substantial delay in the development of the nematode. In humans, an inborn error of the auxiliary pathway for the β-oxidation of fatty acids causes a peroxisomal disorder (Roe *et al.*, 1990).

The third peroxisomal metabolic process that, according to the results of RNAi analysis presented here (Fig. 3.7.1) and by Motley and coworkers (Motley *et al.*, 2000), is required for the normal development of *C. elegans*, involves the biosynthesis of plasmalogen. RNAi experiments with dsRNA to ADHAPS, which catalyzes the second step in plasmalogen biosynthesis, resulted in a substantial delay in the development of the nematode. Likewise, in humans, inborn defects in ADHAPS cause abnormal psychomotor development and result in a lethal peroxisomal disorder, RCDP type 3 (de Vet *et al.*, 1997a; 1999).

Surprisingly, the phenotypes of worms treated with dsRNA to inactivate the processes of acyl-CoA synthetase-mediated activation of fatty acids, the α- and β-oxidation of fatty acids, and the intraperoxisomal decomposition of harmful hydrogen peroxide, were close to that of control worms (Fig. 3.5.2). As a control for the effectiveness of RNAi, immunoblot analysis with antibodies specific to the carboxyl terminus of type 2 thiolase P-

44 demonstrated that the level of this protein was decreased more than 10-fold following injection of dsRNA specific for this gene (Fig. 3.3.2). These results may suggest that, unlike in humans or yeast, these biochemical functions of peroxisomes may not be of major importance for the development of *C. elegans* or are duplicated by cytosolic (*e.g.*, the cytosolic form of catalase) or mitochondrial (*e.g.*, mitochondrial forms of thiolase) orthologs.

CHAPTER 4

ASPECTS OF PEROXISOMAL PROTEIN IMPORT PATHWAYS IN *CAENORHABDITIS ELEGANS*

A version of this chapter has previously been published as "A New Definition for the Consensus Sequence of the Peroxisome Targeting Signal Type 2" (Petriv O.I., L. Tang, V.I. Titorenko and R.A. Rachubinski. 2004. *J. Mol. Biol.*, 341:119-134).

4.1 Overview

Results presented in Chapter 3 demonstrate that *C. elegans* possesses a fully functional PTS1-dependent peroxisomal import pathway with a high degree of similarity to the human PTS1 pathway and its components. However, it remains unclear whether *C. elegans* also possesses a functional PTS2-dependent import pathway. The nematode genome lacks any readily identifiable ortholog of the *PEX7* gene, which encodes the receptor for proteins containing PTS2. In addition, most proteins that are targeted to peroxisomes by PTS2 in other organisms are targeted by PTS1 in *C. elegans* (Motley *et al.*, 2000; Petriv *et al.*, 2004). Moreover, the PTS2 of rat thiolase, a peroxisomal β-oxidation enzyme, was unable to direct a GFP reporter protein to peroxisomes in *C. elegans* (Motley *et al.*, 2000), although the same PTS2 actively targeted reporter proteins to peroxisomes in plants (Flynn *et al.*, 1998) and in trypanosomes (Blattner *et al.*, 1995). These observations prompted a careful analysis of putative nematode peroxisomal proteins in search for polypeptides carrying consensus PTS2, but no PTS1 motifs. Only one such protein, mevalonate kinase, was found. It was shown not to be targeted to peroxisomes in *C. elegans*. Consensus PTS2s from two other *C. elegans* proteins were found to be non-functional in *C. elegans*, mammalian fibroblasts and yeast. These results prompted the analysis of known functional PTS2 motifs and led to a refinement of the existing consensus sequence for the PTS2. To date, PTS2-dependent import of proteins into peroxisomes has been found in all organisms except for *C. elegans* (Motley *et al.*, 2000).

4.2 Search for components of the PTS2-dependent peroxisomal import pathway and PTS2-containing proteins in *C. elegans*

BLAST sequence similarity searches for the *C. elegans* homolog of the human receptor for PTS2 proteins, Pex7p, resulted in the identification of as many as 51 putative homologs. Despite such a high number of hits, none of the identified ORFs was confirmed as the gene encoding the putative PTS2 receptor. It was found that in all cases, the high BLAST score was caused by the match between the six WD40 domains (widespread protein domains of multiple functions) of Pex7p and the WD40 domains in the counterpart ORF. In addition, homologs of the yeast peroxins Pex18p and Pex21p that are known to be involved in PTS2-dependent import in yeast (Purdue *et al.*, 1998), but not humans, were not found in the nematode (Table 3.2.3).

An extensive BLAST sequence similarity search of available *C. elegans* genomic data[11] was performed to identify *C. elegans* genes encoding orthologs of proteins that are known to possess functional PTS2 motifs in other eukaryotes (Table 4.2.1). It appears that most proteins that contain a PTS2 in other eukaryotes possess a PTS1 in *C. elegans*. Some, such as the orthologs of acyl-CoA oxidase and acyl-CoA thioesterase (encoded by the ORFs F59F4.1 and C31H5.6, respectively) have both PTS1 and PTS2 motifs. Only the ortholog of human mevalonate kinase (*Hs*MeK), encoded by the ORF Y42G9A.4, appeared to contain solely a putative PTS2.

---

[11] Databases www.wormbase.org, www.incyte.com

Table 4.2.1. Occurrence of the PTS2 consensus sequence in peroxisomal proteins across different eukaryotes

Protein	Mammals	Plants	Yeasts and trypanosomes	*C. elegans* ortholog
Hsp70	No PTS	PTS2[1]	No PTS	No PTS (C30C11.4, F26D10.3)[a]
Pex8p	No ortholog	No ortholog	PTS1 and PTS2[2]	No ortholog
Pex11p	PTS2[3]	No ortholog	PTS2[3]	No ortholog
Mevalonate kinase	PTS2[4]	PTS2[5]	No PTS	PTS2 (Y42G9A.4)
3-Ketoacyl-CoA thiolase	PTS2[6,7]	PTS2[8-10]	PTS2[11,12-14]	PTS1 (T02G5.8, T02G5.7, T02G5.4)
ADHAPS	PTS2[15,16]	No ortholog	PTS1, PTS2[11]	PTS1 (Y50D7A.7)
Phytanoyl-CoA hydroxylase	PTS2[17]	No ortholog	No PTS	PTS1 (ZK550.6)
Malate dehydrogenase	No PTS	PTS2[18-23]	PTS1[11]	No PTS (F46E10.10)
Peroxisomal citrate synthase	No PTS	PTS2[22]	PTS1[11]	No PTS (T20G5.2)
Acyl-CoA oxidase	PTS1[11]	PTS2[24,25]	PTS1[11]	PTS2 and PTS1 (F59F4.1)
Aspartate aminotransferase	No PTS	PTS2[26]	PTS1[27]	No PTS (T01C8.4, C14E2.2 C44E4.3, C14F11.1)
Aldolase	No PTS	No PTS	PTS2[28]	No PTS (T05D4.1, F01F1.12)
Acyl-CoA thioesterase	No PTS	No ortholog	No ortholog	PTS2 and PTS1 (C31H5.6) PTS1 (K05B2.4) PTS1 (W03D8.8)
HMG-CoA synthase	Functional PTS2-like signal (does not conform to consensus PTS2)[29]	No PTS	No PTS	No PTS (F25B4.6)
Mevalonate-PP decarboxylase		No PTS	No PTS	No PTS (Y48B6A.13)
Farnesyl-PP synthase		No PTS	No PTS	No PTS (R06C1.2)

[a] Numerical designation of ORF encoding *C. elegans* ortholog.

[1], Wimmer *et al.*, 1997; [2], Szilard *et al.*, 1995; [3], Passreiter *et al.*, 1998; [4], Kelley and Herman, 2001; [5], Lluch *et al.*, 2000; [6], Hijikata *et al.*, 1987; [7], Bout *et al.*, 1988; [8], Preisig-Muller and Kindl, 1993; [9], Kato *et al.*, 1996b; [10], Bojorquez and Gomez-Lim, 1995; [11], Motley *et al.*, 2000; [12], Einerhand *et al.*, 1991; [13], Berninger *et al.*, 1993; [14], Kurihara, 1992; [15], de Vet *et al.*, 1997; [16], de Vet *et al.*, 2000; [17], Mihalik *et al.*, 1997; [18], Kim and Smith, 1994; [19], Witt *et al*, 1995; [20], Gietl, 1990; [21], Guex *et al.*, 1995; [22], Kato *et al.*, 1998; [23], Miller *et al.*, 1998; [24], Do and Huang, 1997; [25], Hayashi *et al.*, 1998a; [26], Gebhardt *et al.*, 1998; [27], Verleur *et al.*, 1997; [28], Clayton, 1985; [29], Olivier *et al.*, 2000.

4.3 Subcellular localization of *C. elegans* mevalonate kinase and two other putative PTS2-containing proteins

The ORF Y42G9A.4 encoding *C. elegans* mevalonate kinase (*Ce*MeK) is predicted by WormBase[12] to contain 12 exons and to produce a transcript 11 kilobases in length (Fig. 4.3.1 A). We cloned and sequenced the full-length cDNA for *Ce*MeK by RT-PCR of total *C. elegans* RNA (Fig. 4.3.1 B). The cDNA was 1545 bp in length and was missing the predicted exon 4 (Fig. 4.3.1 A). *Ce*MeK exhibits 33% amino acid identity and 41% amino acid similarity to *Hs*MeK. The amino terminus of *Ce*MeK contains the sequence –KIILFGEHA–, which conforms to the current consensus PTS2 sequence –(R/K)(L/V/I)X_5(H/Q)(L/A)– (Titorenko and Rachubinski, 2001b; Fig. 4.3.1 B). The carboxyl-terminal tripeptide of *Ce*MeK, –KHK, does not conform to the canonical PTS1 sequence –(S/C/A)(K/R/H)(L/M) (Subramani, 1993). To determine its subcellular location, *Ce*MeK was tagged at its amino terminus (GFP-*Ce*MeK) or its carboxyl terminus (*Ce*MeK-GFP) with GFP and transgenic animals were examined by fluorescence microscopy. Both tagged forms of *Ce*MeK localized to the cytosol and not to peroxisomes of *C. elegans* cells (Fig. 4.3.2 A and B).

A search of known and putative *C. elegans* proteins using the Proteome BioKnowledge Library[13] led to the identification of 250 (the search limit of this application) proteins containing the consensus PTS2 sequence close to their amino termini. Only two ORFs, D1053.2 and W10G11.11, encoded proteins in which the consensus PTS2 sequence was immediately next to the initiating methionine. A BLAST search of available databases did not reveal any orthologs of these two putative proteins in other eukaryotes.

---

[12] www.wormbase.org

[13] www.incyte.com

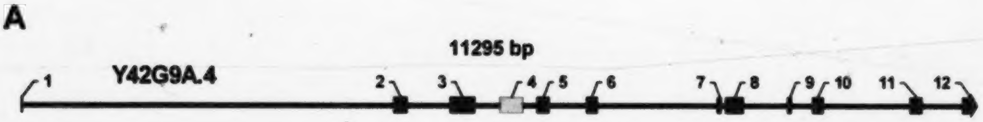

B

```
   1 M   V   V   I   G   G   D   Q   A   L   D   S   P   S   G   S   T   S   R   A
   1 atggtcgtcataggaggtgatcaagccctggactcaccgtcgggaagcacatctcgcgcc
  21 G   S   S   V   S   A   T   A   S   P   M   H   R   N   T   T   S   Q   H   G
  61 ggctcgtcggtgtcggctaccgcgagtccgatgcatcggaacacgacatcacaacatggt
  41 G   L   F   V   S   A   P   G   K   I   I   L   F   G   E   H   A   V   V   Y
 121 ggactgttcgtttcggctcccggaaaaattatttgttcggagagcacgccgtcgtgtat
  61 G   R   T   A   I   A   G   S   I   D   L   R   T   Y   V   S   L   Y   T   S
 181 ggaaggaccgcaatcgccggatcgattgatcttcgcacctacgtttcgctgtacacatcg
  81 A   D   G   R   I   Y   L   S   L   P   D   L   G   V   E   K   T   W   M   L
 241 gcagacggacgcatttatttgagtcttccagaccttggcgtcgaaaagacatggatgctg
 101 K   D   L   L   K   A   A   D   R   L   A   A   E   Y   P   I   E   E   D   Q
 301 aaagatttgttgaaagcggcggatcgtcttgccgcagaatatccgatcgaggaagatcaa
 121 P   P   S   L   E   I   L   V   P   I   A   R   K   L   S   G   S   C   E   D
 361 ccaccatcacttgagattctggtaccgatcgccagaaaattgtcgggttcgtgtgaggat
 141 Q   C   G   V   Q   H   L   A   I   L   A   F   W   Y   L   L   L   G   V   A
 421 cagtgtggtgttcaacatctcgcaattctcgcattttggtatttgttgctcggagttgca
 161 H   R   K   R   D   L   L   A   V   K   A   T   V   R   F   K   L   P   S   C
 481 catcgcaagagagatttgctcgcagtcaaggccacagtccgattcaagcttccaagctgt
 181 V   G   L   G   S   S   G   A   Y   C   V   C   I   A   T   S   L   L   Q   T
 541 gttggattaggatcatctggagcatattgtgtatgcatcgctacatcacttcttcaaact
 201 A   G   L   I   P   P   P   S   I   V   A   D   E   Q   G   N   L   T   W   E
 601 gctggtctcattccaccaccaagtattgtcgccgacgagcaaggcaatttaacatgggaa
 221 E   D   H   L   D   I   I   R   K   W   A   T   A   A   E   S   L   I   H   G
 661 gaagatcatttggacattattcgaaagtggcaactgccgccgaatctcttattcacgga
 241 R   A   S   G   L   D   A   A   V   C   T   F   G   G   V   A   S   F   K   P
 721 cgtgcatcgggtttagacgcggctgtctgcacttttggaggagttgccagcttcaagccg
 261 G   H   R   I   E   H   L   K   N   L   P   D   L   R   V   I   L   V   N   S
 781 ggacacagaattgagcatcttaaaatttacccgatcttcgtgttattcttgtaaattcg
 281 K   V   E   R   N   T   A   R   M   V   Q   T   V   K   E   R   L   K   K   F
 841 aaagttgaaaggaatacggcaagaatggtacaaacagtgaaagaacgattaaagaagttc
 301 P   E   V   V   D   A   M   F   G   S   I   D   A   I   S   L   D   A   A   K
 901 ccagaagttgttgatgcaatgtttggatcaattgatgctatttcacttgatgctgcaaag
 321 I   L   H   R   P   L   L   E   E   N   G   G   G   D   T   G   S   T   V   Q
 961 attctacatcgtccgttgcttgaggagaatggtggtggagatactggatctacagtacag
 341 E   N   G   L   G   P   F   G   G   N   M   V   E   Q   D   H   H   S   L   Q
1021 gaaaatggcctaggaccatttggtggaaatatggtagaacaggatcatcactcccttcag
 361 P   T   R   T   A   S   V   R   S   S   S   L   S   S   Y   V   G   G   G   K
1081 ccaacacgaacagcatcggtacgatcatcatcactttcatcgtatgttggcggtggaaaa
 381 R   N   S   S   A   S   V   I   S   A   T   S   E   K   G   E   N   V   D   T
1141 aggaattcgtcggcttctgtaatctccgcaacttcagaaaaaggagaaaatgtggataca
 401 F   S   K   L   N   D   L   C   R   I   N   N   Q   L   L   I   A   L   G   V
1201 ttcagcaagcttaatgatctatgtcggataaacaatcaattgctcattgcattgggtgtt
 421 G   H   P   K   V   D   L   I   C   T   T   L   A   R   Y   G   I   H   P   K
1261 ggccatccaaaagttgatctcatttgtacgacattggctagatatggaatacatccaaaa
 441 M   T   G   A   G   G   G   G   S   V   F   A   F   L   K   P   N   T   P   Q
1321 atgacgggtgctggtggtggtggatcagttttgcgttcttgaagccaaacacgccacaa
 461 T   L   L   D   M   I   D   G   E   L   R   S   H   G   F   E   V   W   Q   P
1381 actcttctcgacatgattgacggcgagcttcgcagtcatggatttgaagtttggcagcca
 481 P   L   G   G   P   G   V   V   E   H   Q   T   R   P   E   L   F   Q   T   P
1441 ccacttggcggacccggagttgttgaacatcagacacgtcctgagctcttccagacgccc
 501 V   S   S   T   Q   C   S   T   P   A   S   K   H   K   *
1501 gtttcgtcaacacagtgctcaacgccggcttcaaaacataaatga
```

Figure 4.3.1. Gene structure and cDNA sequence for *C. elegans* mevalonate kinase. **A.** Predicted structure of the *Ce*MeK gene. The gene is predicted by WormBase[1] to have 12 exons. Sequencing of the cDNA for *Ce*MeK shows that predicted exon 4 is not present in the final transcript. **B.** Sequence of the coding region of *Ce*MeK cDNA. The full-length cDNA arising from ORF Y42GA.4 was obtained by RT-PCR of total *C. elegans* RNA. The putative PTS2 signal of *Ce*MeK is underlined.

---

[1] www.wormbase.org

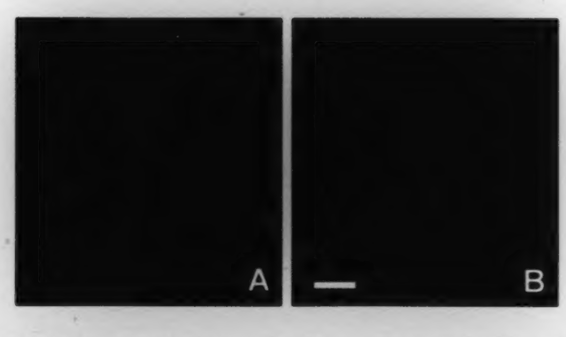

Figure 4.3.2. Subcellular localization of chimeras of *Ce*MeK and GFP. *Ce*MeK-GFP (**A**) and GFP-*Ce*MeK (**B**) localize to the cytosol of cells of *C. elegans*. The head regions of worms are shown. Strong fluorescence is observed in pharyngeal muscle cells. Bar, 20 μm.

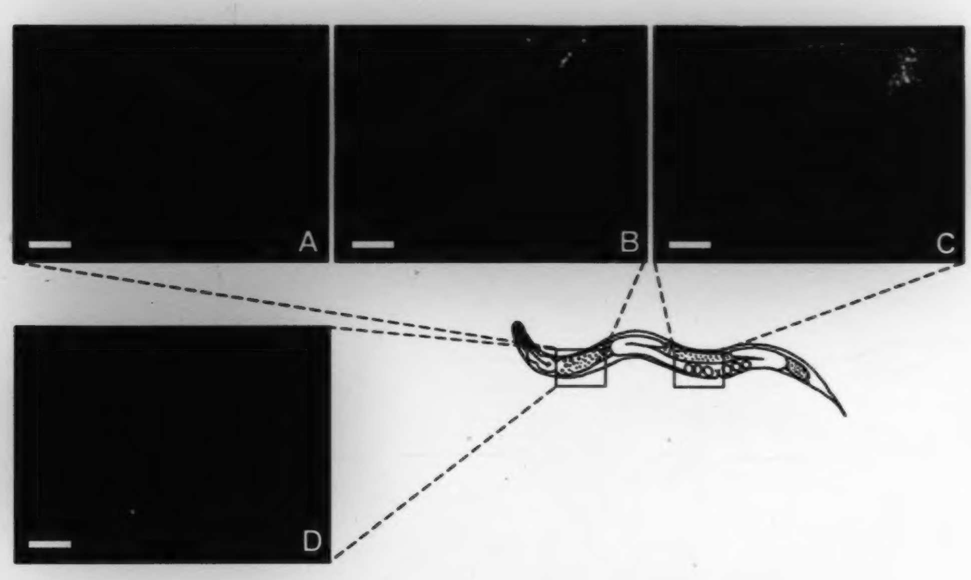

Figure 4.3.3. Subcellular localization of two putative PTS2-containing proteins of *C. elegans*. The proteins encoded by the ORFs W10G11.11 and D1053.2 of the *C. elegans* genome were tagged at their carboxyl termini with GFP, and the localization of the chimeras in cells of *C. elegans* was determined by fluorescence microscopy. **A**, Cytosolic localization of the GFP reporter alone. W10G11.11-GFP (**B**) and D1053.2-GFP (**C**) are localized to the cytosol of cells. **D**, The punctate pattern of peroxisomes labeled by CFP-SKL. The yellow punctate structures visible in panels **A**, **B** and **C** correspond to intestinal lysosomes (Clokey and Jacobson, 1986). Bar, 20 μm.

To investigate if either PTS2-like signal was actually able to function in targeting to the peroxisome, chimeric genes were constructed to code for the unknown proteins tagged at their carboxyl termini with GFP. Like GFP alone (Fig. 4.3.3 A), transgenic animals expressing W10G11.11-GFP (Fig. 4.3.3 B) or D1053.2-GFP (Fig. 4.3.3 C) exhibited a diffuse pattern of fluorescence characteristic of the cytosol and in distinct contrast to the punctate fluorescence pattern of peroxisomes of cells of *C. elegans* expressing a CFP-PTS1 reporter protein (Fig. 4.3.3 D).

We next examined whether the putative PTS2s from D1053.2 and W10G11.11 could function in targeting proteins to peroxisomes in cells known to have a PTS2-targeting system by fusing these putative PTS2s at the amino terminus of GFP or CFP and expressing the chimeric proteins in the yeast *S. cerevisiae*, in murine NIH 3T3 fibroblasts and in the monkey kidney epithelial cell line, COS-7 (Biermann *et al.*, 1999; Schrader, 2001; Iida *et al.*, 2003).

In *S. cerevisiae* cells, PTS2$_{\mathrm{W10G11.11}}$-GFP (Fig. 4.3.4 A) and PTS2$_{\mathrm{D1053.2}}$-GFP (Fig. 4.3.4 E) showed a diffuse fluorescence pattern characteristic of the cytosol, which did not overlap (Fig. 4.3.4 C and G, respectively) with the fluorescent punctate pattern of peroxisomes (Fig. 4.3.4 B and F) in confocal microscopy. In murine NIH 3T3 cells and monkey COS-7 cells, PTS2$_{\mathrm{W10G11.11}}$-CFP and PTS2$_{\mathrm{D1053.2}}$-CFP similarly were cytosolic and not peroxisomal (Fig. 4.3.4 I – T). Therefore, the putative PTS2s from D1053.2 and W10G11.11 do not function as PTSs in systems known to have functional PTS2-dependent import.

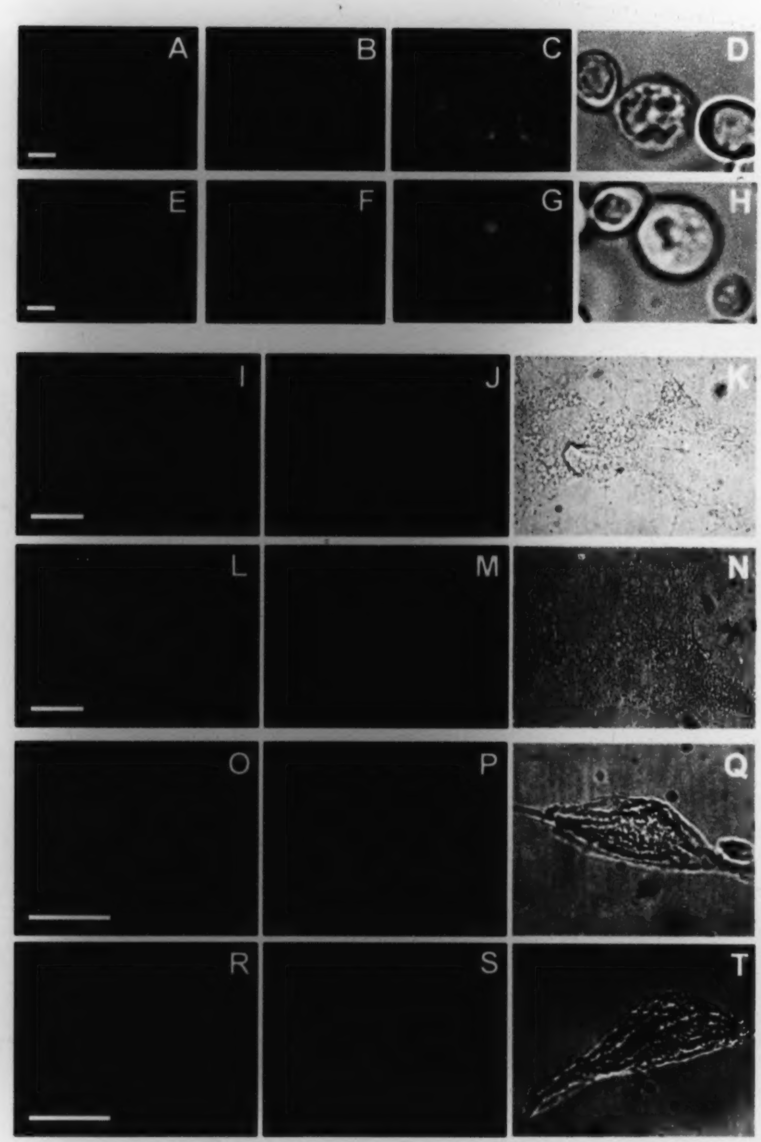

Figure 4.3.4. The PTS2-like sequences of the proteins encoded by the ORFs W10G11.11 and D1053.2 do not function in targeting to peroxisomes in cells from other organisms with functional PTS2 targeting systems. PTS2$_{\text{W10G11.11}}$-GFP (**A**) and PTS2$_{\text{D1053.2}}$-GFP (**E**) were expressed in *S. cerevisiae* cells grown in oleic acid-containing medium to induce peroxisome proliferation and showed a diffuse pattern of fluorescence characteristic of the cytosol and unlike the punctate pattern of peroxisomes labeled with the fluorescent peroxisomal reporter construct Pot1p-mRFP (**B** and **F**). The merged confocal microscopy images showed no colocalization of PTS2$_{\text{W10G11.11}}$-GFP (**C**) or PTS2$_{\text{D1053.2}}$-GFP (**G**) with peroxisomes. Bright field images (**D** and **H**) show cell boundaries. Bars, 2 µm. PTS2$_{\text{W10G11.11}}$-CFP and PTS2$_{\text{D1053.2}}$-CFP were also expressed in NIH 3T3 murine fibroblasts (**I** and **L**, respectively) and monkey kidney epithelial COS-7 cells (**O** and **R**, respectively) and showed a diffuse fluorescence pattern characteristic of the cytosol and not the punctate pattern of peroxisomes labeled with the reporter construct DsRed-2-SKL (**J**, **M**, **P** and **S**). Bright field images (**K**, **N**, **Q**, and **T**) show cell boundaries. Bars, 10 µm.

4.4 Computational analysis of PTS2 motifs from eukaryotic genomes

We analyzed the complete sets of proteins encoded by the genomes of *Homo sapiens*, *C. elegans*, *Arabidopsis thaliana* and *S. cerevisiae* (Fig. 4.4.1) for the occurrence of the currently accepted PTS2 consensus sequence, –(R/K)(L/V/I)X_5(H/Q)(L/A)– (Rachubinski and Subramani, 1995; Titorenko and Rachubinski, 2001b). This PTS2 motif was encountered in approximately 10% of encoded proteins and was distributed with relatively equal frequency along the entire primary sequence except for the carboxyl-terminal ends of proteins encoded by the analyzed genomes (Fig. 4.4.1 A). An analysis of the amino acid composition of the five previously undefined internal positions of the motif indicated that no particular amino acid is overrepresented at any of these positions in any of the organisms studied. Even though some PTS2s have been shown to be functional at any location along a protein, even at the carboxyl terminus (Rehling *et al.*, 1996) and in the middle of the protein (Subramani, 1996; Legaskis and Terlecky, 2001;), most functional PTS2 signals from known peroxisomal proteins are found at the amino termini. Therefore, we also analyzed the amino acid composition of PTS2 motifs found in the amino-terminal 20% of proteins encoded by the same genomes. Again, no specific amino acid was found to be significantly overrepresented in any of the five internal positions of the PTS2 motif for the tested organisms. Using protein sequences from the well annotated Swiss-Prot protein database as input data, we generated a learning database consisting of 993 entries of proteins annotated as being localized to peroxisomes. Proteins that could be targeted to peroxisomes by a PTS1 were removed from the set using software available at http://mendel.imp.univie.ac.at/PTS1/. Of the 845 peroxisomal proteins that do not contain a PTS1, 131 appeared to contain at least one putative consensus PTS2 motif. The PTS2

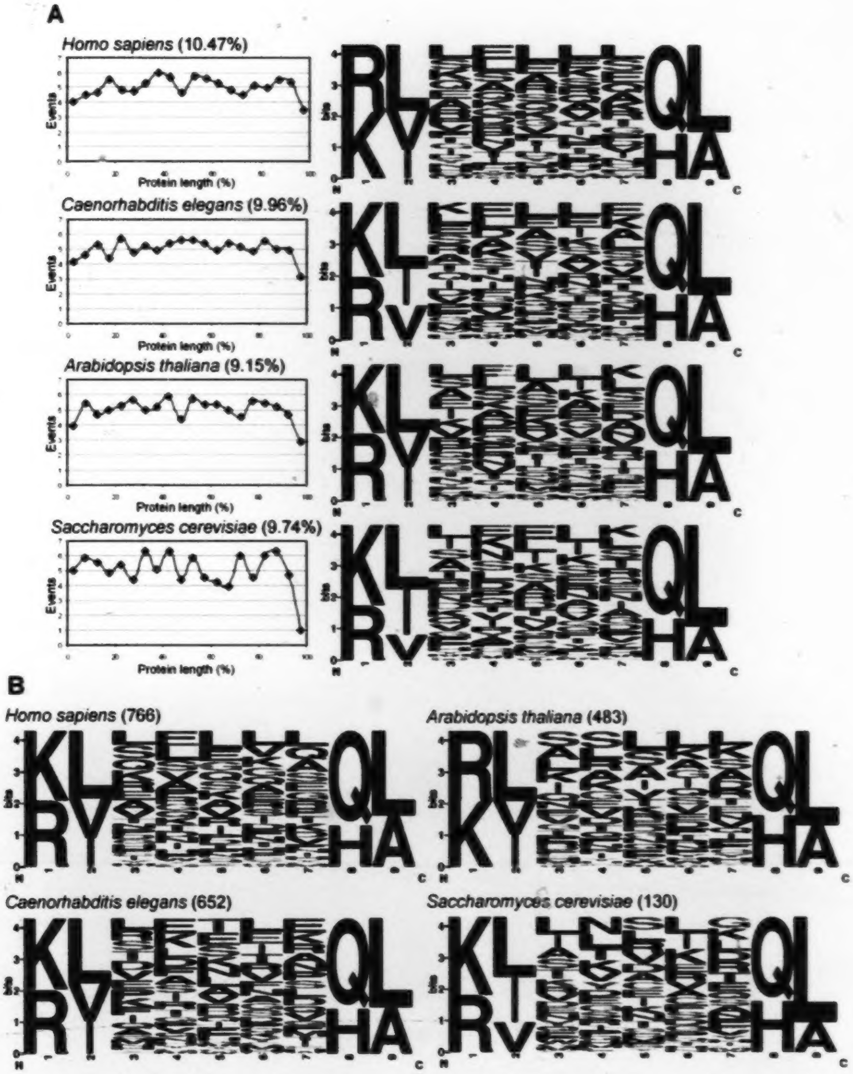

Figure 4.4.1. Distribution and composition of PTS2 motifs. A, Distributions along primary sequences of proteins and amino acid compositions of PTS2 motifs with consensus –(R/K)(L/V/I)X_5(H/Q)(L/A)– in proteins encoded by different eukaryotic genomes. The percentages of proteins encoded by a particular genome and which contain the consensus PTS2 motif are given in brackets at the top of each graph. The abscissa in graphs represents the lengths of proteins in percent, with 0 corresponding to the amino terminus and 100 corresponding to the carboxyl terminus. The ordinate in graphs represents the frequency of the PTS2 motif. **B**, Amino acid compositions of the PTS2 motifs located at a distance within 20% of the amino termini of proteins encoded by the different eukaryotic genomes The number of total PTS2 motifs found for each organism is shown in brackets. Graphics were generated using WebLogo[1]

---

[1] http://weblogo.berkeley.edu/

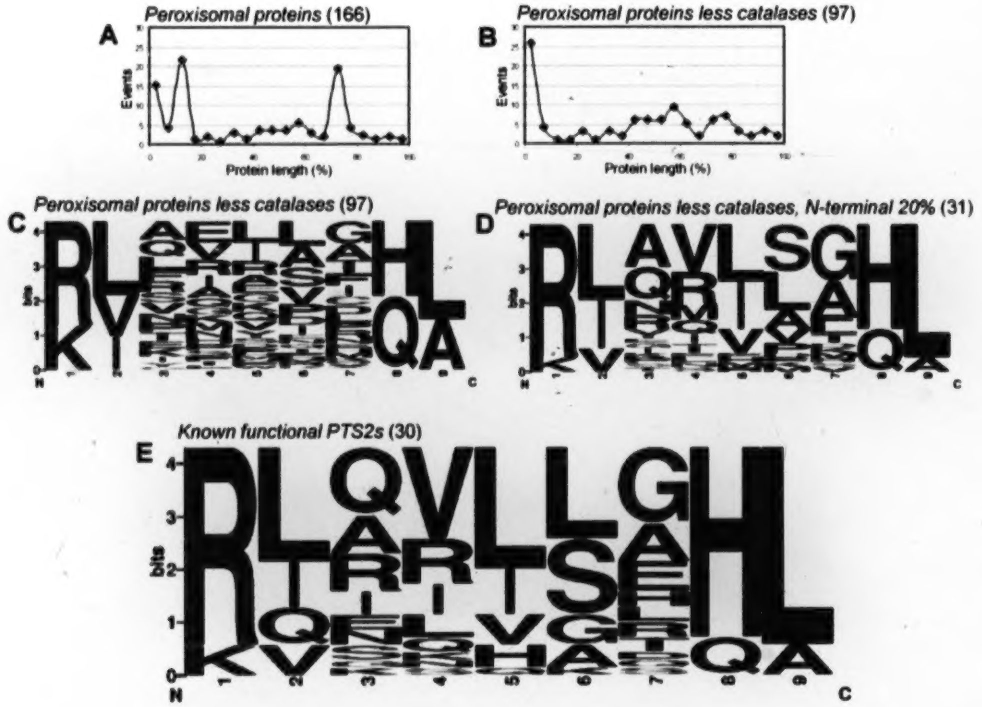

Peroxisomal proteins (166)

Peroxisomal proteins less catalases (97)

Peroxisomal proteins less catalases (97)

Peroxisomal proteins less catalases, N-terminal 20% (31)

Known functional PTS2s (30)

Figure 4.4.2. Distribution and amino acid composition of PTS2 motifs with consensus –(R/K)(L/V/I)X_5(H/Q)(L/A)– in peroxisomal proteins. Proteins designated as peroxisomal by annotation in the Swiss-Prot protein data were analyzed before (**A**) and after (**B**) removal of catalase sequences from the learning database. The abscissa in graphs represents the lengths of proteins in percent, with 0 corresponding to the amino terminus and 100 corresponding to the carboxyl terminus. The ordinate in graphs represents the frequency of the PTS2 motif. The amino acid compositions of the PTS2 motifs of peroxisomal proteins were determined after removal of catalase sequences and were determined for all PTS2 motifs (**C**), for those PTS2 motifs located within 20% of the amino termini of peroxisomal proteins (**D**), and (**E**) for those PTS2 motifs experimentally shown to function in targeting to peroxisomes. The numbers of PTS2 motifs analyzed are given in brackets. Graphics were generated using WebLogo[1].

---

[1] http://weblogo.berkeley.edu/

motifs were not uniformly distributed along the primary sequences of the 131 proteins but were concentrated in regions at distances of 12% and 72% from their amino termini (Fig. 4.4.2 A). The 131 proteins contained a large number of catalases from different organisms. Catalases exhibit extensive sequence similarity amongst themselves and contain two consensus PTS2 motifs at distances of 12% and 72% from their amino termini. Since no catalase has been reported to be targeted to peroxisomes by one or the other of these PTS2 motifs (Purdue *et al.*, 1996), we removed all catalase sequences from the learning database and analyzed the restructured learning database as before. Most of the proteins remaining in the learning database have their PTS2 motifs localized towards their amino termini (Fig. 4.4.2 B). There was no strong enrichment for any particular amino acid at positions 3 to 7 of the nonapeptide PTS2 motif if all peroxisomal protein sequences except for catalase were considered (Fig. 4.4.2 C). However, if the analysis was restricted only to those sequences with a PTS2 motif towards their amino termini, then at least one internal position of the PTS2 motif (position 5 of the nonapeptide) displayed a strong preference for particular amino acid residues (L/I/V; Fig. 4.4.2 D). Specific amino acids were also enriched at positions 3 (A, Q), 4 (V, R), 6 (S, L) and 7 (G, A) of the nonapeptide PTS2 of the proteins in this subset.

We next defined the amino acid compositions at positions 3 to 7 of PTS2 motifs experimentally demonstrated to function in targeting to peroxisomes. The sequences of these PTS2s are presented in Table 4.4.1. The relative abundance of particular amino acids at positions 3 to 7 of these PTS2s (Fig. 4.4.2 E) is similar to that observed for the corresponding amino acid positions of PTS2s of all catalase-less peroxisomal proteins present in the Swiss-Prot protein database (Fig. 4.4.2 D). Position 5 of functional PTS2s is

Table 4.4.1. Sequences of functional PTS2 motifs

Accession Number	Sequence of amino terminus including PTS2 motif	Protein name	Species[a]
XP_027151	MLSEVLLVSAPG**KVILHGEHA**VVHGKV	Mevalonate kinase	*Hs*[1-3]
NP_112325	MLSEVLLVSAPG**KVILHGEHA**VVHGKV		*Rn*[4]
NP_076045	MLSEALLVSAPG**KVILHGEHA**VVHGKV		*Mm*[5]
AAB81834	MEQLRAAA**RLQIVLGHL**GRPSAG	Phytanoyl-CoA α-hydroxylase	*Hs*[6]
P57093	MDYTRAGA**RLQVLLGHL**GRPSAL		*Rn*[7]
NP_034856	MNLTRAGA**RLQVLLGHL**GRPSAP		*Mm*[8]
NP_003650	MAEAAAAAGGTGLGAGASYGSAADRDRDPDPDRAGR**RLRVLSGHL**LGRPRE	Alkyldihydroxy acetone phosphate synthase	*Hs*[9]
P97275	MAEAAAAAAAAAAAGETSASSGSAAERDPDQDRAGR**RLRVLSGHL**LGRPQE		*Cv*[10,11]
NP_445802	MAEAAGEAGASERDPDAVRARR**RLRVLSGHL**LGRPQE		*Rn*[9]
AAH00635	MQ**RLQVVLGHL**RGPADS	3-ketoacyl-CoA thiolase	*Hs*[12,13]
P07871	MH**RLQVVLGHL**AGRSES		*Rn*[13-16]
AAC23571	MERAME**RQKILLRHL**NPVSSS		*At*[17]
S33637	MEKAIN**RQSILLHHL**RPSSSA		*Cs*[18]
P07871	MH**RLQVVLGHL**AGRSES		*Rn*[13-16]
CAA53078	MEKAIN**RQQVLLQHL**RPSNSS		*Mi*[19]
CAA63598	MEKAME**RQRVLLEHL**RPSSSS		*Bn*[20]
S72532	MEKAIN**RQSILLHHL**RPSSSA		*Csp*[21]
P33291	MD**RLNQLSGQL**KPNAKQ		*Ct*[13]
CAA86118	MSQ**RLQSIKDHL**VESAMG		*Sc*[13]
Q05493	MD**RLNNLATQL**EQNPAK		*Yl*[13]
NP_196528	MEFRGDANQ**RIARISAHL**TPQMEA	Malate dehydrogenase	*At*[22]
DEPUGW	MQPIPDVNQ**RIARISAHL**HPPKSQ		*Cl*[23,24]
AAC41647	MQPIPDVNQ**RIARISAHL**HPPKYQ		*Cs*[25]
	MKPIPDVNE**RIARISAHL**QPPKSQ		*Csp*[26]
AAR00586	MFTRPMEGGGMTKEAQMTSLASEHDTQRALR**RIQKLSLHL**LQPSPF	Acyl-CoA oxidase	*Ph*[14]
T07901	MASPGEPNRTAEDESQAAAR**RIERLSLHL**TPIPLD		*Csp*[21]
P49299	MPTDMELSPSNVARH**RLAVLAAHL**SAASLE	Citrate synthase	*Cm*[21, 27]
P07752	MSK**RVEVLLTQL**PAYNRL	Fructose-bisphosphate aldolase	*Tb*[21]
BAB40976	M**RLTLPRLNA**AYIVGA	Acetoacetyl-CoA thiolase	*Yl*[28]
CAA82928	MQPWYH**KLGRQGRQL**AEQWQT	Pex8p	*Hp*[29]
AAC03416	MASSTVQIHGLGAPSFAAASMRKSNHVSS**RTVFFGQKL**GNSSAF	HSP 70	*Cl*[30]
P12807	ME**RLRQIASQA**TAASAA	Methylamine oxidase	*Pa*[31]
AAC50014	MRPPVILKTTTSLLDSSSSSPPCDR**RLNTLARHF**LPQMAS	Aspartate amino-transferase	*Gm*[32]

[a]*Hs*, *Homo sapiens*; *Rn*, *Rattus norvegicus*; *Mm*, *Mus musculus*; *Cp*, *Cavia porcellus*; *At*, *Arabidopsis thaliana*; *Cs*, *Cucumis sativus*; *Cm*, *Cucurbita maxima*; *Cl*, *Citrullus lanatus*; *Mi*, *Mangifera indica*; *Bn*, *Brassica napus*; *Csp*, *Cucurbita sp*; *Ph*, *Phalaenopsis cv. 'True Lady'*; *Gm*, *Glycine max*; *Tb*, *Trypanosoma brucei brucei*; *Sc*, *Saccharomyces cerevisiae*; *Yl*, *Yarrowia lipolytica*; *Hp*, *Hansenula polymorpha*; *Ct*, *Candida tropicalis*.

[1], Wanders and Romeijn, 1998; [2], Olivier *et al*., 2000; [3], Biardi *et al*., 1994; [4], Stamellos *et al*., 1992; [5], Hogenboom *et al*., 2002; [6], Maeda *et al*., 2001; [7], Jansen *et al*., 1997; [8], de Vet *et al*., 2000; [9], Kurihara *et al*., 1992; [10], de Vet *et al*., 1997; [11], de Vet *et al*., 1997b; [12], Schram *et al*., 1987; [13], Glover *et al*., 1994; [14], Blattner *et al*., 1995; [15], Flynn *et al*., 1998; [16], Tsukamoto *et al*., 1994; [17], Hayashi *et al*., 1998a; [18], Kato *et al*., 1996b; [19], Bojorquez and Gomez-Lim, 1995; [20], Olesen *et al*., 1997; [21], Hayashi *et al*., 1998b; [22], Gietl, 1992; [23], Gietl *et al*., 1994; [24], Gietl, 1990; [25], Kim and Smith, 1994; [26], Kato *et al*., 1998; [27], Kato *et al*., 1996a; [28], Yamagami *et al*., 2001; [29], Waterham *et al*., 1994; [30], Wimmer *et al*., 1997; [31] Bruinenberg *et al*., 1990; [32], Gebhardt *et al*., 1998.

strongly conserved, with only amino acids L, I, V, H and Q being found. Position 6 also displays a high degree of conservation and is occupied only by L, S, G, A and K. Positions 3, 4 and 7 are much less conserved in their amino acid composition, although there is overrepresentation of particular amino acids at each of these three positions (Q, A, R and I at position 3; V, R, I and L at position 4; G, A and E at position 7). Moreover, in addition to amino acids L, V and I enriched at position 2 of all PTS2 motifs (see Fig. 4.4.1 and Fig. 4.4.2 C and D), functional PTS2 motifs often contain glutamine (Q) residues at this position (Fig. 4.4.2 E).

4.5 DISCUSSION

4.5.1 No evidence for the PTS2-dependent import pathway in *C. elegans*

The conclusion that the PTS2-targeting pathway is not present in *C. elegans* is based on the observations that 1) most, but not all, PTS2-containing orthologous proteins from other eukaryotes possess a PTS1 in *C. elegans* (Motley *et al.*, 2000), 2) no ortholog of the PTS2 receptor Pex7p is predicted for *C. elegans* (Motley *et al.*, 2000), 3) *Ce*Pex5p is expressed as a short form, lacking the Pex7p interaction motif (Thieringer *et al.*, 2003) found in long form of Pex5p from mammals (Dodt *et al.*, 2001), and 4) the PTS2 from murine peroxisomal thiolase does not function as a PTS in the nematode (Motley *et al.*, 2000). We now show that there is in *C. elegans* at least one PTS2-containing ortholog of a protein known to be peroxisomal in other organisms (Stamellos *et al.*, 1992; Wanders and Romeijn, 1998; Hogenbloom *et al.*, 2002), the enzyme mevalonate kinase (MeK). The PTS2-containing region of MeKs from different organisms is highly conserved (Table 4.5.1); however, this homology does not extend to the subcellular localization of *Ce*MeK. We

Table 4.5.1. Comparison of PTS2 sequences of MeKs from different eukaryotes

PTS2	Organism	Localization[a]
VSAPG**KVILHGEHA**VVHGK	*Homo sapiens*	P[1,2,3]
VSAPG**KVILHGEHA**VVHGK	*Mus musculus*	P[4]
VSAPG**KVILHGEHA**VVHGK	*Rattus norvegicus*	P/C[5]
DRAGR**RLRVLSGHL**LGRPQ	*Cavia porcellus*	
VSAPG**KVIVFGEHA**VVHGK	*Neurospora crassa*	C[6]
TSAPG**KVIIFGEHS**AVYNK	*Saccharomyces cerevisiae*	C[7]
ARAPG**KIILAGEHA**VVHGS	*Arabidopsis thaliana*	
VHSPG**KVILHGEHA**VVYHR	*Drosophila melanogaster*	
ARAPG**KIILSGEHA**VVHGS	*Hevea brasiliensis*	
ARAPG**KIILAGEHA**VVHGS	*Oryza sativa*	
VSAPG**KIILFGEHA**VVYGR	*Caenorhabditis elegans*	C[This study]
VSAPG**KIILFGEHA**VVYGR	*Caenorhabditis briggsae*	Worm Base

[a] P, peroxisomal; C, cytosolic. [1], Wanders and Romeijn, 1998; [2], Olivier *et al.*, 2000; [3], Biardi *et al.*, 1994; [4], Hogenboom *et al.*, 2002; [5], Stamellos *et al.*, 1992; [6], Imblum and Rodwell, 1974; [7], Oulmoulden and Karst, 1991.

showed *Ce*MeK to be localized to the cytosol of cells of *C. elegans*, while MeK is peroxisomal in cells of rat (Stamellos *et al.*, 1992), mouse (Hogenbloom *et al.*, 2002) and human (Wanders and Romeijn, 1998). The putative PTS2 sequence of *Neurospora crassa* MeK is almost identical to that of *Ce*MeK (Table 4.5.1). *Nc*MeK appears to be cytosolic (Imblum and Rodwell, 1974), even though there is a functional PTS2-dependent targeting system in *N. crassa*.

MeK catalyzes the phosphorylation of mevalonate to mevalonate 5-phosphate (Stamellos *et al.*, 1992). In higher eukaryotes, mevalonate and mevalonate phosphate are intermediates in the biosynthesis of a highly diverse group of metabolically active compounds including cholesterol, ubiquinone, and vitamin D. *C. elegans* appears to be auxotrophic for sterols, because it does not possess the enzymes necessary for *de novo* sterol biosynthesis (Matyash *et al.*, 2001). Sequence similarity searches predict that *C. elegans* has all the enzymes necessary for the early steps of steroid compound biosynthesis but lacks any recognizable squalene modifying enzymes such as squalene synthase, epoxidase and oxidosqualene cyclase. MeK is one of the enzymes that catalyze early reactions in the sterol metabolism pathway, and its physiological importance is underscored by known MeK deficiencies in humans that result in mevalonic aciduria (Kelley and Herman, 2001). RNAi experiments did demonstrate a requirement for *Ce*MeK for normal nematode development (Kamath *et al.*, 2003; Simmer *et al.*, 2003; WormBase[14]).

---

[14] www.wormbase.org

4.5.2 A new definition for the consensus sequence of the peroxisome targeting signal type 2

Proteins encoded by the *C. elegans* ORFs D1053.2 and W10G11.11 contain putative PTS2s at their extreme amino termini but show no apparent similarity to known peroxisomal proteins. GFP-chimeras of both proteins did not localize to peroxisomes but instead were found in the cytosol of cells of *C. elegans*. These motifs, which conform to the current consensus PTS2 sequence –(R/K)(L/V/I)X_5(H/Q)(L/A)–, are nonfunctional not only in *C. elegans* but also in yeast and mammalian cells known to have functional PTS2-dependent targeting machinery. Our findings suggest that the current consensus PTS2 sequence is too redundant and in need of revision. In fact, the consensus PTS2 sequence for plants has been revised to –(R/K)X_6(H/Q)(A/L/F)– (Flynn *et al.*, 1998), and the importance of individual amino acid residues for the functionality of the PTS2 motif is being elucidated further (Gietl *et al.*, 1994; Tsukamoto *et al.*, 1994; Flynn *et al.*, 1998; Olivier *et al.*, 2000).

Computational analysis has shown that the currently accepted PTS2 consensus, –(R/K)(L/V/I)X_5(H/Q)(L/A)–, is a ubiquitous and frequently found sequence in eukaryotic proteins. This sequence is found even in viral proteins, although it does not show conservation across different strains of the same virus, unlike PTS1 (Mohan and Atreya, 2003). These observations and the finding that there is no preference of the consensus PTS2 sequence for a particular position along the length of proteins (Fig. 4.4.1 A) suggest that the current PTS2 consensus sequence is too broad in its definition to be used reliably as a determinant for the peroxisomal localization of a protein of unknown subcellular location. Although all functional PTS2s conform to the current PTS2 consensus sequence,

–(R/K)(L/V/I)X_5(H/Q)(L/A)–, not all sequences in proteins conforming to this consensus sequence function as PTS2s in targeting proteins to peroxisomes. The five positions of the PTS2 consensus sequence that are currently defined as being able to be occupied by any amino acid are in effect occupied by specific subsets of amino acids. Combining computational data on the preferences for particular amino acids at the nine positions of PTS2 motifs known to function in targeting to peroxisomes (Fig. 4.4.2 E), together with data on the subcellular locations of all proteins containing consensus PTS2 sequences or of peroxisomal proteins mutated in their functional PTS2 sequences (Table 4.5.2), suggests the following amino acid possibilities at the nine positions of the PTS2 motif:

Position 1. R is almost exclusive at this position in functional PTS2s. K substitutes for R in mammalian MeK (Table 4.4.1), which has been shown to be peroxisomal or partially peroxisomal (Stamellos *et al.*, 1992; Biardi *et al.*, 1994; Wanders and Romeijn, 1998), and in Pex8p, a peroxisomal peroxin of the yeast *Hansenula polymorpha* (Table 4.4.1). *Hp*Pex8p has a PTS1 in addition to its PTS2, although the PTS2 has been shown to function autonomously (Waterham *et al.*, 1994). Amino acids S, G, H, Q, N, T, E, L and V (Table 4.5.2, rows 27, 29, 40-46) cannot substitute for R at position 1. Data permitting an A at position 1 of a functional PTS2 are contradictory (Table 4.5.2, rows 3 and 47) and can be explained by the presence of so called "accessory sequences" (Klein *et al.*, 2002) that can modulate receptor binding to the PTS2. The presence of "accessory sequences" may explain why in some cases the presence of K at position 1 compromises the functionality of PTS2 (Table 4.5.2, rows 28 and 39).

Position 2. L appears to be the predominant amino acid at this position, with possible substitution by I, Q or V. Mutational analysis has shown that in some cases Q

Table 4.5.2. List of PTS2 sequences and their variants tested for their functionality in importing proteins into peroxisomes

	PTS2 sequence[a]	Localization[b]
1.	MHRLQV[illegible]LGHLAG	P[1]
2.	MHRLQVVLGH[illegible]AG	P[1]
3.	MSQ[illegible]LQSIKDH[illegible]	P[2]
4.	MSQRL[illegible]SIKDHL	P[2]
5.	MSQRLQSIKD[illegible]L	P[2]
6.	MSQRL[illegible]SIKD[illegible]L	P[2]
7.	MSQRLRSIKD[illegible]L	P[2]
8.	MSQRLQSIKDH[illegible]	P[2]
9.	MSQRLQSIKDH[illegible]	P[2]
10.	MSQRLQSIKDH[illegible]	P[2]
11.	MSQRLQSIKDH[illegible]	P/C[2]
12.	MSQRLQSIKD[illegible]L	P/C[2]
13.	MHRLQVVLG[illegible]LAG	P/C[1,3]
14.	MHR[illegible]QV[illegible]LGHLAG	P/C[1]
15.	MHRLQV[illegible]LGHLAG	P/C[1]
16.	MHR[illegible]QV[illegible]L[illegible]HLAG	P/C[1]
17.	MHR[illegible]V[illegible]LGHLAG	P/C[1]
18.	INR[illegible]QV[illegible]L[illegible]HLAG	P/C[1]
19.	RIARISA[illegible]	C[4]
20.	[illegible]ARISAHL	C[4]
21.	MHRLQVVLG[illegible]LAG	C[1,3]
22.	MHR[illegible]QVVLGHLAG	C[1]
23.	MHR[illegible]QV[illegible]LGHLAG	C[1]
24.	MHRLQV[illegible]LGHLAG	C[1]
25.	MHR[illegible]LAG	C[1,5]
26.	MHRLQVVLG[illegible]LAG	C[1,3]
27.	MSQ[illegible]LQSIKDHL	C[2]
28.	MSQ[illegible]LQSIKDHL	C[2]
29.	MSQ[illegible]LQSIKDHL	C[2]
30.	MSQR[illegible]QSIKDHL	C[2]
31.	MSQR[illegible]QSIKDHL	C[2]
32.	MSQR[illegible]SIKDHL	C[2]
33.	MSQRL[illegible]SIKDHL	C[2]
34.	MSQRL[illegible]SIKD[illegible]L	C[2]
35.	MSQRLQSIKDH[illegible]	C[2]
36.	MSQR[illegible]QSIKDHL	C[2]
37.	MRLLP[illegible]LAQAVPKSF	C[This Study]
38.	MRIFL[illegible]VHLFALCA	C[This Study]
39.	MH[illegible]LQVVLGHLAGRSG	C[3]
40.	MH[illegible]LQVVLGHLAGRSG	C[3]
41.	MH[illegible]LQVVLGHLAGRSG	C[3]
42.	MH[illegible]LQVVLGHLAGRSG	C[3]
43.	MH[illegible]LQVVLGHLAGRSG	C[3]
44.	MH[illegible]LQVVLGHLAGRSG	C[3]
45.	MH[illegible]LQVVLGHLAGRSG	C[3]
46.	MH[illegible]LQVVLGHLAGRSG	C[3]
47.	MH[illegible]LQVVLGHLAGRSG	C[3]
48.	MHRLQVVLG[illegible]LAGRSG	C[3]
49.	MHRLQVVLG[illegible]LAGRSG	C[3]
50.	MHRLQVVLG[illegible]LAGRSG	C[3]
51.	MHRLQVVLG[illegible]LAGRSG	C[3]
52.	MHRLQVVLG[illegible]LAGRSG	C[3]
53.	MHRLQVVLG[illegible]LAGRSG	C[3]
54.	APGKVIV[illegible]GEHAVVHGK	C[6]
55.	APGKVII[illegible]GEH[illegible]AVYNK	C[6]

[a] Mutated amino acid residues and residues of interest are highlighted in black and grey respectively.

[b] P, peroxisomal; C, cytosolic.

[1] Flynn *et al.*, 1998

[2] Glover *et al.*, 1994

[3] Tsukamoto *et al.*, 1994

[4] Gietl *et al.*, 1994

[5] Wimmer *et al.*, 1997

[6] Imblum and Rodwell, 1974

(Table 4.5.2, rows 22 and 30) as well as R (Table 4.5.2, rows 31 and 36) can render the PTS2 nonfunctional.

Position 3. A variable position. Q, A, R, I, E, N, S, G, and K are the most likely amino acids to be found at this position. Some amino acids (*e.g.*, P) at this position may render the PTS2 nonfunctional (Table 4.5.2, row 33); however, the presence of H at position 3 apparently does not compromise the functionality of PTS2 (Table 4.5.2, row 4).

Position 4. Another variable position, with a preference for amino acids V, R, I, L, Q, K, N and S.

Position 5. We suggest that this position is very important for the functionality of PTS2, due to its occupancy by a limited number of amino acids. L, V and I are preferred at position 5, although H and Q function at this position in mammalian MeK and *Hp*Pex8p (Table 4.4.1). E or S at position 5 reduces or negates, respectively, the functionality of PTS2 (Table 4.5.2, rows 15 and 24).

Position 6. A relatively variable position occupied by one of five amino acids: L, S, G, A or K. K is found at this position only in the enzyme 3-ketoacyl-CoA thiolase of *S. cerevisiae* (Table 4.4.1).

Position 7. A variable position with a preference for the amino acids G, A, E, H, L, R, T, D, Q and S. This position appears to be relatively unimportant, as any amino acid substitution is readily accepted without affecting PTS2 functionality.

Position 8. A highly conserved position occupied exclusively by H or Q. Substitution by L, N or T at this position does not affect the functionality of PTS2 (Table 4.5.2, rows 5-7), but G, K, N, S, D, R, L and V are excluded (Table 4.5.2, rows 21, 26, 48-53).

Position 9. The last position is occupied mainly by L and occasionally by A. In rare cases, position 9 can be occupied by F (Glover *et al.*, 1994; Flynn *et al.*, 1998; Gebhardt *et al.*, 1998). The fact that F, as well as M and V, can substitute for L at position 9 is supported by mutational analysis (Table 4, rows 8, 9 and 10). The presence of amino acids such as W and S at position 9 affects the functionality of PTS2 (Table 4.5.2, rows 11 and 35).

An integration of this analysis suggests two new versions of the consensus PTS2 sequence: –R(L/V/I/Q)XX(L/V/I/H)(L/S/G/A)X(H/Q)(L/A)– describes the most common of the PTS2 variants, while –(R/K)(L/V/I/Q)XX(L/V/I/H/Q)(L/S/G/A/K)X(H/Q) (L/A/F)– describes almost all known PTS2 variants. The putative PTS2s of the proteins encoded by the ORFs D1053.2 and W10G11.11 (Table 4.5.2, rows 37 and 38) do not correspond to either of the two proposed consensus PTS2 sequences, with amino acid residues at position 5 for D1053.2 and at positions 5 and 6 for W10G11.11 being inappropriate for PTS2 activity as discussed above. The putative PTS2s of *Ce*MeK and *Nc*MeK are not functional, presumably because of the presence of a F residue at position 5 (Table 4.5.1) in these proteins, with L/V/I/H or L/V/I/H/Q being the only predicted permissible residues at position 5.

A search of the Proteome database[15] with the PTS2 consensus sequence –R(L/V/I/Q)XX(L/V/I/H)(L/S/G/A)X(H/Q)(L/A)– identified many known peroxisomal proteins targeted by the PTS2-dependent pathway from organisms such as human, mouse, rat and yeast. An analogous search of all putative *C. elegans* ORFs did not result in any protein known to be peroxisomal in the nematode or in other organisms. This finding, combined with the demonstration that *Ce*MeK localizes to the cytosol and previous findings (Motley *et al.*, 2000), shows unequivocally that the PTS2-dependent peroxisomal import pathway does not function in the nematode *C. elegans*, possibly due to the switching of targeting signals found in peroxisomal proteins that occurred during evolution of *C. elegans* (Motley *et al.*, 2000).

---

[15] www.incyte.com

CHAPTER 5

ROLE OF PEROXISOMAL CATALASE
IN
CAENORHABDITIS ELEGANS LONGEVITY

A version of this chapter has previously been published as "Lack of peroxisomal catalase causes a progeric phenotype in *Caenorhabditis elegans*". (Petriv, O.I., and R.A. Rachubinski. 2004. *J. Biol. Chem.* 19:19996-20001).

5.1 Overview

This chapter describes data obtained from molecular and biochemical analysis of a deficiency in peroxisomal catalase, CTL-2.

Despite the lack of an obvious RNAi phenotype, CTL-2 protein deficiency was found to affect aging and the developmental program of *C. elegans*. *Δctl-2* worms lay fewer eggs and age more rapidly than controls. The *Δctl-2* mutation also shortens the lifespan of the long-living mutant, *Δclk-1*. Surprisingly, the progeric phenotype of *Δctl-2* mutants is not due to increased carbonylation of the major *C. elegans* proteins. Peroxisomes are proposed to be the primary location affected by the absence of catalase. Abnormalities within the organelle therefore affect the entire developmental program of the nematode.

5.2 Characterization of the catalase genes of *C. elegans* and analysis of catalase enzymatic activity in the nematode

The *C. elegans* genome contains three catalase genes in tandem: *ctl-3*, *ctl-1* and *ctl-2* (Figs. 5.2.1 and 5.2.2) (Lewis and Fleming, 1995). DAF-16 binding motifs (McElwee *et al.*, 2003) are present upstream and downstream of all three genes (Fig. 5.2.1). The catalase genes exhibit extensive sequence identity. *ctl-1* is identical to *ctl-2* between nucleotides 1 and 304 and to *ctl-3* from nucleotide 304 until its end (Figs. 5.2.1 and 5.2.2). The coding region of *ctl-2* exhibits 76.7% sequence identity to the coding region of *ctl-3* (Figs. 5.2.1, 5.2.2 and 5.2.3). The intervening region between the *ctl-1* and *ctl-3* genes is 100% identical in sequence to the intervening region between the *ctl-1* and *ctl-2* genes (Figs. 5.2.1 and 5.2.2). Extensive sequence identity among the catalase genes makes it difficult to analyze their individual expression by techniques such as

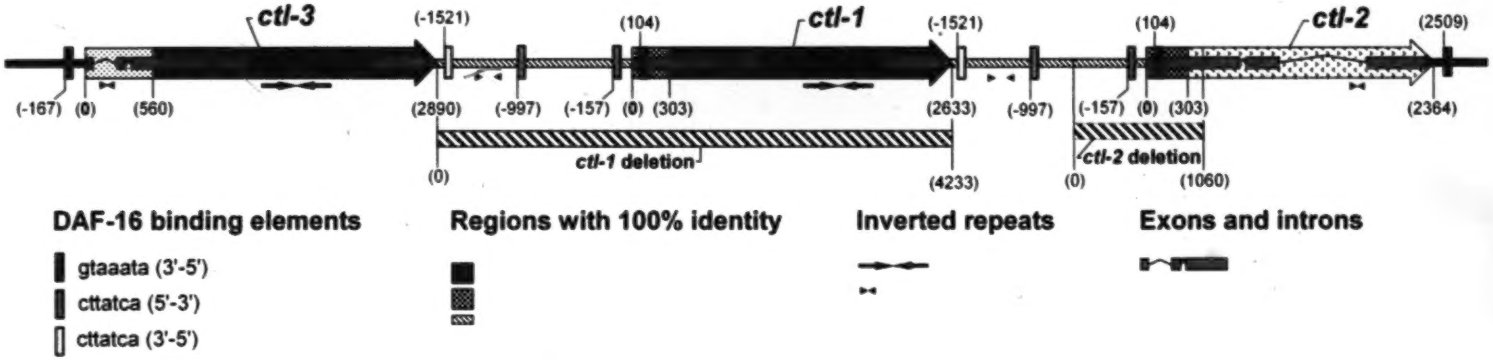
ctl-3
(-1521)
(104)
ctl-1
(-1521)
(104)
ctl-2
(2509)
(-167)
(0)
(560)
(2890)
(-997)
(-157)
(0)
(303)
(2633)
(-997)
(-157)
(0)
(303)
(2364)
ctl-1 deletion
(0)
(4233)
ctl-2 deletion
(0)
(1060)
DAF-16 binding elements
gtaaata (3'-5')
cttatca (5'-3')
cttatca (3'-5')
Regions with 100% identity
Inverted repeats
Exons and introns

Figure 5.2.1. Structure of the *ctl* loci in the *C. elegans* genome. A genomic DNA fragment 12 Kbp in length and encompassing the three catalase genes of *C. elegans* is presented. This region contains several consensus binding sites for the transcription factor DAF-16 and a large number of inverted DNA repeats. The adenosyl residue of the translation initiating codon of each catalase gene is designated "0" and serves as the point of reference for numbering the nucleotide sequence upstream (negative values) and downstream (positive values) of a particular catalase gene. Identical shading represents regions with 100% identity between genes.

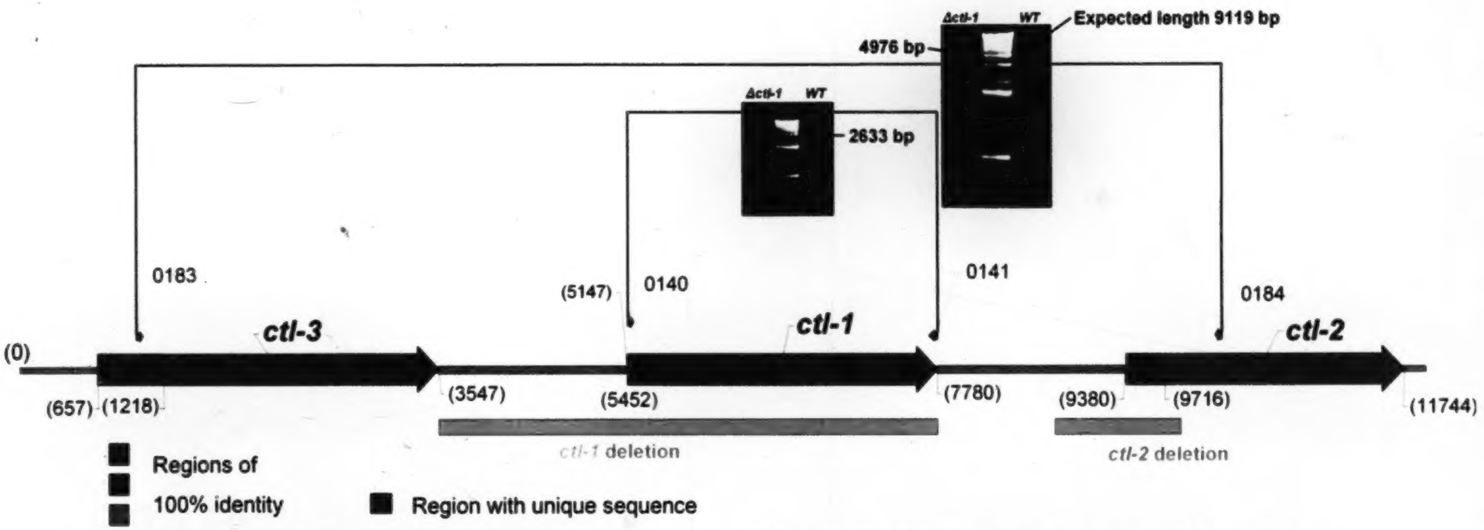
Δctl-1 WT
Expected length 9119 bp
4976 bp
Δctl-1 WT
2633 bp
0183
(5147)
0140
0141
0184
(0)
ctl-3
ctl-1
ctl-2
(657)
(1218)
(3547)
(5452)
(7780)
(9380)
(9716)
(11744)
ctl-1 deletion
ctl-2 deletion
Regions of 100% identity
Region with unique sequence

Pairwise comparison of *ctl* genes

Pairs	Gene identity, %	cDNA identity, %
ctl-1:ctl-2	66.8	82.0
ctl-1:ctl-3	87.8	94.1
ctl-2:ctl-3	58.1	76.7

Oligonucleotide sequences for Δ*ctl-1 screening*

0183	ATCAATTTCAGCGATTTTCTTCGCA
0184	AGTTGGAAATTATAGACCGA
0140	TCGGTACCATGCCAAACGATCCATCGG
0141	CTGCTAGCTTAATGCTTCTTCTGGCAGAGC

Figure 5.2.2. Detection of the deletions of catalase genes. Structure of the *ctl* loci of the *C. elegans* genome and of *Δctl-1 (u800)* and *Δctl-2 (ua90)* deletions. Orange bars illustrate deletion spans. Identity between catalase genes is indicated. Oligonucleotides used for nested PCR to detect the *Δctl-1* deletion are presented. PCR products, showing the *Δctl-1* deletion are represented.

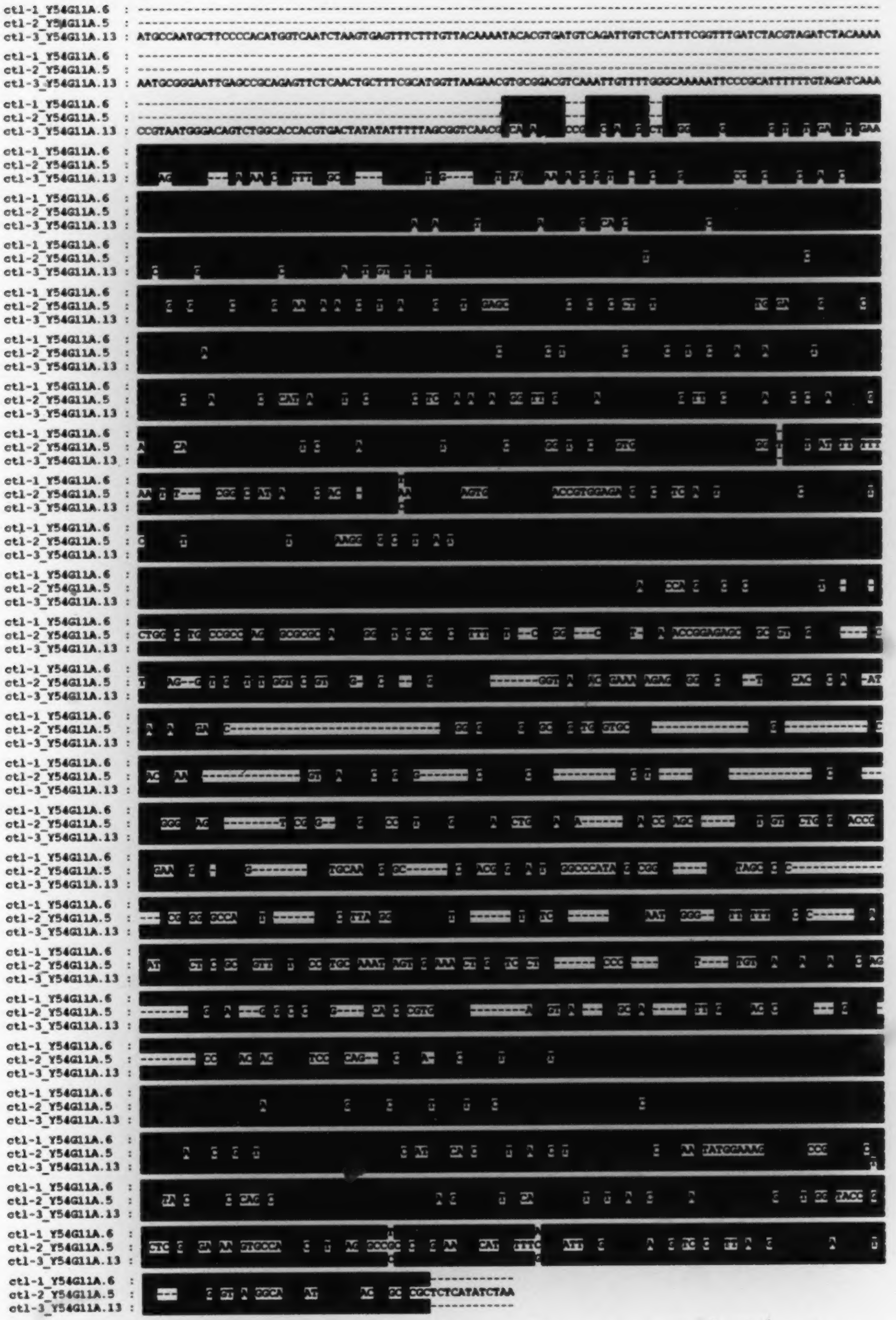

Figure 5.2.3. Multiple alignment of *C. elegans* catalase genes. ClustalW[1] software was used to align and compare sequences of the nematode catalase genes. Black - identical nucleotides.

---

[1] http://www.ebi.ac.uk/clustalw/

Northern blotting, or *in situ* hybridisation. The results of RNA interference and gene microarray analysis also should be interpreted with caution.

The catalases themselves can be distinguished from one another through differences in their biochemical properties. Because the pIs of the three catalases differ significantly (Table 5.2.1), they can be readily separated by native gel electrophoresis and detected by staining for enzymatic activity (see Materials and Methods) (Fig. 5.2.4 A). We isolated a worm strain, *ctl-2(ua90)II*, harboring a deletion of the *ctl-2* gene (Figs. 5.2.1 and 5.2.2, *Δctl-2*). The *Δctl-2* mutant strain exhibits no detectable CTL-2 enzymatic activity (Fig. 5.2.4 A). DNA sequencing of the strain *ctl-1(u800)II*, which has been claimed to exhibit decreased catalase activity due to a premature termination codon in the *ctl-1* gene (Taub *et al.*, 1999), showed that the entire *ctl-1* gene and extensive sequence upstream are missing in this mutant (Figs. 5.2.1 and 5.2.2, *Δctl-1*). Native gel electrophoresis confirmed the absence of CTL-1 enzymatic activity in the *Δctl-1* strain (Fig. 5.2.4 A). Attempts to isolate mutants of the *ctl-3* gene were unsuccessful. In dauer larvae, a developmental stage during which animals do not feed and fat metabolism is shifted to fat storage (Guarente *et al.*, 1998), the level of CTL-1 activity is increased, while the level of peroxisomal CTL-2 activity appears to be similar to that found in wild-type worms (Fig. 5.2.4 A). *Δctl-2* and *Δctl-1* mutants are able to enter the dauer stage normally.

Quantitative colorimetric analysis of catalase activity showed that deletion of the *ctl-2* gene (Fig. 5.2.4 B, *Δctl-2* and Table 5.2.2) reduced catalase activity to approximately 20% of the total catalase activity observed in wild-type worms, while deletion of the *ctl-1* gene (Fig. 5.2.4 B, *Δctl-1* and Table 5.2.2) led to a much smaller reduction in catalase activity to approximately 75% of the total catalase activity observed in wild-type worms.

Table 5.2.1. Three genes encoding catalases in *C. elegans*

Gene	ORF designation	cDNA length (base pairs)	Protein MW[a]	Protein pI
ctl-1	Y54G11A.6	1494	57.3	6.71
ctl-2	Y54G11A.5(A)	1503	57.5	8.02
ctl-3	Y54G11A.13	1539	59	6.66

[a] Predicted molecular weight, in kDa.

Table 5.2.2. Lifespan, catalase activity and brood size in *C. elegans* mutants

Strain[†]	Mean lifespan, days from hatching [a]	Maximum lifespan, days from hatching [a]	Catalase activity *in vitro*, % of wild-type	Eggs laid/worm (n=20 worms)
Wild-Type	14.6 ± 1.4 (n[b] = 717)	20.8 ± 3.1 (n[e] = 6)	100	310 ± 31
Δctl-1	15.3 ± 1.2 (n = 364) [b]	21.7± 0.5 (n = 4) [b]	74.6 ± 6.7 (n = 8)	332 ± 25
Δctl-2	12.1 ± 0.9 (n = 365) [c,*]	16.6 ± 1.1 (n = 5) [b,**]	19.6 ± 6.1 (n = 11)	231 ± 22
Δclk-1	24.7 ± 2.7 (n = 277)	32.7 ± 1.5 (n = 3)	171.5 ± 19.8 (n = 4)	160 ± 20
Δclk-1; Δctl-2	24.3 ± 1.6 (n = 161) [d]	29.3 ± 1.2 (n = 3) [c,**]	nd [f]	130 ± 24

[†] alleles used: *Δctl-1 (u800), Δctl-2 (ua90), Δclk-1(qm30).*

[a] Based on unpaired t-test for two populations.

[b] number of animals counted in a number of independent experiments shown in [e].

[c] Comparison to wild-type strain.

[d] Comparison to *clk-1* strain.

[e] number of independent experiments in which [b] total number of worms was counted.

[f] Not determined.

* Significantly different at $P < 0.01$.

** Significantly different at $0.01 < P < 0.05$.

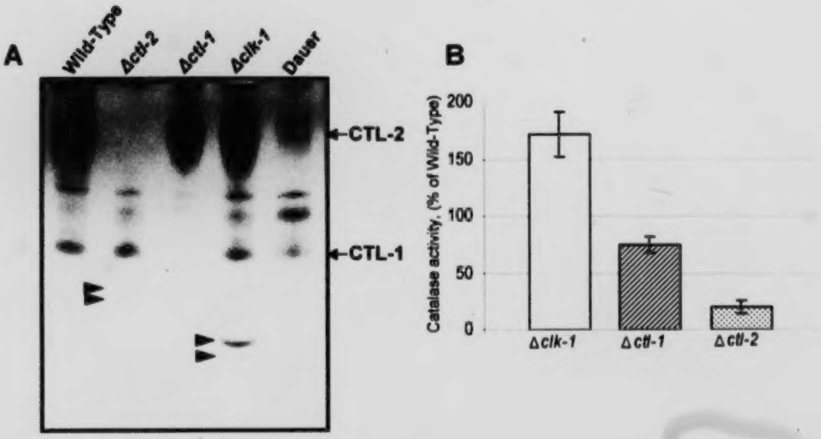

Figure 5.2.4. Activity of catalases in *C. elegans*. ***A***. Native gel of total nematode lysates stained for catalase activity. In mutant worms, enzymes other than the three catalases that manifest catalase activity are upregulated (*arrowheads*). Equal amounts of protein were loaded in each lane except for the lane labeled "Dauer", which contained 7.5 times less protein than each of the other lanes. ***B***. Total catalase activity measured *in vitro* in mutant mixed stage worms as a percentage of total catalase activity in wild-type worms.

Therefore, peroxisomal catalase CTL-2 contributes most of the total catalase activity in *C. elegans*.

5.3 Lack of peroxisomal, but not cytosolic, catalase causes a progeric phenotype in *C. elegans*

We compared the mean and maximum lifespan and brood size of catalase mutant worms versus wild-type worms to determine whether the different catalases in *C. elegans* could have a role in the development and aging of the nematode. *Δctl-1* mutants showed no difference in lifespan or brood size when compared to wild-type worms, while *Δctl-2* mutants had a significantly shortened (16% less) lifespan and decreased brood size (Fig. 5.3.1 and Table 5.2.2). Introduction of the *Δctl-2* mutation into long-lived *Δclk-1* mutant worms did not result in a shortening of their mean lifespan (Fig. 5.3.1 and Table 5.2.2), consistent with a previous finding that the extended lifespan of *Δclk-1* mutant worms is not related directly to the antioxidant action of catalase (Braeckman *et al.*, 2002). Nevertheless, we observed a significantly shortened (14% less) maximum lifespan and an acceleration of approximately 12 hours in the onset of the egg laying period in *Δclk-1*; *Δctl-2* double mutant worms as compared to *Δclk-1* mutant worms (Fig. 5.3.1 and Table 5.2.2).

Increased protein carbonylation has been observed during cell aging (Goto *et al.*, 1999). Carbonylation of major worm proteins such as vitellogenin-6 (Nakamura *et al.*, 1999) increases at 10 days of age relative to 10 days in both wild-type worms and *Δctl-1* and *Δctl-2* mutant worms, but the overall increase in carbonylation is less for both mutants than for wild-type worms (see Materials and Methods) (Fig. 5.3.2). This smaller increase

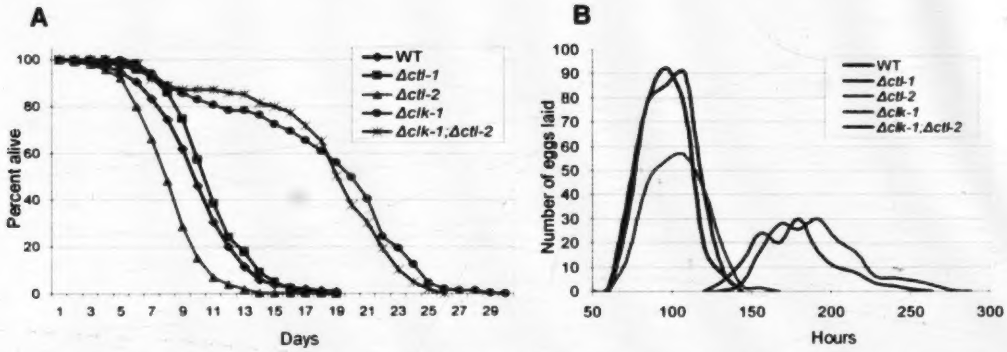

Figure 5.3.1. Effects of mutation of the *ctl-1* and *ctl-2* genes on lifespan and brood size of wild-type and *Δclk-1* mutant worms. (See also Table 5.2.2). **(A)**, mutation of the *ctl-2* gene (*Δctl-2*) shortens the mean lifespan of wild-type (WT) worms (strain N2) by 16% and the maximum lifespan of the *Δclk-1* long-living mutant by 14%. In contrast, the *Δctl-1* mutation does not influence significantly the mean lifespan of wild-type worms. **(B)**, *Δctl-2* mutants lay 25% fewer eggs than do wild-type (WT) or *Δctl-1* mutant worms. Lack of CTL-2 also advances the egg-laying period in the *Δclk-1* mutant by 12 h.

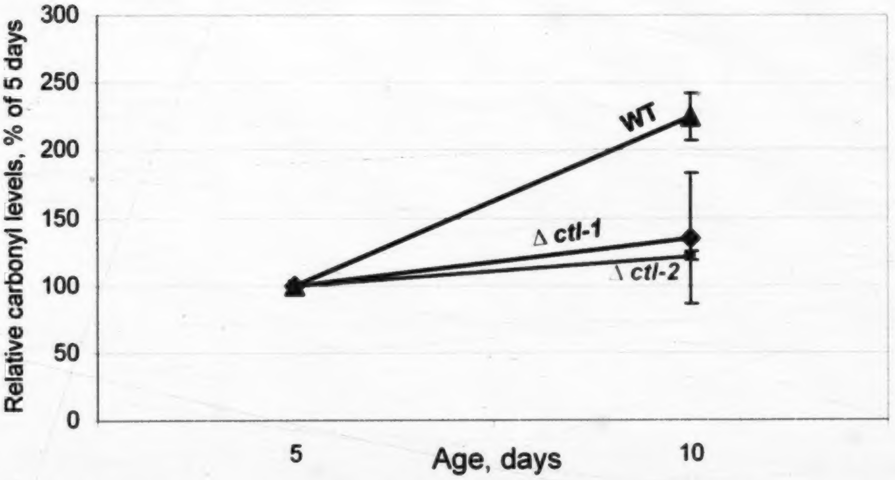

Figure 5.3.2. Carbonylation levels of the major proteins of wild-type and catalase mutant worms. Protein carbonylation was determined as described in Materials and Methods. Carbonylation levels at 5 days were taken as 100%. Carbonylation levels at 10 days are 224 ± 17% in wild-type worms (WT), 134 ± 48% in *Δctl-1* worms and 121 ± 4% in *Δctl-2* worms. Data derived from three independent experiments.

in carbonylation observed for the *Δctl-1* and *Δctl-2* mutants may result from a compensatory upregulation of other antioxidant enzymes in these mutants. Evidence for such compensatory changes in the synthesis of unidentified enzymes with catalase activity could be seen for the *Δctl-1* and *Δctl-2* mutants (Fig. 5.2.4 A, arrowheads). The carbonylation of major protein species therefore appears not to be the cause of the progeric phenotype of the *Δctl-2* mutant.

5.4 Cells of the *Δctl-2* mutant exhibit abnormal peroxisome morphology

A deficiency in the peroxisomal β-oxidation enzyme acyl-CoA oxidase leads to increased levels of intracellular H_2O_2 and alters the morphology of peroxisomes (Fan *et al.*, 1998). A lack of peroxisomal catalase CTL-2 might be expected to exert a similar effect on peroxisome morphology due to decreased breakdown of intraperoxisomal H_2O_2. We therefore examined the morphology of peroxisomes in wild-type and *Δctl-2* mutant worms by fluorescent confocal microscopy and electron microscopy. Morphometric analysis indicates that the mean diameter of peroxisomes is increased in *Δctl-2* mutant worms versus wild-type worms (Fig. 5.4.1 A), and peroxisomes tend to cluster in the *Δctl-2* mutant (Fig. 5.4.1 A). Electron microscopy revealed that these clustered peroxisomes are often associated with lipid vesicles (Fig. 5.4.2 B, left panel) or with specific multivesicular structures of unknown origin and function (Fig. 5.4.2 B, right panel). Fat metabolism is apparently normal in *Δctl-2* mutant worms, as they accumulate lipid droplets in their cells of the same size accumulated by cells of wild-type worms (Fig. 5.4.1 B).

In an attempt to detect peroxides of fatty acids, methyl esters of total lipids derived from catalase mutant and wild-type worms were analyzed by gas chromatography-mass

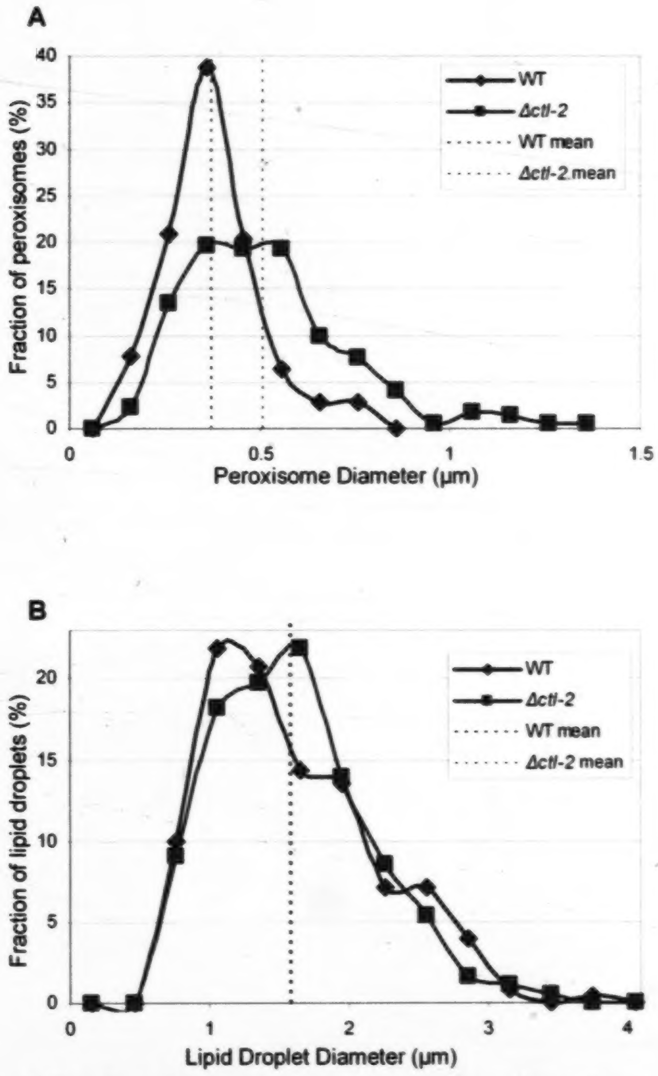

Figure 5.4.1. Cells of *Δctl-2* mutant worms contain enlarged peroxisomes but lipid droplets of normal size. (**A**), Distribution of range of diameter and mean diameter of peroxisomes in hypodermal cells of the *Δctl-2* mutant (0.38 µm, n = 206) and wild-type (WT) (0.51 µm, n = 223) worms. (**B**), Distribution of range of diameter and mean diameter of lipid droplets from gut cells of wild-type (WT) (5.48 µm, n = 251) and *Δctl-2* mutant (5.51 µm, n = 187) worms.

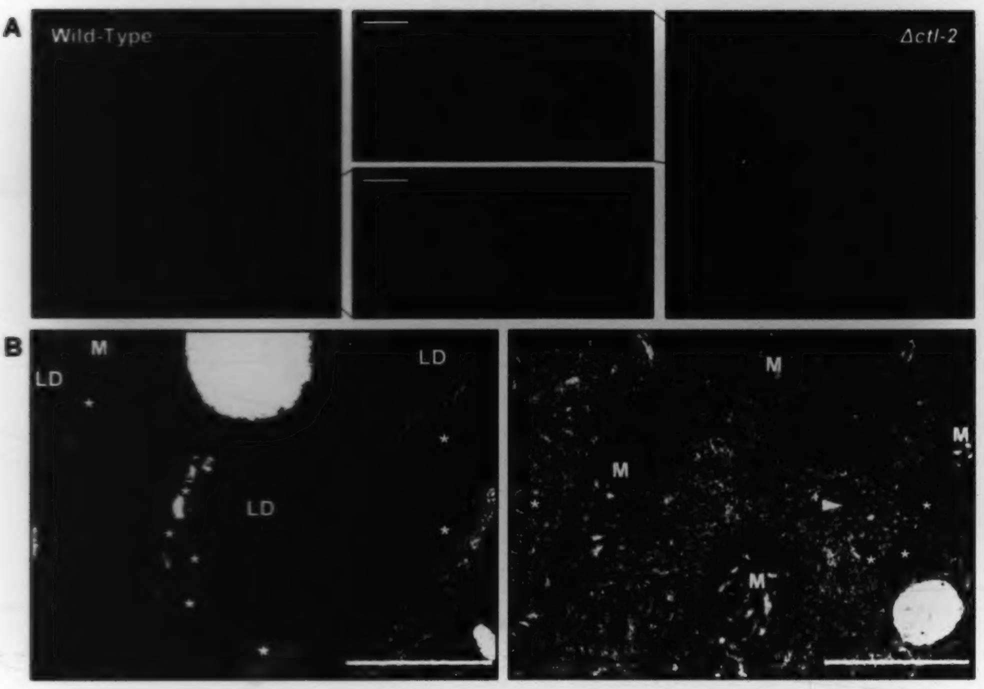

Figure 5.4.2. Peroxisomes exhibit altered morphology in *Δctl-2* mutant worms. (*A*). Peroxisomes were detected by fluorescence confocal microscopy of GFP tagged with the tripeptide PTS1, Ser-Lys-Leu (Pertriv et al., 2002). Peroxisomes are larger and form aggregates in cells of the *Δctl-2* mutant as compared to peroxisomes in cells of wild-type worms. Bar, 5 μm. (***B***). Electron microscopy of gut cells (left panel) or hypodermal cells (right panel) of *Δctl-2* worms showing that peroxisomes (⋆) are often associated with lipid droplets (LD) or vesicular structures of unknown origin (*arrowhead*). M, mitochondrion. Bar, 1 μm.

spectrometry (Fig. 5.4.3). No significant difference in the spectra of total lipids was observed for wild-type and mutant worms 7 days after hatching.

5.5 DISCUSSION

Similarly to superoxide dismutases (SOD), catalases are scavengers of H_2O_2 and reactive oxygen species (ROS), respectively, and have been suggested to play important roles in the aging process in *C. elegans* (Vanfleteren, 1993). Catalase levels are increased in the long-lived *C. elegans* mutants *age-1* (Larsen, 1993; Vanfleteren, 1993; Yanase *et al.*, 2002), *eat-2* (Houthoofd *et al.*, 2002b) and *daf-2* (Hekimi *et al.*, 2001; Houthoofd *et al.*, 2003), while catalase gene expression is decreased in a short-lived strain mutated for DAF-16 (Wolkow *et al.*, 2000). The *daf-16* mutation also largely suppresses the increases in catalase activity observed in *age* mutants (Houthoofd *et al.*, 2003).

Catalases genes are among the direct targets (Lee et al, 2003; McElwee *et al.*, 2003) of the FOXO-family transcription factor, DAF-16 (Ogg *et al.*, 1997), a key regulator of the insulin/IGF-I signaling pathway implicated in the aging process (Hsu *et al.*, 2003; McElwee *et al.*, 2003). These target genes usually contain specific nucleotide sequences in their upstream regulatory regions capable of binding DAF-16 and can be directly repressed or activated upon binding of DAF-16 (Murphy *et al.*, 2003). Specific transcriptional regulation of target genes by DAF-16 is purported to lead to an extended or shortened lifespan for the nematode. Among the genes regulated by DAF-16 are those encoding heat-shock proteins and cytochrome P450s involved in the cell stress-response and genes encoding proteins responsible for antioxidant defense, such as the mitochondrial superoxide dismutase SOD-3, the metallothionein homolog MTL-1, and the catalases

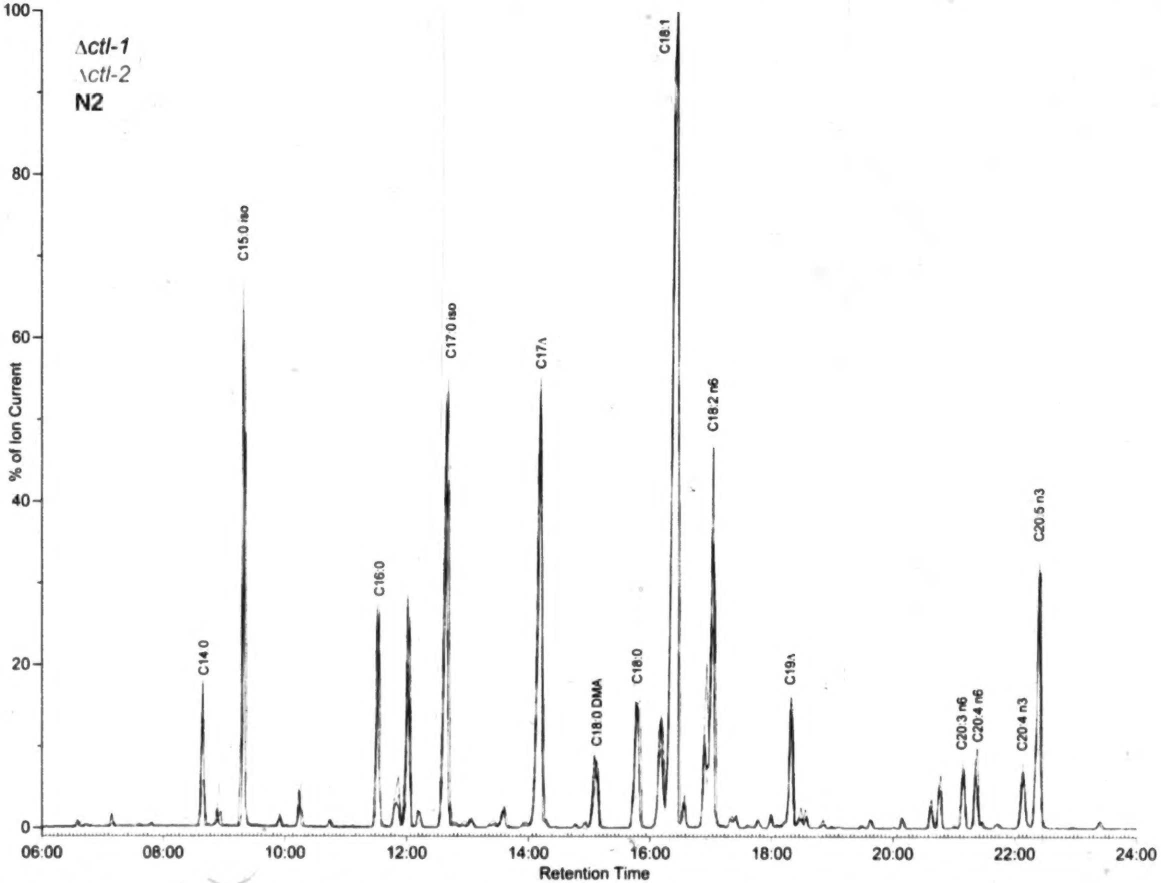

Figure 5.4.3. Gas chromatography spectra of methyl esters of fatty acids derived from *C. elegans* wild-type (N2) and catalase mutant (Δ*ctl-1*, Δ*ctl-2*) worms. Triacylglycerols from nematodes were hydrolyzed and derivatized to methyl esters (see Materials and Methods). C17 Δ and C19 Δ, cyclopropane-containing fatty acids. DMA, dimethyl acetal.

CTL-1 and CTL-2 (Murphy *et al.*, 2003).

In addition to the insulin/IGF-I signaling pathway, dietary restriction and oxidative stress are also thought to be major determinants of the aging process in *C. elegans* and other model organisms (Jazwinski, 1998; Houthoofd *et al.*, 2003). Under conditions of dietary restriction that extend monoxenic, and especially axenic, worm lifespan, catalase and SOD levels have been found to be increased dramatically in a DAF-16-independent manner (Houthoofd *et al.*, 2003). A correlation between increases in SOD and catalase activity and hyperresistance to oxidative stress has also been observed in some long-lived mutants (Larsen, 1993). During the dauer larval stage when the nematode is developmentally arrested, non-feeding and exhibits a lifespan several times larger than normal, catalase and/or SOD activities are substantially upregulated (Larsen, 1993; Houthoofd *et al.*, 2002a). Moreover, treatment of worms with SOD/catalase mimetics extends their lifespans (Melov *et al.*, 2000; Gill *et al.*, 2003). These and other findings from different model organisms (Mackay and Bewley, 1989; Longo *et al.*, 1996; Jazwinski, 1998; Boulianne, 2001; van Zandycke *et al.*, 2002) suggest that catalases play an important role in the aging process; however, a definitive statement on the role of individual catalases in the aging process in *C. elegans* requires an investigation of this process in mutant strains deleted for the individual catalase genes.

Two forms of catalase, the cytosolic CTL-1 and the peroxisomal CTL-2, have been reported for *C. elegans* (Taub *et al.*, 1999; Togo *et al.*, 2000). A previous attempt to involve CTL-1 directly in the control of aging in *C. elegans* was unsuccessful (Taub *et al.*, 1999). Molecular features of the catalase gene locus in *C. elegans*, namely the presence of different catalase genes exhibiting a high level of sequence identity, make it difficult, if not impossible, to interpret adequately the results of methods such as RNAi (Hsu *et al.*, 2003; Murphy *et al.*, 2003; Petriv *et al.*, 2002). To permit definitive statements on the roles of individual catalases in the aging process of *C. elegans*, individual gene knockouts are required. The *C. elegans* strains mutated in two different catalase genes described here represent the first genetic evidence directly implicating peroxisomal catalase, CTL-2, but not cytosolic catalase, CTL-1, in the aging process and developmental program of *C. elegans* and show that a lack of CTL-2 causes a progeric phenotype in the nematode.

The *C. elegans* genome contains three genes encoding different catalases. No other metazoan has been reported to have multiple catalase genes. The most active form of catalase in *C. elegans* is peroxisomal catalase, CTL-2, which contributes approximately 80% of total catalase activity in the nematode. The remaining catalase activity is contributed by cytosolic catalase, CTL-1, a previously unreported catalase, CTL-3, encoded by the open reading frame Y54G11A.13, and unknown enzymes exhibiting catalase activity (Fig. 5.2.4 A). Attempts to obtain a strain mutant for the *ctl-3* gene were unsuccessful; however, expression of a GFP reporter under the control of a flanking region extending 657 bp upstream from the *ctl-3* initiating codon was localized to pharyngeal muscle cells and neurons (Fig. 5.5.1).

Previous results from studies employing RNAi had suggested the importance of CTL-2 function for longevity in *C. elegans* (Murphy *et al.*, 2003). However, because of the high degree of nucleotide identity among the catalase genes, the results of RNAi studies must be interpreted with caution. Worms deleted for the *ctl-2* gene have demonstrated directly for the first time that a lack of peroxisomal catalase accelerates aging in *C. elegans*. A lack of CTL-2 resulted in a 16% reduction in the mean lifespan of

Figure 5.5.1. Reporter GFP expression from the *ctl-3* gene upstream region. GFP lozalization to pharyngeal muscle cells (**A**), and neurons (**B** and **C**; **A**, arrows).

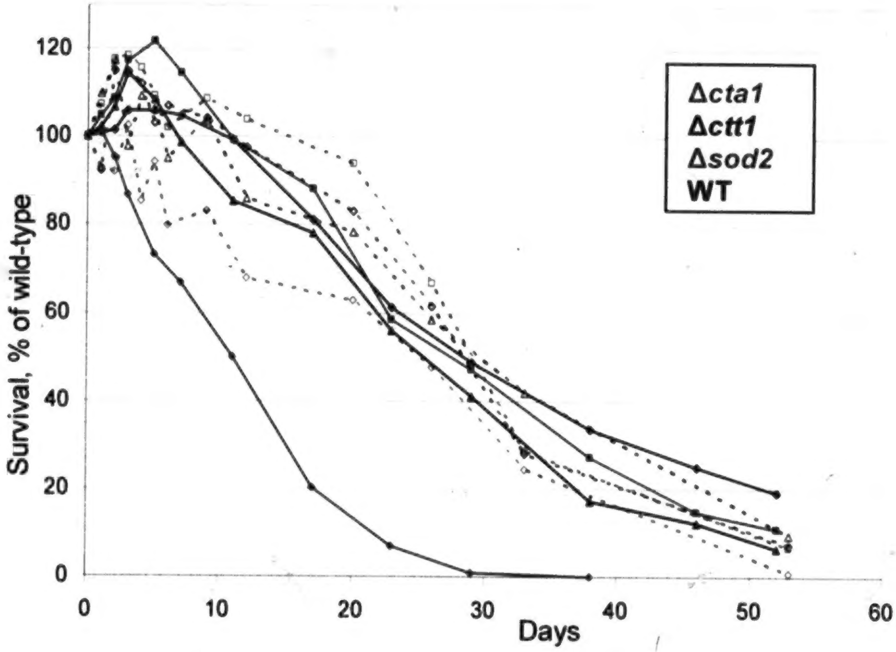

Figure 5.5.2. Survival of *S. cerevisiae* wild-type (WT) and mutant strains lacking cytosolic (Δ*ctt1*) or peroxisomal (Δ*cta1*) catalase. The number of cells in experiments varied from 3 cells/µl (solid lines) to 10000 cells/µl (hatched lines). A mutant of mitochondrial SOD (Δ*sod2*) served as a negative control (Longo *et al*., 1996).

worms. The reduced viability of *Δctl-2* mutant worms was also reflected in the significantly smaller number of eggs they laid and their slightly delayed and extended egg laying period. Importantly, a deletion of the *ctl-1* gene did not affect either lifespan or egg laying capacity of the nematode, demonstrating that the effects of the *ctl-2* deficiency on these characteristics were not simply the result of reduced overall catalase activity. Introduction of the *Δctl-2* mutation into the long-lived *Δclk-1* mutant increased the survival of *Δclk-1*; *Δctl-2* double mutant worms during the first 19 days of life but led to the rapid death of this strain after 19 days (Fig. 5.3.1 A), thus resulting in a shortened maximum lifespan but no overall change in mean lifespan. These findings are consistent with previous data showing that the extended mean lifespan of the *Δclk-1* mutant is not related directly to the antioxidant action of catalase (Braeckman *et al.*, 1992). Interestingly, introduction of the *Δctl-2* mutation into the *Δclk-1* mutation background accelerated the egg laying period of the *Δclk-1*; *Δctl-2* double mutant by 12 hours compared to the *Δclk-1* mutant. Development and behavior are considerably retarded and reproduction is strongly reduced in *Δclk-1* mutant worms as compared to wild-type worms (Wong *et al.*, 1995). Reduced reproduction in *Δclk-1* worms is the result of slower germline development, which in turn is dependent on ROS-mediated oxidation of low density lipoprotein (LDL)-like lipoproteins (Shibata *et al.*, 2003). Suppression of the *sod-1* gene encoding cytosolic SOD has been shown to stimulate germline development, apparently through the increased oxidation of lipoproteins (Shibata *et al.*, 2003). The synthesis of complex lipids and the assembly of lipoproteins depend on peroxisomes (Wetterau *et al.*, 1992; Segrest *et al.*, 2001). An expected increase in the levels of ROS resulting from increased levels of H_2O_2 inside peroxisomes lacking catalase would be expected to lead to increased oxidation of lipids, including those that are assembled into LDLs in the nematode. Oxidation of lipids in cells of *Δctl-2* mutant worms could also happen outside peroxisomes due to leakage of H_2O_2 from abnormal peroxisomes. Both confocal and electron microscopy showed the presence of peroxisomes with abnormal morphology in cells of *Δctl-2* mutant worms (Fig. 5.4.2). Therefore, the progeric phenotype of *Δctl-2* mutant worms and the observed advancement in the egg laying period of the *Δclk*-1; *Δctl-2* double mutant may be due to increased levels of local ROSs produced in the absence of CTL-2 that act in the oxidation of lipids both within and outside the peroxisome. This is particularly significant given that the carbonylation of major protein species is not the cause of the progeric phenotype of the *Δctl-2* mutant. Peroxidation of major lipids was also not observed in the *Δctl-2* mutant nematode (Fig. 5.4.3), but this is most likely due to the low sensitivity of the detection method used. Some patients with Zellweger-like clinical features suffer from severe neurological abnormalities resulting from the mislocalization of peroxisomal catalase to the cytosol (Singh *et al.*, 1997). Lack of catalase in the peroxisomes of skin fibroblasts from these patients results in the inactivation of multiple enzyme activities in peroxisomes, probably due to increased levels of ROS (O_2^- and H_2O_2) and subsequent oxidative injury to proteins or lipids in the peroxisomes. The enzymatic deficiencies were corrected by targeting catalase to peroxisomes in these mutant cells (Sheikh *et al.*, 1998).

The effects of a lack of peroxisomal catalase on organismal longevity is not restricted to *C. elegans*. In the fly *Drosophila melanogaster*, a complete loss of catalase activity confers a severe viability deffect (Mackay and Bewley, 1989). In *S. cerevisiae*, the activity of cytosolic catalase (catalase T, *CTT1*) is required for normal replicative lifespan on repressing (glucose-containing) or derepressing (ethanol-containing) growth medium.

Peroxisomal catalase (catalase A, *CTA1*), however, is required only on derepressing medium (van Zandycke *et al.*, 2002). Loss of cytosolic catalase T has little effect on the chronological lifespan of *S. cerevisiae*, even though its levels are highly induced during the stationary phase of growth (Longo *et al.*, 1996).

To date, no data have been available for the role of catalase A in the chronological lifespan of *S. cerevisiae*. We therefore measured the chronological lifespan of wild-type *S. cerevisiae* and of the mutants *Δcta1* and *Δctt1* and of the mutant *Δsod2* (mitochondrial SOD) as a negative control (see Material and Methods). No significant decrease in the viability of yeast carrying the *Δcta1* or the *Δctt1* mutation was found in comparison to the wild-type strain (Fig. 5.5.2). These data suggest that both catalases may play an important anti-aging role during cell division rather than during stationary growth of *S. cerevisiae*.

In closing, lack of peroxisomal catalase, CTL-2, but not cytosolic catalase, CTL-1, causes a progeric phenotype in the nematode *C. elegans*. The *Δctl-2* mutant of *C. elegans* represents a convenient model not only to study the process of aging but possibly also for the study of the human diseases acatalasemia and hypocatalasemia (Ogata, 1991; Petriv *et al.*, 2002; Thieringer *et al.*, 2003). Our results support and extend recent findings that peroxisomes not only have important roles in cell metabolism but also are involved in the developmental processes of eukaryotic organisms (Titorenko and Rachubinski, 2001a; Legaskis *et al.*, 2002; Petriv *et al.*, 2002; Thieringer *et al.*, 2003).

CHAPTER 6

FUNCTIONAL DISSECTION OF THE THIOLASE AND STEROL-CARRIER DOMAINS OF SCPx OF *CAENORHABDITIS ELEGANS*

6.1 Overview

This chapter provides a molecular analysis of the biological effects caused by a deficiency in 3-oxoacyl CoA thiolase type II, P-44, a peroxisomal enzyme discussed in detail in Chapter 3. Unlike thiolase type I, which catalyzes the thiolytic reaction with straight-chain fatty acids as a substrate, thiolase type II acts on methyl-branched fatty acids. Accumulation of branched fatty acid, phytanic in the human plasma is thought to be the main cause of Refsum deasease.

P-44 deficiency was found to extend the egg laying period of *C. elegans*, to cause a decrease in body size and to induce the proliferation of peroxisomes. Surprisingly, the expected accumulation of branched fatty acids such as phytanic acid and pristanic acid was not detected in mutant worms. Nevertheless, *C. elegans* worms deficient in P-44 exhibit a defect of branched fatty acid catabolism. Interestingly, a similar phenotype is observed in worms deficient in fat-2, the nematode homolog of the SCP2 domain of SCPx, which plays a sterol-carrier role.

The nature of the P-44 and fat-2 mutant phenotypes suggests that they are caused by elevated levels of branched fatty acids or very-long chain fatty acids.

6.2 Genetic and phenotypic characterization of *C. elegans* P-44 deficiency

C. elegans P-44 thiolase is homologous to the catalytic thiolase domain of mammalian SCPx protein (Fig. 6.2.1). DNA sequencing demonstrated that the deletion allele *ok693* in the mutant RB859 removes the greater part of the gene encoding P-44, Y57A10C.6 (Fig. 6.2.2 A). Only a short truncated protein missing most of the thiolase domain could potentially be synthesized from the remainder of the gene. P-44 deficiency affects worm size, egg laying and peroxisome morphology. Mutant worms (1.18 ± 0.14

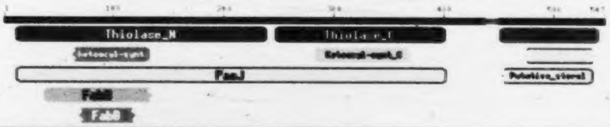	Nematode gene	Tripeptide at C-terminus	Worm Base ORF #
Score = 382 bits (1266), Expect = e-105 Identities = 238/408 (58%), Positives = 311/408 (75%), Gaps = 5/408 (1%) 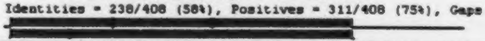	P-44	-SKI	Y57A10C.6
Score = 82.8 bits (203), Expect = 3e-14 Identities = 40/108 (37%), Positives = 67/108 (62%), Gaps = 2/108 (1%) 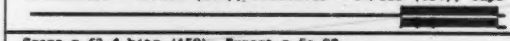	NLT-1	-AKL	ZK892.2
Score = 62.4 bits (150), Expect = 5e-08 Identities = 43/142 (30%), Positives = 73/142 (51%), Gaps = 5/142 (3%) 	fat-2	-SKL	M03A8.1
Score = 67.0 bits (162), Expect = 2e-09 Identities = 93/380 (24%), Positives = 143/380 (37%), Gaps = 61/380 (16%) 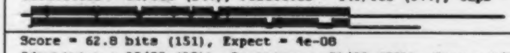		-LGL	F53A2.7
Score = 62.8 bits (151), Expect = 4e-08 Identities = 35/88 (39%), Positives = 52/88 (58%), Gaps = 1/88 (1%) 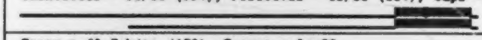	dhs-6	-GKL	C17G10.8
Score = 63.5 bits (153), Expect = 2e-08 Identities = 91/407 (22%), Positives = 153/407 (37%), Gaps = 81/407 (19%) 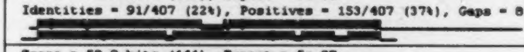	kat-1	-QKL	T02G5.8
Score = 58.9 bits (141), Expect = 5e-07 Identities = 94/417 (22%), Positives = 158/417 (37%), Gaps = 84/417 (20%) 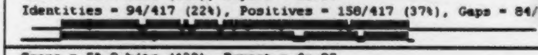		-YGK	B0303.3
Score = 52.0 bits (123), Expect = 6e-05 Identities = 87/370 (23%), Positives = 141/370 (37%), Gaps = 68/370 (18%) 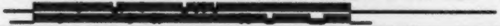		-KKL	T02G5.7

Figure 6.2.1. Alignment of human SCPx and *C. elegans* homologs. Amino acids 1-400 of SCPx form the thiolase domain. Amino acids 450-547 form the sterol carrier domain. A typical result of the automatic detection of protein domains of SCPx using BLAST[1] is shown at top. PaaJ, catalytic domain of acetyl-CoA acetyltransferase. Alignments: upper protein, SCPx; lower protein, *C. elegans* homolog. Blue denotes region of homology. Red denotes gaps. Potential peroxisome targeting signals found in *C. elegans* homologs of SCPx that conform or resemble the consensus PTS1 sequence, –(S/C/A)(K/R/H)(L/M), are -SKI, -AKL, -SKL, - QKL and -KKL.

---

[1] http://www.ncbi.nlm.nih.gov/BLAST/

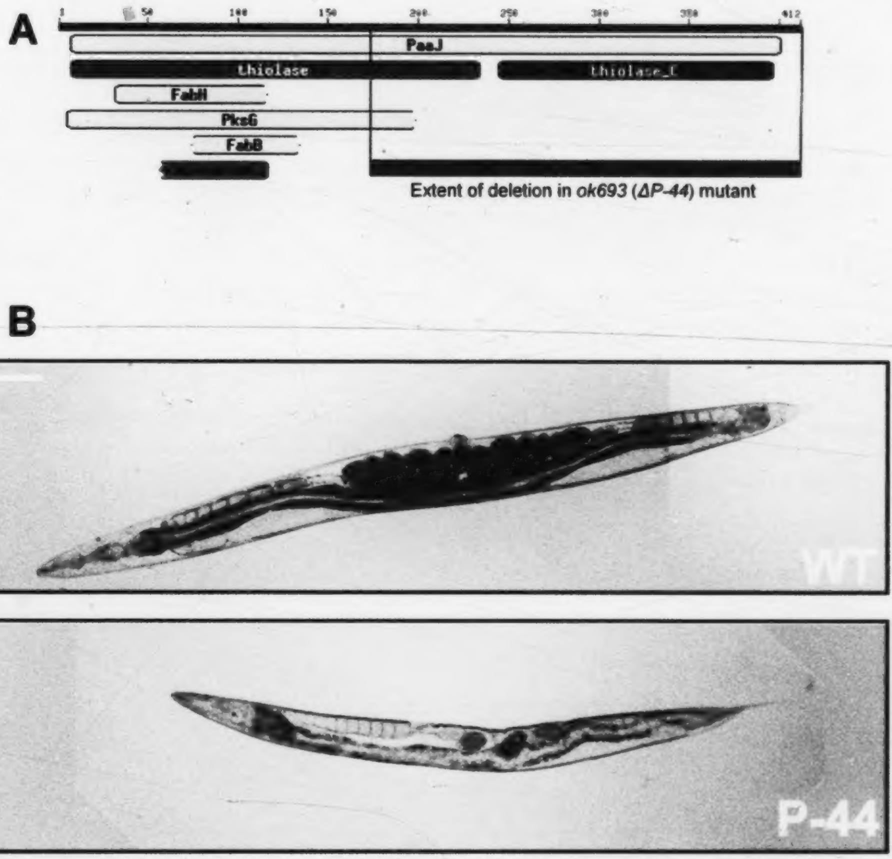
A
1
50
100
150
200
250
300
350
412
PaaJ
thiolase
thiolase_C
FabH
PksG
FabB
Extent of deletion in *ok693* (*ΔP-44*) mutant
B
WT
P-44

Figure 6.2.2. Molecular and phenotypic features of thiolase type I deficiency in the *Δp-44* mutant strain RB859. (**A**). Detection of conserved protein domains in P-44 using BLAST on-line application. PaaJ, the catalytic domain of acetyl-CoA acetyltransferase. Deletion *ok693* (the deletion is shown in purple) removes the greater part of thiolase domain of P-44. (**B**). Sizes of age-matched wild-type and P-44 mutant worms. Bar, 0.1 mm. The average length of wild-type worms was 1.57 ± 0.06 mm and of P-44 mutant worms, 1.18 ± 0.14 mm.

mm) are 25% shorter in length than wild-type worms (1.57 ± 0.06 mm) 4 days after hatching (Fig. 6.2.2 B). Mutant worms lay similar numbers of eggs as wild-type worms (283 ± 31 and 272 ± 29 eggs, respectively), but the egg laying period of P-44 deficient nematodes is longer than that of wild-type worms. When worms were fed phytanic acid, development of both strains was severely affected (Fig. 6.2.3). Peroxisomes in P-44 mutants are irregularly shaped and abnormally distributed (Fig. 3.5.3). Electron microscopy studies also demonstrated that peroxisomes in the gut cells of P-44 mutant worms cluster in large groups and often are accompanied by unusual membranes not found in wild-type worms. Moreover, peroxisomes of P-44 mutant worms are often found in immediate proximity to unusually large lipid vesicles (Fig. 6.2.4).

6.3 Fatty acid composition of P-44 mutant and wild-type *C. elegans*

As reported previously (Bun-ya *et al.*, 1998), P-44 is a type II thiolase, the closest nematode homolog of mammalian SCPx protein. In contrast to thiolase type I, which acts only on straight-chain substrates, P-44 thiolase catalytic activity was also observed with the 2-methylhexadecenoyl-CoA and oxo-forms of bile acids as substrates. The same catalytic activity is characteristic of SCPx (Bun-ya *et al.*, 1998). SCPx is also known to take part in the catabolism of methyl-branched fatty acids such as phytanic acid (3,7,11,15-tetramethylhexadecanoic) and pristanic acid (2,6,10,14-tetramethylpentadecanoic) (Seedorf *et al.*, 1998). Therefore, in analogy to SCPx, P-44 has been suggested as a candidate enzyme that could take part in branched fatty acid catabolism in the nematode (Bun-ya *et al.*, 1997; Maebuchi *et al.*, 1999). The peroxisomal location of P-44 and expression pattern of the gene for P-44 during nematode ontogenesis also suggest that P-44 and SCPx play

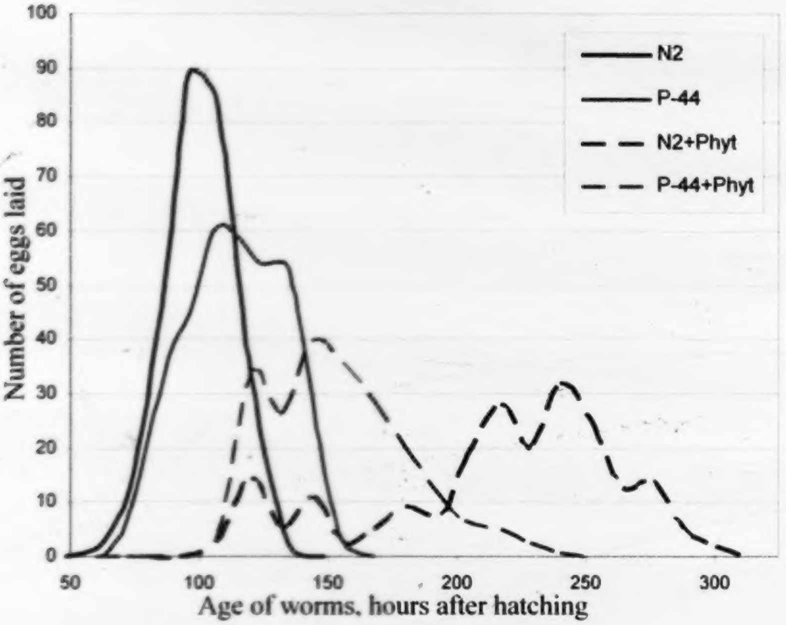

Figure 6.2.3. Egg laying in wild-type and P-44 mutant worms. Egg laying in P-44 mutant worms is delayed in comparison to wild-type worms (N2). Both strains lay equal numbers of eggs (283 ± 31 eggs for the wild-type and 272 ± 29 eggs for the P-44 mutant, n=24). Supplementing the nematode diet with phytanic acid delays and extends the egg laying period of both P-44 mutant (P-44+Phyt) and wild-type (N2+Phyt) worms. This effect is more pronounced in wild-type worms.

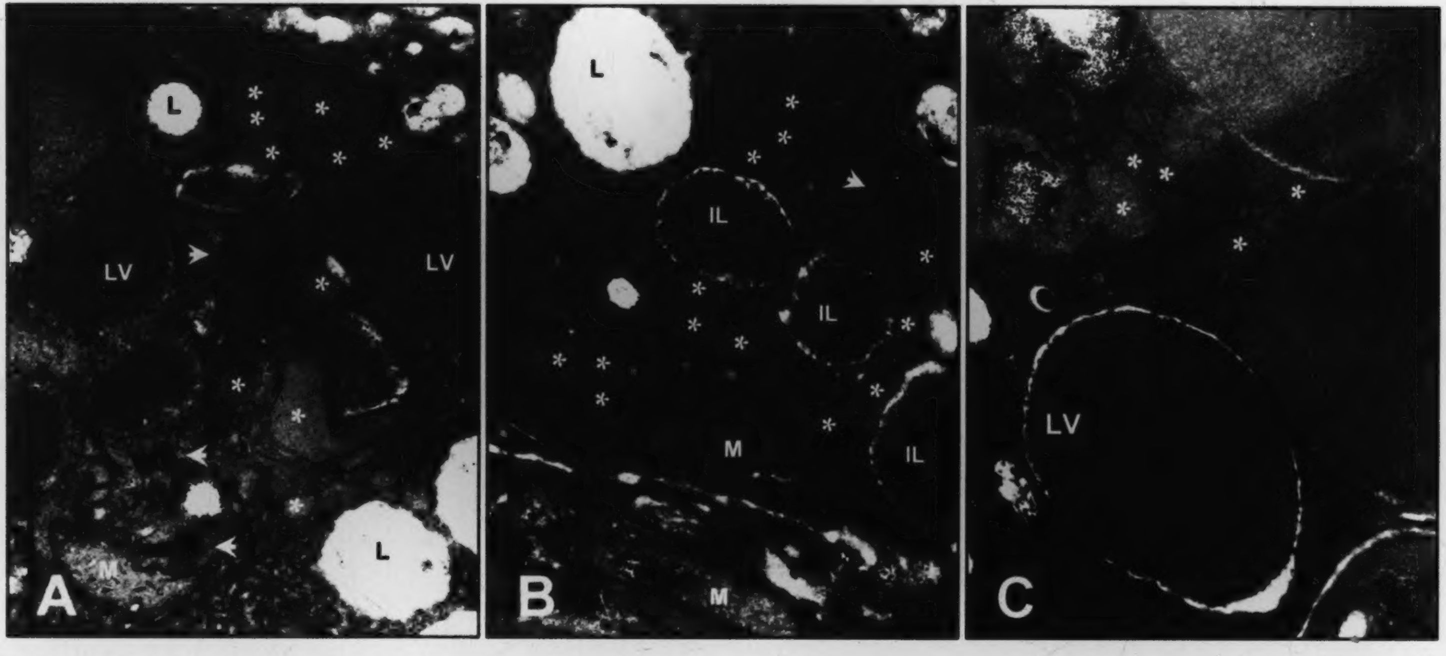

Figure 6.2.4. Electron microscopy of peroxisomes in *ok693* (ΔP-44) mutant worms. (**A**) and (**B**), Clusters of peroxisomes (asterisks) and unidentified membranes (arrowheads). (**C**), Enlarged lipid vesicles (LV) surrounded by peroxisomes. M, mitochondria; L, lysosomes; IL, intestinal lysosomes (gut granules (Clokey and Jacobson, 1986)).

common physiological roles (Maebuchi *et al.*, 1999). Thus, it is expected that mutant worms deficient in P-44 will have defects in branched fatty acid metabolism.

Gas chromatography-mass spectroscopy (GC-MS) spectra of total lipid extracts from P-44 mutant worms fed on *E. coli* strain OP50 did not differ significantly from the spectra obtained from wild-type worms (Fig. 6.3.1). Most likely, in a natural environment, the source of branched fatty acids for *C. elegans* is from the remains of animals, plants, and soil microorganisms, particularly cyanobacteria. Under laboratory conditions, *C. elegans* feed on *E. coli* OP50 (Stiernagle, 1999). *E. coli*, like most other Gram-negative bacteria, do not synthesize branched fatty acids (Smirnova and Reynolds, 2001; Lu *et al.*, 2004). GC-MS analysis of total lipids from *E. coli* OP50 identifies straight chain, hydroxy-containing, and cyclopropane-containing fatty acids (Fig. 6.3.2). Phytanic acid and pristanic acid are formed by the oxidation of isoprenoids (Verhoeven and Jakobs, 2001; Rontani *et al.*, 2002). Little information is available as to whether *E. coli* is a natural source of compounds containing the isoprenoid chain, such as benzoquinones, naphthoquinones, carotenes, tocopherols, farnesol, geranylgeranol and phytol (Lehninger, 2005). Most likely these compounds cannot be considered a potential source for branched-chain fatty acids for *C. elegans*, which feed on *E. coli*. Indeed, identification of individual fatty acids in total lipid extracts from *C. elegans* fed on *E. coli* did not reveal any branched-chain fatty acid except for mono-methyl branched iso- and cyclopropane-forms (See Fig. 6.3.3 for lipid data and Table 6.3.1 for the nomenclature of fatty acids). Lipids were identified by their behavioral profile in GC-MS versus the profiles of different lipids in standard lipid mixtures and by MS spectra analysis (See Appendix).

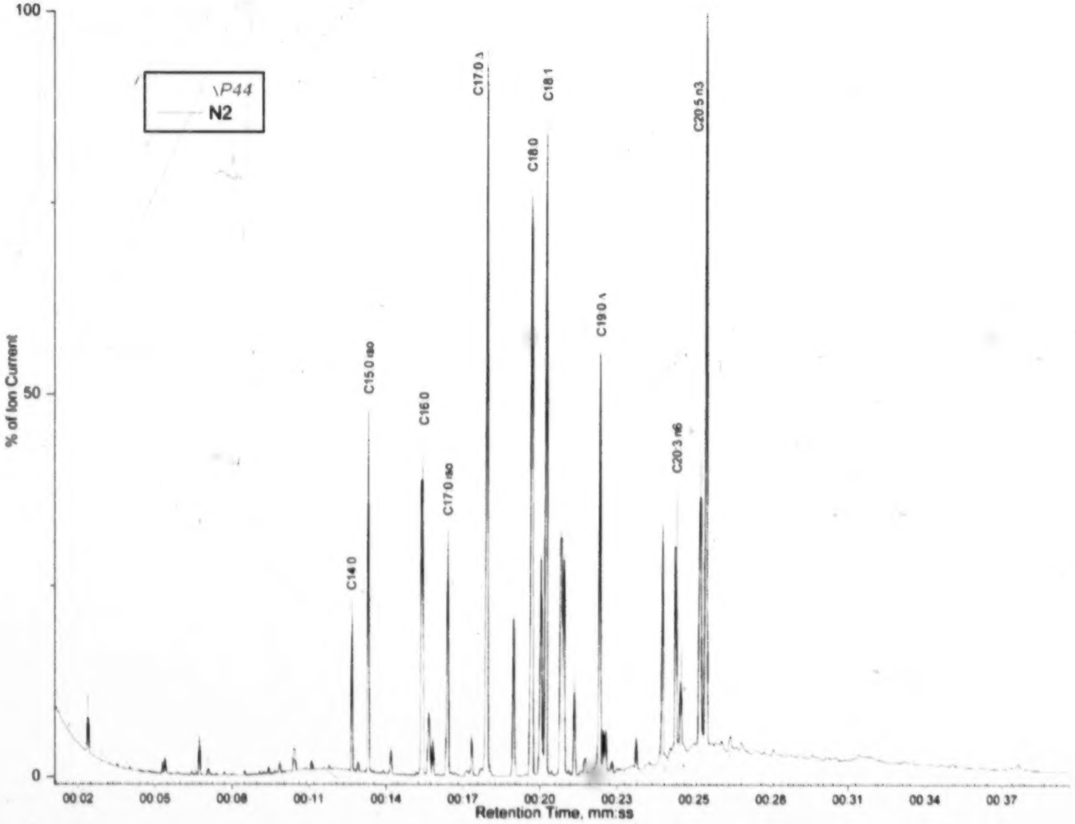

Figure 6.3.1. Gas chromatogram of total lipids derived from *C. elegans* wild-type (N2) and P-44 mutant worms fed *E. coli* OP50. Only major peaks are identified. For a more detailed annotation of peaks, see Fig. 6.3.3.

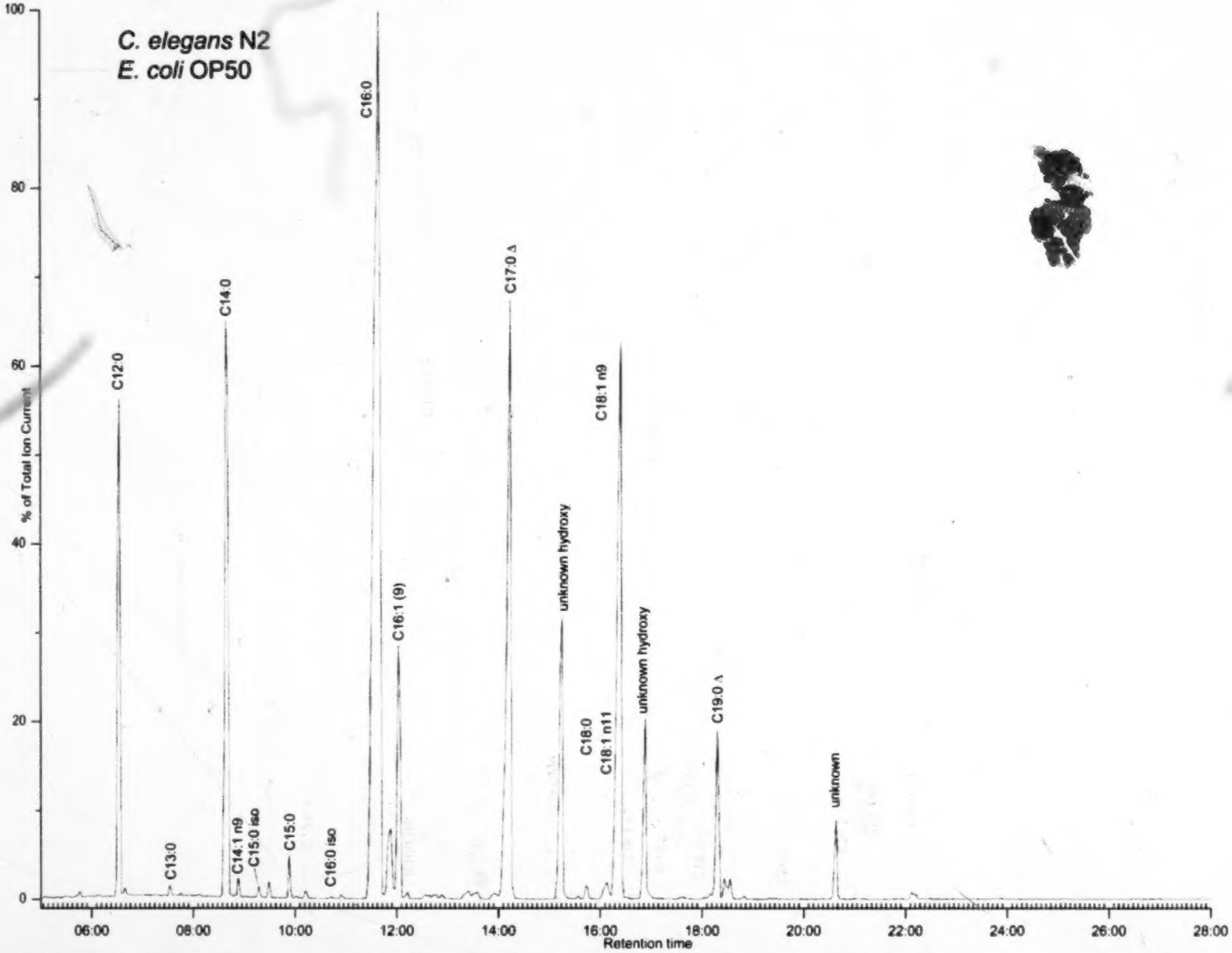

Figure 6.3.2. Gas chromatogram of methyl esters of fatty acids extracted from *E. coli* OP50. For comparison, the spectrum is overlapped with a spectrum derived from nematode lipids. Individual peaks were identified by mass spectrometry.

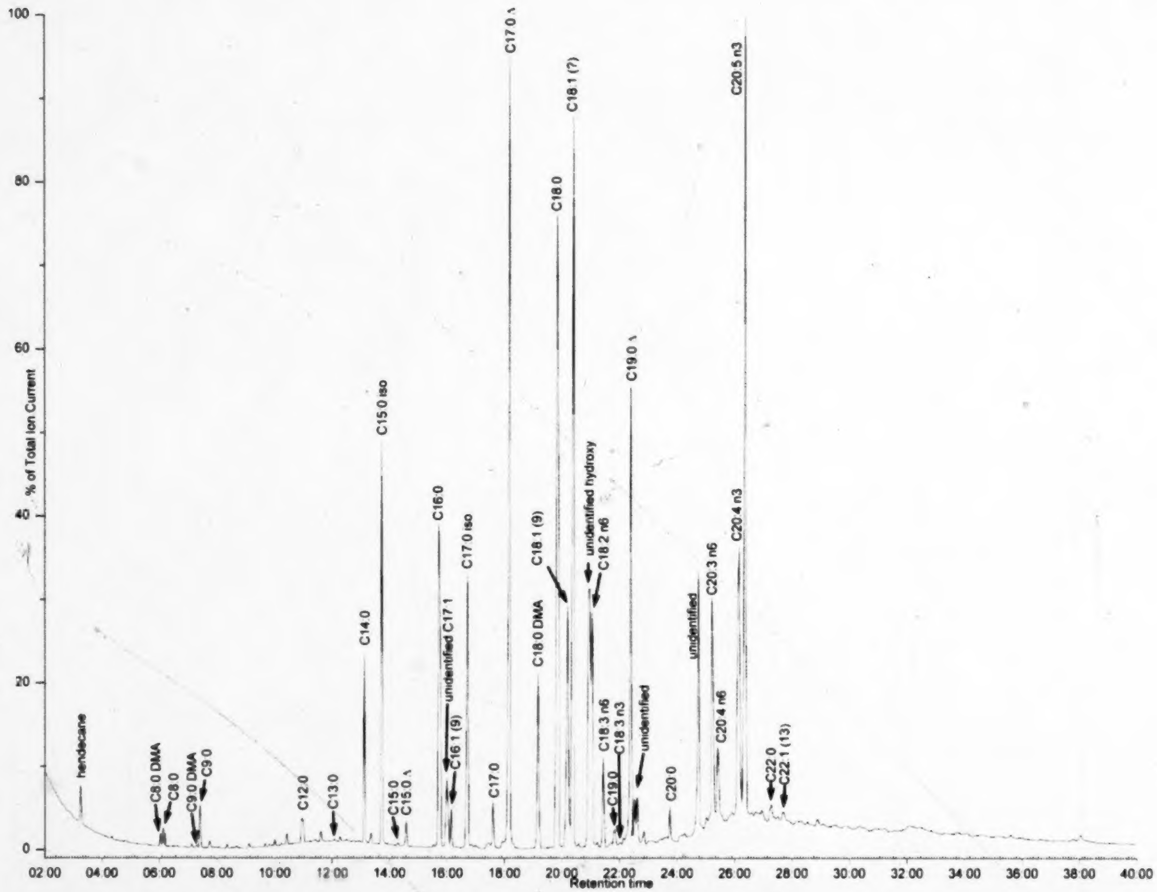

Figure 6.3.3. Gas chromatogram of lipids extracted from wild-type worms fed *E. coli* OP50. Triacylglycerols were hydrolyzed and derivatized to methyl esters (see Materials and Methods). For fatty acid nomenclature, see Table 6.3.1.

Table 6.3.1. Structure of some fatty acids and their derivatives

Abbreviation	Structure	Chemical name of acid
C17:0	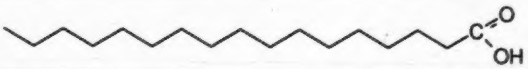	heptadecanoic
C17:0 iso	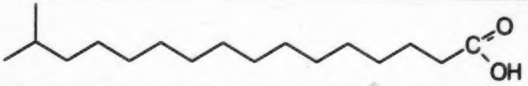	15-methyl hexadecanoic
C17:0 aiso	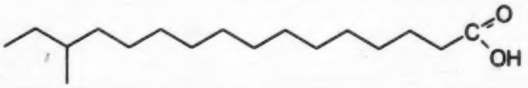	14-methyl hexadecanoic
C18:3 (6,9,12)	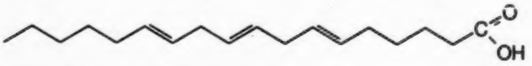	6,9,12-octadeca-trienoic
C20:5 n3	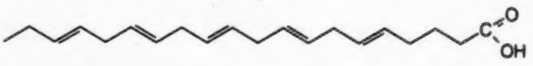	5,8,11,14,17-eicosa-pentanoic
C19 Δ	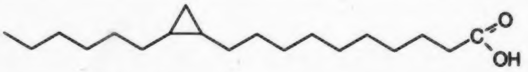	11,12-methylene-octadecanoic
C17 Δ	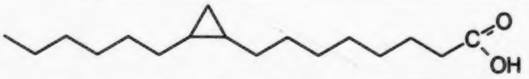	9,10-methylene-hexadecanoic
C15 Δ	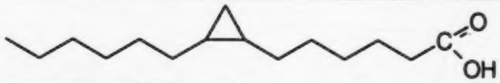	7,8-methylene-hexadecanoic
18:0DMA[1]	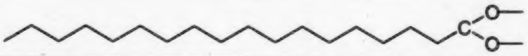	octadecanal-dimethyl acetal
phytanic	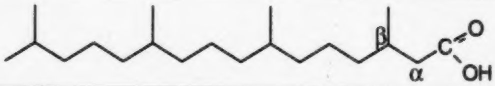	3,7,11,15-tetramethyl-hexadecanoic
pristanic	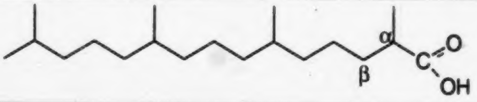	2,6,10,14-tetramethyl-pentadecanoic
TMTD	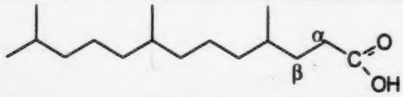	4,8,12 trimethyl-tridecanoic

---

[1] DMA is a derivative of plasmalogens formed during esterification of phospholipids.

The effect of supplementing the diet of wild-type and P-44 mutant worms with the branched fatty acid, pristanic acid, was then investigated. When *C. elegans* was incubated in a buffer containing pristanic acid, it was detected among the other fatty acids found in the nematode. In addition, an intermediate of pristanic acid catabolism, 4,8,12 trimethyltridecanoate, could be detected in wild-type worms but not in P-44 mutant worms (Figs. 6.3.4 and 6.3.5). Also, an unknown fatty acid was found to be present only in wild-type worms (Fig. 6.3.4). The ion impact mass spectrum of this fatty acid was very similar to the spectra of the known cyclopropane-containing fatty acids C17Δ (9,10-methylenehexadecanoic) and C19Δ (11,12-methyleneoctadecanoic) (Fig. 6.3.6). Retention time of this unknown acid was consistent with C15Δ. Moreover, *C. elegans* fed on *E. coli* strain FT17, which is unable to synthesize cyclopropane-containing lipids (Grogan and Cronan, 1986) did not contain this fatty acid (Fig. 6.3.7). Therefore, the unknown fatty acid is most likely *cis*-7,8-methylene tetradecanoic acid, the member of the family of cyclopropane-containing fatty acids that includes C17Δ and C19Δ lipids.

Mammalian SCPx protein consists of two functional domains, the thiolase domain and the SCP2 (sterol carrier protein 2) domain (Fig. 6.2.1) (Ohba *et al.*, 1994). As the *SCPx* gene has two independent promoters that control transcription from alternative start sites, both the SCPx (thiolase domain fused to SCP2) and the SCP2 (displaying only sterol carrier activity) proteins are synthesized in mammals (Ohba *et al.*, 1995). According to immunolot analysis, SCPx knockout mice appear to lack both proteins (Seedorf *et al.*, 1998). No mammalian system lacking only SCP2 but not the thiolase domain of SCPx has been reported to date. Interestingly, the thiolase and SCP2 domains of SCPx have nematode homologs that are encoded by two different genes, P-44 and *fat-2*, respectively,

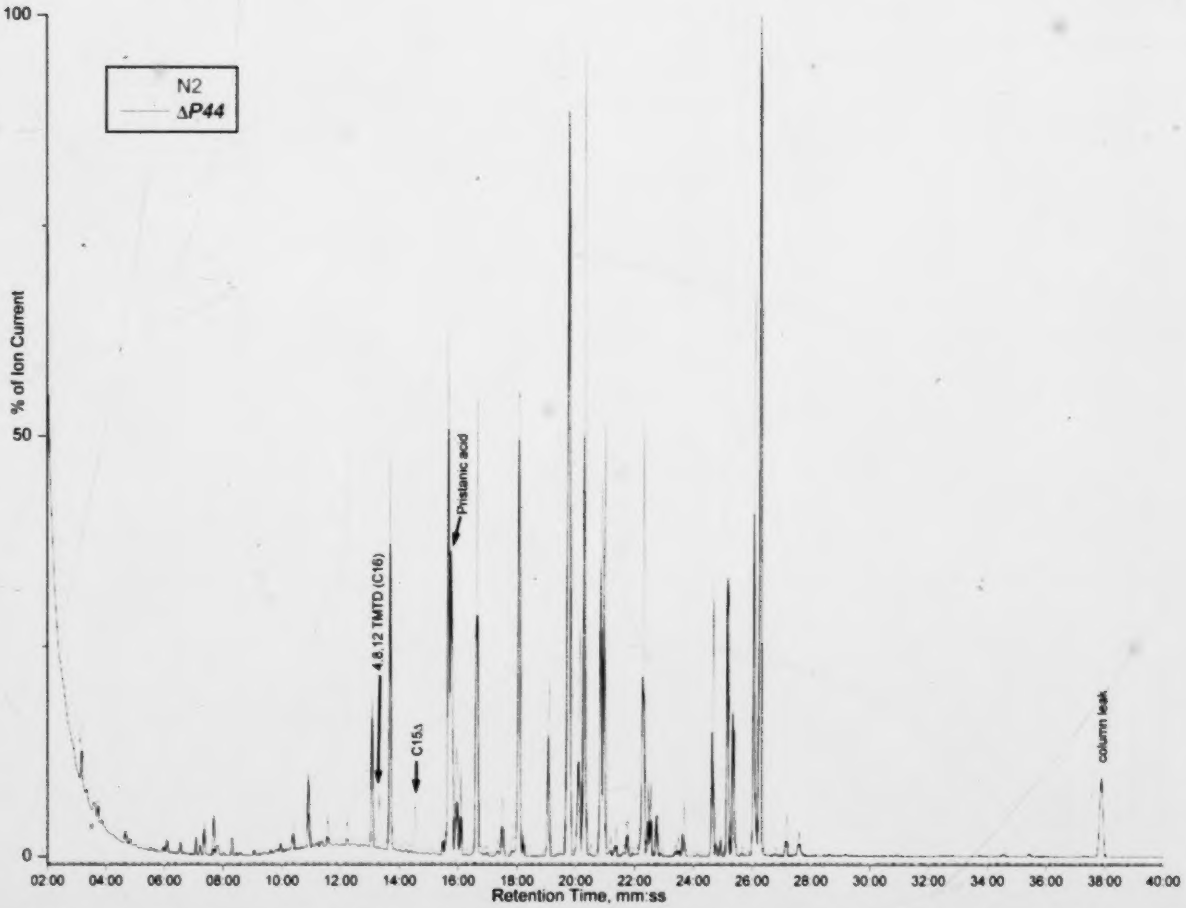

Figure 6.3.4. Gas chromatogram of methyl esters of fatty acids derived from *C. elegans* wild-type (N2) and P-44 mutant worms fed pristanic acid. Only relevant peaks are annotated. TMTD, trimethyltridecanoic acid. C15Δ, cyclopropane-containing fatty acid.

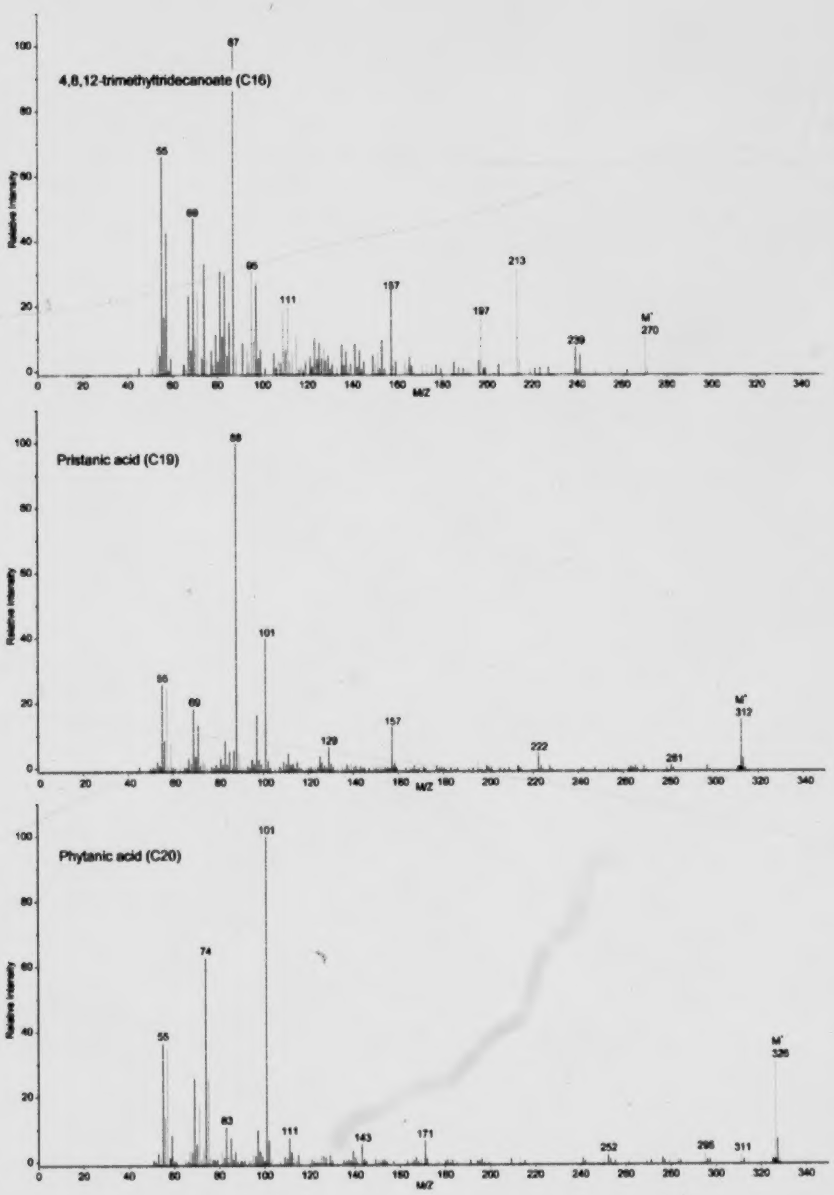

Figure 6.3.5. Ion impact mass spectra of phytanic, pristanic, and TMTD acids. Molecular ions, M^+, represent the molecular mass of a compound.

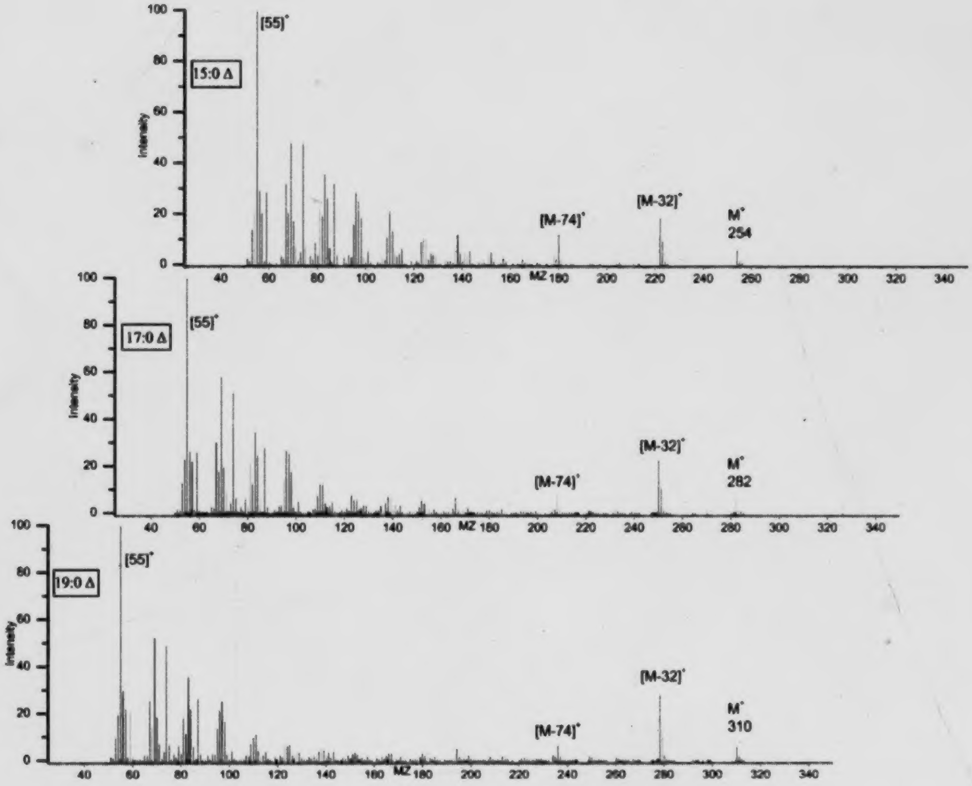

Figure 6.3.6. Comparison of ion impact mass spectra obtained from an unknown C15 fatty acid and the cycplopropane-containing fatty acids C17Δ and C19Δ. Molecular ions, M^+, represent the molecular mass of a compound. All three compounds generate very similar pattern of ion spectra upon ionization.

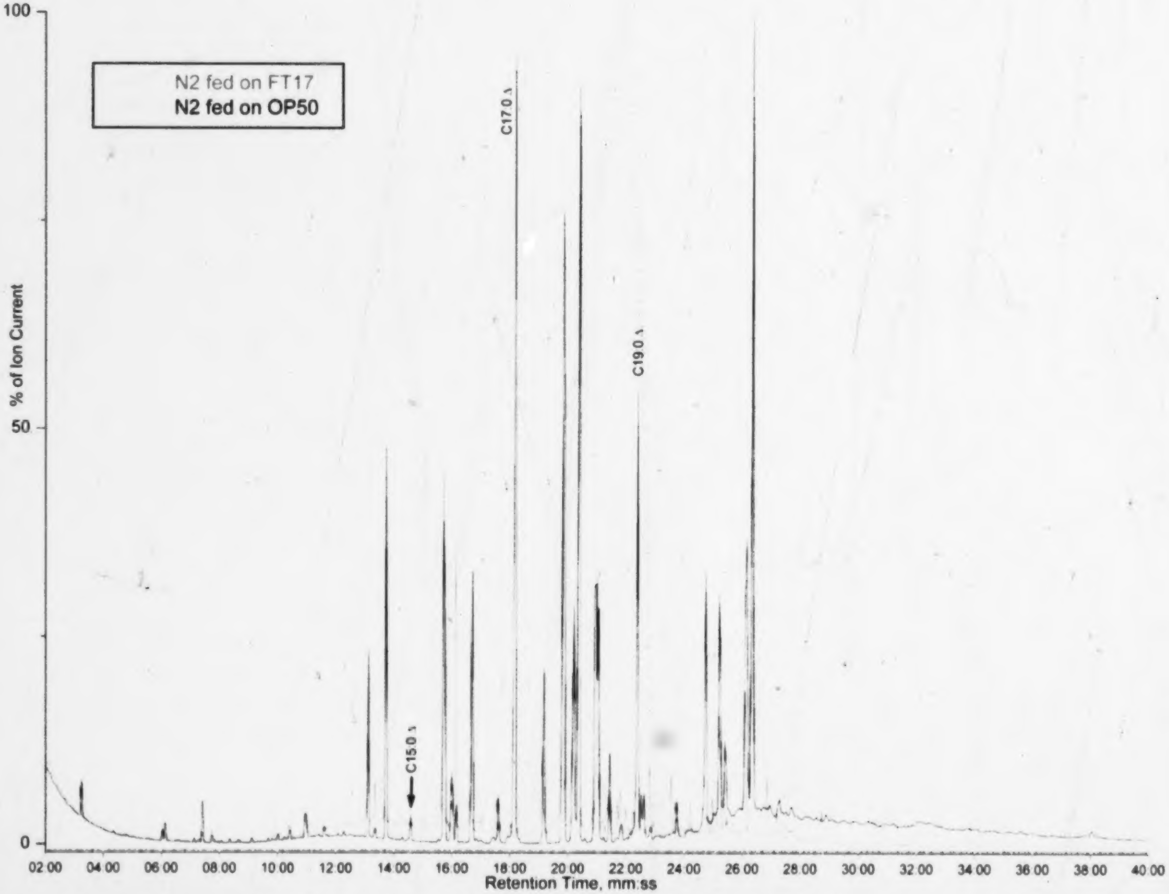

Figure 6.3.7. Gas chromatogram of methyl esters of fatty acids extracted from wild-type worms fed *E. coli* strains OP50 and FT17. The strain FT17 is deficient in the synthesis of cyclopropane-containing fatty acids. Only peaks of interest are annotated. Worms fed *E.coli* strain FT17 lack C15, C17 and C19 cyclopropane-containing fatty acids.

in the *C. elegans* genome (Fig. 6.2.1). This offers a unique possibility to dissect the molecular functions of the two domains of SCPx by comparing the total lipid extracts derived from fat-2 knockout and P-44 knockout worms. GC-MS analysis of total nematode lipids demonstrated that worms lacking FAT-2, the nematode homologue of SCP2, accumulate neither 4,8,12 trimethyltridecanoate nor C15Δ fatty acid when fed pristanic acid (Fig. 6.3.8). Thus, the effect of a FAT-2 deficiency is similar to that of a P-44 thiolase deficiency.

6.4 DISCUSSION

In mammals, SCPx has 3-oxoacyl-CoA thiolase activity and catalyses the thiolytic step in both the breakdown of phytanic/pristanic branched-chain fatty acids and in the formation of the CoA esters of cholic acid and chenodeoxycholic acid from di- and trihydroxycholestanoic acid (Antonenkov *et al.*, 1997). Both processes take place in peroxisomes. In peroxisomes, phytanic acid undergoes one round of α-oxidation to form pristanic acid (Fig. 6.4.1) (Lehninger, 2005). In turn, pristanic acid undergoes only three cycles of β-oxidation, after which the products acetyl-CoA, propionyl-CoA and 4,8-dimethylnonanoyl-CoA exit the peroxisome (Wanders *et al.*, 2000). The final step (Fig 6.4.1, Step 10) of at least the first β-oxidation cycle is catalyzed by SCPx. No human disorder has been described in which either peroxisomal thiolase 1 or thiolase 2 (SCPx) is deficient (Wanders *et al.*, 2001). Nevertheless, an accumulation of phytanic acid was detected in patients suffering from Refsum disease (Klenk and Kahike, 1963), some cases of Zellweger's syndrome, Rhizomelic chondrodysplasia punctata, Sjögren-Larsson syndrome, and α-methylacyl-CoA epimerase deficiency (Mukherji *et al.*, 2003). The

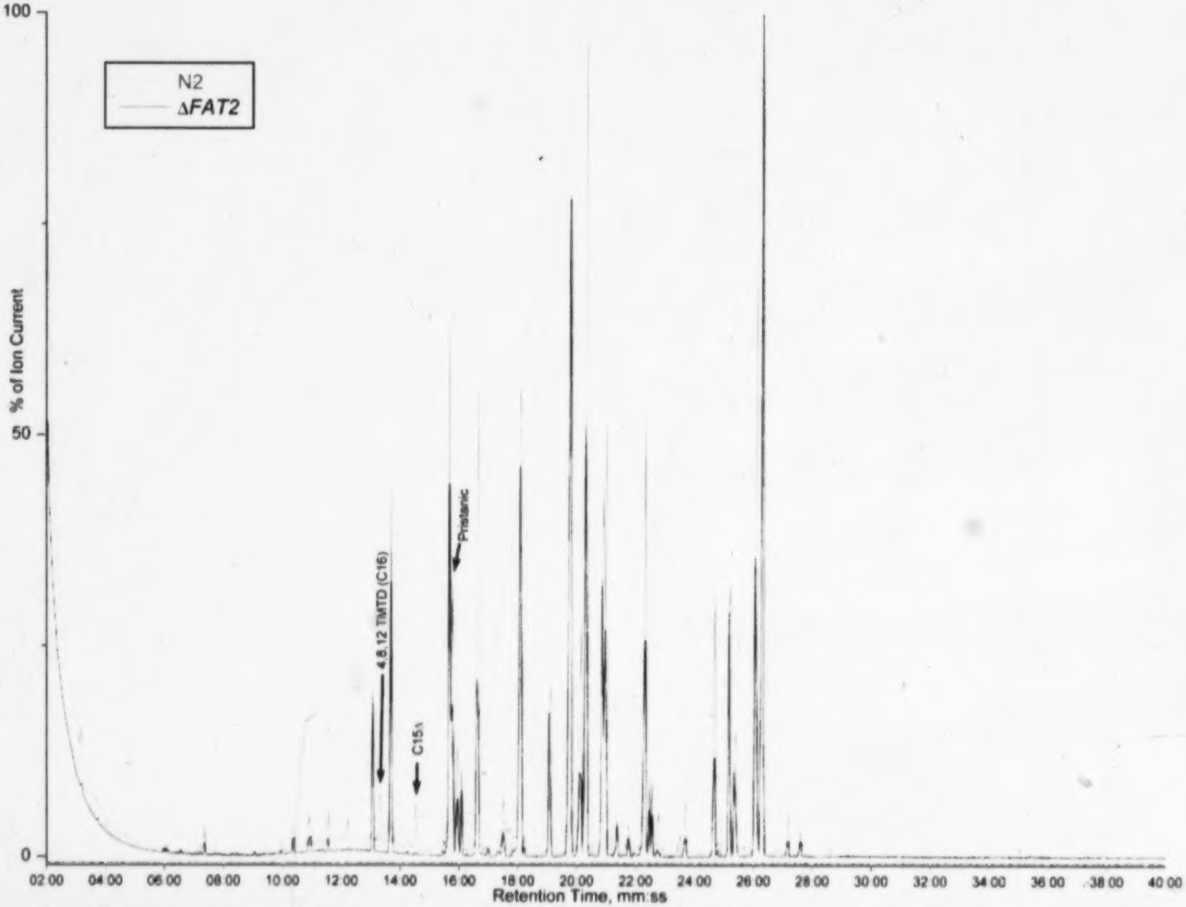

Figure 6.3.8. Gas chromatogram of methyl esters of fatty acids derived from *C. elegans* wild-type (N2) and *fat-2* mutant worms fed with pristanic acid. Only relevant peaks are annotated. TMTD, trimethyltridecanoic acid. C15Δ, cyclopropane-containing fatty acid.

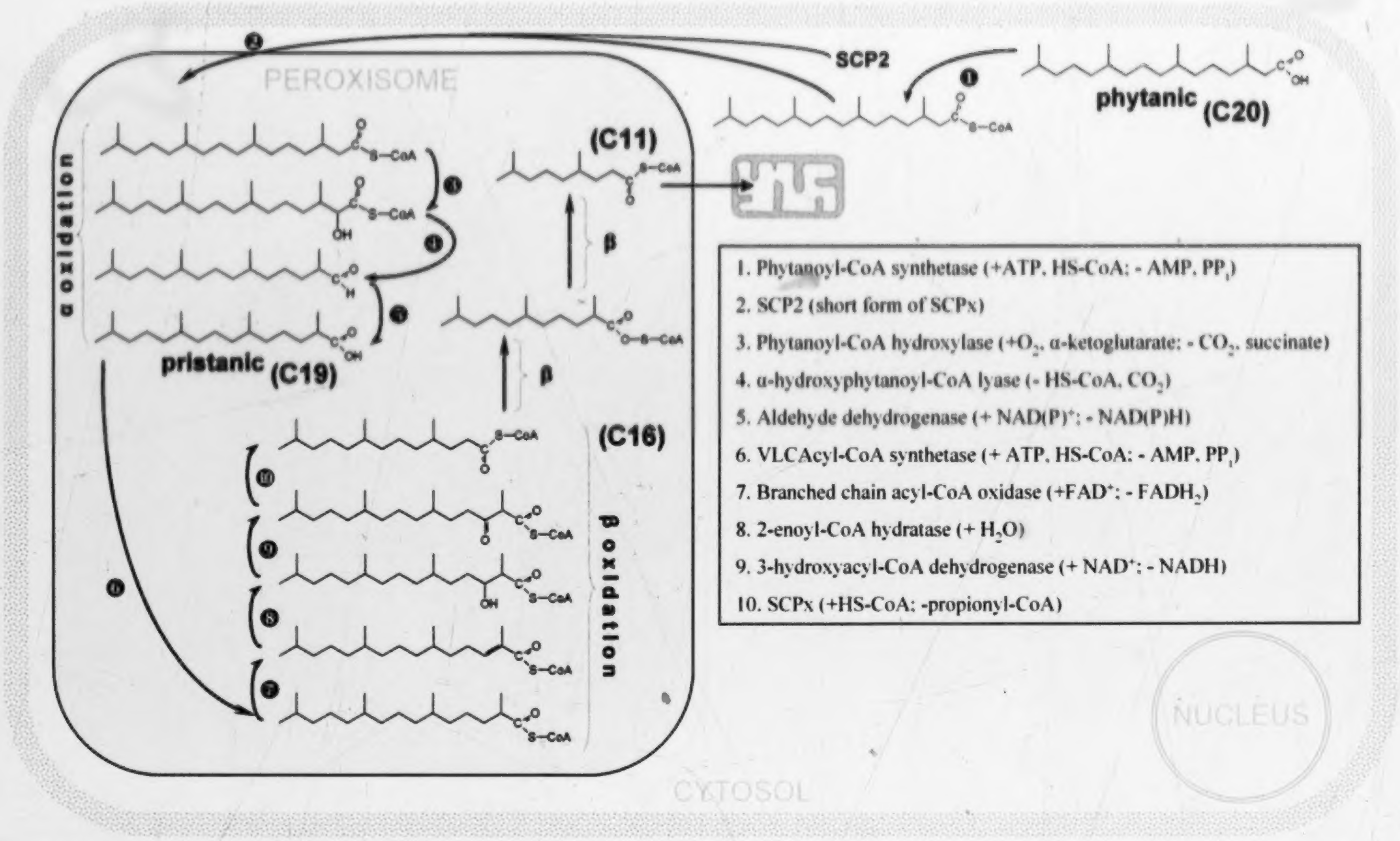
PEROXISOME
SCP2
phytanic (C20)
(C11)
β
β
α oxidation
pristanic (C19)
(C16)
β oxidation
NUCLEUS
CYTOSOL

1. Phytanoyl-CoA synthetase (+ATP, HS-CoA: - AMP, PP_i)
2. SCP2 (short form of SCPx)
3. Phytanoyl-CoA hydroxylase (+O_2, α-ketoglutarate: - CO_2, succinate)
4. α-hydroxyphytanoyl-CoA lyase (- HS-CoA, CO_2)
5. Aldehyde dehydrogenase (+ $NAD(P)^+$; - NAD(P)H)
6. VLCAcyl-CoA synthetase (+ ATP, HS-CoA: - AMP, PP_i)
7. Branched chain acyl-CoA oxidase (+FAD^+; - $FADH_2$)
8. 2-enoyl-CoA hydratase (+ H_2O)
9. 3-hydroxyacyl-CoA dehydrogenase (+ NAD^+; - NADH)
10. SCPx (+HS-CoA: -propionyl-CoA)

Figure 6.4.1. Catabolism of phytanic acid in humans. Reactions of the first α- and the following three β-oxidation cycles take place in the peroxisome. 4,8-dimethylundecanoate (C11) synthesized in the peroxisome is then transported to the mitochondrion for further catabolism. Enzymes involved in the peroxisomal catabolic reactions are presented in the box.

knockout of SCPx in mice has a marked effect on hepatic gene expression, peroxisome proliferation, and causes hypolipidemia, impaired body weight control and neuropathy (Seedorf *et al.*, 1998).

The dietary source of phytanic acid for humans is mainly dairy products and ruminant fats. Ruminants accumulate phytanic acid after phytol, the side chain of chlorophyll, is released and oxidized to phytanate in their digestive system by gastrointestinal microorganisms (Verhoeven and Jakobs, 2001). The high sequence similarity between the nematode P-44 protein and mammalian SCPx makes similar biochemical functions for these proteins likely. Experimental data demonstrate that this is in fact the case. The presence of an intermediate of pristanic acid catabolism, 4,8,12 trimethyltridecanoate, in wild-type worms, but not in P-44 mutant worms fed pristanic acid indicate that the β-oxidation of pristanic acid is blocked in P-44 mutant worms (Fig. 6.3.4). These worms also lack C15Δ fatty acid. Cyclopropane-containing fatty acids are seldomly found in eukaryotic lipids (Body, 1972; Kaneda, 1991; Grogan and Cronan, 1997; Cronan, 2002). As feeding of nematodes on *E. coli* defective in the synthesis of cyclopropane fatty acids shows, they are not synthesized *de novo* in *C. elegans* (Fig. 6.3.7). C15Δ is therefore most likely a product of the β-oxidation of C17Δ and C19Δ lipids. Cyclopropane rings in the carbohydrate chains of delta-fatty acids put them into a class of lipids that is distinct from straight-chain fatty acids but similar to the methyl-branched lipids (Table 6.3.1). The catabolism of delta-fatty acids has so far only been studied in microorganisms (Tipton and al-Shathir, 1974). The identity of the thiolase that catalyzes one of the intermediate steps in the β-oxidation of C17Δ and C19Δ fatty acids in nematodes is unknown, but data presented here suggest that it is the type II 3-oxoacyl CoA thiolase, P-44.

Remarkably, deficiency in the FAT-2 protein, the *C. elegans* homolog of the sterol carrier domain of SCPx, which is identical to SCP2, has a similar effect on the composition of *C. elegans* lipids as the P-44 deficiency. *fat-2* mutant worms also develop more slowly than wild-type animals (data not shown). SCP2 does not possess individual catalytic activity (Seedorf *et al.*, 2000). SCP2 was found to be involved in the formation of a substrate complex for the enzyme PhyH (Mukherji, 2002). PhyH is defective in patients with Refsum's disease (Mihalik *et al.*, 1997). It was also proposed that SCP2 may form substrate complexes with all enzymes of the α-oxidation pathway (Mukherji, 2003). The two most likely explanations for the identical phenotypes of the nematode fat-2 and P-44 deficiencies are that P-44 catalyses thiolytic reactions only in fat-2/substrate complexes or that fat-2 is required for the translocation of substrates for P-44 across the peroxisomal membrane. The latter hypothesis is also supported by findings that SCP2 possesses a non-specific lipid transfer function (Seedorf et al., 2000).

Some data indicate that SCPx, together with the thiolase type I, is involved in the oxidation of the very-long straight-chain fatty acids C24:0 and C26:0 (Ferdinandusse, 2004) and C24:6n-3 (Feridandusse, 2001). No significant accumulation of these fatty acids was observed in P-44 and fat-2 mutants (Figs. 6.3.4 and 6.3.8), suggesting that the oxidation of these very-long straight-chain fatty acids was unaffected or that they are not synthesized in the nematode.

The physiological effect of the P-44 deficiency on nematode size, egg laying and peroxisome phenotype, and the *fat-2* deficiency on nematode development are less clear. Cyclopropane fatty acids are dispensable for nematode development, as *C. elegans* living on bacteria that do not synthesise delta-fatty acids develop at the same rate as worms feeding on the *E. coli* strain OP50. P-44- and FAT-2-deficient nematodes fed on *E. coli* do not accumulate detectable amounts of uncatabolized branched fatty acids or very-long chain fatty acids. Interestingly, spontaneous peroxisome proliferation and significant alteration of gene expression in liver are early events in SCPx/SCP2-deficient (Ellinghaus *et al.*, 1999) and acyl-CoA oxidase-deficient (Fan *et al.*, 1996) mice. These effects can be attributed to the biological activities of the SCPx and acyl-CoA oxidase substrates, phytanic acid and very-long chain fatty acids. They are biological ligands for the peroxisome proliferator-activated receptor α (PPARα) (Fan *et al.*, 1998; Ellinghaus *et al.*, 1999; Seedorf *et al.*, 2000). Although GS-MS analysis did not detect these forms of fatty acids in P-44 mutant and fat-2 mutant worms fed *E. coli*, an increased concentration of these molecules in mutant worms cannot be ruled out. In fact, the biological effect of dietary phytanic acid on the nematode resembles that of P-44 deficiency but is more prominent. When P-44 mutant worms or wild-type worms were fed phytanic acid added to the *E. coli* lawn, development of both strains was severely affected (Fig. 6.2.3, dashed lines).

In conclusion, this work demonstrates that both the P-44 and fat-2 proteins are involved in the catabolism of the same specific types of fatty acids in *C. elegans*. Therefore, it can be assumed that both the thiolase and sterol carrier domains of SCPx are of equal functional importance in the catabolism of certain classes of lipids in mammals.

CHAPTER 7

PERSPECTIVES

7.1 Peroxisome biogenesis and peroxisome biogenesis diseases in the nematode *C. elegans* and in humans

This work describes a functional analysis of 11 *C. elegans* ORFs that encode potential nematode peroxins. These ORFs were selected based on their sequence similarity to genes encoding 14 known human peroxins (Table 3.2.1). All 11 genes were tested for their necessity for normal nematode development, as well as for the role in peroxisome biogenesis by RNAi. Assuming that all RNAi experiments were effective, it was demonstrated that only 6 of 11 genes (*i.e.*, the genes encoding Pex3p, Pex5p, Pex12p, Pex13p, Pex14p and Pex19p) that were initially selected as candidates for genes encoding nematode peroxins were in fact necessary for normal peroxisome biogenesis or peroxisome-related processes. In contrast, RNAi treatment against the genes encoding the potential nematode homologs of Pex1p, Pex2p, Pex6p, Pex10p and Pex11p did not result in an obvious disruption of peroxisomal function. One possible reason for the absence of the expected phenotypes for some RNAi experiments is a misprediction of the homologs in the worm. As described in Section 3.7, this is especially true for the genes encoding Pex1p and Pex6p. Indeed, less than 1% of $\text{RNAi}_{\text{Pex6p}}$ animals displayed a diffuse pattern of staining for CFP-SKL. This suggests that the injected $\text{dsRNA}_{\text{Pex6p}}$ may have interfered with another mRNA that is transcribed from the true nematode Pex6p gene. This may be the mRNA encoding Pex1p, as both genes share significant structural, as well as functional, redundancy (Geisbrecht *et al.*, 1998).

In humans, mutations in the PEX1 and PEX6 genes account for 80% of all cases of Zellweger syndrome, neonatal adrenoleukodystrophy, and infantile Refsum disease (Geisbrecht *et al.*, 1998). The identification of *C. elegans* Pex1p and Pex6p would therefore be of interest in this context. A thorough RNAi analysis with the remaining nematode genes found to be potential homologs of human Pex1p and Pex6p (Tables 3.7.1 and 3.7.2) will be necessary. Also, double $\text{RNAi}_{\text{Pex1p/Pex6p}}$ is necessary to assess a possible functional redundancy of both proteins. Finally, true *pex1* and *pex6* gene knockouts must be generated to avoid all caveats associated with RNAi technology.

An attempt to replace the tetratricopeptide repeat (TPR) domain of *S. cerevisiae* Pex5p with the TPR domain from the predicted *C. elegans* Pex5p protein (Gurvitz *et al.*, 2001) showed that the nematode Pex5p may functionally replace its human counterpart. It is tempting to expect similar redundancy between other nematode and human peroxins. This is another research direction to be developed in the future.

Although the complete set of proteins that regulate peroxisome biogenesis in the nematode has yet to be clarified, some important general conclusions can be drawn. As described in Section 3.2, the degree of sequence identity is minimal between nematode and yeast peroxins, but high with the human peroxins. (Table 3.2.3). This suggests that the processes of peroxisome biogenesis and maintenance may be more closely related between nematodes and humans than between nematodes and yeast (Thieringer *et al.*, 2003). In addition to this, its developed nervous system makes *C. elegans* a very attractive model for peroxisome-related research, since most peroxisomal disorders affect the nervous system. This is also true for a much wider spectrum of neurodegenerative diseases such as neurodegenerative tauopathy (Goedert, 2003), Tay-Sachs disease, Niemann-Pick disease, human mucolipidosis type IV, Alzheimer disease, Parkinson disease, polyglutamine-expansion disorders that include Huntington disease, spinobulbar muscular atrophy, dentatorubral pallidoluysian atrophy, and others (Driscoll and Gerbstbrein, 2003). With this in mind, *C. elegans* may make an excellent model organism for research related to neurodegenerative diseases.

7.2 Peroxisomal import pathways in *C. elegans*

The results presented in Chapter 4 show that the only identified PTS2-containing nematode protein known to localize to peroxisomes in other organisms, mevalonate kinase, is not peroxisomal in *C. elegans*. Therefore, the possibility that *C. elegans* possesses a PTS2-dependant peroxisome import pathway can be ruled out. This is the first case where this pathway is not found in a eukaryote. This may be a common feature for all *Caenorhabditis* species, as no distinctive Pex7p homologs can be found in *Caenorhabditis briggsae*, and the PTS2 motif from *C. briggsae* MeK is identical with the PTS2 motif from *Ce*MeK. Yet, the statement that "*Caenorhabditis elegans* has a single pathway to target matrix proteins to peroxisomes" made by Motley and coworkers (Motley *et al.*, 2000) cannot be considered conclusive, as there is the possibility that unique nematode peroxisomal targeting signals different from PTS1 and PTS2 will be discovered. It will only be possible to evaluate this hypothesis after more data have been obtained on peroxisomal proteins in nematodes.

7.3 Nematode catalases and longevity

A number of putative nematode homologs of human peroxisomal enzymes were tested for their importance in nematode ontogenesis (Table 3.2.2). As described in Section 1.9, only catalase CTL-2 and thiolase P-44 were localized to peroxisomes in *C. elegans*.

Using *ctl-2* and P-44 gene deletions, the role of CTL-2 in the nematode longevity and a biochemical function for P-44 were examined in this thesis (Chapter 5).

One of the six different mechanisms (Houthoofd *et al.*, 2004) by which the lifespan of *C. elegans* can be extended is by reduced insulin/IGF-I signaling (Hsu *et al.*, 2003). This pathway manifests its effect on the regulation of organismal longevity through its action on a subset of target genes. These include a variety of stress-response genes, among them genes encoding catalases (Murphy *et al.*, 2003). Another mechanism by which the longevity of most organisms, including mammals, can be increased, is dietary restriction (Houthoofd *et al.*, 2003). As in the first case, antioxidant enzymes, including catalase, were found to be upregulated under conditions of dietary restriction in worms (Houthoofd *et al.*, 2003). These data make catalase an attractive target for an important role in aging. However, no evidence directly implicating catalases in the aging process of nematodes or other organisms had been presented.

This thesis shows that lack of the peroxisomal catalase CTL-2 causes an earlier death in *C. elegans*. Lack of peroxisomal catalase also affects the developmental program of *C. elegans*, as *Δctl-2* mutants exhibit decreased brood size. In contrast, lack of cytosolic catalase CTL-1 has no effect on either nematode aging or brood size. The *Δctl-2* mutation also shortens the maximum lifespan of the long-lived *Δclk-1* mutant and accelerates the onset of its egg laying period. The more rapid aging of *Δctl-2* worms is apparently not due to increased carbonylation of the major *C. elegans* proteins, although altered peroxisome morphology in the *Δctl-2* mutant suggests that changes in peroxisomal function, including increased production of reactive oxygen species, underlie the progeric phenotype of the *Δctl-2* mutant.

The data obtained on total protein carbonylation and on total lipid oxidation (Section 5.4) may indicate that the methods employed are not sensitive enough to detect molecular changes in peroxisomal lipids and proteins, since they constitute only a very small fraction of total proteins and lipids in the worm. Therefore, it would be advantageous to establish a method that allows the purification of nematode peroxisomes. Analyses of protein carbonylation and lipid peroxidation in purified peroxisomes from wild-type and catalase deletion worms would clarify whether aging can be attributed to peroxisomal functions in worms.

As discussed in Section 5.5, *C. elegans* is the only known metazoan to have three catalase genes. Unlike the ubiquitously expressed CTL-1 and CTL-2, the upstream region of the *ctl-3* catalase gene can drive reporter gene expression only in a specific subset of *C. elegans* cells - pharyngeal muscle cells and neurons (Fig. 5.5.1). The CTL-3-GFP chimeric protein has a high tendency to aggregate in the cell but localizes to cytosol. The unusual expression pattern of the third catalase gene suggests that it may play a specialized role in *C. elegans* antioxidant protection and, possibly, longevity. As the upstream region of the *ctl-3* gene is active in pharyngeal muscle cells, one possible role for CTL-3 would be protection against H_2O_2 that has been found to be used by some bacteria to kill the nematode (Jansen *et al.*, 2002).

Finally, the neuronal expression of the CTL-3 gene suggests another possible role for CTL-3 - regulating oxidative stress signaling in neurons. Reactive oxygen species (ROS) signaling plays an important role in the pathology of neurodegenerative diseases such as Alzheimer disease (Zhu *et al.*, 2004).

A reliable experimental evaluation of the role of CTL-3 will only be possible after the generation of a *ctl-3* gene knockout mutant.

7.4 Nematode metabolism of specific classes of fatty acids

The results presented in Chapter 6 of this thesis represent an example of how the nematode model can be advantageous for resolving the biochemical problems arising in a mammalian organism. The principal advantage of *C. elegans* in defining human SCPx function is that the two domains found in the human SCPx protein are encoded by two separate genes in the nematode, permitting ready dissection of SCPx function. Using strains deleted for genes encoding the P-44 type II thiolase and the FAT-2 protein, which are homologs of human SCPx, it was demonstrated that functioning of both the P-44 type II thiolase and the FAT-2 protein are necessary for the catabolism of branched chain fatty acids in the nematode. It is not clear whether FAT-2 plays the role of a carrier of these fatty acids across the peroxisomal membrane or whether it is necessary for the formation of a substrate complex with the fatty acids in the peroxisomal matrix, or both.

It is also of interest to understand the molecular mechanism that retards the development of P-44 and *fat-2* mutant worms when they are fed bacteria, a diet potentially low in branched FAs and VLCFAs. SCPx was found to be implicated in the conversion of the CoA esters of different derivatives of cholestanoic acid (Antonenkov *et al.*, 1997). The nematode is known to have very low amounts of cholesterol in membranes, but it is also known that nematode development is regulated by sterol-derived signaling molecules (Kurzchalia and Ward, 2003). Therefore, P-44 and FAT-2 may be involved in the biosynthesis of these specific forms of signaling molecules. Sensitive techniques such as

Time-of-Flight Secondary-Ion Mass Spectrometry (TOF-SIMS) (Seedorf *et al.*, 1998) allow the detection of cholesterol derivatives in complex biological mixtures. This may be the method of choice for future analyses of the molecular basis of the P-44 and fat-2 phenotypes.

Another interesting problem that arises is whether there is functional redundancy between mammalian SCPx and the nematode P-44/Fat-2 proteins? Heterologous expression of the thiolase and SCP2 domains of SCPx, as well as of full-length SCPx, in the nematode P-44Δ and *fat-2*Δ genetic backgrounds should provide an answer to this question.

7.5 Is *C. elegans* a good system to model human peroxisome function?

C. elegans meets the basic criteria for a model organism for peroxisome research as set out in Chapter 1.6. *C. elegans* is multicellular. It has a structured nervous system that is made up of the different types of neurons found in humans and which use the same neurotransmitters as human neurons (White *et al.*, 1986; Thomas and Lockery, 1999). In contrast to *Drosophila*, the neurotransmitter at the neuromuscular junction in *C. elegans* is acetylcholine, as in vertebrates (Buckingham *et al.*, 2004). Self-fertilization, the facile generation of homozygous mutants, relatively simple biology and a short lifecycle also make *C. elegans* an advantageous animal model. In addition, *C. elegans* exhibits a diverse repertoire of behaviors that can be used for a variety of physiological tests.

Observation of axonal migration and connectivity is much simplified in *C. elegans* with its invariant postembryonic cell lineage (Sulston and Horvitz, 1977), transparent cuticle and reconstructed pattern of synaptic connectivity (Hall and Russel, 1991). A drawback of the *C. elegans* nervous system *vis-à-vis* a vertebrate nervous system is the lack of a myelin sheath around nematode axons. Demyelination of cortical neurons is observed in the brains of adrenoleukodystrophy patients (Lazarow and Moser, 1989). Another drawback of *C. elegans* is that its small size limits the use of electrophysiological interrogation of its neurons, but recent advances in the culturing of nematode neurons that appear to permit the treatment of neurons by RNAi (Christensen, 2002) should facilitate the implementation of this technically demanding technique in *C. elegans*.

C. elegans genetics is well developed, and *C. elegans* is the best understood experimental animal for investigating human disease-related genes (Buckingham *et al*., 2004). It has been estimated that the *C. elegans* genome contains the counterparts of up to 50% of human disease genes (Culetto and Sattelle, 2000). This thesis demonstrates that the *C. elegans* genome contains ORFs encoding proteins with high identity to 11 of 14 human peroxins. Many yeast peroxins find few if any counterparts in the nematode. RNAi with six predicted nematode peroxins did result in the impairment of peroxisomal functions and developmental arrest in the worm. Thus, *C. elegans* is a preferred system with which to model the human peroxisomal disorders. *C. elegans* orthologs of human disease genes offer insights into the functions of the human genes. Available genetic methods in *C. elegans* allow the discovery of genes that, when mutated, could either enhance or suppress a particular molecular process and, as such, their products may represent novel candidate drug targets. Also, by screening for and analyzing mutants that either suppress or enhance already characterized mutations (so-called synthetic mutants), functionally interacting gene products can be identified. Both strategies can be readily employed in *C. elegans*, and only with much more difficulty in vertebrate organisms. Lastly, *C. elegans* is one of the foremost model systems used in developmental genetics. This thesis extends the variety of human developmental disorders that can be successfully modeled in *C. elegans*.

CHAPTER 8

REFERENCES

AbdelRaheim, S.R., and A.G. McLennan. 2002. The *Caenorhabditis elegans* Y87G2A.14 Nudix hydrolase is a peroxisomal coenzyme A diphosphatase. *BMC Biochem.* 3:5.

Alberts, B., D. Bray, J. Lewis, M. Raff, K. Roberts, and P. Walter. 2002. Molecular Biology of the Cell. Fourth edition. Garland Publishing Inc. New York. 1463 pp.

Antonenkov, V.D., P.P. Van Veldhoven, E. Waelkens, and G.P. Mannaerts. 1997. Substrate specificities of 3-oxoacyl-CoA thiolase A and sterol carrier protein 2/3-oxoacyl-CoA thiolase purified from normal rat liver peroxisomes. Sterol carrier protein 2/3-oxoacyl-CoA thiolase is involved in the metabolism of 2-methyl-branched fatty acids and bile acid intermediates. *J. Biol. Chem.* 272:26023-26031.

Barstead, R.J. 1999. Reverse genetics. *In C. elegans.* A Practical Approach. I. A Hope, editor. Oxford University Press, Oxford. 112-113.

Berninger, G., R. Schmidtchen, G.Casel, A. Knorr, K. Rautenstrauss, W.-H. Kunau, and E. Schweizer. 1993. Structure and metabolic control of the *Yarrowia lipolytica* peroxisomal 3-oxoacyl-CoA-thiolase gene. *Eur. J. Biochem.* 216:607-613.

Berteaux-Lecellier, V., M. Picard, C. Thompson-Coffe, D. Zickler, A. Panvier-Adoutte, and J.M. Simonet. 1995. A nonmammalian homolog of the PAF1 gene (Zellweger syndrome) discovered as a gene involved in caryogamy in the fungus *Podospora anserina*. *Cell* 81:1043-1051.

Biardi, L., A. Sreedhar, A. Zokaei, N.B. Vartak, R.L. Bozeat, J.E. Shackelford, G.-A. Keller, and S.K. Krisans. 1994. Mevalonate kinase is predominantly localized in peroxisomes and is defective in patients with peroxisome deficiency disorders. *J. Biol. Chem.* 269:1197-1205.

Biermann, J., J. Gootjes, B.M. Humbel, T.B. Dansen, R.J. Wanders, and H. van den Bosch. 1999. Immunological analyses of alkyl-dihydroxyacetone-phosphate synthase in human peroxisomal disorders. *Eur. J. Cell Biol.* 78:339-348.

Blattner, J., H. Dorsam, and C.E. Clatyon. 1995. Function of N-terminal import signals in trypanosome microbodies. *FEBS Lett.* 360:310-314.

Blaxter, M. 1998. *Caenorhabditis elegans* is a nematode. *Science* 282:2041-2046.

Blumenthal, T, and K.S. Gleason. 2003. *Caenorhabditis elegans* operons: form and function. *Nat. Rev. Genet.* 4:112-120.

Body, D.R. 1972. The occurrence of cyclopropane fatty acids in the phospholipids of sheep rumen tissues. *FEBS Lett.* 27:5-8.

Boeckmann, B., A. Bairoch, R. Apweiler, M.-C. Blatter, A. Estreicher, E. Gasteiger, M.J. Martin, K. Michoud, C. O'Donovan, I. Phan, S. Pilbout, and M. Schneider. 2003. The

Swiss-Prot protein knowledgebase and its supplement TrEMBL in 2003. *Nucleic Acids Res*. 31:365-370.

Bojorquez, G., and M.A. Gomez-Lim. 1995. Peroxisomal thiolase mRNA is induced during mango fruit ripening. *Plant Mol. Biol.* 28:811-820.

Bosher, J.M., and M. Labouesse. 2000. RNA interference: genetic wand and genetic watchdog. *Nature Cell Biol.* 2:E31-E36.

Boulianne, G.L. 2001. Neuronal regulation of lifespan: clues from flies and worms. *Mech. Ageing Dev*. 122:883-894.

Bout, A., Y. Teunissen, T. Hashimoto, R. Benne, and J.M. Tager. 1988. Nucleotide sequence of human peroxisomal 3-oxoacyl-CoA thiolase. *Nucleic Acids Res.* 16:10369.

Braeckman, B.P., K. Houthoofd, K. Brys, I. Lenaerts, A. De Vreese, S. Van Eygen, H. Raes, and J.R. Vanfleteren. 2002. No reduction of energy metabolism in Clk mutants. *Mech. Ageing Dev. 123:1447-1456.*

Braverman, N., G. Dodt, S.J. Gould, and D. Valle. 1998. An isoform of pex5p, the human PTS1 receptor, is required for the import of PTS2 proteins into peroxisomes. *Hum. Mol. Genet*. 7:1195-1205.

Brenner, S. 1974. The genetics of *Caenorhabditis elegans*. *Genetics*. 77:71-94.

Bruinenberg, P.G., M. Blaa[illegible], B. Kazemier, and G. AB. 1990. Cloning and sequencing of the malate synthase gene from *Hansenula polymorpha*. *Yeast*. 6:245-254.

Buckingham, S.D., B. Esmaeili, M. Wood, D.B. Sattelle. 2004. RNA interference: from model organisms towards therapy for neural and neuromuscular disorders. *Hum. Mol. Genet*. 13:R275-R288.

Bun-ya, M., M. Maebuchi, S.H. Togo, T. Kurosawa, T. Hashimoto, and T. Kamiryo. 2000. Metabolic significance and expression of *Caenorhabditis elegans* type II 3-oxoacyl-CoA thiolase. *Cell Biochem. Biophys*. 32:291-293.

Bun-ya, M., M. Maebuchi, T. Hashimoto, S. Yokota, and T. Kamiryo. 1997. A second isoform of 3-ketoacyl-CoA thiolase found in *Caenorhabditis elegans*, which is similar to sterol carrier protein x but lacks the sequence of sterol carrier protein 2. *Eur. J. Biochem*. 245:252-259.

Bun-ya, M., M., Maebuchi, T. Kamiryo, T. Kurosawa, M. Sato, M. Tohma, L.L. Jiang, and T. Hashimoto. 1998. Thiolase involved in bile acid formation. *J. Biochem (Tokyo). 123*:347-352.

C. elegans Sequencing Consortium, The. 1998. Genome sequence of the nematode *C. elegans*: a platform for investigating biology. *Science*. 282:2012-2018.

Campbell, R.E., O. Tour, A.E. Palmer, P.A. Steinbach, G.S. Baird, D.A. Zacharias, and R.Y. Tsien. 2002. A monomeric red fluorescent protein. *Proc. Natl. Acad. Sci. USA*. 99:7877-7882.

Chang, C.C., S. South, D. Warren, J. Jones, A.B. Moser, H.W. Moser, and S.J. Gould. 1999. Metabolic control of peroxisome abundance. *J. Cell Sci.* 112:1579-1590.

Christensen, M., A. Estevez, X. Yin, R. Fox, R. Morrison, M. McDonnell, C. Gleason, D.M. Miller 3rd, K. Strange. 2002. A primary culture system for functional analysis of C. elegans neurons and muscle cells. *Neuron*. 33:503-514.

Church, D.L., K.L. Guan, and E.J. Lambie. 1995. Three genes of the MAP kinase cascade, *mek-2*, *mpk-1/sur-1* and *let-60 ras*, are required for meiotic cell cycle progression in *Caenorhabditis elegans*. *Development*. 121:2525–2535.

Clayton, C.E. 1985. Structure and regulated expression of genes encoding fructose biphosphate aldolase in *Trypanosoma brucei*. *EMBO J.* 4:2997-3003.

Clokey, G.V., and L.A. Jacobson. 1986. The autofluorescent "lipofuscin granules" in the intestinal cells of *Caenorhabditis elegans* are secondary lysosomes. *Mech. Ageing Dev.* 35:79-94.

Cooper, G.M. 2000. The Cell - A Molecular Approach. Second edition. Sinauer Associates, Sunderland. 690 pp.

Cronan, J.E.Jr. 2002. Phospholipid modifications in bacteria. *Curr. Opin. Microbiol.* 5:202-205.

Culetto, E., D.B. Sattelle. 2000. A role for *Caenorhabditis elegans* in understanding the function and interactions of human disease genes. *Hum. Mol.Genet*. 9:869-877.

Datta, N.S., G.N. Wilson, and A.K. Hajra. 1984. Deficiency of enzymes catalyzing the biosynthesis of glycerol-ether lipids in Zellweger syndrome. A new category of metabolic disease involving the absence of peroxisomes. *N. Engl. J. Med.* 311:1080-1083.

de Duve, C., and P. Baudhuin. 1966. Peroxisomes (microbodies and related particles). *Physiol. Rev*. 46:323-357.

de Hoop, M.J., and G. AB. 1992. Import of proteins into peroxisomes and other microbodies. *Biochem. J.* 286:657-669.

de Vet, E.C., B.T. van den Broek, and H. van den Bosch. 1997a. Nucleotide sequence of human alkyl-dihydroxyacetonephosphate synthase cDNA reveals the presence of a peroxisomal targeting signal 2. *Biochim. Biophys. Acta.* 1346:25-29.

de Vet, E.C., A.W. Zomer, G.J. Lahaut, and H. van den Bosch. 1997b. Polymerase chain reaction-based cloning of alkyl-dihydroxyacetonephosphate synthase complementary DNA from guinea pig liver. *J. Biol. Chem.* 272:798-803.

de Vet, E.C., H.C. Prinsen, and H. van den Bosch. 1998. Nucleotide sequence of a cDNA clone encoding a *Caenorhabditis elegans* homolog of mammalian alkyl-dihydroxyacetonephosphate synthase: evolutionary switching of peroxisomal targeting signals. *Biochem. Biophys. Res. Commun.* 242:277-281.

de Vet, E.C., L. Ijlst, W. Oostheim, C. Dekker, H.W. Moser, H. van den Bosch, and R.J. Wanders. 1999. Ether lipid biosynthesis: alkyl-dihydroxyacetonephosphate synthase protein deficiency leads to reduced dihydroxyacetonephosphate acyltransferase activities. *J. Lipid Res.* 40:1998-2003.

de Vet, E.C., Y.H. Hilkes, M.W. Fraaije, and H. van den Bosch. 2000. Alkyl-dihydroxyacetonephosphate synthase. Presence and role of flavin adenine dinucleotide. *J. Biol. Chem.* 275:6276-6283.

Dean, M., Y. Hamon, and G. Chimini. 2001. The human ATP-binding cassette (ABC) transporter superfamily. *J. Lipid Res.* 42:1007-1017.

Do, Y.Y., and P.L. Huang. 1997. Characterization of a pollination-related cDNA from *Phalaenopsis* encoding a protein which is homologous to human peroxisomal acyl-CoA oxidase. *Arch. Biochem. Biophys.* 344:295-300.

Dodt, G., D. Warren, E. Becker, P. Rehling, and S.J. Gould. 2001. Domain mapping of human PEX5 reveals functional and structural similarities to *Saccharomyces cerevisiae* Pex18p and Pex21p. *J. Biol. Chem.* 276:41769-41781.

Dowell, P., T.C. Otto, S., Adi, and M.D. Lane. 2003. Convergence of peroxisome proliferator-activated receptor gamma and Foxo1 signaling pathways. *J. Biol. Chem.* 278:45485-45491.

Driscoll, M., and B. Gerstbrein. 2003. Dying for a cause: invertebrate genetics takes on human neurodegeneration. *Nat. Rev. Genet.* 4:181-194.

Einerhand, A.W., T.M. Voorn-Brouwer, R. Erdmann, W.-H. Kunau, and H. F. Tabak. 1991. Regulation of transcription of the gene coding for peroxisomal 3-oxoacyl-CoA thiolase of *Saccharomyces cerevisiae*. *Eur. J. Biochem.* 200:113-122.

Elgersma, Y., A. Vos, M. van den Berg, C.W. van Roermund, P. van der Sluijs, B. Distel, and H.F. Tabak. 1996. Analysis of the carboxyl-terminal peroxisomal targeting signal 1 in a homologous context in *Saccharomyces cerevisiae*. *J. Biol. Chem.* 271:26375-26382.

Elgersma, Y., C.W. van Roermund, R.J. Wanders, and H.F. Tabak. 1995. Peroxisomal and mitochondrial carnitine acetyltransferases of *Saccharomyces cerevisiae* are encoded by a single gene. *EMBO J.* 14:3472-3479.

Ellinghaus, P., C. Wolfrum, G. Assmann, F. Spener, and U. Seedorf. 1999. Phytanic acid activates the peroxisome proliferator-activated receptor alpha (PPARα) in sterol carrier protein 2-/ sterol carrier protein x-deficient mice. *J. Biol. Chem.* 274:2766-2772.

Erdmann, R., and G. Blobel. 1995. Giant peroxisomes in oleic acid-induced *Saccharomyces cerevisiae* lacking the peroxisomal membrane protein Pmp27p. *J. Cell Biol.* 128:509-523.

Fan, C.Y., J. Pan, N. Usuda, A.V. Yeldandi, M.S. Rao, and J.K. Reddy. 1998. Steatohepatitis, spontaneous peroxisome proliferation and liver tumors in mice lacking peroxisomal fatty acyl-CoA oxidase. Implications for peroxisome proliferator-activated receptor α natural ligand metabolism. *J. Biol. Chem.* 273:15639-15645.

Fan, C.Y., J. Pan, R. Chu, D. Lee, K.D. Kluckman, N. Usuda, I. Singh, A.V. Yeldandi, M.S. Rao, N. Maeda, and J.K. Reddy. 1996. Hepatocellular and hepatic peroxisomal alterations in mice with a disrupted peroxisomal fatty acyl-coenzyme A oxidase gene. *J. Biol. Chem.* 271:24698-24710.

Ferdinandusse, S., S. Denis, C.W. Van Roermund, R.J. Wanders, and G. Dacremont. 2004. Identification of the peroxisomal β-oxidation enzymes involved in the degradation of long-chain dicarboxylic acids. *J. Lipid Res.* 45:1104-1111.

Ferdinandusse, S., S. Denis, P.A. Mooijer, Z. Zhang, J.K. Reddy, A.A. Spector, and R.J. Wanders. 2001. Identification of the peroxisomal beta-oxidation enzymes involved in the biosynthesis of docosahexaenoic acid. *J. Lipid Res.* 42:1987-1995.

Ferdinandusse, S., S. Denis, P.T. Clayton, A. Graham, J.E. Rees, J.T. Allen, B.N. McLean, A.Y. Brown, P. Vreken, H.R. Waterham, and R.J. Wanders. 2000. Mutations in the gene encoding peroxisomal α-methylacyl-CoA racemase cause adult-onset sensory motor neuropathy. *Nat. Genet.* 24:188-191.

Filppula, S.A., A.I. Yagi, S.H. Kilpelainen, D. Novikov, D.R. Fitzpatrick, M. Vihinen, D. Valle, and J.K. Hiltunen. 1998. $\Delta^{3,5}$-$\Delta^{2,4}$-dienoyl-CoA isomerase from rat liver. Molecular characterization. *J. Biol. Chem.* 273: 349-355.

Flynn, C.R., R.T. Mullen, and R.N. Trelease. 1998. Mutational analyses of a type 2 peroxisomal targeting signal that is capable of directing oligomeric protein import into tobacco BY-2 glyoxysomes. *Plant J.* 16:709-720.

Fujiki, Y. 2000. Peroxisome biogenesis and peroxisome biogenesis disorders. *FEBS Lett.* 476:42-46.

Fujino, T., M.J. Kang, H. Suzuki, H. Iijima, and T. Yamamoto. 1996. Molecular characterization and expression of rat acyl-CoA synthetase 3. *J. Biol. Chem.* 271: 16748-16752.

Gebhardt, J.S., G.J. Wadsworth, and B.F. Matthews. 1998. Characterization of a single soybean cDNA encoding cytosolic and glyoxysomal isozymes of aspartate aminotransferase. *Plant Mol. Biol.* 37:99-108.

Ghenea, S., M. Takeuchi, J. Motoyama, K. Sasamoto, W.-H. Kunau, T. Kamiryo, and M. Bun-Ya. 2001. The cDNA sequence and expression of the AAA-family peroxin genes *pex-1* and *pex6* from the nematode *Caenorhabditis elegans*. *Zool. Sci.* 18: 675-681.

Giaever, G., A.M. Chu, L. Ni, C. Connelly, L. Riles, S. Veronneau, S. Dow, A. Lucau-Danila, K. Anderson, B. Andre, A.P. Arkin, A. Astromoff, M. El-Bakkoury, R. Bangham, R. Benito, S. Brachat, S. Campanaro, M. Curtiss, K. Davis, A. Deutschbauer, K.D. Entian, P. Flaherty, F. Foury, D.J. Garfinkel, M. Gerstein, D. Gotte, U. Guldener, J.H. Hegemann, S. Hempel, Z. Herman, D.F. Jaramillo, D.E. Kelly, S.L. Kelly, P. Kotter, D. LaBonte, D.C. Lamb, N. Lan, H. Liang, H. Liao, L. Liu, C. Luo, M. Lussier, R. Mao, P. Menard, S.L. Ooi, J.L. Revuelta, C.J. Roberts, M. Rose, P. Ross-Macdonald, B. Scherens, G. Schimmack, B. Shafer, D.D. Shoemaker, S. Sookhai-Mahadeo, R.K. Storms, J.N. Strathern, G. Valle, M. Voet, G. Volckaert, C.Y. Wang, T.R. Ward, J. Wilhelmy, E.A. Winzeler, Y. Yang, G. Yen, E. Youngman, K. Yu, H. Bussey, J.D. Boeke, M. Snyder, P. Philippsen, R.W. Davis, and M. Johnston. 2002. Functional profiling of the *Saccharomyces cerevisiae* genome. *Nature*. 418:387-391.

Gietl, C. 1990. Glyoxysomal malate dehydrogenase from watermelon is synthesized with an amino-terminal transit peptide. *Proc. Natl. Acad. Sci. USA*. 87:5773-5777.

Gietl, C. 1992. Malate dehydrogenase isoenzymes: cellular locations and role in the flow of metabolites between the cytoplasm and cell organelles. *Biochim. Biophys. Acta*. 1100:217-234.

Gietl, C., K.N. Faber, I.J. van der Klei, and M. Veenhuis. 1994. Mutational analysis of the N-terminal topogenic signal of watermelon glyoxysomal malate dehydrogenase using the heterologous host *Hansenula polymorpha*. *Proc. Natl. Acad. Sci. USA*. 91:3151-3155.

Gill, M.S., A. Olsen, J.N. Sampayo, and G.J. Lithgow. 2003. An automated high-throughput assay for survival of the nematode *Caenorhabditis elegans*. *Free Radic. Biol. Med.* 35, 558-565

Glover, J.R., D.W. Andrews, S. Subramani, and R.A. Rachubinski. 1994. Mutagenesis of the amino targeting signal of *Saccharomyces cerevisiae* 3-ketoacyl-CoA thiolase reveals conserved amino acids required for import into peroxisomes *in vivo*. *J. Biol. Chem.* 269:7558-7563.

Goedert, M. 2003. Neurodegenerative tauopathy in the worm. *Proc. Natl. Acad. Sci. USA.* 100:9653-9655.

Gonczy, P., G. Echeverri, K. Oegema, A. Coulson, S.J. Jones, R.R. Copley, J. Duperon, J. Oegema, M. Brehm, E. Cassin, E. Hannak, M. Kirkham, S. Pichler, K. Flohrs, A. Goessen, S. Leidel, A.M. Alleaume, C. Martin, N. Ozlu, P. Bork, and A.A. Hyman. 2000. Functional genomic analysis of cell division in *C. elegans* using RNAi of genes on chromosome III. *Nature.* 408:331-336.

Goto, S., A. Nakamura, Z. Radak, H. Nakamoto, R. Takahashi, K. Yasuda, Y. Sakurai, and N. Ishii. 1999. Carbonylated proteins in aging and exercise: immunoblot approaches. *Mech. Ageing Dev.* 107:245-253.

Gould, S.J., and D. Valle. 2000. Peroxisome biogenesis disorders: genetics and cell biology. *Trends Genet.* 16:340-345.

Grogan, D.W., and J.E.Jr Cronan. 1986. Characterization of *Escherichia coli* mutants completely defective in synthesis of cyclopropane fatty acids. *J. Bacteriol.* 1986. 166:872-877.

Guarente, L., G. Ruvkun, and R. Amasino. 1998. Aging, life span, and senescence. *Proc. Natl. Acad. Sci. USA.* 95:11034-11036.

Guex, N., H. Henry, J. Flach, H. Richter, and F. Widmer. 1995. Glyoxysomal malate dehydrogenase and malate synthase from soybean cotyledons (*Glycine max L.*): enzyme association, antibody production and cDNA cloning. *Planta.* 197:369-375.

Gurvitz, A., L. Wabnegger, S. Langer, B. Hamilton, H. Ruis, and A. Hartig. 2001. The tetratricopeptide repeat domains of human, tobacco, and nematode PEX5 proteins are functionally interchangeable with the analogous native domain for peroxisomal import of PTS1-terminated proteins in yeast. *Mol. Genet. Genomics.* 265:276-286.

Gurvitz, A., S. Langer, M. Piskacek, B. Hamilton, H. Ruis, and A. Hartig. 2000. Predicting the function and subcellular location of *Caenorhabditis elegans* proteins similar to *Saccharomyces cerevisiae* β-oxidation enzymes. *Yeast.* 17:188-200.

Hajra, A.K., and A.K. Das. 1996. Lipid biosynthesis in peroxisomes. *Ann. N. Y. Acad. Sci.* 804:129-141.

Hall, D.H. 1995. Electron microscopy and three-dimensional image reconstruction. *Methods Cell Biol.* 48:395-436.

Hall, D.H., R. L. Russell. 1991. The posterior nervous system of the nematode *Caenorhabditis elegans*: serial reconstruction of identified neurons and complete pattern of synaptic interactions. *J. Neurosci.* 11:1-22.

Hashimoto, T. 1999. Peroxisomal β-oxidation enzymes. *Neurochem. Res.* 24:551-563.

Hayashi, H., L. De Bellis, K. Yamaguchi, A. Kato, M. Hayashi, and M. Nishimura. 1998a. Molecular characterization of a glyoxysomal long chain acyl-CoA oxidase that is synthesized as a precursor of higher molecular mass in pumpkin. *J. Biol. Chem.* 273:8301-8307.

Hayashi, M., K. Toriyama, M. Kondo, and M. Nishimura. 1998b. 2,4-dichlorophenoxybutyric acid-resistant mutants of *Arabidopsis* have defects in glyoxysomal fatty acid β-oxidation. *Plant Cell.* 10:183-195.

Hazra, P.P., I. Suriapranata, W.B. Snyder, and S. Subramani. 2002. Peroxisome remnants in pex3delta cells and the requirement of Pex3p for interactions between the peroxisomal docking and translocation subcomplexes. *Traffic.* 3:560-574.

Hekimi, S., J. Burgess, F. Bussiere, Y. Meng, and C. Benard. 2001. Genetics of lifespan in *C. elegans*: molecular diversity, physiological complexity, mechanistic simplicity. *Trends Genet.* 17:712-718.

Hettema, E.H., B. Distel, and H.F. Tabak. 1999. Import of proteins into peroxisomes. *Biochim. Biophys. Acta.* 1451:17-34.

Hijikata, M., N. Ishii, H. Kagamiyama, T. Osumi, and T. Hashimoto. 1987. Structural analysis of cDNA for rat peroxisomal 3-ketoacyl-CoA thiolase. *J. Biol. Chem.* 262:8151-8158.

Hirsch D., A. Stahl, and H.F. Lodish. 1998. A family of fatty acid transporters conserved from mycobacterium to man. *Proc. Natl. Acad. Sci. USA.* 95:8625-8629.

Hogenboom, S., G.J. Romeijn, S.M. Houten, M. Baes, R.J. Wanders, and H.R. Waterham. 2002. Absence of functional peroxisomes does not lead to deficiency of enzymes involved in cholesterol biosynthesis. *J. Lipid Res.* 43:90-98.

Holzinger, A., P. Mayerhofer, J. Berger, P. Lichtner, S. Kammerer, and A.A. Roscher. 1999. Full length cDNA cloning, promoter sequence, and genomic organization of the human adrenoleukodystrophy related (ALDR) gene functionally redundant to the gene responsible for X-linked adrenoleukodystrophy. *Biochem. Biophys. Res. Commun.* 258:436-442.

Hope, I.A. 1999. Background on *Caenorhabditis elegans*. *In C. elegans*. A Practical Approach. Hope, I.A., editor. Oxford University Press, Oxford. 1-15.

Hope, I.A. 2001. Broadcast interference - functional genomics. *Trends Genet.* 17:297-299.

Houthoofd, K., B.P. Braeckman, T.E. Johnson, J.R. Vanfleteren. 2004. Extending life-span in *C. elegans*. *Science*. 305:1238-1239.

Houthoofd, K., B.P. Braeckman, I. Lenaerts, K. Brys, A. De Vreese, S. Van Eygen, and J.R. Vanfleteren. 2002a. Ageing is reversed, and metabolism is reset to young levels in recovering dauer larvae of *C. elegans*. *Exp. Gerontol.* 37:1015-1021.

Houthoofd, K., B.P. Braeckman, I. Lenaerts, K. Brys, A. De Vreese, S. Van Eygen, and J.R. Vanfleteren. 2002b. No reduction of metabolic rate in food restricted *Caenorhabditis elegans*. *Exp. Gerontol.* 37:1359-1369.

Houthoofd, K., B.P. Braeckman, T.E. Johnson, and J.R. Vanfleteren. 2003. Life extension via dietary restriction is independent of the Ins/IGF-1 signalling pathway in *Caenorhabditis elegans*. *Exp. Gerontol.* 38:947-954.

Hsu, A.L., C.T. Murphy, and C. Kenyon. 2003. Regulation of aging and age-related disease by DAF-16 and heat-shock factor. *Science.* 300:1142-1145.

Huang, L.S., and P.W. Sternberg. 1995. Genetic dissection of developmental pathways. *Methods Cell Biol.* 48:97-122.

Iida, R., T. Yasuda, E. Tsubota, H. Takatsuka, M. Masuyama, T. Matsuki, and K. Kishi. 2003. M-LP, Mpv17-like protein, has a peroxisomal membrane targeting signal comprising a transmembrane domain and a positively charged loop and up-regulates expression of the manganese superoxide dismutase gene. *J. Biol. Chem.* 278:6301-6306.

Imblum, R.L., and V.W. Rodwell. 1974. 3-Hydroxy-3-methylglutaryl CoA reductase and mevalonate kinase of *Neurospora crassa*. *J. Lipid Res.* 15:211-222.

Jansen, G.A., D.M. van den Brink, R. Ofman, O. Draghici, G. Dacremont, and R.J. Wanders. 2001. Identification of pristanal dehydrogenase activity in peroxisomes: conclusive evidence that the complete phytanic acid α-oxidation pathway is localized in peroxisomes. *Biochem. Biophys. Res. Commun.* 283:674-679.

Jansen, G.A., R. Ofman, S. Ferdinandusse, L. Ijlst, A.O. Muijsers, O.H. Skjeldal, O. Stokke, C. Jakobs, G.T. Besley, J.E. Wraith, and R.J. Wanders. 1997. Refsum disease is caused by mutations in the phytanoyl-CoA hydroxylase gene. *Nature Genet.* 17:190-193.

Jansen, W.T., M. Bolm, R. Balling, G.S. Chhatwal, and R. Schnabel. 2002. Hydrogen peroxide-mediated killing of *Caenorhabditis elegans* by *Streptococcus pyogenes*. *Infect. Immun.* 70:5202-5207.

Jazwinski, S.M. 1998. Genetics of longevity. *Exp. Gerontol.* 33:773-783.

Jedd, G., and N.-H.Chua. 2000. A new self-assembled peroxisomal vesicle required for efficient resealing of the plasma membrane. *Nature Cell Biol.* 2:226-231.

Kamath, R.S., A.G. Fraser, Y. Dong, G. Poulin, R. Durbin, M. Gotta, A. Kanapin, N. Le Bot, S. Moreno, M. Sohrmann, D.P. Welchman, P. Zipperlen, and J. Ahringer. 2003. Systematic functional analysis of the *Caenorhabditis elegans* genome using RNAi. *Nature.* 421:231-237.

Kaminaka, H., S. Morita, T. Masumura, and K. Tanaka. 1998. Molecular cloning and characterization of a cDNA encoding glyoxysomal malate dehydrogenase from rice (*Oryza sativa L.*). GenBank Accession Number Q42972.

Kaneda, T. 1991. Iso- and anteiso-fatty acids in bacteria: biosynthesis, function, and taxonomic significance. *Microbiol. Rev.* 55:288-302.

Kato, A., M. Hayashi, M. Kondo, and M. Nishimura. 1996a. Targeting and processing of a chimeric protein with the N-terminal presequence of the precursor to glyoxysomal citrate synthase. *Plant Cell.* 8:1601-1611.

Kato, A., M. Hayashi, Y. Takeuchi, and M. Nishimura. 1996b. cDNA cloning and expression of a gene for 3-ketoacyl-CoA thiolase in pumpkin cotyledons. *Plant Mol. Biol.* 31:843-852.

Kato, A., Y. Takeda-Yoshikawa, M. Hayashi, M. Kondo. I. Hara-Nishimura, and M. Nishimura. 1998. Glyoxysomal malate dehydrogenase in pumpkin: cloning of a cDNA and functional analysis of its presequence. *Plant Cell Physiol.* 39:186-195.

Kelley, R.I., and G.E. Herman. 2001. Inborn errors of sterol biosynthesis. *Annu. Rev. Genomics Hum. Genet.* 2:299-341.

Kennedy, S., D. Wang, and G. Ruvkun. 2004. A conserved siRNA-degrading RNase negatively regulates RNA interference *in C. elegans. Nature.* 427:645-649.

Kim, D.J., and S.M. Smith. 1994. Expression of a single gene encoding microbody NAD-malate dehydrogenase during glyoxysome and peroxisome development in cucumber. *Plant Mol. Biol.* 26:1833-1841.

Kim, S.K., J. Lund, M. Kiraly, K. Duke, M. Jiang, J.M. Stuart, A. Eizinger, B.N. Wylie, and G.S. Davidson. 2001. A gene expression map for *Caenorhabditis elegans. Science.* 293:2087-2092.

Klein, A.T., M. van den Berg, G. Bottger, H.F. Tabak, and B. Distel. 2002. *Saccharomyces cerevisiae* acyl-CoA oxidase follows a novel, non-PTS1, import pathway into peroxisomes that is dependent on Pex5p. *J. Biol. Chem.* 277:25011-25019.

Klenk, E., and W. Kahike. 1963. On the presence of 3,7,11,15-tetramethylhexadecanoic acid (phytanic acid) in the cholesterol esters and other lipoid fractions of the organs in a case of a disease of unknown origin (possibly heredopathia atactica polyneuritiformis, Refsum's syndrome). *Hoppe Seylers Z. Physiol. Chem.* 333:133-139.

Koushika, S.P., and M.L. Nonet. 2000. Sorting and transport in *C. elegans*: a model system with a sequenced genome. *Curr. Opin. Cell Biol.* 12:517-523.

Kragler, F., A. Langeder, J. Raupachova, M. Binder, and A. Hartig. 1993. Two independent peroxisomal targeting signals in catalase A of *Saccharomyces cerevisiae*. *J. Cell Biol.* 120:665-673.

Kunau, W.-H. 1998. Peroxisome biogenesis: from yeast to man. *Curr. Opin. Microbiol.* 1:232-237.

Kurihara, T., M. Ueda, N. Kanayama, J. Kondo, Y. Teranishi, and A. Tanaka. 1992. Peroxisomal acetoacetyl-CoA thiolase of an *n*-alkane-utilizing yeast, *Candida tropicalis*. *Eur. J. Biochem.* 210:999-1005.

Kurzchalia, T.V., and S. Ward. 2003. Why do worms need cholesterol? *Nat. Cell Biol.* 5:684-688.

Laemmli, U.K. 1970. Cleavage of structural proteins during the assembly of the head of bacteriophage T4. *Nature*. 227:680-685.

Larsen, P.L. 1993. Aging and resistance to oxidative damage in *Caenorhabditis elegans*. *Proc. Natl. Acad. Sci. U S A*. 90:8905–8909.

Lazarow, P.B., and H.W. Moser. 1989. Disorders of peroxisome biogenesis. *In* The metabolic Basis of inherited Disease. Scriver, C.R., A.L. Beaudet, W.S. Sly, D. Valle, editors. Vol II. Sixth edition. McGraw-Hill, New York. 1479-1509.

Lazarow, P.B., and Y. Fujiki. 1985. Biogenesis of peroxisomes. *Annu. Rev. Cell Biol.* 1:489-530.

Lee, S.S., S. Kennedy, A.C. Tolonen, and G. Ruvkun. 2003. DAF-16 target genes that control *C. elegans* life-span and metabolism. *Science*. 300:644-647.

Legakis, J.E., and S.R. Terlecky. 2001. PTS2 protein import into mammalian peroxisomes. *Traffic*. 2:252-260.

Legakis, J.E., J.I. Koepke, C. Jedeszko, F. Barlaskar, L.J. Terlecky, H.J. Edwards, P.A. Walton, and S.R. Terlecky. 2002. Peroxisome senescence in human fibroblasts. *Mol. Biol. Cell*. 12:4243-4255.

Leighton, F., B. Poole, H. Beaufay, P. Baudhuin, J.W. Coffey, S. Fowler, and C. de Duve. 1968. The large-scale separation of peroxisomes, mitochondria, and lysosomes from the livers of rats injected with triton WR-1339. Improved isolation procedures, automated analysis, biochemical and morphological properties of fractions. *J. Cell Biol.* 37:482-513.

Lewis, J.A., and J.T. Fleming. 1995. Basic culture methods. *Methods Cell Biol.* 48:3-29.

Li, X., E. Baumgart, G.X. Dong, J.C. Morrell, G. Jimenez-Sanchez, D. Valle, K.D. Smith, and S.J. Gould. 2002. PEX11α is required for peroxisome proliferation in response to 4-phenylbutyrate but is dispensable for peroxisome proliferator-activated receptor α-mediated peroxisome proliferation. *Mol. Cell. Biol.* 22:8226–8240.

Lin Y., L. Sun, L.V. Nguyen, R.A. Rachubinski, and H.M. Goodman. 1999. The Pex16p homolog SSE1 and storage organelle formation in *Arabidopsis* seeds. *Science.* 284:328-330.

Lluch, M.A., A. Masferrer, M. Arro, A. Boronat, and A. Ferrer. 2000. Molecular cloning and expression analysis of the mevalonate kinase gene from *Arabidopsis thaliana. Plant Mol. Biol.* 42:365-376.

Longo, V.D., E.B. Gralla, and J.S. Valentine. 1996. Superoxide dismutase activity is essential for stationary phase survival in *Saccharomyces cerevisiae*. Mitochondrial production of toxic oxygen species *in vivo*. *J. Biol. Chem.* 271:12275-12280.

Lu, Y.J., Y.M. Zhang, and C.O. Rock. 2004. Product diversity and regulation of type II fatty acid synthases. *Biochem. Cell Biol.* 82:145-155.

Mackay, W.J., and G.C. Bewley. 1989. The genetics of catalase in *Drosophila melanogaster*: isolation and characterization of acatalasemic mutants. *Genetics.* 122:643-652.

Maduro, M., and D. Pilgrim. 1995. Identification and cloning of *unc-119*, a gene expressed in the *Caenorhabditis elegans* nervous system. *Genetics.* 141:977-988.

Maebuchi, M., S.H. Togo, S. Yokota, S. Ghenea, M. Bun-Ya, T. Kamiryo, and A. Kawahara. 1999. Type-II 3-oxoacyl-CoA thiolase of the nematode *Caenorhabditis elegans* is located in peroxisomes, highly expressed during larval stages and induced by clofibrate. *Eur. J. Biochem.* 264: 509-515.

Maeda, I., Kohara, Y., Yamamoto, M. and Sugimoto, A. 2001. Large-scale analysis of gene function in *Caenorhabditis elegans* by high-throughput RNAi. *Curr. Biol.* 11, 171-176.

Maniatis, T., E.F. Fritsch, and J. Sambrook. 1982. Molecular cloning. A laboratory Manual. Cold Spring Harbor Laboratory, Cold Spring Harbor, NY.

Marzioch, M., R. Erdmann, M. Veenhuis, and W.-H. Kunau. 1994. *PAS7* encodes a novel yeast member of the WD-40 protein family essential for import of 3-oxoacyl-CoA thiolase, a PTS2-containing protein, into peroxisomes. *EMBO J.* 13:4908-4918.

Matsumoto, N., S. Tamura, and Y. Fujiki. 2003. The pathogenic peroxin Pex26p recruits the Pex1p-Pex6p AAA ATPase complexes to peroxisomes. *Nat. Cell Biol.* 5:454-460.

Matyash, V., C. Geier, A. Henske, S. Mukherjee, D. Hirsh, C. Thiele, B. Grant, F.R. Maxfield, and T.V. Kurzchalia. 2001. Distribution and transport of cholesterol in *Caenorhabditis elegans*. *Mol. Biol. Cell.* 12:1725-1736.

McElwee, J., K. Bubb, and J.H. Thomas. 2003. Transcriptional outputs of the *Caenorhabditis elegans* forkhead protein DAF-16. *Aging Cell.* 2:111-121.

McGuinness, M.C., H. Wei, and K.D. Smith. 2000. Therapeutic developments in peroxisome biogenesis disorders. *Expert Opin. Investig. Drugs*. 9:1985-1992.

Mello, C., and A. Fire. 1995. DNA transformation. *Methods Cell Biol.* 48:451-482.

Mellor, J., M.J. Dobson, N.A. Roberts, M.F. Tuite, J.S. Emtage, S. White, P.A. Lowe, T. Patel, A.J. Kingsman, and S.M. Kingsman. 1983. Efficient synthesis of enzymatically active calf chymosin in *Saccharomyces cerevisiae*. *Gene*. 24:1-14.

Melov, S., J. Ravenscroft, S. Malik, M.S. Gill, D.W. Walker, P.E. Clayton, D.C. Wallace, D. Malfroy, S.R. Doctorow, and G.J. Lithgow. 2000. Extension of life-span with superoxide dismutase/catalase mimetics. *Science*. 289:1567–1569.

Michalik, L., B. Desvergne, N.S. Tan, S. Basu-Modak, P. Escher, J. Rieusset, J.M. Peters, G. Kaya, F.J. Gonzalez, J. Zakany, D. Metzger, P. Chambon, D. Duboule, and W. Wahli. 2001. Impaired skin wound healing in peroxisome proliferator-activated receptor (PPAR)α and PPARβ mutant mice. *J. Cell Biol.* 154:799-814.

Mihalik, S.J., J.C. Morrell, D. Kim, K.A. Sacksteder, P.A. Watkins, and S.J. Gould. 1997. Identification of PAHX, a Refsum disease gene. *Nature Genet.* 17:185-189.

Miller, D.M., and D.C. Shakes. 1995. Immunofluorescence microscopy. *Methods Cell Biol.* 48:365-394.

Miller, S.S., B.T. Driscoll, R.G. Gregerson, J.S. Gantt, and C.P. Vance. 1998. Alfalfa malate dehydrogenase (MDH): molecular cloning and characterization of five different forms reveals a unique nodule-enhanced MDH. *Plant J.* 15:173-184.

Mizuno, T., K. Ito, C. Uchida, M. Kitagawa, A. Ichiyama, S. Miura, K. Fujita, and T. Oda. 2002. Analyses in transfected cells and *in vitro* of a putative peroxisomal targeting signal of rat liver serine:pyruvate aminotransferase. *Histochem. Cell Biol.* 118:321-328.

Mohan, K.V., and C.D. Atreya. 2003. Novel organelle-targeting signals in viral proteins. *Bioinformatics*. 19:10-13.

Moser, H.W. 1999. Genotype-phenotype correlations in disorders of peroxisome biogenesis. *Mol. Genet. Metab.* 68:316-327.

Mosser, J., A.M. Douar, C.O. Sarde, P. Kioschis, R. Feil, H. Moser, A.M. Poustka, J.L. Mandel, and P. Aubourg. 1993. Putative X-linked adrenoleukodystrophy gene shares unexpected homology with ABC transporters. *Nature*. 361:726-730.

Motley, A.M., E.H. Hettema, R. Ketting, R. Plasterk, and H.F. Tabak. 2000. *Caenorhabditis elegans* has a single pathway to target matrix proteins to peroxisomes. *EMBO Rep.* 1:40-46.

Mukherji, M., N.J. Kershaw, C.J. Schofield, A.S. Wierzbicki, and M.D. Lloyd. 2002. Utilization of sterol carrier protein-2 by phytanoyl-CoA 2-hydroxylase in the peroxisomal alpha oxidation of phytanic acid. *Chem. Biol.* 9:597-605.

Mukherji, M., C.J. Schofield, A.S. Wierzbicki, G.A. Jansen, R.J. Wanders, and M.D. Lloyd. 2003. The chemical biology of branched-chain lipid metabolism. *Prog. Lipid Res.* 42:359-376.

Mullen, R. T., M.S. Lee, C.R. Flynn, and R.N. Trelease. 1997. Diverse amino acid residues function within the type 1 peroxisomal targeting signal. Implications for the role of accessory residues upstream of the type 1 peroxisomal targeting signal. *Plant Physiol.* 115:881-889.

Mullen, R.T., and R.N. Trelease. 1996. Biogenesis and membrane properties of peroxisomes: does the boundary membrane serve and protect? *Trends Plant Sci.* 1:389-394.

Murphy, C.T., S.A. McCarroll, C.I. Bargmann, A. Fraser, R.S. Kamath, J. Ahringer, H. Li, and C. Kenyon. 2003. Genes that act downstream of DAF-16 to influence the lifespan of *Caenorhabditis elegans*. *Nature*. 424:277-284.

Nakamura, A., K. Yasuda, H. Adachi, Y. Sakurai, N. Ishii, and S. Goto. 1999. Vitellogenin-6 is a major carbonylated protein in aged nematode, *Caenorhabditis elegans*. *Biochem. Biophys. Res. Commun.* 264:580-583.

Neuberger, G., S. Maurer-Stroh, B. Eisenhaber, A. Hartig, and F. Eisenhaber. 2003a. Motif refinement of the peroxisomal targeting signal 1 and evaluation of taxon-specific differences. *J. Mol. Biol.* 328:567-579.

Neuberger, G., S. Maurer-Stroh, B. Eisenhaber, A. Hartig, and F. Eisenhaber. 2003b. Prediction of peroxisomal targeting signal 1 containing proteins from amino acid sequence. *J. Mol. Biol.* 328:581-592.

Ogata, M. 1991. Acatalasemia. *Hum. Genet.* 86:331-340.

Ogg, S., S. Paradis, S. Gottlieb, G.I. Patterson, L. Lee, H.A. Tissenbaum, and G. Ruvkun. 1997. The Fork head transcription factor DAF-16 transduces insulin-like metabolic and longevity signals in *C. elegans*. *Nature*. 389:994-999.

Ohba, T., H. Rennert, S.M. Pfeifer, Z. He, R. Yamamoto, J.A. Holt, J.T. Billheimer, and J.F.3rd Strauss. 1994. The structure of the human sterol carrier protein X/sterol carrier protein 2 gene (SCP2). *Genomics*. 24:370-374.

Ohba, T., J.A. Holt, J.T. Billheimer, and J.F.3rd Strauss. 1995. Human sterol carrier protein x/sterol carrier protein 2 gene has two promoters. *Biochemistry*. 34:10660-10668.

Oikawa, E., H. Iijima, T. Suzuki, H. Sasano, H. Sato, A. Kamataki, H. Nagura, M.J. Kang, T. Fujino, H. Suzuki, and T.T. Yamamoto. 1998. A novel acyl-CoA synthetase, ACS5, expressed in intestinal epithelial cells and proliferating preadipocytes. *J. Biochem. (Tokyo)*. 124:679-685.

Olesen, C., K.K. Thomsen, I. Svendsen, and A. Brandt. 1997. The glyoxysomal 3-ketoacyl-CoA thiolase precursor from *Brassica napus* has enzymatic activity when synthesized in *Escherichia coli*. *FEBS Lett.* 412:138-140.

Olivier, L.M., W. Kovacs, K. Masuda, G.-A. Keller, and S.K. Krisans. 2000. Identification of peroxisomal targeting signals in cholesterol biosynthetic enzymes. AA-CoA thiolase, HMG-CoA synthase, MPPD, and FPP synthase. *J. Lipid Res.* 41:1921-1935.

Oulmouden, A., and F. Karst. 1991. Nucleotide sequence of the *ERG12* gene of *Saccharomyces cerevisiae* encoding mevalonate kinase. *Curr. Genet.* 19:9-14.

Passreiter, M., M. Anton, D. Lay, R. Frank, C. Harter, F.T. Wieland, K. Gorgas, and W.W. Just. 1998. Peroxisome biogenesis: involvement of ARF and coatomer. *J. Cell Biol.* 141:373-383.

Petriv, O.I., D.B. Pilgrim, R.A. Rachubinski, and V.I. Titorenko. 2002. RNA interference of peroxisome-related genes in *C. elegans*: a new model for human peroxisomal disorders. *Physiol. Genomics*. 10:79-91.

Plasterk, R.H. 1995. Reverse genetics: from gene sequence to mutant worm. *Methods Cell Biol* 48:59-80.

Pollard, T.D., and W.C. Earnshaw. Cell Biology. 2002. Elsevier Science, Philadelphia. 805 pp.

Poll-Thé, B.T., F. Roels, H. Ogier, J. Scotto, J. Vamecq, R.B. Schutgens, R.J. Wanders, C.W. van Roermund, M.J. van Wijland, A.W. Schram, J.M. Tager, and J.M. Saudubray. 1988. A new peroxisomal disorder with enlarged peroxisomes and a specific deficiency of acyl-CoA oxidase (pseudo-neonatal adrenoleukodystrophy). *Am. J. Hum. Genet.* 42:422-434.

Porter, K.R., and J.B. Kaulfield. 1958. Proseedings of the Fourth International Congress Electron Microscopy. Springer-Verlag. Berlin. 2:503

Powers, J.M., and H.W. Moser. 1998. Peroxisomal disorders: genotype, phenotype, major neuropathologic lesions, and pathogenesis. *Brain Pathol.* 8:101-120.

Preisig-Muller, R., and H. Kindl. 1993. Thiolase mRNA translated *in vitro* yields a peptide with a putative N-terminal presequence. *Plant Mol. Biol.* 22:59-66.

Purdue, P.E, S.M. Castro, V. Protopopov, and P.B. Lazarow. 1996. Targeting of human catalase to peroxisomes is dependent upon a novel C-terminal peroxisomal targeting sequence. *Ann. N. Y. Acad. Sci.* 804:775-776.

Purdue, P.E., M. Skoneczny, X. Yang, J.W. Zhang, and P.B. Lazarow. 1999. Rhizomelic chondrodysplasia punctata, a peroxisomal biogenesis disorder caused by defects in Pex7p, a peroxisomal protein import receptor: a minireview. *Neurochem. Res.* 24:581-586.

Purdue, P.E., X. Yang, and P.B. Lazarow. 1998. Pex18p and Pex21p, a novel pair of related peroxins essential for peroxisomal targeting by the PTS2 pathway. *J. Cell Biol.* 143:1859-1869.

Rachubinski, R.A., and S. Subramani. 1995. How proteins penetrate peroxisomes. *Cell.* 83:525-528.

Rand, J.B., and C.D. Johnson. 1995. Genetic pharmacology: interactions between drugs and gene products in *Caenorhabditis elegans*. *Methods Cell Biol.* 48:187-204.

Rehling, P., M. Marzioch, F. Niesen, E. Wittke, M. Veenhuis, and W.-H. Kunau. 1996. The import receptor for the peroxisomal targeting signal 2 (PTS2) in *Saccharomyces cerevisiae* is encoded by the *PAS7* gene. *EMBO J.* 15:2901-2913.

Rhodin, J. 1954. Aktiebolaget Godvil Stockholm. Karolinska Institute, Dissertation.

Riddle, D.L. 1988. The Dauer larva. *In* The nematode *Caenorhabditis elegans.* Wood, W.B., editor. Cold spring Laboratory Press, Cold Spring Harbor. 393-412.

Roe, C.R., D.S. Millington, D.L. Norwood, N. Kodo, H. Sprecher, B.S. Mohammed, M. Nada, H. Schulz, and R. McVie. 1990. 2,4-Dienoyl-coenzyme A reductase deficiency: a possible new disorder of fatty acid oxidation. *J. Clin. Invest.* 85:1703-1707.

Rontani, J.F., A. Mouzdahir, V. Michotey, and P. Bonin. 2002. Aerobic and anaerobic metabolism of squalene by a denitrifying bacterium isolated from marine sediment. *Arch Microbiol.* 178:279-287.

Rottensteiner, H., K. Stein, E. Sonnenhol, and R. Erdmann. 2003. Conserved function of pex11p and the novel pex25p and pex27p in peroxisome biogenesis. *Mol. Biol. Cell.* 14:4316-4328.

Sacksteder, K.A., and S.J. Gould. 2000. The genetics of peroxisome biogenesis. *Annu Rev. Genet.* 34:623-652, 2000.

Sacksteder, K.A, J.M. Jones, S.T. South, X. Li, Y. Liu, and S.J. Gould. 2000. PEX19 binds multiple peroxisomal membrane proteins, is predominantly cytoplasmic, and is required for peroxisome membrane synthesis. *J. Cell Biol.* 148:931-944.

Sambrook, J., and D.W. Russell. 2001. Molecular cloning. A laboratory manual. Cold spring Laboratory Press, Cold Spring Harbor. V.1:5.9.

Sandhir, R., M. Khan, and I. Singh. 2000. Identification of the pathway of α-oxidation of cerebronic acid in peroxisomes. *Lipids.* 35:1127-1133.

Sanger, F., S. Nicklen, and A.R. Coulson. 1977. DNA sequencing with chain-terminating inhibitors. *Proc. Natl. Acad. Sci. USA.* 74:5463-5467.

Schrader, M. 2001. Tubulo-reticular clusters of peroxisomes in living COS-7 cells: dynamic behavior and association with lipid droplets. *J. Histochem Cytochem.* 49:1421-1429.

Schrader, M., B.E. Reuber, J.C. Morrell, G. Jimenez-Sanchez, C. Obie, T.A. Stroh, D. Valle, T.A. Schroer, and S.J. Gould. 1998. Expression of PEX11β mediates peroxisome proliferation in the absence of extracellular stimuli. *J. Biol. Chem.* 273:29607-29614.

Schram, A.W., S. Goldfischer, C.W.T. van Roermund, E.M. Brouwer-Kelder, J. Collins, T. Hashimoto, H.S.A. Heymans, H. van den Bosch, R.B.H. Schutgens, J.M. Tager, and R.J.A. Wanders. 1987. Human peroxisomal 3-oxoacyl-coenzyme A thiolase deficiency. *Proc. Natl. Acad. Sci. USA.* 84:2494-2496.

Seedorf, U., M. Raabe, P. Ellinghaus, F. Kannenberg, M. Fobker, T. Engel, S. Denis, F. Wouters, K.W. Wirtz, R.J. Wanders, N. Maeda, and G. Assmann. 1998. Defective peroxisomal catabolism of branched fatty acyl coenzyme A in mice lacking the sterol carrier protein-2/sterol carrier protein-x gene function. *Genes Dev.* 12:1189-1201.

Segrest, J.P., M.K. Jones, H. De Loof, and N. Dashti. 2001. Structure of apolipoprotein B-100 in low density lipoproteins. *J. Lipid Res*. 42:1346-1367.

Sheikh, F.G., K. Pahan, M. Khan, E. Barbosa, and I. Singh. 1998. Abnormality in catalase import into peroxisomes leads to severe neurological disorder. *Proc. Natl. Acad. Sci. USA*. 95:2961-2966.

Shibata, Y., R. Branicky, I.O. Landaverde, and S. Hekimi. 2003. Redox regulation of germline and vulval development in *Caenorhabditis elegans*. *Science*. 302:1779-1782.

Shimozawa, N., T. Tsukamoto, T. Nagase, Y. Takemoto, N. Koyama, Y. Suzuki, M. Komori, T. Osumi, G. Jeannette, R.J. Wanders, and N. Kondo. 2004. Identification of a new complementation group of the peroxisome biogenesis disorders and *PEX14* as the mutated gene. *Hum. Mutat*. 23:552-558.

Sikorski, R.S., and P. Hieter. 1989. A system of shuttle vectors and yeast host strains designed for efficient manipulation of DNA in *Saccharomyces cerevisiae*. *Genetics*. 122:9-27.

Simmer, F., C. Moorman, A.M. Van Der Linden, E. Kuijk, P.V. Van Den Berghe, R. Kamath, A.G. Fraser, J. Ahringer, and R.H. Plasterk. 2003. Genome-Wide RNAi of *C. elegans* Using the Hypersensitive rrf-3 Strain Reveals Novel Gene Functions. *PLoS Biol*. 1:E12.

Singh, H., and A. Poulos. 1988. Distinct long chain and very long chain fatty acyl CoA synthetases in rat liver peroxisomes and microsomes. *Arch. Biochem. Biophys*. 266:486-495.

Singh, I., O. Lazo, G.S. Dhaunsi, and M. Contreras. 1992. Transport of fatty acids into human and rat peroxisomes. Differential transport of palmitic and lignoceric acids and its implication to X-adrenoleukodystrophy. *J. Biol. Chem*. 267:13306-13313.

Singh, I., R.G. Voigt, F.G. Sheikh, K. Kremser, and F.R.3rd Brown. 1997. Biochemical features of a patient with Zellweger-like syndrome with normal PTS-1 and PTS-2 peroxisomal protein import systems: a new peroxisomal disease. *Biochem. Mol. Med*. 61:198-207.

Smirnova, N., and K.A. Reynolds. 2001. Branched-chain fatty acid biosynthesis in *Escherichia coli*. *J. Ind. Microbiol. Biotechnol*. 27:246-251.

Smith, J.J., T.W. Brown, G.A. Eitzen, and R.A. Rachubinski. 2000. Regulation of peroxisome size and number by fatty acid β-oxidation in the yeast *Yarrowia lipolytica*. *J. Biol. Chem*. 275:20168-20178.

Smith, J.J., M. Marelli, R.H. Christmas, F.J. Vizeacoumar, D.J. Dilworth, T. Ideker, T. Galitski, K. Dimitrov, R.A. Rachubinski, and J.D. Aitchison. 2002. Transcriptome profiling to identify genes involved in peroxisome assembly and function. *J. Cell Biol.* 158:259-271.

St. Jules, R., W. Setlik, J. Kennard, and E. Holtzman. 1990. Peroxisomes in the head of *Drosophila melanogaster*. *Exp Eye Res* 51:607-617.

Stamellos, K.D., J.E. Shackelford, R.D. Tanaka, and S.K. Krisans. 1992. Mevalonate kinase is localized in rat liver peroxisomes. *J. Biol. Chem.* 267:5560-5568.

Stanczak, H., J.J. Stanczak, and I. Singh. 1992. Chromosomal localization of the human gene for palmitoyl-CoA ligase (FACL1). *Cytogenet. Cell Genet.* 59:17-19.

Steinberg, S.J., S.J. Mihalik, D.G. Kim, D.A. Cuebas, and P.A. Watkins. 2000. The human liver-specific homolog of very long-chain acyl-CoA synthetase is cholate:CoA ligase. *J. Biol. Chem.* 275:15605-15608.

Steinberg, S.J., S.J. Wang, D.G. Kim, S.J. Mihalik, and P.A. Watkins. 1999. Human very-long-chain acyl-CoA synthetase: cloning, topography, and relevance to branched-chain fatty acid metabolism. *Biochem Biophys Res Commun.* 257:615-621.

Sternberg, P.W. 2001. Working in the post-genomic *C. elegans* world. *Cell.* 105:173-176.

Stiernagle, T. 1999. Maintenance of *C. elegans*. *In C. elegans*. A Practical Approach. Hope, I.A., editor. Oxford University Press, Oxford. 112-113.

Subramani, S, A. Koller, and W.B. Snyder. 2000. Import of peroxisomal matrix and membrane proteins. *Annu. Rev. Biochem.* 69:399-418.

Subramani, S. 1993. Protein import into peroxisomes and biogenesis of the organelle. *Annu. Rev. Cell Biol.* 9:445-478.

Subramani, S. 1996. Convergence of model systems for peroxisome biogenesis. *Curr. Opin. Cell Biol.* 8:513-518.

Subramani, S. 1997. *PEX* genes on the rise. *Nature Genet.* 15:331-333.

Sulston, J.E., E. Schierenberg, J.G. White, and J.N. Thomson. 1983. The embryonic cell lineage of the nematode *Caenorhabditis elegans*. *Dev. Biol.* 100:64-119.

Sulston, J.E., H.R. Horvitz. 1977. Post-embryonic cell lineages of the nematode, *Caenorhabditis elegans*. *Dev. Biol.* 56:110-156.

Swinkels, B.W., S.J. Gould, and S. Subramani. 1992. Targeting efficiencies of various permutations of the consensus C-terminal tripeptide peroxisomal targeting signal. *FEBS Lett.* 305:133-136.

Szilard, R.K., V.I. Titorenko, M. Veenhuis, and R.A. Rachubinski. 1995. Pay32p of the yeast *Yarrowia lipolytica* is an intraperoxisomal component of the matrix protein translocation machinery. *J. Cell Biol.* 131:1453-1469.

Tam, Y.Y., J.C. Torres-Guzman, F.J. Vizeacoumar, J.J. Smith, M. Marelli, J.D. Aitchison, and R.A. Rachubinski. 2003. Pex11-related proteins in peroxisome dynamics: a role for the novel peroxin Pex27p in controlling peroxisome size and number in Saccharomyces cerevisiae. *Mol. Biol. Cell.* 14:4089-4102.

Tanaka, A., K. Okumoto, and Y. Fujiki. 2003. cDNA cloning and characterization of the third isoform of human peroxin Pex11p. *Biochem. Biophys. Res. Commun.* 300:819-823.

Taub, J., J.F. Lau, C. Ma, J.H. Hahn, R. Hoque, J. Rothblatt, and M. Chalfie. 1999. A cytosolic catalase is needed to extend adult lifespan in *C. elegans daf-C* and *clk-1* mutants. *Nature.* 399:162-166.

Taub, J., J.F. Lau, C. Ma, J.H. Hahn, R. Hoque, J. Rothblatt, and M. Chalfie. 2003. Retraction of: A cytosolic catalase is needed to extend adult lifespan in *C. elegans daf-C* and *clk-1* mutants. *Nature.* 421:764.

Terlecky, S.R., and M. Fransen. 2000. How peroxisomes arise. *Traffic* 1:465-473.

Terlecky, S.R., W.M. Nuttley, D. McCollum, E. Sock, and S. Subramani, S. 1995. The *Pichia pastoris* peroxisomal protein PAS8p is the receptor for the C-terminal tripeptide peroxisomal targeting signal. *EMBO J.* 14:3627-3634.

Thieringer, H., B. Moellers, G. Dodt, W.-H. Kunau, and M. Driscoll. 2003. Modeling human peroxisome biogenesis disorders in the nematode *Caenorhabditis elegans*. *J. Cell Sci.* 116:1797-1804.

Thomas, J.H., and S. Lockery. 1999. Neurobiology. *In C. elegans.* A Practical Approach. Hope, I.A., editor. Oxford University Press, Oxford.143-179.

Tipton, C.L., and N.M. al-Shathir. 1974. The metabolism of cyclopropane fatty acids by *Tetrahymena pyriformis*. *J. Biol. Chem.* 249:886-889.

Titorenko, V.I., and R.A. Rachubinski. 2001a. Dynamics of peroxisome assembly and function. *Trends Cell Biol.* 11:22-29.

Titorenko, V.I., and R.A. Rachubinski. 2001b. The life cycle of the peroxisome. *Nature Rev. Mol. Cell Biol.* 2:357-368.

Titorenko, V.I., D.M. Ogrydziak, and R.A. Rachubinski. 1997. Four distinct secretory pathways serve protein secretion, cell surface growth, and peroxisome biogenesis in the yeast *Yarrowia lipolytica*. *Mol. Cell Biol.* 17:5210-5226.

Togo, S.H., M. Maebuchi, S. Yokota, M. Bun-Ya, A. Kawahara, and T. Kamiryo. 2000. Immunological detection of alkaline-diaminobenzidine-negative peroxisomes of the nematode *Caenorhabditis elegans*. Purification and unique pH optima of peroxisomal catalase. *Eur. J. Biochem* 267:1307-1312.

Tolbert, N.E., and E. Essner. 1981. Microbodies: peroxisomes and glyoxysomes. *J. Cell Biol.* 91:271s-283s.

Tsukamoto, T., S. Hata, S. Yokota, S. Miura, Y. Fujiki, M. Hijikata, S. Miyazawa, T. Hashimoto, and T. Osumi. 1994. Characterization of the signal peptide at the amino terminus of the rat peroxisomal 3-ketoacyl-CoA thiolase precursor. *J. Biol. Chem.* 269:6001-6010.

van den Bosch, H., R.B. Schutgens, R.J. Wanders, and J.M. Tager. 1992. Biochemistry of peroxisomes. *Annu. Rev. Biochem.* 61:157-197.

van Grunsven, E.G., E. van Berkel, P.A. Mooijer, P.A. Watkins, H.W. Moser, Y. Suzuki, L.L. Jiang, T. Hashimoto, G. Hoefler, J. Adamski, and R.J. Wanders. 1999. Peroxisomal bifunctional protein deficiency revisited: resolution of its true enzymatic and molecular basis. *Am. J. Hum. Genet.* 64:99-107.

van Roermund, C.W., H.F. Tabak, M. van den Berg, R.J. Wanders, and E.H. Hettema. 2000. Pex11p plays a primary role in medium-chain fatty acid oxidation, a process that affects peroxisome number and size in *Saccharomyces cerevisiae*. *J. Cell Biol.* 150:489-498.

van Zandycke, S.M., P.J. Sohier, and K.A. Smart. 2002. The impact of catalase expression on the replicative lifespan of *Saccharomyces cerevisiae*. *Mech. Ageing Dev.* 123:365-373.

Vanfleteren, J.R. 1993. Oxidative stress and ageing in *Caenorhabditis elegans*. *Biochem. J.* 292:605-608.

Verhoeven, N.M., and C. Jakobs. 2001. Human metabolism of phytanic acid and pristanic acid. *Prog. Lipid Res.* 40:453-466.

Verleur, N., Y. Elgersma, C.W. van Roermund, H.F. Tabak, and R.J. Wanders. 1997. Cytosolic aspartate aminotransferase encoded by the *AAT2* gene is targeted to the peroxisomes in oleate-grown *Saccharomyces cerevisiae*. *Eur. J. Biochem.* 247:972-980.

Wanders, R.J., and J.M. Tager. 1998. Lipid metabolism in peroxisomes in relation to human disease. *Mol. Aspects Med.* 19:69-154.

Wanders, R.J., E.G. van Grunsven, and G.A. Jansen. 2000. Lipid metabolism in peroxisomes: enzymology, functions and dysfunctions of the fatty acid α- and β-oxidation systems in humans. *Biochem. Soc. Trans.* 28:141-149.

Wanders, R.J., P. Vreken, S. Ferdinandusse, G.A. Jansen, H.R. Waterham, C.W. van Roermund, and E.G. van Grunsven. 2001. Peroxisomal fatty acid α- and β-oxidation in humans: enzymology, peroxisomal metabolite transporters and peroxisomal diseases. *Biochem. Soc. Trans.* 29:250-267.

Wanders, R.J., P.G. Barth, R.B.H. Schutgens, and H.S.A. Heymans. 1996. Peroxisomal disorders: post- and prenatal diagnosis based on a new classification with flowcharts. *Int. Pediatrics.* 11:203-214.

Wanders, R.J.A. 1999. Peroxisomal disorders: clinical, biochemical, and molecular aspects. *Neurochem. Res.* 24:565-580.

Wanders, R.J.A., and G.J. Romeijn. 1998. Differential deficiency of mevalonate kinase and phosphomevalonate kinase in patients with distinct defects in peroxisome biogenesis: evidence for a major role of peroxisomes in cholesterol biosynthesis. *Biochem. Biophys. Res. Commun.* 247:663-667.

Waterham, H.R., V.I. Titorenko, P. Haima, J.M. Cregg, W. Harder, and M. Veenhuis. 1994. The *Hansenula polymorpha PER1* gene is essential for peroxisome biogenesis and encodes a peroxisomal matrix protein with both carboxy- and amino-terminal targeting signals. *J. Cell Biol.* 127:737-749.

Watkins, P.A. 1997. Fatty acid activation. *Prog. Lipid Res.* 36:55-83.

Watkins, P.A., A.E. Howard, and S.J. Mihalik. 1994. Phytanic acid must be activated to phytanoyl-CoA prior to its alpha-oxidation in rat liver peroxisomes. *Biochim Biophys Acta.* 1214:288-294.

Watts, J.L., and J. Browse. 2002. Genetic dissection of polyunsaturated fatty acid synthesis in *Caenorhabditis elegans*. *Proc. Natl. Acad. Sci. USA.* 99:5854-5859.

Wetterau, J.R., L.P. Aggerbeck, M.E. Bouma, C. Eisenberg, A. Munck, M. Hermier, J. Schmitz, G. Gay, D.J. Rader, and R.E. Gregg. 1992. Absence of microsomal triglyceride transfer protein in individuals with abetalipoproteinemia. *Science.* 258:999-1001.

White, J.G., E. Southgate, J.N. Thomson, and S. Brenner. 1986. The structure of the Nervous system of the nematode *Caenorhabditis elegans*. *Phil. Trans. R. Soc. Lond. B. Biol. Sci.*, B314:1-340.

Wimmer, B., F. Lottspeich, I. van der Klei, M. Veenhuis, and C. Gietl. 1997. The glyoxysomal and plastid molecular chaperones (70-kDa heat shock protein) of watermelon cotyledons are encoded by a single gene. *Proc. Natl. Acad. Sci. USA*. 94:13624-13629.

Witt, U., S. Rehberg, and W.O. Abel. 1995. A full-Length cDNA (Accession No. X92512) coding for glyoxysomal malate dehydrogenase from *Brassica napus L. Plant Physiol.* 110:336-336.

Wolfrum, C., P. Ellinghaus, M. Fobker, U. Seedorf, G. Assmann, T. Borchers, and F. Spener. 1999. Phytanic acid is ligand and transcriptional activator of murine liver fatty acid binding protein. *J. Lipid Res*. 40:708-714.

Wolkow, C.A., K.D. Kimura, M.S. Lee, and G. Ruvkun. 2000. Regulation of *C. elegans* life-span by insulinlike signaling in the nervous system. *Science*. 290:147-150.

Wong, A., P. Boutis, and S. Hekimi. 1995. Mutations in the *clk-1* gene of *Caenorhabditis elegans* affect developmental and behavioral timing. *Genetics*. 139:1247-1259.

Woodbury, W., A.K. Spencer, and M.A. Stahman. 1971. An improved procedure using ferricyanide for detecting catalase isozymes. *Anal. Biochem*. 44:301-305.

Yamagami, S., T. Iida, Y. Nagata, A. Ohta, and M. Takagi. 2001. Isolation and characterization of acetoacetyl-CoA thiolase gene essential for *n*-decane assimilation in yeast *Yarrowia lipolytica. Biochem. Biophys. Res. Commun*. 282:832-838.

Yanase, S., K. Yasuda, and N. Ishii. 2002. Adaptive responses to oxidative damage in three mutants of *Caenorhabditis elegans* (*age-1*, *mev-1* and *daf-16*) that affect life span. *Mech. Ageing Dev*. 123:1579-1587.

Yokota, S., S.H. Togo, M. Maebuchi, M. Bun-Ya, C.M. Haraguchi, and T. Kamiryo. 2002. Peroxisomes of the nematode *Caenorhabditis elegans*: distribution and morphological characteristics. *Histochem. Cell Biol*. 118:329-336.

Zhu, X., A.K. Raina, H.G. Lee, G. Casadesus, M.A. Smith, and G. Perry. 2004. Oxidative stress signalling in Alzheimer's disease. *Brain Res*. 1000:32-39.

APPENDIX

Comparison of spectra of fatty acid methyl esters and mixtures of methyl ester lipid standards.

ST1 - Mixture Me 100 (Larodan)

ST2 - Mixture Me 93 (Larodan)

ST3 - Combined mixtures BR 2 and BR 3 (Larodan)

ST4 - Mixture HAM 14 (Larodan)

ST5 - Mixture of phytanic, hydroxyphytanic, pristanic, 2-methylbutyric, and 3-methylvaleric (Sigma), C15:0 aiso, 2-methylhexadecanoic, *cis*-9,10-methyleneoctadecanoic (generic acids, gift from Dr. L. Ruthven, Department of Biochemistry, University of Alberta) acids. Fatty acids were derivatized to methyl esters (see Materials and Methods).

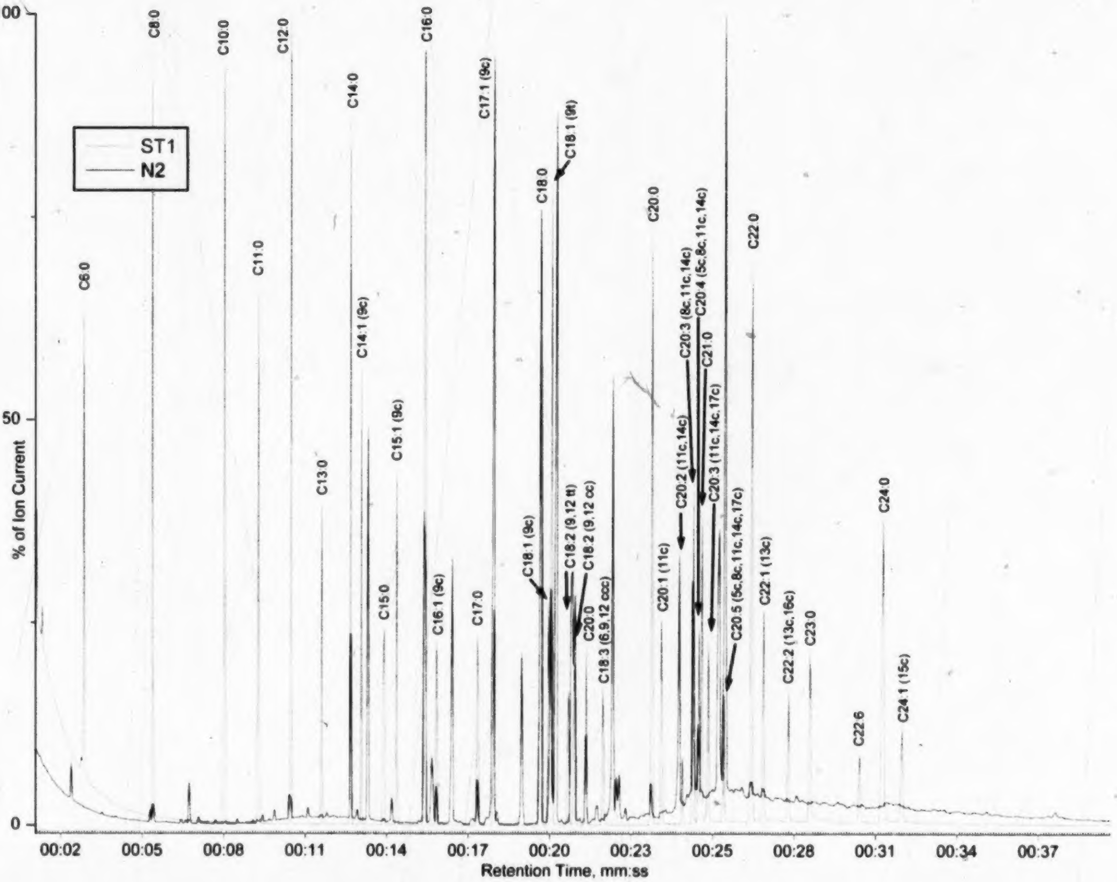

Figure A1. Gas chromatogram spectra of the standard lipid mixture ST1 and of lipids extracted from wild-type worms fed *E. coli* OP50.

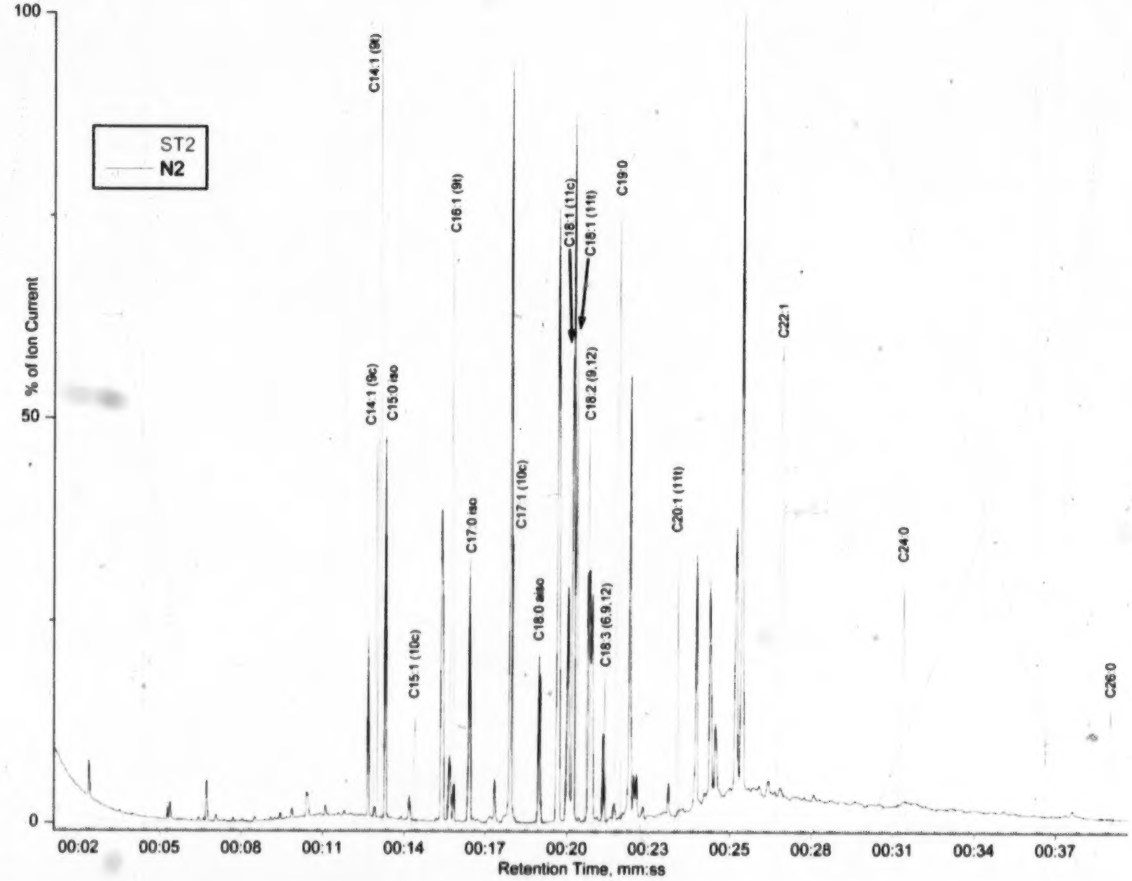

Figure A2. Gas chromatogram spectra of the standard lipid mixture ST2 and of lipids extracted from wild-type worms fed *E. coli* OP50.

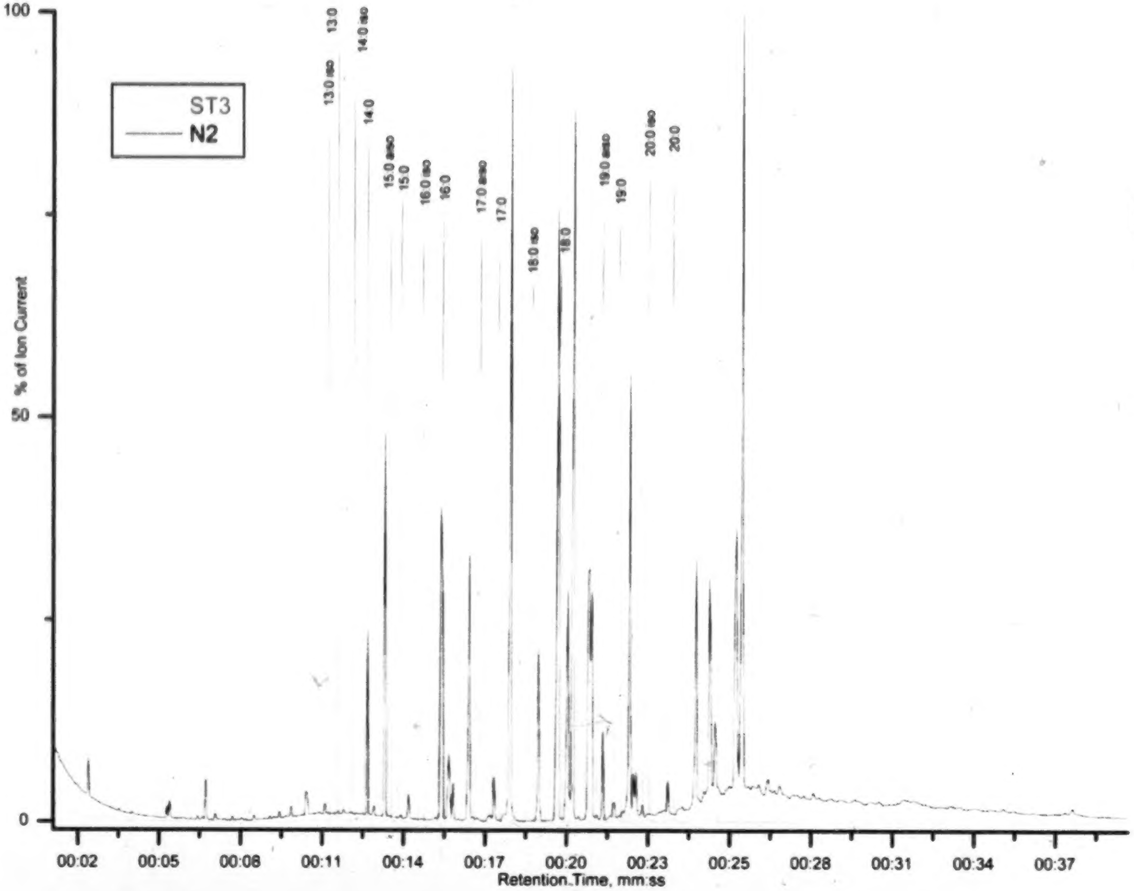

Figure A3. Gas chromatogram spectra of the standard lipid mixture ST3 and of lipids extracted from wild-type worms fed *E. coli* OP50.

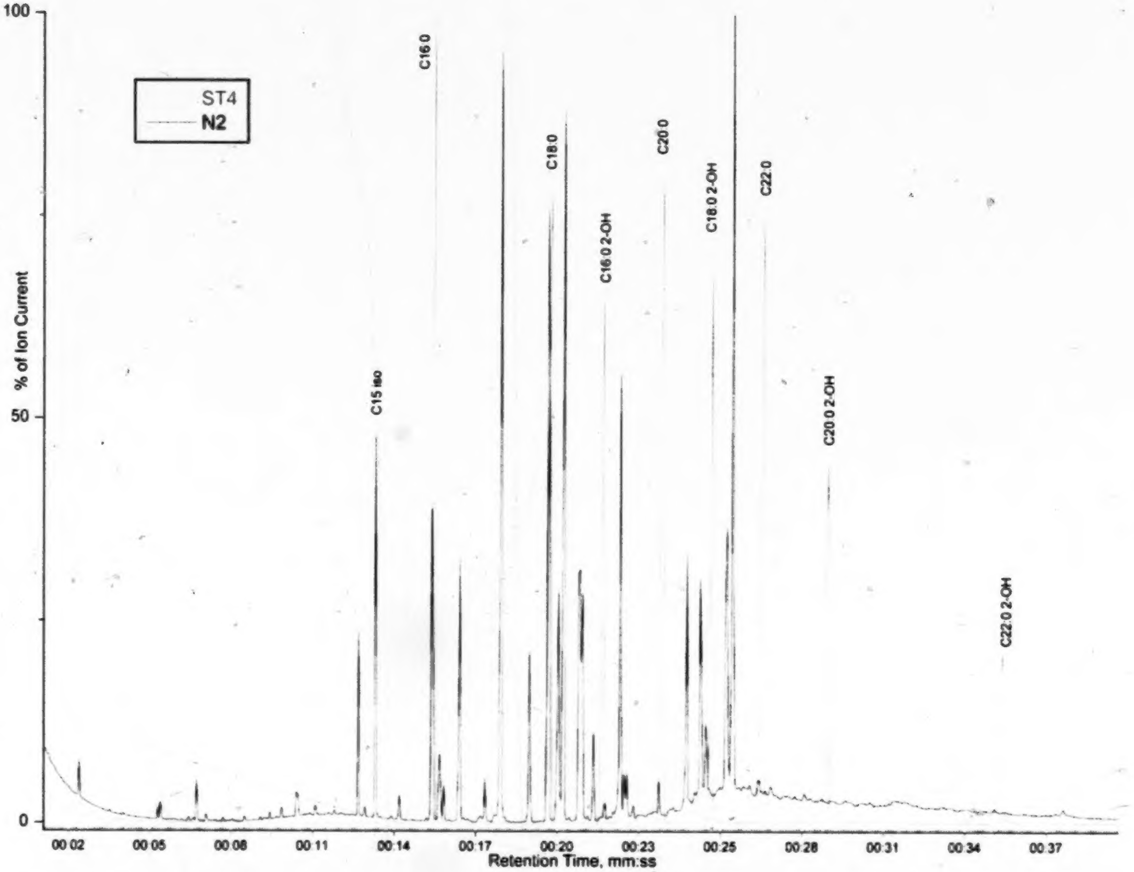

Figure A4. Gas chromatogram spectra of the standard lipid mixture ST4 and of lipids extracted from wild-type worms fed *E. coli* OP50.

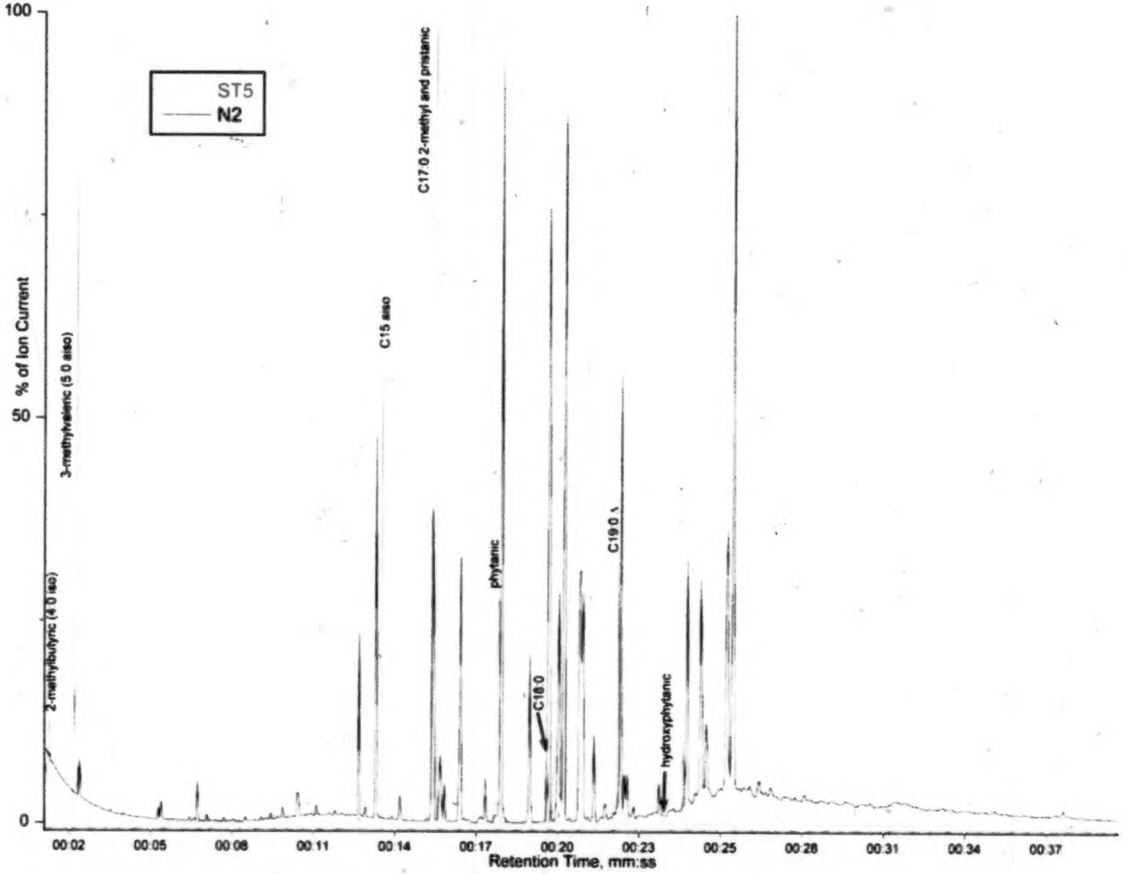

Figure A5. Gas chromatogram spectra of the standard lipid mixture ST5 and of lipids extracted from wild-type worms fed *E. coli* OP50.